ISSN 2071-4726
2071-0305

Инженерно-строительный журнал

НАУЧНОЕ ИЗДАНИЕ

№5(73) 2017

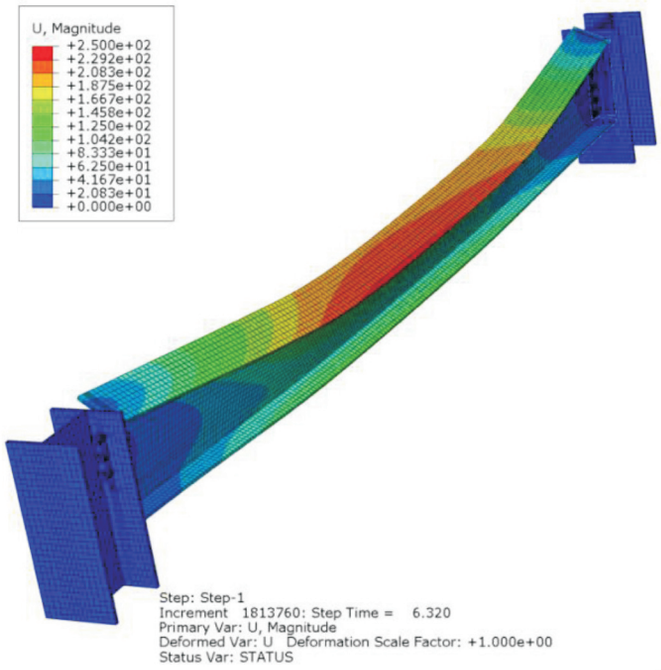

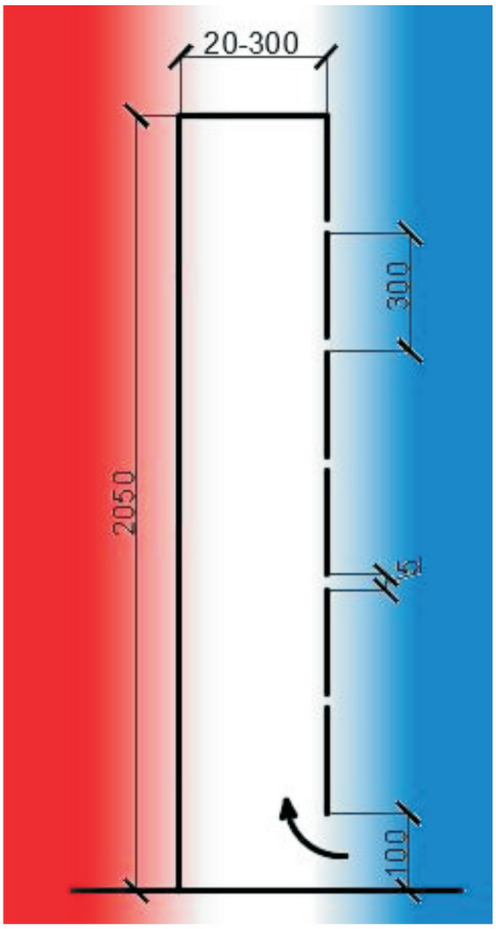

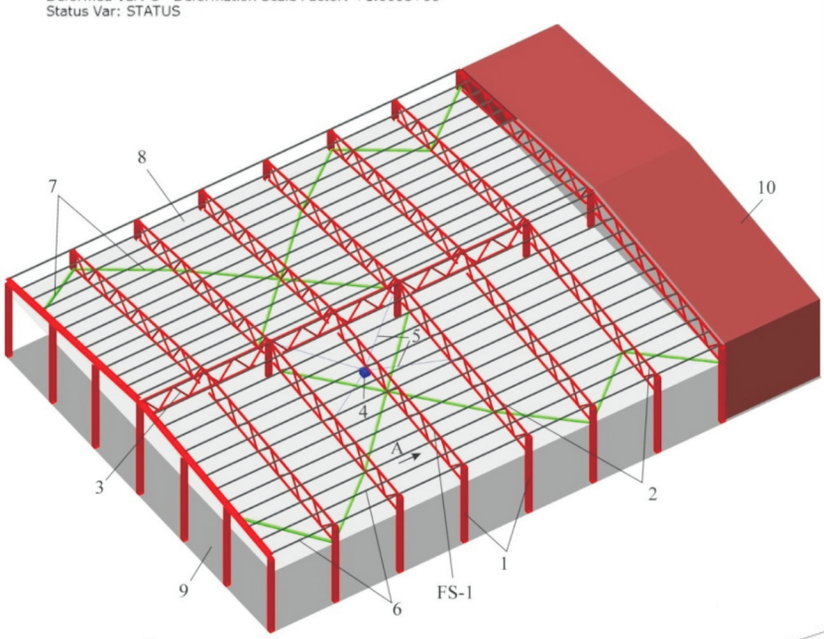

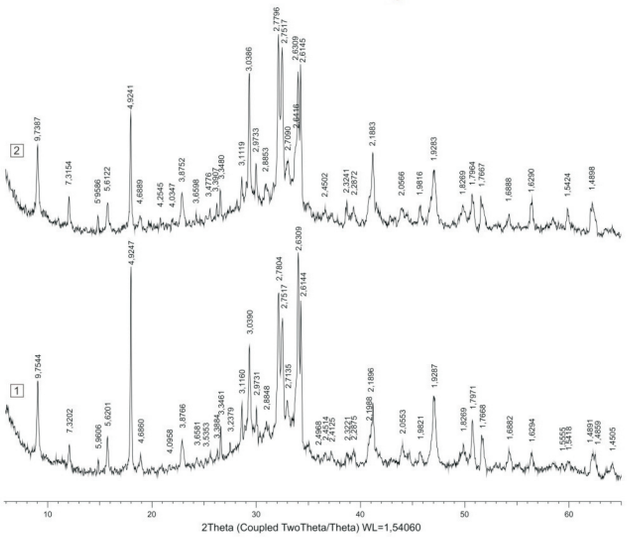

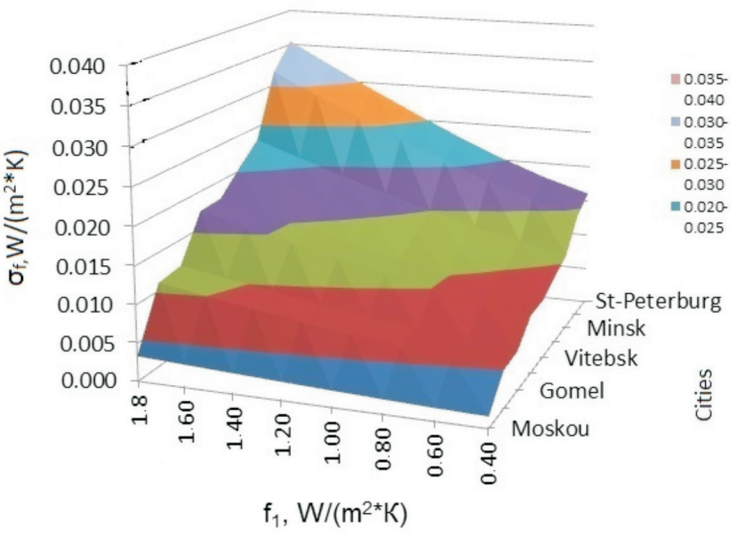

Федеральное государственное автономное образовательное учреждение высшего образования
Санкт-Петербургский политехнический университет Петра Великого

ПОЛИТЕХ
Санкт-Петербургский политехнический университет Петра Великого

Инженерно-строительный институт
Центр дополнительных профессиональных программ

195251, г. Санкт-Петербург, Политехническая ул., 29,
тел/факс: 552-94-60, www.stroikursi.spbstu.ru,
stroikursi@mail.ru

Приглашает специалистов организаций, вступающих в СРО, на курсы повышения квалификации (72 часа)

Код	Наименование программы	Виды работ*
	Курсы по строительству	
БС-01-04	«Безопасность и качество выполнения общестроительных работ»	п.1,2, 3, 5, 6, 7, 9, 10, 11, 12, 13, 14
БС-01	«Безопасность и качество выполнения геодезических, подготовительных и земляных работ, устройства оснований и фундаментов»	1,2,3,5
БС-02	«Безопасность и качество возведения бетонных и железобетонных конструкций»	6,7
БС-03	«Безопасность и качество возведения металлических, каменных и деревянных конструкций»	9,10,11
БС-04	«Безопасность и качество выполнения фасадных работ, устройства кровель, защиты строительных конструкций, трубопроводов и оборудования»	12,13,14
БС-05	«Безопасность и качество устройства инженерных сетей и систем»	15,16,17,18,19
БС-06	«Безопасность и качество устройства электрических сетей и линий связи»	20,21
БС-08	«Безопасность и качество выполнения монтажных и пусконаладочных работ»	23,24
БС-12	«Безопасность и качество устройства мостов, эстакад и путепроводов»	29
БС-13	«Безопасность и качество выполнения гидротехнических, водолазных работ»	30
БС-14	«Безопасность и качество устройства промышленных печей и дымовых труб»	31
БС-15	«Осуществление строительного контроля»	32
БС-16	«Организация строительства, реконструкции и капитального ремонта. Выполнение функций технического заказчика и генерального подрядчика»	33
	Курсы по проектированию	
БП-01	«Разработка схемы планировочной организации земельного участка, архитектурных решений, мероприятий по обеспечению доступа маломобильных групп населения»	1,2,11
БП-02	«Разработка конструктивных и объемно-планировочных решений зданий и сооружений»	3
БП-03	«Проектирование внутренних сетей инженерно-технического обеспечения»	4
БП-04	«Проектирование наружных сетей инженерно-технического обеспечения»	5
БП-05	«Разработка технологических решений при проектировании зданий и сооружений»	6
БП-06	«Разработка специальных разделов проектной документации»	7
БП-07	«Разработка проектов организации строительства»	8
БП-08	«Проектные решения по охране окружающей среды»	9
БП-09	«Проектные решения по обеспечению пожарной безопасности»	10
БП-10	«Обследование строительных конструкций и грунтов основания зданий и сооружений»	12
БП-11	«Организация проектных работ. Выполнение функций генерального проектировщика»	13
Э-01	«Проведение энергетических обследований с целью повышения энергетической эффективности и энергосбережения»	
	Курсы по инженерным изысканиям	
И-01	«Инженерно-геодезические изыскания в строительстве»	1
И-02	«Инженерно-геологические изыскания в строительстве»	2,5
И-03	«Инженерно-гидрометеорологические изыскания в строительстве»	3
И-04	«Инженерно-экологические изыскания в строительстве»	4
И-05	«Организация работ по инженерным изысканиям»	7

***(согласно приказам Минрегионразвития РФ N 624 от 30 декабря 2009 г.)**

По окончании курса слушателю выдается удостоверение о краткосрочном повышении квалификации установленного образца (72 ак. часа)

Для регистрации на курс необходимо выслать заявку на участие, и копию диплома об образовании по телефону/факсу: 8(812) 552-94-60, 535-79-92, , e-mail: stroikursi@mail.ru.

http://www.engstroy.spbstu.ru – полнотекстовая версия журнала в сети Интернет.
Бесплатный доступ, обновление с каждым новым выпуском

Инженерно-строительный журнал
НАУЧНОЕ ИЗДАНИЕ

ISSN 2071-4726, 2071-0305

Свидетельство о государственной регистрации: ПИ №ФС77-38070, выдано Роскомнадзором

Специализированный научный журнал. Выходит с 09.2008.

Включен в Перечень ведущих периодических изданий ВАК РФ

Периодичность: 8 раз в год

Учредитель и издатель:

Санкт-Петербургский политехнический университет Петра Великого

Адрес редакции:

195251, СПб, ул. Политехническая, д. 29, Гидрокорпус-2, ауд. 227А

Главный редактор:
Екатерина Александровна Линник

Научный редактор:
Николай Иванович Ватин

Технический редактор:
Ксения Дмитриевна Борщева

Содержание

На обложке: иллюстрации авторов к статьям номера

Контакты:
Тел. +7(812)535-52-47 E-mail: mce@spbstu.ru
Web: http://www.engstroy.spbstu.ru

http://www.engstroy.spbstu.ru – full-text open-access version in Internet. It is updated immediately with each new issue.

Magazine of Civil Engineering
SCHOLAR JOURNAL

ISSN 2071-4726
Peer-reviewed scientific journal
Start date: 2008/09
8 issues per year

Publisher:
Peter the Great St. Petersburg Polytechnic University

Indexing:
Scopus, Russian Science Citation Index (WoS), Compendex, DOAJ, EBSCO, Google Academia, Index Copernicus, ProQuest, Ulrich's Serials Analysis System

Corresponding address:
227a Hydro Building, 29 Polytechnicheskaya st., Saint-Petersburg, 195251, Russia

Contents

On the cover: authors' illustrations

+7(812) 535-52-47
E-mail: mce@spbstu.ru
Web: http://www.engstroy.spbstu.ru/eng/index.html

doi: 10.18720/MCE.73.1

Deformations of steel roof trusses under shock emergency action

Деформации стальных стропильных ферм при ударных аварийных воздействиях

A.V. Alekseytsev,
National Research Moscow State Civil Engineering University, Moscow, Russia
N.S. Kurchenko,
Bryansk State University of Engineering and Technology, Bryansk, Russia

канд. техн. наук, доцент А.В. Алексейцев,
Национальный исследовательский Московский государственный строительный университет, г. Москва, Россия
канд. техн. наук, доцент Н.С. Курченко,
Брянский государственный инженерно-технологический университет, г. Брянск, Россия

Key words: truss; technological equipment; emergency impact; experiment; shock effects; crate system; cable sensor; dynamic loads; displacements in time; strains in time

Ключевые слова: стропильная ферма; технологическое оборудование; аварийное воздействие; эксперимент; ударные воздействия; крейтовая система; тросовый датчик; динамические догружения; перемещения во времени; деформации во времени

Abstract. The problems of experimental and theoretical research on the stressed and deformed state of steel structures under emergency actions are particularly relevant. This paper proposes experimental and theoretical research methodology, which is used on the basis of an example of research on a full-length truss as part of the frame for an industrial buildings workshop. Components of the stressed-strained state of the structure are determined experimentally in the course of a simulated emergency situation. As emergency impacts, this paper considers the detachment of the air-cooling unit attached to a node of the lower chord of the truss. Experimental data is gathered through the joint use of the crate system, cable sensor and PC. The finite-element modelling of the structure behavior is performed based on the direct integration of differential equations of motion of the system subject to the local dynamic effects, and a comparison of data obtained with experiments results. As a result of using the test methodology we obtained the maximum weight of technological equipment fastened to the roof truss, while ensuring its normal operation in case of an emergency related to the failure to affix the equipment.

Аннотация. Предлагается методика экспериментально-теоретических исследований стальных конструкций при не учитываемых в нормативных документах запроектных воздействиях, которая реализуется на примере стропильной фермы в составе каркаса цеха промышленного здания. Экспериментальным путем определяются компоненты напряженно-деформированного состояния конструкции при моделировании аварийной ситуации. В качестве запроектного воздействия рассматривается отрыв воздухоохладительной установки, закрепленной к узлу нижнего пояса фермы. Сбор экспериментальных данных осуществляется при совместном использовании крейтовой системы, тросового датчика и персонального компьютера. Выполняется конечно-элементное моделирование поведения конструкции на основе прямого интегрирования дифференциальных уравнений движения системы, подверженной локальным динамическим воздействиям, и сопоставление полученных данных с результатами экспериментов. В результате определена максимальная масса технологического оборудования, закрепляемого к стропильной ферме, при обеспечении ее нормальной эксплуатации в случае возникновения ненормируемой аварийной ситуации, связанной с отказом крепления оборудования.

Алексейцев А.В., Курченко Н.С. Деформации стальных стропильных ферм при ударных аварийных воздействиях // Инженерно-строительный журнал. 2017. № 5(73). С. 3–13.

Introduction

The most important requirement when designing construction facilities is to ensure the mechanical safety of buildings and structures. Many researchers consider issues aimed at improving structural systems at ability to endure local damage. Of particular importance is the design of facilities with high level of responsibility, for which it is necessary to take into account actions that are not covered under buildings normal operation (so-called beyond-design actions). Incomplete or inadequate research on such action may result in severe socio-economic consequences. Research related to the design of safety design systems is one of the priority areas in the development of architectural engineering. Much attention is paid to the study of concrete and steel structures. As an example of emergency situations, a number of authors [1–6] have considered the processes of dynamic added stress on concrete systems, when excluding individual support links. An analysis of the ultimate static and dynamic effects in steel structures under emergency action, related to the maximum permissible loading or the exclusion of individual elements or supports from the design scheme, is reflected in papers [7–13].

Experimental and theoretical research on full-sized steel trusses and beams are of particular interest. In this case, experimental research is carried out both on designed [14, 15] and reconstructed [16] facilities. Through experiments, such basic observed values as the deformation of the rods [15], prestress levels of elements [14], and the parameters that describe the behaviour of nodal joints under static and dynamic loads [13, 17] are simulated for the designed structures. Much attention is awarded to emergencies. The most common beyond-design actions on building structures involve localised damage to one element or a group of elements as a result of fire exposure [18], ultimate loading [9, 19], removal of individual supports (pillars of the post-and-beam system) [13], or a number of scenarios involving mechanical local damage [12], dynamic pressure pulsations born by the structure, or [20] the actual load on the damaged system [21].

There is considerable interest in the theoretical and experimental analysis of beyond-design actions on structures. It should be noted that the literature has rather neglected the description of methodologies and the instrument basis for experimental research on building structures under local dynamic actions. In this paper, we propose a method for experimental research on dynamic displacements and deformations in steel structures under emergency impact, set forth using the example of testing of a steel truss spanning 18m as part of the building frame. This method determines the value of the dynamic added stress and the structure's dynamic displacement. Local dynamic actions were modelled using methods for analysing damaged structures, the main provisions of which are set out in [22].

Methods

When designing various industrial facilities, the safety of production and technological processes must be ensured. At the same time, in some cases, the normative documents do not take all possible types of production-related accidents into account. Thus, safety requirements shall be established in accordance with client's technical requirements. To implement such requirements, when considering the operating conditions of structural engineering objects, we propose that the following steps be taken:

- identify and classify possible emergency actions;
- develop and actually implement the test scheme, simulating an emergency situation. In this case, the structure or design system used in the building shall be tested.
- perform a finite-element simulation and design calculation in the dynamic formulation for the considered beyond-design actions, and calculate natural oscillations in the linear and non-linear formulations;
- determine the simulated level of emergency loading. The size of the experimental quasi beyond-design basis load (intensity, duration and other action parameters) shall be determined, taking the scale factor into account, and making it possible to avoid real damage to the structure. For example, the load on the structure (foundation subsidence) should be small enough that, when loading, no substantial plastic strain (deformation) occurs, and that system returns to its original state following quasi beyond-design actions;
- conduct an experiment simulating a possible accident. Determine the experimental values of coefficients of structural and inertia (if any) damping. Gathering data on the dynamic behaviour of these structures must be performed using modern industrial systems to record the values of the monitored parameters with a frequency of at least 50 Hz.

- conduct a structural analysis, taking into account the damping of vibrations and comparison of the results obtained with the experimental data, and a debugging test scheme with a calculation scheme that is adjusted if necessary;
- determine the parameters required, according to the security conditions, for the supporting frame system and equipment during beyond-design actions.

Setting tasks for experimental investigations. It is necessary to perform a dynamic analysis of roof truss FS-1, which is in extremely stressed-strained condition and is installed in the meat product storage building frame of the meat industry (Fig. 1). As beyond-design actions, it is necessary to consider the breakage of rope R (Fig. 2) connected to the node of the lower chord of the truss and with a load 4, while simulating the presence of the air-cooling device.

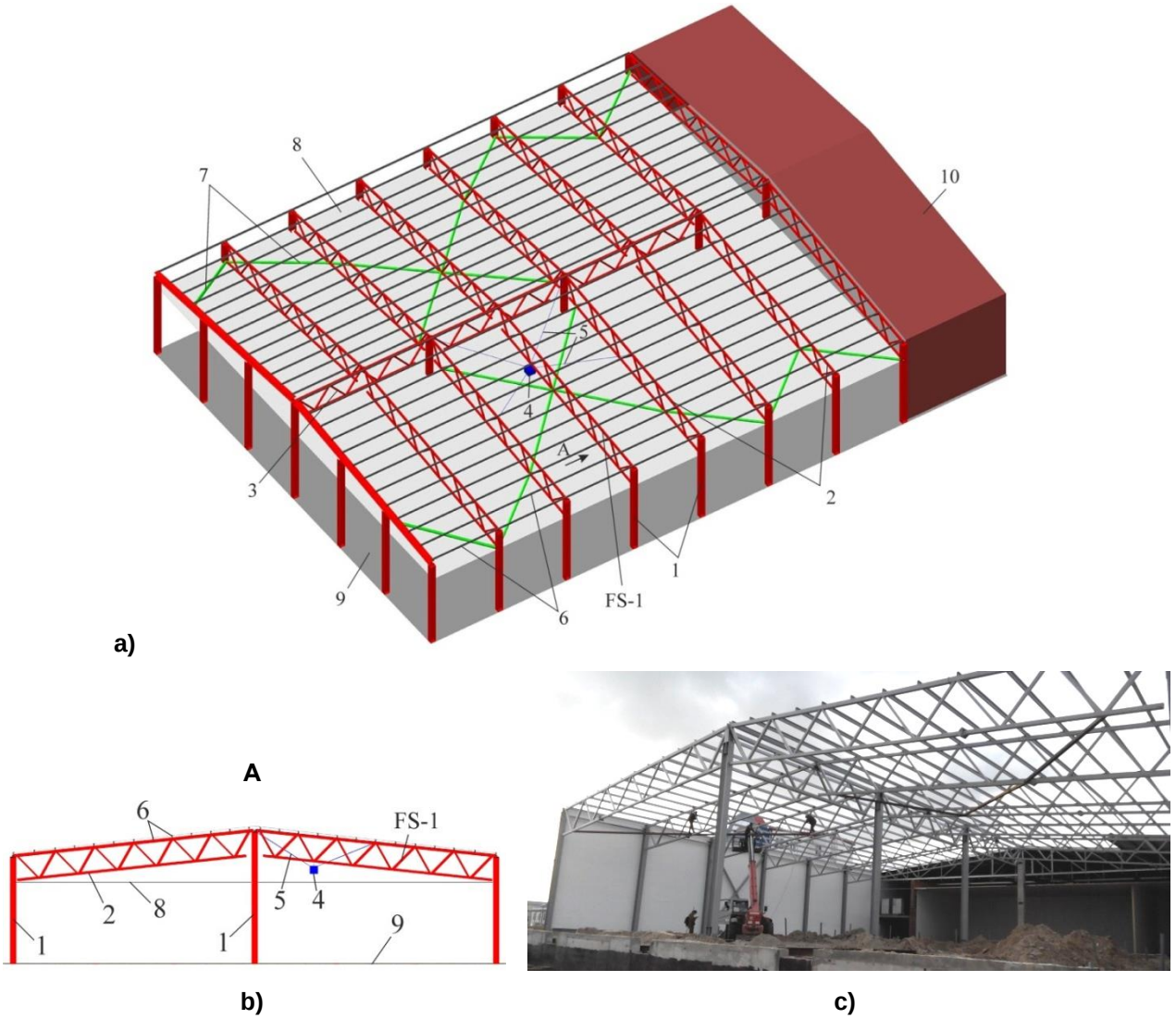

Figure 1. Object of the experiment: a – solid model: 1 – column 2 – roof trusses, 3 – secondary truss, 4 – load, 5 – safety ropes, 6 – girders, 7 – braces on bottom chord of a truss, 8 – suspended ceiling of the sandwich panels, 9 – polymer floor of the shop, 10 – operated additional building; b – view A on the row of transverse frame, c – a photo of the object in the course of erection at the stage of installation of braces on bottom chords of trusses

In this case, it is necessary to measure values of the dynamic *displacement* in the span and deformation of the individual structural elements and determine the values of the arising dynamic effects. According to the experiment's results, it is necessary to determine the maximum weight of the air-cooling device in ensuring the elastic behaviour of a truss in the event of an emergency situation under consideration.

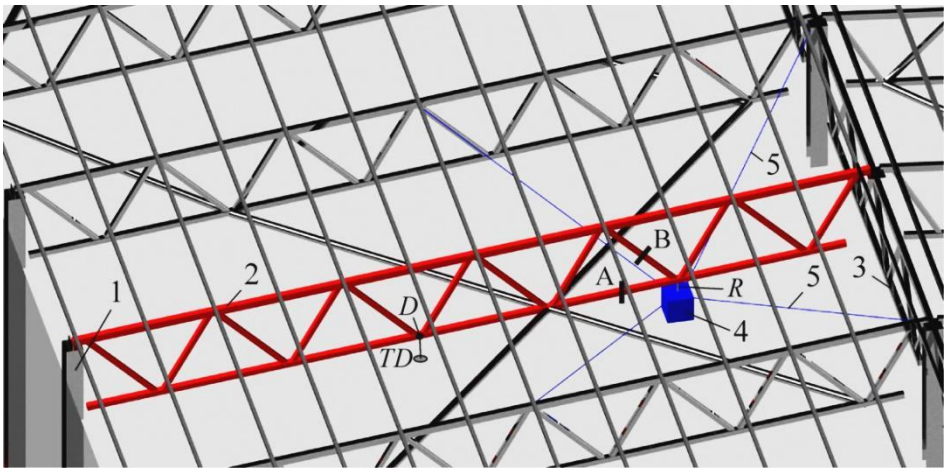

Figure 2. The scheme of tests: 1 – column 2 – truss FS-1 investigated, 3 – secondary roof truss, 4 – load, 5 – safety ropes, R – cut rope, RD – cable sensor, A, B – the location of the sections of rods with strain gauges installed

Description of the structural system to be tested. The object of the experiment is a flat roof truss FS-1 spanning 18 m as part of the frame of an industrial building workshop (Fig. 1a). The truss is made of square and rectangular pipes as per Russian State Standard GOST 30245-2003: the bottom chord of a profile is 140x6, the upper one is 180x6, and the grille is 100x4. The node for connecting rods is welded. The truss connections with the column and secondary truss are made of joint-fixed support nodes. From the plane, the truss is fastened with braces on the upper and bottom chords. At the level of the upper chord, the braces are located in the middle third of the truss span. At the level of the bottom chord, they are situated according to the scheme of the support braces' location, as shown in Fig. 1, pos. 7, and the one node is fastened. During the tests, the coating weight was taken into account and there was no snow load, but in the final calculation of the stress-deformed state, it was ultimately taken into account.

Load 4 is suspended using rope R in the assembly of the bottom chord (Fig. 3). In addition, safety ropes 5 are attached to the load in order to ensure the load transfer to the adjacent trusses in the case that rope R breaks. The safety ropes and suspension rope were used according to DIN 3055 with a diameter of 5/6 mm, type of stranding 6x7 + FC with a breaking force of not less than 11.2 kN. The load was made as a steel box, which is filled with steel plates. The total weight of the load is 180 kg. The picture of the truss test scheme fragment and assembly with a load is shown in Figure 3. The weight of the load was determined on the basis of preliminary calculations in a dynamic setting, taking into account the condition that the additional dynamic added load associated with emergency impact did not cause the appearance of plastic deformations in the structure.

Result and Discussion

Experiment plan. The dynamic test of the truss was planned by the quick mechanical destruction of rope R with a load (Fig. 3,b). The state of the truss, through which operational loads were formed, including the structure's own weight and that of the girders and coating, load and safety system, was considered as the initial. In this state, it was planned to activate data collection systems for the measured values, and using the angle grinder to exclude rope R of the load from loading. According to the results of the preliminary dynamic calculation for the impact considered by us, it is necessary to measure displacements in time in node D of the truss (Fig. 2), and relative deformations in time in two rods: on the bottom chord and in the diagonal member, connected to the assembly from the side of the rest onto the column (cross-sections A, B on Fig. 2). Based on the results of measurements, it was planned to determine the level of maximum dynamic added loading (increase stress) in rods and maximum increase in displacements in case of emergency situation related to the breakage of the real technological equipment (air-cooled devices) with different weights.

a) **b)**

Figure 3. Photo of preparing a design for testing: a – general scheme: FS-1 – the truss tested in span of 18 m; MMS – mobile measuring station; b – the load on the suspension R and safety ropes

The measurement scheme, devices and equipment. In each of the cross-sections A, B (Figs. 2, 4, 6), a group of strain gauges TD1-TD4 of the type KF 5P1-3-200B12 with a base of 5 mm and a resistance of 200 ohm ± 0.2 were installed. Resistive strain gauge bases were placed in parallel to the longitudinal axis of the rod. To affix gauges on the truss, the glue of cold hardening cyanoacrylate "Tsiakrin AO" was used. Output signals of the strain amplifier were recorded using a crate data acquisition system L-CARD LTR EU-2 with chips ADC LTR-212, allowing to carry out a survey of gauges with frequency up to 3,000 Hz. The mode information collection with a frequency of 1,536 Hz was used in the experiment. Data obtained by the crate system was transmitted to a computer and processed by an electronic recorder Lgraph 2.0, which has the ability to visualize the measured deformations in time. At point D (see Fig. 2), vertical displacements were measured using the cable sensor SX50-1250-16-L-SR with the accuracy of 524 pulses within 1 mm of the cable stroke ($2 \cdot 10^{-3}$ mm), a digital indicator PAX-I, and video camera with a recording frequency of 60 frames per second. This cable sensor was attached to a steel rod that passed through cover 8 (Figure 1) and attached to a ladder standing on floor 9 of the shop. The diagrams of displacements were based on a non-interlaced scan of a video file with the recording of the readings of the indicator PAX-I in each of the frames and their further processing. Discrete data obtained about the displacements and deformation of the frame were processed in the soft MATLAB 2015a with use of the one-dimensional wavelet transform using Meyer wavelet, which allowed the removal of noise and maintained continuous dependencies corresponding to the main frequency of the truss' own vibrations. The mechanical properties of steel, which the truss is made from, were taken from the test report attached to the steel certificate. Yield stress of the material $\sigma_m = 340 \pm 20\,MPa$, relative deformations $\varepsilon_m = 0.0015 \pm 0.0004$.

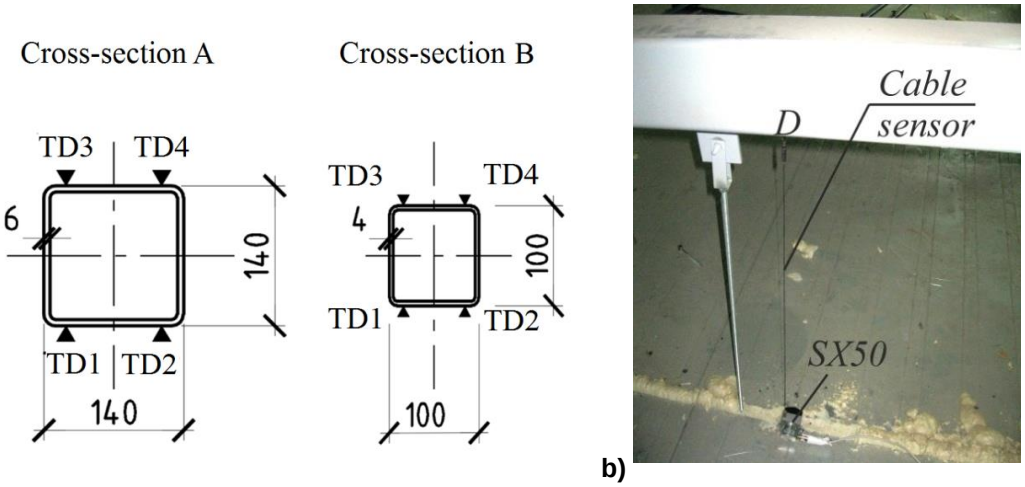

a) **b)**

Figure 4. Location of strain gauges in sections A, B (a) and scheme of installation of the cable sensor (b)

Алексейцев А.В., Курченко Н.С. Деформации стальных стропильных ферм при ударных аварийных воздействиях // Инженерно-строительный журнал. 2017. № 5(73). С. 3–13.

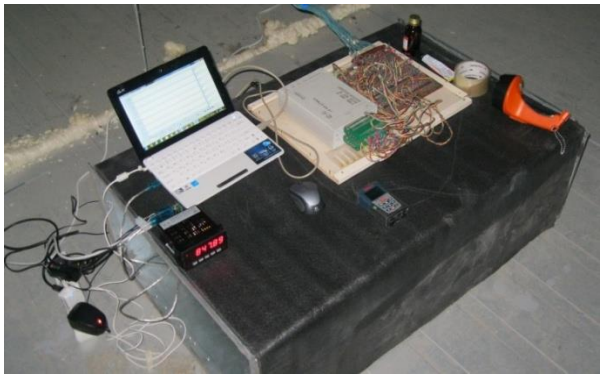

Figure 5. MMS: crate system, cable sensor and an indicator connected to a computer

Figure 6. Installation of strain gauges on the truss rods

At the emergency impact considered, the additional loading of the truss has not caused a significant formation of permanent deformations. The view of the load 4 (Fig. 2) after the rope R breakage is shown in Figure 7.

Figure 7. The load on the safety ropes

Figure 8. Installed air-cooling devices

The damping of the structure's vibrations was observed for 0.4–0.7 seconds after the emergency impact. Figure 9 shows the data of the measured values of longitudinal deformations ε and the vertical displacement of point D (see Fig. 3, 4, b), which shows that the maximum modulus of the values of displacements and deformations are achieved in the first quarter of the period for the main form of vibrations.

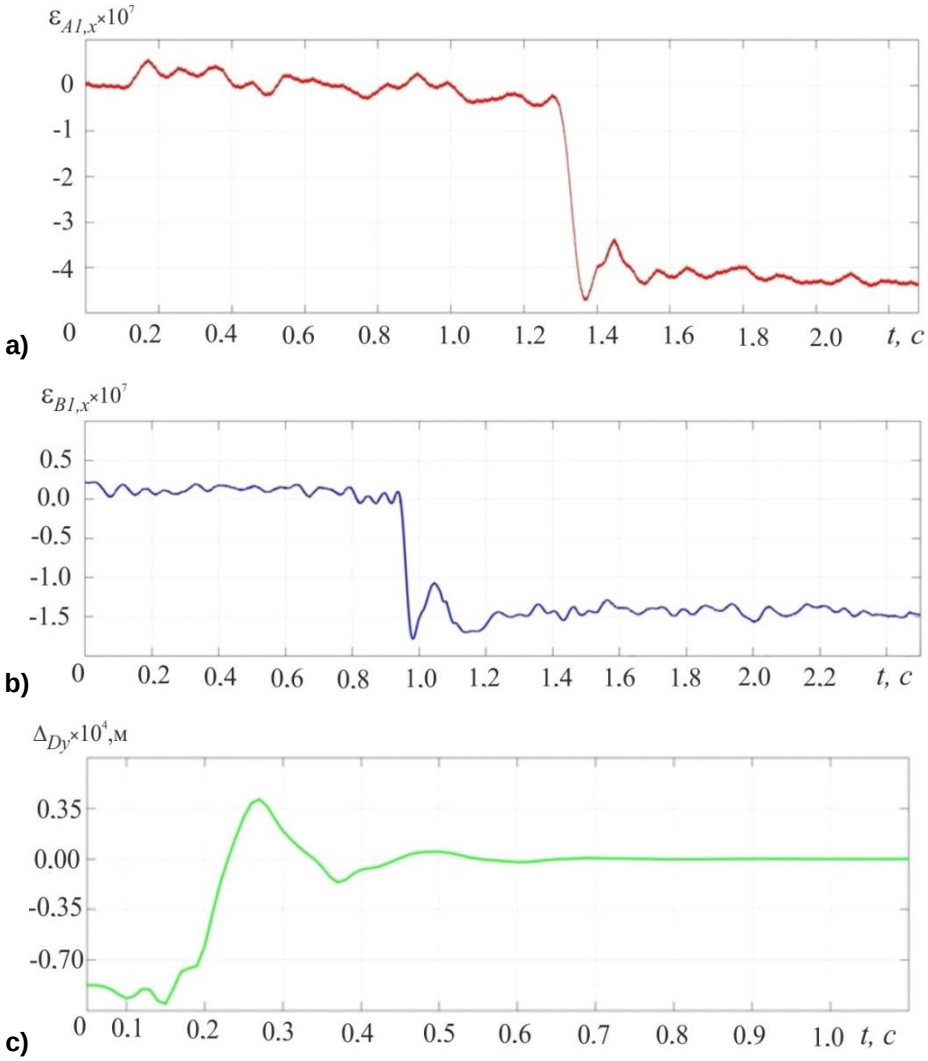

Figure 9. Graphs of changes of deformations in time:
a – deformations registered by the strain gauge TD1 on the lower chord;
b – readings of the gauge TD2 on the diagonal member compressed;
c – the vertical displacements of the point D measured using the cable sensor

Calculation of beyond-design *actions*. The truss calculation was performed in a dynamic setting, taking into account the material's linear-elastic behaviour and based on the methodology described in [22]. To analyse the dynamic behaviour of the truss system, the equation was used:

$$\left[M\left(\{Z\}\right)\right]\left\{\ddot{Z}\right\} + \left[C\left(\{Z\}\right)\right]\left\{\dot{Z}\right\} + \left\{R\left(\{Z\}\right)\right\} = \left\{F(t)\right\} + G\chi(t), \quad (1)$$

where $\left[M\left(\{Z\}\right)\right]$, $\left[C\left(\{Z\}\right)\right]$ – matrices of the masses and damping; $\left\{R\left(\{Z\}\right)\right\}$, $\{Z\}$ – vectors of nodal reactions and generalized nodal displacements; $\left\{F(t)\right\}$ – vector of loads acting on the normative actions; G – vector, defined by gravity forces of drop; $\chi(t)$ – Heaviside function.

On the basis of applying the method of the peaks set forth in the paper [23], the value of the structural damping coefficient $\beta = 0.02$ was calculated. In the case of load impact, the dynamic yield limit σ_m^D shall be determined in a simplified way according to the recommendations of [23]: $\sigma_m^D = 1.1 \cdot \omega^{1/17} \cdot \sigma_m$ where ω is the lowest frequency of the structure's vibrations. According to experimental measurements, it is $\omega = 27.1$Hz for the investigated structure. Then we have $\sigma_m^D = 1.1 \cdot 27.1^{1/17} \cdot 320 \approx 427$ MPa. We introduced single supporting fastenings at the joints with braces at the upper and bottom chords of the adjacent trusses. The object's deformations were described

by the rod finite elements. The secondary roof truss was discretised in a simplified way, as its stress-deformed state was not considered in detail (Fig. 10).

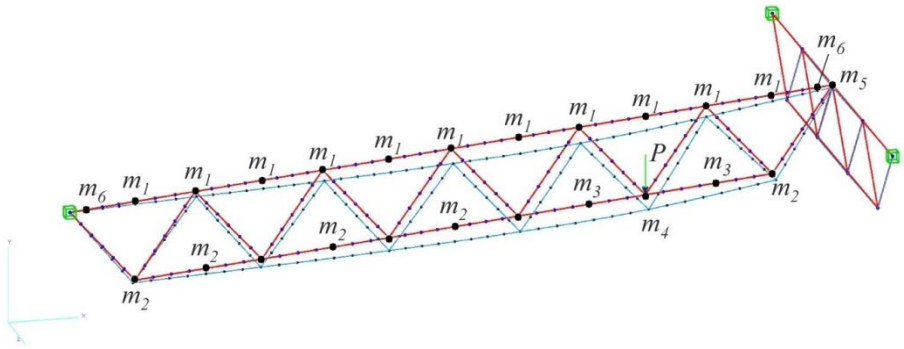

Figure 10. Design and deformed scheme of the truss at time t0 before removing the load

The actions from operating loads on the truss were taken into account in the form of concentrated nodal masses m_1- m_6 on vertical degrees of freedom. The mass m_1 takes into account the presence of girders and cover structures of the shop, m_2 – the ceiling affixed on suspensions (see Figure 3,a), $m_3 = m_2 + m_4$, m_4 – one-third of the weight of the installer cutting the rope, m_5 – mass born by the secondary roof structure from the action of the truss and structures resting on it in a nearby span, $m_6 = m_2 /2$. The force of gravity of the load P_y = -1765 N (Fig. 11) was taken into account. The value t_0 was determined under the condition of damping for vibrations of the system after the load is affixed on the structure. After this time, the load was removed.

Figure 12 reflects the truss deformation according to beyond-design actions at $t = 0.375$ s, which corresponds to its maximum bending. The scale of movements has increased 100 times in comparison with the scale of the object image. The graph of the point D movement is shown in Fig. 13. The table compares the results of theoretical analysis of the truss with experimental data, according to the values of the modulus of maximum vertical displacement in time at the point D $\left(\left|V_D\right|_{\max}\right)$ and the maximum in time stresses in the rods. Table 1 shows that calculated and experimental data are satisfactorily matched. The results of the actual additional loading on the truss, depending on the weight $m_{\max}$ of refrigeration systems, are shown in Table 2. Here, $\Delta\sigma_{\max}$ is the truss margin of safety.

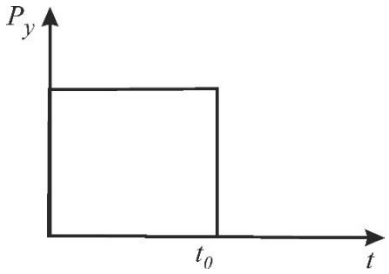

Figure 11. Change in force in time

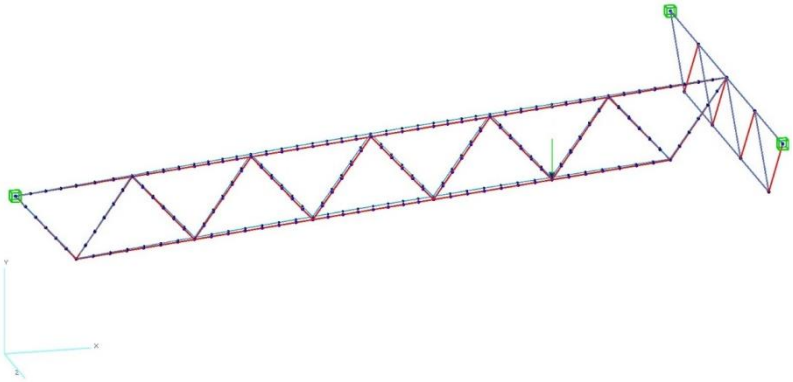

Figure 12. The design and deformed scheme of the truss at time t=0.375 s after removing the load

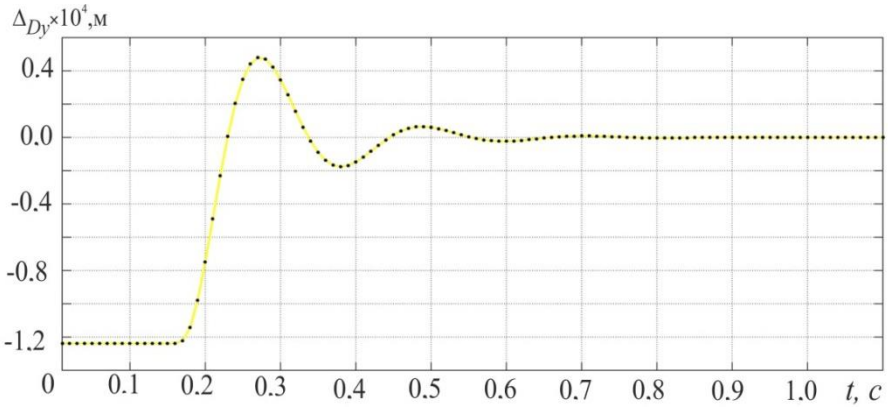

Figure 13. Results of the theoretical calculation of point D displacement in time

Table 1. Results of experimental and theoretical research on truss FM-1

Measurements using a cable sensor and strain gauges (Figs. 2, 4)		$\lvert V_D\rvert_{\max}\cdot10^4$, **m**		σ_{S1}, **kPa**		σ_{S2}, **kPa**	
		Experiment	**Calculation**	**Experiment**	**Calculation**	**Experiment**	**Calculation**
Node	*TD*	1.340	1.678	-	-	-	-
Lower chord rod	TD1	-	-	9500	11000	-	-
	TD2	-	-	4400	7900	-	-
	TD3	-	-	7300	11000	-	-
	TD4	-	-	6100	7900	-	-
Diagonal member	TD1	-	-	-	-	3100	4100
	TD2	-	-	-	-	8400	4600
	TD3	-	-	-	-	5500	4100
	TD4	-	-	-	-	2100	4600

Table 2. Results of experimental and theoretical research on truss FS-1

Name	**Values of dynamic additional loads at the breakage of the air-cleaning device at a mass $m_{\max}$ kg**							
	180*	200	500	800	1100	1400	1700	2000
$\Delta\sigma_{\max}$, MPa	**11***	12	31	49	67	86	104	122

* the value is obtained experimentally, and the remaining values obtained by the linear interpolation.

We did not find in the literature of similar facilities to compare the results of experimental studies. However, the overall behavior of the object under emergency exposures, which are considered, perfectly corresponds to the dynamics of structures, studied in the works [11, 12, 21], with similar effects.

Conclusions

This paper has proposed a method for experimental and theoretical research on the stressed and deformed state of steel structures under emergency actions not taken into account in design standards.

1. We have established that calculations and tests on the truss as part of the building frame under actual impact have confirmed the efficiency of the proposed methodology of the investigation designs in emergency situations, as well as the accuracy of the paper proposed by the authors [22] about modifying the method for calculating systems damaged by directly integrating equations for objects' motion.

2. We have found that, for the considered beyond-design impacts on the truss, the maximum values of displacements and deformations were observed in the first quarter of the period of the main form of vibrations, which can be used in assessing such structural systems' ability to survive.

Алексейцев А.В., Курченко Н.С. Деформации стальных стропильных ферм при ударных аварийных воздействиях // Инженерно-строительный журнал. 2017. № 5(73). С. 3–13.

3. When solving the problem of determining the mass of the air-cooling device, the breakage of which has had a impact on the design of the truss, we found that the level of dynamic additional loading in the rods, at the values of this mass not exceeding 500 kg, has had no significant effect on the support system's stress-strain state.

Acknowledgement

Work was performed under the grant program of the Russian Fundamental Research Fund as project 16-38-00041 "Optimization for steel load-bearing structures of buildings and facilities with the normal and high levels of responsibility".

References

1. Kolchunov V.I., Skobeleva Ye.A., Klyuyeva N.V. Experimental researches of deformations and crack resistance of reinforced concrete structures with composite section strain. *Structural Mechanics of Engineering Constructions and Buildings.* 2008. No. 1. Pp. 54–60. (rus).
2. Bondarenko V.M., Klyuyeva N.V., Degtyar A.N. Optimizatsiya zhivuchesti konstruktivno nelineynykh zhelezobet-onnykh ramno-sterzhnevykh sistem pri vnezapnykh strukturnykh [The optimisation of the survivability of structurally nonlin-ear reinforced concrete frame-bar systems at sudden structural loads]. *Izvestiya-Orel GTU. Seriya "Stroitel'stvo. Transport".* 2007. No. 4. Pp. 5–10. (rus).
3. Klyuyeva N.V., Shuvalov K.A. Methods of experimental determination of parameters of deformation and destruction of statically indeterminate pre-stressed reinforced concrete beam systems in the out-of-limit state. *Vestnik MGSU.* 2012. No. 11. Pp. 61–66. (rus).
4. Tamrazyan A.G. Rekomendatsii k razrabotke trebovaniy k zhivuchesti zdaniy i sooruzheniy [Recommendations to the development of requirements for survivability of buildings and structures]. *Vestnik MGSU.* 2011. No. 2. Vol. 1. Pp. 77–83. (rus).
5. Kolchunov V.I., Perelygin S.S. Eksperimental'nyye issledovaniya ramno-sterzhnevykh konstruktivnykh sistem s el-ementami sostavnogo secheniya pri vnezapnom vyklyuchenii svyazey [Experimental investigations of the frame-rod struc-tural systems with elements of the composite section at the sudden exclusion of braces]. *Stroitelnaya mekhanika inzhenernykh konstruktsiy i sooruzheniy.* 2006. No. 2. Pp. 115–121. (rus).
6. Schramm B., Richard H.A., Kullmer G. Theoretical, experimental and numerical investigations on crack growth in fracture mechanical graded structures. *Engineering Fracture Mechanics.* 2016. No. 167. Pp. 188–200.
7. Gordon V.A., Klyuyeva N.V., Poturayeva T.V. Raschet dinamicheskikh usiliy v konstruktivno-nelineynykh elemen-takh sterzhnevykh prostranstvennykh sistem pri vnezapnykh strukturnykh izmene-niyakh [Calculation of dynamic forces in structural and non-linear elements of spatial rod systems at sudden structural changes]. *Stroitelnaya mekhanika i raschet sooruzheniy.* 2008. No. 6. Pp. 26–30. (rus).
8. Fedorov V.S., Mednov E.A. Vliyaniye iskhodnogo napryazhenno-deformirovannogo sostoyaniya i urovnya nagru-zheniya na voznikayushchiy dinamicheskiy effekt pri avariynom razrushenii opory v nerazreznykh stalnykh balkakh [The effect of initial stressed and deformed state and the level of loading on the dynamic effect occurring in case of emergency support destruction in solid steel beams]. *Stroitelstvo i rekonstruktsiya.* 2010. No. 6. Pp. 48-52. (rus).
9. Serpik I.N., Leletko A.A., Alekseytsev A.V. Evolyutsionnyy sintez metallicheskikh ploskikh ram v sluchaye otsenki nesushchey sposobnosti po metodu predelnogo ravnovesiya [The evolutionary synthesis of metallic flat frames in the case of evaluation of the bearing capacity using the method of limit equilibrium]. *News of higher educational institutions. Construction.* 2007. No. 8. Pp. 4–9.

Литература

1. Колчунов В.И., Скобелева Е.А., Клюева Н.В. Экспериментальные исследования деформативности и трещи-ностойкости железобетонных конструкций составного сечения // Строительная механика инженерных конструкций и сооружений. 2008. № 1. С. 54–60.
2. Бондаренко В.М., Клюева Н.В., Дегтярь А.Н. Оптимизация живучести конструктивно нелинейных железобе-тонных рамно-стержневых систем при внезапных структурных // Известия ОрелГТУ. Серия «Строительство. Транспорт». 2007. № 4. С. 5–10.
3. Клюева Н.В., Шувалов К.А. Методика экспериментального определения параметров деформирования и раз-рушения преднапряженных железобетонных статически неопределимых балочных систем в запредельных состо-яниях // Вестник МГСУ. 2012. № 11. С. 61-66.
4. Тамразян А.Г. Рекомендации к разработке требований к живучести зданий и сооружений // Вестник МГСУ. 2011. № 2. Т. 1. С. 77–83.
5. Колчунов В.И., Перелыгин С.С. Экспериментальные исследования рамно-стержневых конструктивных си-стем с элементами составного сечения при внезапном выключении связей // Строительная механика инженерных конструкций и сооружений. 2006. № 2. С. 115–121.
6. Schramm B., Richard H.A., Kullmer G. Theoretical, experimental and numerical investigations on crack growth in fracture mechanical graded structures // Engineering Fracture Mechanics. 2016. No. 167. Pp. 188–200.
7. Гордон В.А., Клюева Н.В., Потураева Т.В. Расчет динамических усилий в конструктивно-нелинейных эле-ментах стержневых пространственных систем при внезапных структурных изменениях // Строительная механика и расчет сооружений. 2008. № 6. С. 26–30.
8. Федоров В.С., Меднов Е.А. Влияние исходного напряженно-деформированного состояния и уровня нагруже-ния на возникающий динамический эффект при аварийном разрушении опоры в неразрезных стальных балках // Строительство и реконструкция. 2010. № 6. С. 48–52.
9. Серпик И.Н., Лелетко А.А., Алексейцев А.В. Эволюционный синтез металлических плоских рам в случае оценки несущей способности по методу предельного равновесия // Известия высших учебных заведений. Строи-тельство. 2007. № 8. С. 4–9.
10. Алексейцев А.В., Курченко Н.С. Поиск рациональных параметров стержневых металлоконструкций на ос-нове адаптивной эволюционной модели // Строительная механика инженерных конструкций и сооружений. 2011. № 3. С. 7–14.
11. Gade V.P. Sahoo D.R Evaluation of collapse-resistance of special truss moment frames as per FEMAp695 ap-proach // Engineering Structures. 2016. No. 126. Pp. 505–515.
12. Brunell G., Kim Y.J. Effect of local damage on the behavior of a laboratory-scale steel truss bridge // Engineering Structures. 2013. No. 48. Pp. 281–291.
13. Bo Y., Kang H.T. Experimental tests of different types of

Alekseytsev A.V., Kurchenko N.S. Deformations of steel roof trusses under shock emergency action. *Magazine of Civil Engineering.* 2017. No. 5. Pp. 3–13. doi: 10.5862/MCE.73.1.

(rus).

10. Alekseytsev A.V., Kurchenko N.S. Poisk ratsional'nykh parametrov sterzhnevykh metallokonstruktsiy na osnove adaptivnoy evolyutsionnoy modeli [The search for rational parameters of the rod metal structures on the basis of adaptive evolution model]. *Stroitelnaya mekhanika inzhenernykh konstruktsiy i sooruzheniy.* 2011. No. 3. Pp. 7–14. (rus).
11. Gade V.P., Sahoo D.R. Evaluation of collapse-resistance of special truss moment frames as per FEMAp695 ap-proach. *Engineering Structures.* 2016. No. 126. Pp. 505–515.
12. Brunell G., Kim Y.J. Effect of local damage on the behaviour of a laboratory-scale steel truss bridge. *Engineering Structures.* 2013. No. 48. Pp. 281–291.
13. Bo Y., Kang H.T. Experimental tests of different types of bolted steel beam–column joints under a central-column-removal scenario. *Engineering Structures.* 2013. No. 54. Pp. 112–130.
14. Gosaye J., Gardner L., Wadee M.A., Ellen M.E. Tensile performance of pre-stressed steel elements. *Engineering Structures.* 2014. No. 79. Pp. 234–243.
15. M. Theofanous, A. Liew, and L. Gardner. Experimental study of stainless steel angles and channels in bending // Structures. 2015. No. 4. pp. 80-90.
16. 16. A. Farsi, F. Keshavarzi, P. Pouladi and R. Mirghaderi. Experimental study of a replaceable steel coupling beam with an end-plate connection // Journal of Constructional Steel Research. 2016. No. 122. pp. 138-150.
17. Andrade S.A.L., Vellasco P.C.G., Silva J.G.S., Lima L.R.O., D'Este A.V. Tubular space trusses with simple and reinforced end-flattened nodes-an overview and experiments. *Journal of Constructional Steel Research.* 2005. No. 61. Pp. 1025–1050.
18. Liu M., Zhao J., Jin M. An experimental study of the mechanical behaviour of steel planar tubular trusses in a fire. *Journal of Constructional Steel Research.* 2010. No. 66. Pp. 504–511.
19. Jankowska-Sandberg J., Kołodziej J. Experimental study of steel truss lateral–torsional buckling. *Engineering Structures.* 2013. No. 46. Pp. 165–172.
20. Yuan Y., Tan P.J., Shojaei K.A., Wrobe P. Large deformation, damage evolution and failure of ductile structures to pulse-pressure loading. *International Journal of Solids and Structures.* 2016. No. 96. Pp. 320–339.
21. Attar M., Karrech A., Regenauer-Lieb K.. A lattice spring model for dynamic analysis of damaged beam-type structures under moving loads. *European Journal of Mechanics - A/Solids.* 2016. No. 60. Pp. 196–207.
22. Serpik I.N., Kurchenko N.S., Alekseytsev A.V. Analysis of the dynamic behavior of plane frames at emergency actions considering geometrical, material and structural nonlinearities. *Promyshlennoye i grazhdanskoye stroitelstvo.* 2012. No. 10. Pp. 49–51. (rus).
23. Deb K. *Optimisation for engineering design*. New Delhi: Prentice-Hall of India Private Limited, 2005. 383 p.

bolted steel beam-column joints under a central column removal scenario // Engineering Structures. 2013. No. 54. Pp. 112–130.

14. Gosaye J., Gardner L., Wadee M.A., Ellen M.E. Tensile performance of prestressed steel elements // Engineering Structures. 2014. No. 79. Pp. 234–243.
15. Theofanous M., Liew A., Gardner L. Experimental study of stainless steel angles and channels in bending // Structures. 2015. No. 4. Pp. 80–90.
16. Farsi A., Keshavarzi F., Pouladi P., Mirghaderi R. Experimental study of a replaceable steel coupling beam with an end-plate connection // Journal of Constructional Steel Research. 2016. No. 122. Pp. 138–150.
17. Andrade S.A.L., Vellasco P.C.G., Silva J.G.S., Lima L.R.O., D'Este A.V. Tubular space trusses with simple and reinforced end-flattened nodes-an overview and experiments // Journal of Constructional Steel Research. 2005. No. 61. Pp. 1025–1050.
18. Liu M., Zhao J., Jin M. An experimental study of the mechanical behavior of steel planar tubular trusses in a fire // Journal of Constructional Steel Research. 2010. No. 66. Pp. 504–511.
19. Jankowska-Sandberg J., Kołodziej J. Experimental study of steel truss lateral-torsional buckling // Engineering Structures. 2013. No. 46. Pp. 165–172.
20. Yuan Y., Tan P.J., Shojaei K.A., Wrobe P. Large deformation, damage evolution and failure of ductile structures to pulse-pressure loading // International Journal of Solids and Structures. 2016. No. 96. Pp. 320–339.
21. Attar M., Karrech A., Regenauer-Lieb K. A lattice spring model for dynamic analysis of damaged beam-type structures under moving loads // European Journal of Mechanics - A/Solids. 2016. No. 60. Pp. 196–207.
22. Серпик И.Н., Курченко Н.С., Алексейцев А.В. Анализ в геометрически, физически и конструктивно нелинейной постановке динамического поведения плоских рам при запроектных воздействиях // Промышленное и гражданское строительство. 2012. № 10. С. 49–51.
23. Deb K. Optimization for engineering design. New Delhi: Prentice-Hall of India Private Limited, 2005. 383 p.

Anatoly Alekseytsev,
+7(960)5643358; aalexw@mail.ru

Natalya Kurchenko,
+7(920)602-32-40; ms.kurchenko@mail.ru

Анатолий Викторович Алексейцев,
+7(960)5643358; эл. почта: aalexw@mail.ru

Наталья Сергеевна Курченко,
+7(920)602-32-40; эл. почта:
ms.kurchenko@mail.ru

Алексейцев А.В., Курченко Н.С. Деформации стальных стропильных ферм при ударных аварийных воздействиях // Инженерно-строительный журнал. 2017. № 5(73). С. 3–13.

doi: 10.18720/MCE.73.2

Process of hydration and structure formation of the modified self-compacting concrete

Процессы гидратации и структурообразования модифицированного самоуплотняющегося бетона

R.R. Bogdanov,
R.A. Ibragimov,
Kazan State University of Architecture and Engineering, Kazan, Russia

Ассистент Р.Р. Богданов,
канд. техн. наук, доцент Р.А. Ибрагимов,
Казанский государственный архитектурно-строительный университет, г. Казань, Россия

Key words: modifying; admixture; superplasticizing admix; hydrophobisator; metakaolin; self-compacting concrete; hydration

Ключевые слова: модификация; добавки; суперпластификатор; гидрофобизатор; метакаолин; самоуплотняющийся бетон; гидратация

Abstract. The article reviews the research results of influence of a complex modifying agent on rheological properties of cement-water paste and cement stone strength. The article describes the processes of hydration and structure formation of cement stone, the special aspects of the phase constitution of Portland cement hydration products in the process of modifying by complex admixture. The behavior of cement hydration in composition with the complex modifying agent have been shown by means of measuring the hydrogen-ion concentration, by sedimentation, contraction and heat emission of cement suspension. There is the decreasing of the degree of cement stone hydration because of blocking action of the superplasticizing admix and hydrophobisator during the initial stage. Studying the cement stone spalls with the aid of electron microscopy has showed that there are the crystallized hydrated newgrowths with smaller dispersive capacity in composition with the complex modifying agent than the ones without introduction of admixtures. The increasing of concentration of hydrated calcium sulfoaluminate in pores and capillaries, the increasing of the specific surface area of hydrated phases both in the general structure of cement stone and in structure with regions of imperfections, the voids content decreasing lead to the material hardening. The way of cement stone structure formation in composition with the complex modifying agent is found by means of differential thermal and X-ray phase analyses. This way is shown in the composition with a complex modifying agent manifested in blocking effect SP and HP, resulting in a reduced amount of portlandite and high content of the starting phase the cement clinker, wherein the MTK is reacted with calcium hydroxide, which helps to seal material. Reduction of ettringite in the composition with a complex modifying agent is associated with precipitation of superplasticizing admix molecules on C3A particles, which limits interaction with water.

Аннотация. В статье рассмотрены вопросы повышения эксплуатационных характеристик самоуплотняющегося бетона, путем модифицирования структуры цементного камня разработанным комплексным модификатором. Изучено влияние комплексного модификатора и его компонентов: гиперпластификатора (ГП), гидрофобизатора (ГФ), метакаолина (МтК) на реологию, тепловыделение, контракцию цементного теста, а также на предел прочности при сжатии, микроструктуру и фазовый состав цементного камня. Введение комплексного модификатора позволяет повысить прочность цементного камня на 75 % по сравнению с контрольным. Определение кинетики изменения показателя pH, седиментации, контракции и тепловыделения цементных суспензий выявлен характер гидратации цемента в составе с комплексным модификатором, проявляющийся в начальном замедлении степени гидратации цементного камня из-за блокирующего действия гиперпластификатора и гидрофобизатора. Изучение сколов цементного камня с помощью электронной микроскопии показало, что в составе с комплексным модификатором кристаллические новообразования формируются значительно меньшей дисперсности, чем в составе без добавки. Увеличение концентрации гидросульфоалюмината кальция в порах и капиллярах, увеличение удельной поверхности гидратных фаз, как в общей структуре цементного камня, так и в дефектных областях пространственного скелета, уменьшение пористости приводит к упрочнению материала. Методами дифференциально термического и рентгенофазового анализа установлен механизм

структурообразования цементного камня в составе с комплексным модификатором, проявляющийся в блокирующем эффекте ГП и ГФ, что выражается в пониженном количестве портландита и большем содержании исходных фаз цементного клинкера, при этом МТК взаимодействует с гидроксидом кальция, что способствует уплотнению материала. Уменьшение эттрингита в составе с комплексным модификатором связано с осаждением молекул гиперпластификатора на частицы С3А, ограничивающем взаимодействие с водой.

Introduction

The problem of high-functional durable concrete production is topical to the present day. Such kind of concrete is usually used as underlay of buildings. Moreover, structuring the hardened cement paste, that has high density, low capillary porosity and consists of predominantly low-basic hydrated phases, is top priority [1–4]. One of the simplest and most effective methods of improving the cement composition properties is introduction of complex admixtures, which contains effective superplasticizing admixes, hydrophobic waterproofing agents and active mineral admixtures. Literature review and data analysis of these components have shown the following.

The effective superplasticizing admix is an important part of self-compacting concrete (SCC) [5]. This modifying agent makes it possible not only to increase the concrete consistency under the low water to cement proportion, but also to get high-performance, durable concrete with high density. Furthermore, most advanced superplasticizing admixes based on polycarboxylic ethers are the most effective [6-8, 13].

The increasing of freeze-thaw resistance, waterproofing capacity and exterior resistance can be achieved by introduction of water-repellent admixtures [9-11]. The silicone waters based on sodium and potassium siliconates are of primary concern. Moreover, consideration must be given to retardancy of cement hydration under the high hydrophobisator' dosages because of hydrophobic film occurring on the surface of reactants and impeding the process of hydration during the initial period [12].

With the purpose of optimizing the SCC's grain size composition and exclusion of water gain and concrete disintegration it is necessary to add fine-dispersed components to concrete composition. Ground meal, microsilicasuspension, boiler fly ash, rice husk ash, floured glass sand and metakaolin are used for this component. Scientists highlight metakaolin among the above listed [14-16], which has stable content and properties. Besides, metakaolin has a pozzolanic effect, as it reacts with $Ca(OH)_2$ during the late curing time and therewith increases the resistance to aggressive media and cement stone strength[17, 18].

The authors have developed a complex modifying agent for self-compacting concrete, comprising: superplasticizer – 1.5 %, hydrophobisator – 0.15 %, metakaolin – 5 % by weight of cement. Optimization of complex modifying agent components is shown in [19, 20].

Therefore the aim of the research is studying the influence of the complex modifying agent and its components on the special aspects of micropatterning and structuring phase composition of cement stone.

The effective and simple way of achievement of the polyfunctional effect and the full realization of a capability of all the components is introduction of complex admixtures. There are famous scientists S.S. Kaprielov, V.I. Kalashnikov, L.Ya. Kramar, A.V. Sheinfeld, B.Ja. Trofimov, H.-S. Kim, S.-H. Lee celebrated for scientific research of the investigation the influence of the complex admixtures, consist of plasticizing agents and active mineral admixtures (AMA), on process of hydration and structure formation of cement stone [2, 17, 18, 21, 22]. V.G. Batrakov's studies about the complexes with plasticizing agent and hydrophobisator are also well known [12]. But the complexes which contain a plasticizing agent based on polycarboxylic ether, an organosilicone hydrophobisator and metakaolin as AMA are underinvestigated. Consequently, the investigation of the influence of superplasticizing admixture, hydrophobisator and metakaolin in composition of complex modifying agent on the strength, micropatterning and structuring phase composition of cement stone is the site of special scientific interest.

The object of the research is studying the influence of the complex modifying agent and its components on the special aspects of micropatterning and structuring phase composition of cement stone.

In order to learn these aspects it is necessary to get around the following problems:

– to learn the influence of complex modifying agent and its components on setting up time of cement-water paste and on the strength of cement stone;

- to learn the influence of the complex modifying agent and its components on the processes of hydration by means of calorimetric measurements, contraction of cement-water paste, determination cement suspension hydrogen-ion concentration (pH-value);
- to learn the influence of the complex modifying agent on the microstructure of cement stone with the aid of electron microscopy;
- to learn the influence of the complex modifying agent on the phase composition of cement stone hydrated newgrowths by means of differential thermal analysis and X-ray phase analysis.

Materials and Methods of Research

The Portland cement CEM II/A-S 32.5 corresponding to Russian State Standard GOST 31108-2003 “Cements. Technical conditions” produced by Holsim (Rus) (“Volskcement” Open Joint Stock Company), and Portland cement CEM II/A-S 32.5 corresponding to Russian State Standard GOST 31108-2003 “Cements. Technical conditions”, produced by Ulyanovskcement LLC (hereafter brands of Portland cement will be denoted by C1 and C2 correspondingly) were used as a cementitious matter. The C1 consists of the following main minerals: C_3S - 68 %, C_2S - 10 %, C_3A - 3.7 %, C4AF - 15 % and admixtures: gaize - 6 %, SO_3 - 2.2 %. The C2 consists of the following main minerals: C_3S - 57 %, C_2S - 17 %, C_3A - 7.5 %, C_4AF - 12.8 % and admixtures: gaize - 9.1 %, SO_3 - 2.36 %.

In the research the following admixtures are used as modifying agents: superplasticizer (SP) Remicrete SP 10 produced by SCHOMBURG GmbH company (Germany) (admixture is compatible with PN-EN 934-2:T3.1 и 3.2), organosilicone hydrophobisator (HP) “Tiprom S” produced by “Proizvodstvennoe obedinenie “SAZI” LLC (TS 2229-069-32478306-2003). Metakaolin (MtK) was used as active mineral admixture - noncrystalline aluminium silicate occurrence in ZHuravlinyj Log (TS 5729-095-51460677-2009).

The research of heat emission kinetics of cement-water paste was made by means of calorimetric measurements with the use of a measuring system Termokhron DS1921.

The research of contraction of cement-water paste was made by means of the measurement procedures MI 2486-98 and MI 2487-98 on the contraction measuring tester of cement activity “Cement-prognoz”.

The hydrogen-ion concentration of cement-water paste liquidus was measured with the use of pH-meter pH-metra testo 206-pH1.

The kinetics of sedimentation of cement suspension (1:100) was experimented in spirit on the torsion balance sort of BT 500.

X-ray patterns were measured on the automatic X-ray diffractometer D2 Phaser (manufacturing company Bruker AXS GmbH). Processing the received interference spectrums was made with the use of the DIFFRAC.SUITE software package. The diffractive database named ICDD PDF-2 Release 2013 helped to make the phase identification with the use of the DIFFRAC.EVA-v3.1 program module. The statement of amount of the phases was made by Rietveld method with the use of DIFFRAC.TOPAS-v4.2 program module.

Microstructure of cement stone was determined by means of a high-resolution autoemissive electronic scanning microscope Merlin produced by CARL ZEISS Company. The spalls of cement stone samples were mist by composite metal Au/Pd in the ratio 80/20 on the high-vacuum unit named Quorum T150 ES.

Differential scanning calorimetry was studied by means of the instrument of synchronal thermoanalysis STA 443 F3 Jupiter (Netzsch, Germany). During the assay performance the sample’s weight was 30-50 mg, the rate of temperature elevation was 10 °C/min, the temperature interval was from 30 °C to 1000 °C.

Results and Discussion

The results of the research of the influence of the complex modifying agent and its components on the water-reducing effectiveness, on the setting up time of cement-water paste and on the cement stone strength are shown in Table 1.

Table 1. The influence of the complex modifying agent and its components on the normal consistency, setting up time of cement-water paste

No.	Name of admixture	Admixtures content, %	Normal consistency of cement-water paste, %		Setting up time, min		Cement stone compressive strength (MPa)	
			C1	C2	beginning	ending	C1	C2
1	-	–	0.29 100 %	0.27 100 %	195 190	290 280	45.38 100 %	44.97 100 %
2	Remicrete SP 10	1,5	0.21 72.4 %	0.203 75.2 %	410 390	650 610	74.1 163 %	72.6 161 %
3	HP Tiprom S	0.15	0.284 98 %	0.266 98.5 %	620 630	830 810	45.83 101 %	46.3 103 %
4	MtK	5	0.324 112 %	0.292 108 %	180 190	320 330	56.83 125 %	55.16 123 %
5	Complex modifying agent	6.65	0.235 81 %	0.215 79.6 %	530 510	740 720	79.41 175 %	77.68 173 %

Note: For the setting up time there are results for C1 above the line and amounts for C2 under the line. The numerator is strength of compression in MPa, the denominator is fractional strength of compression in %.

As you can see in the table (Table1), water to cement proportion (WC) decreases by 1.5-27.6 % during the introduction of admixtures, moreover, water to cement proportion (WC) increases by 8-12 % during the introduction of metakaolin. The increasing of cement-water paste setting up time for all studied admixtures (except metakaolin), especially for the cement with superplasticizing admix, and HP can be observed.

Adding the complex modifying agent to the cement-water paste increases the cement stone compressive strength by 73-75 %, depending on the type of cement. Furthermore, during the introduction of superplasticizing admix and MtK severally cement stone compressive strength increases by 61-63 % and 25-23 % correspondingly, and the introduction of HP doesn't have influence on the increasing of compressive strength. The combined effect of introduction of all complex modifying agent components helps to increase compressive strength by 73-75 %, which shows the synergism of chemical admixtures.

Degree of hydration of cement stone was analyzed by measuring the hydrogen-ion concentration of cement-water paste liquidus, the heat emission, by the sedimentation of cement suspension (the Portland cement made at the Ulyanovskiy factory), by the contraction on both types of cement.

Here are the research results of measuring the hydrogen-ion concentration of cement-water paste liquidus (1:10) under the influence of the complex modifying agent and its components.

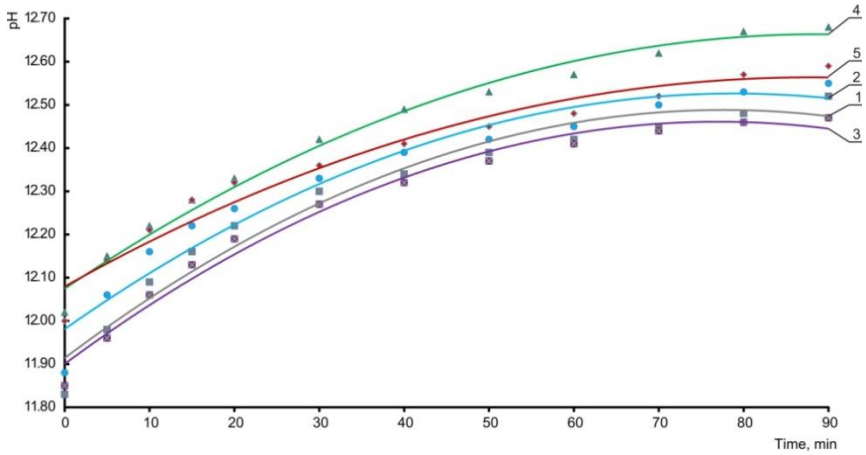

Figure 1. The influence of complex modifying agent and its components on changing the hydrogen-ion concentration of cement-water paste liquidus:
1 – with no admixtures; 2 – 1.5 % Remicrete SP 10; 3 – 0.15 % Tiprom S; 4 – 5 % MtK;
5 – 6.65 % complex modifying agent by weight of cement

In accordance with the findings in Figure 1, the hydrogen-ion concentration of separate components of complex modifying agent (superplasticizing admix and hydrophobisator) is less than the hydrogen-ion concentration of complex modifying agent. The decrease of hydrogen-ion concentration of superplasticizing admix and HP are connected with the blocking action of their molecules during the cement hydration. Furthermore, the hydrogen-ion concentration of cement with complex modifying agent is higher in comparison with compositions with mono-admixtures (superplasticizing admix and HP), which is probably connected with the superplasticizing admix and HP molecules adsorbtion by metakaolin and finally leads to the hydrogen-ion concentration increase in comparison with compositions with mono-admixtures (superplasticizing admix and HP). The hydrogen-ion concentration of complex modifying agent is more than 12.4, which is the condition of formation and accretion of the calcium hydroxide nucleating seeds and C-S-H phase.

The increasing of the hydrogen-ion concentration of cement suspensions is connected with intensive cement hydration. In view of this, there are the results of sedimentary test of cement suspensions in Figure 2. According to the data from Figure 2, the rate of cement sedimentation with admixtures is highly decreased, especially with Remicrete SP 10 modifying agent and the complex modifying agent, which is the result of the more intensive physical-chemical cement dispersion, which leads to strengthening of the degree of hydration. The superplasticizing admix mechanism of action is based on the quick molecules adsorption of the admix on the surface of cement. The molecules of admix are adsorbed on the surface of cement clinker, besides this, intensive cement dispersion in liquidus is due to the steric effect of the molecules action of superplasticizing admix. The intensity of dispersion in composition with complex modifying agent is less in comparison with composition with HP (by 17 %), which is also connected with local superplasticizing admix molecules adsorption on the particles of MtK.

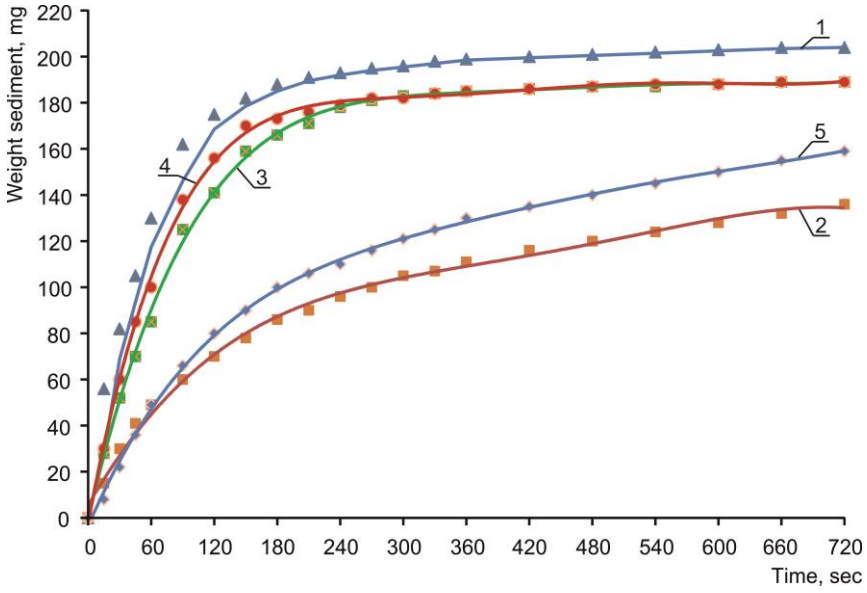

Figure 2. Kinetics of cement sedimentation with admixtures. Conventional signs are shown in the Figure 1

Intensive cement dispersion and increasing of the hydrogen-ion concentration of cement suspensions with complex modifying agent comes with changing the absolute volume of the hydrating cement-water paste. For this reason we have measured the contraction of cement-water paste (Figure 3).

As you can see in Figure 3, the highest rate of contraction of cement-water paste with MtK during the initial stage of hydration can be observed, which illustrates the increasing of degree of hydration with this admixture. There is the decreasing of the contraction rate in composition with complex modifying agent during the first hours of cement hardening due to the hydrophobisator's blocking action.

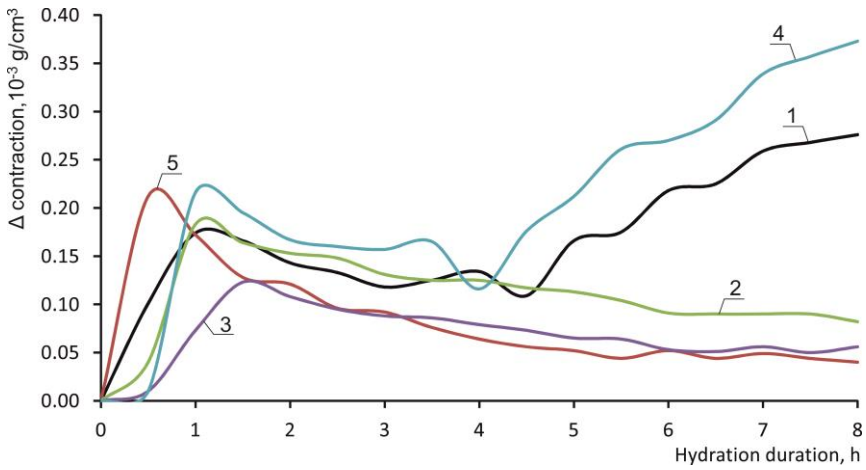

Figure 3. The rate of contraction of cement-water paste differential curve. Conventional signs are shown in the Figure 1

The contraction of cement-water paste closely connected with heat emission kinetics. In connection with this, the heat emission curves of cement-water paste with admixtures are shown in Figure 4.

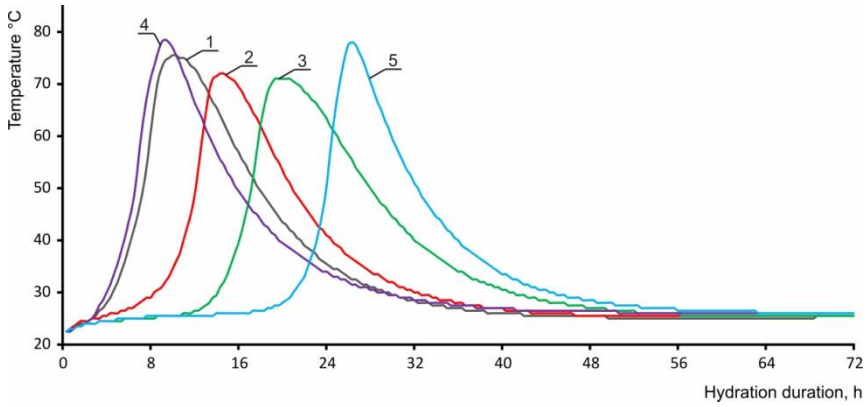

Figure 4. The heat emission during the hydration of Portland cement. Conventional signs are shown in the Figure 1

It can be seen from Figure 4 that the duration of induction process over superplasticizing admix, HP and the complex modifying agent is longer by 4, 8 and 6 hours in comparison with composition with no admixture correspondingly and shorter during the introduction of MtK. In accordance with the opinion of Batrakov V.G. [12] the slowing-down effect of hydration during the introduction of HP is explained, on the one hand, by the interaction of potassium alkylsiliconate and calcium hydroxide, accompanied by the release of hydrogen, which envelops cement particles and prevents the hydration, and on the other hand, by accumulation the admixtures interaction products and cement grains in the system.

The MtK admixture leads to an increase in the rate of heat emission of cement-water paste and the maximum temperature of hydration. HP and superplasticizing admix reduces the hydration, which becomes evident in the shifting the temperature peaks to the right by 8-12 hours. However, there is the reducing of hydration by 20 hours in composition with complex modifying agent, what is the result of hydrophobisator and superplasticizing admix synergistic effect. Nevertheless, the highest amount of waste heat in composition with complex modifying agent can be observed, that becomes evident in the increasing the degree of hydration of cement-water paste.

Studying the structure formation of cement stone with addition the complex modifying agent is a one of the top scientific problems.

There is an intricate structure of cement in Figure 5. There are needle crystals of ettringite in jellous mass of hydrated newgrowths in composition with complex admixture, which fill pore spaces in cement stone. According to the data from X-ray phase analysis, the hydrated newgrowths of ettringite are also produced in free volume in the sample without admix.

The increasing of hydrated calcium sulfoaluminate concentration in pore spaces, specific surface area of hydrated phases lead to the hardening of material both in the general structure of cement stone and in structure with regions of imperfections.

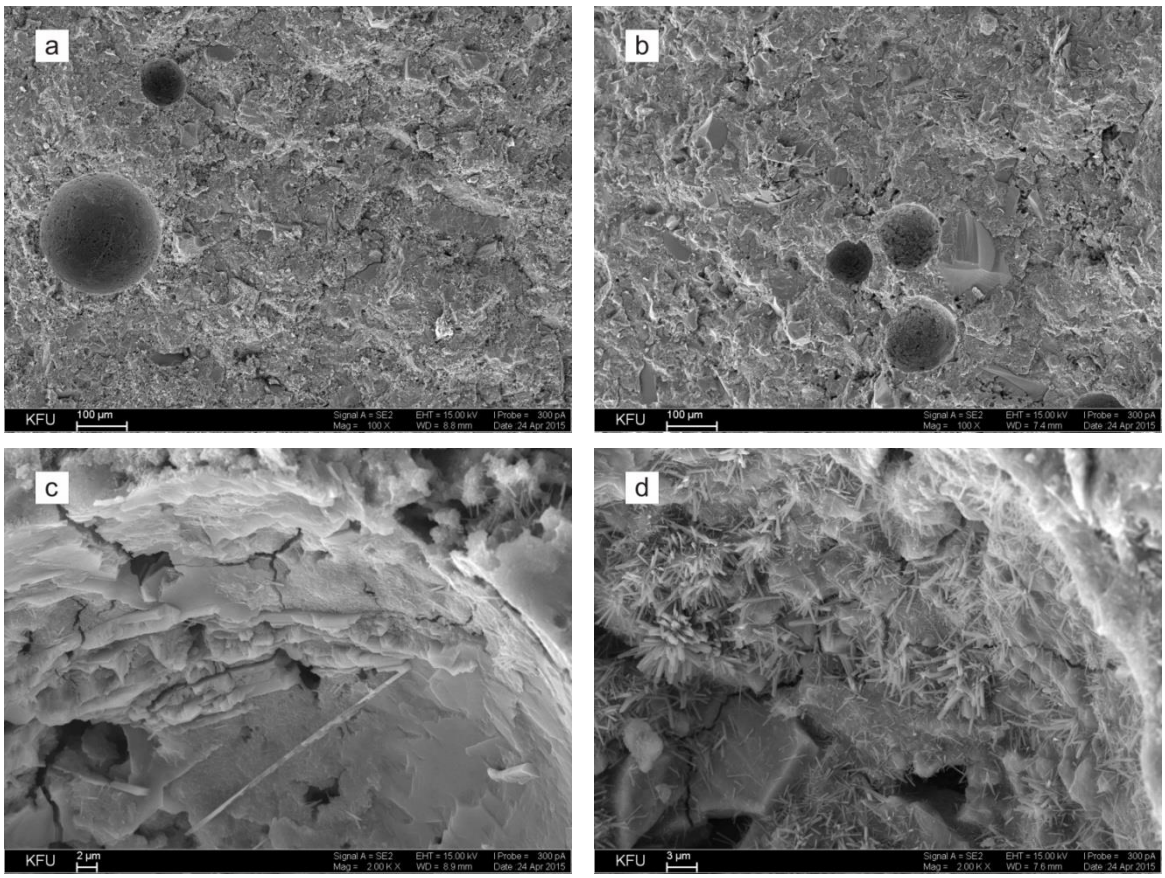

Figure 5. Electron microphotographs of samples of cement stone:
a, c – spall of the sample with no admixture;
b, d – spall of the sample with complex modifying agent.
Remarks: a, b – magnification 100^x
c, d – magnification 2000^x

The special aspect of influence of complex modifying agent is the fact that new crystallized formations have lower dispersion than formations in composition with no admixture. Moreover, the hydrated newgrowths crystallized in composition with complex modifying agent colmatage pores of cement stone, also hardening it.

Volume increasing and decreasing of the hydration products can be measured on the samples of cement stone hardening under normal conditions during 28 days by means of differential thermal (Figure 6) and X-ray phase analyses (Figure 7).

The first endoeffect at a temperature of 100–102 °C is connected with removal of gravitational moisture from pores and capillaries, and also with the fractional dehydration of ettringite. This effect is bigger in composition 1, what is confirmed by lower voids content in composition with complex modifying agent and by a high content of ettringite in composition 1, which is conformed to the data from X-ray phase analyses.

The second endoeffect at a temperature of 470–480 °C is connected with decompounding of $Ca(OH)_2$., and this effect is bigger in composition 1, which is also conformed to the data from X-ray phase analyses. Furthermore, there is the banding the free Portlandite with metakaolin and formation of calcium silicate hydrate (CSH) with lowered basicity in composition 2 [2, 17].

The third endoeffect is probably connected with decompounding of calcium carbonate. This effect is equal in both compositions, which is confirmed by the data from X-ray phase analyses, videlicet by the Rietveld method calculation (taking into account 20% of add phase); the effect is up by 8% in the sample with no admix in comparison with the sample with the complex modifying agent. Also endoeffect at a temperature 830–860 °C can be associated with dehydration of low-basic calcium hydrosilicates. At the same time, no endoeffect is observed in the DTA curves at a temperature of 830–860 °C.

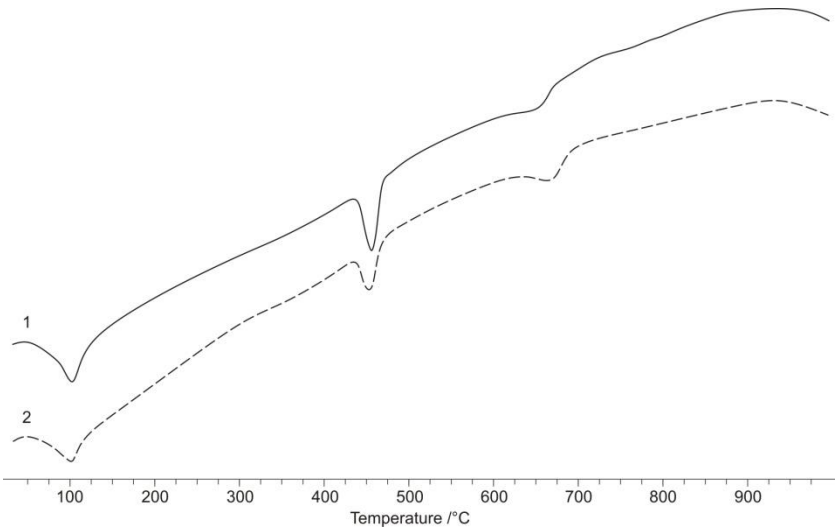

Figure 6. The curves of differential thermal analysis:
1 – the sample, 2 – the sample with complex modifying agent

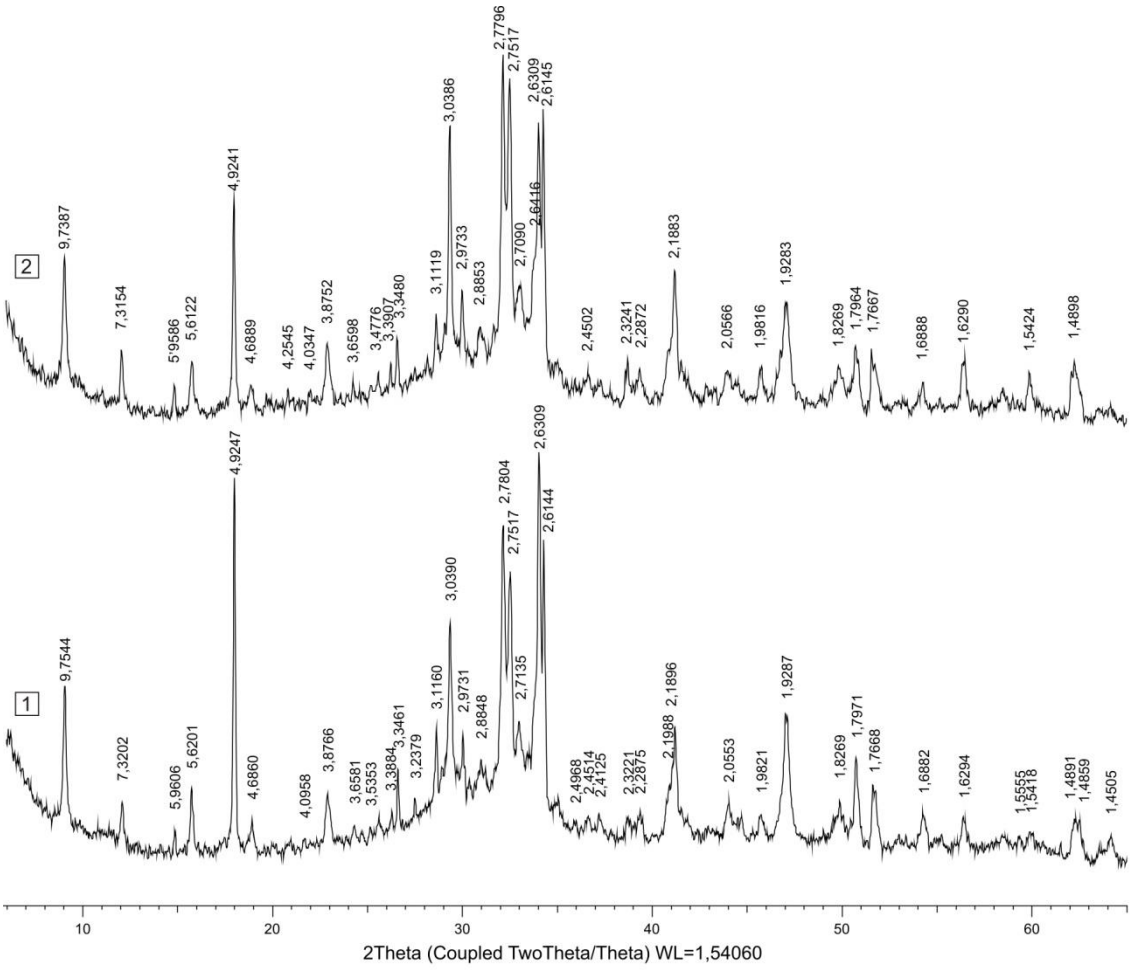

Figure 7. The curves of the X-ray phase analysis of cement stone: 1 – the sample, 2 – the sample with complex modifying agent

X-ray phase analysis of samples of cement stone without additive and with the complex modifying agent was performed (Figure 7). A quantitative calculation was also made using by the Rietveld method taking into account 20% of add phase. It has been established that the amount of the initial phase - alite (C_3S d = 3.0386; 2.7796; 2.7517; 2.6145; 2.3241; 2.1883; 1.7667; 1.6290 Å) is observed in the composition with a complex modifier and tricalcium aluminate (C3A d = 2.7090, 1.5555 Å) is 43 % higher than the control composition (C_3S d = 3.0390; 2.7804; 2.7517; 2.6144; 2.3221; 2.1988; 1.7668; 1.6294 Å;

C_3A d = 2.7135; 1.5555 Å), which indicates a delay in hydration of cement due to the blocking effect of SP and HP, while the amount of whitet decreases by 35% (C_2S d = 2.8853; 2.7796; 2.7517; 2.7090; 2.2872; 2.1883 Å). This effect is probably due to the fact that the adsorption of the superplasticizing admix occurs on hydrated neoplasms, and the greatest adsorption capacity is possessed by C_3A, the smallest C_2S [12]. The decrease in the amount of portlandite ($Ca(OH)_2$ d = 4.9241, 3.1119, 2.6309, 1.9283, 1.7964, 1.6888, 1.4859, 1.4505 Å) in the composition with a complex modifying agent (by 50 %) is due to the interaction of portlandite with metakaolin. This helps to compact the material, which is indirectly confirmed by a decrease in the amount of calcium carbonate ($CaCO_3$ d = 3.8752, 3.0386, 2.6309 Å) by 8 %, which increases the resistance of the material to carbonization. In the composition with the complex modifying agent, the amount of ettringite (d = 9.7387, 5.6122, 4.6889, 3.8752, 2.1988, 2.1504 Å) decreases by 32 %, which is possibly due to a large amount of unreacted C_3A in the composition with a complex modifying agent (43 %). And a decrease in the concentration of calcium hydroxide in solution, while according to electron microscopy, ettringite crystallizes in the pore spaces and cracks, consolidating and strengthening the structure of the material.

Taken all round according to the data from X-ray phase analysis, differential thermal analysis, electron microscopy, the mechanism of action of the complex modifying agent is manifested in the blocking effect of SP and HP, which is expressed in a reduced amount of portlandite and a greater content of the initial phases of cement clinker, while MTK interacts with calcium hydroxide, which contributes to the compaction of the material. Reduction of ettringite in the composition with a complex modifying agent is associated with precipitation of superplasticizing admix molecules on C_3A particles, which limits interaction with water.

Conclusions

1. The complex modifying agent for self-compacting concrete has been developed. We have researched the influence of the complex modifying agent on setting up time of cement-water paste and on the cement stone strength depending on Portland cement mineralogical composition.

2. The behavior of cement hydration in composition with the complex modifying agent have been shown by means of measuring the hydrogen-ion concentration, by sedimentation, contraction and heat emission of cement suspension. There is the decreasing of the degree of cement stone hydration because of blocking action of the superplasticizing admix and hydrophobisator during the initial stage.

3. Studying the cement stone spalls with the aid of electron microscopy has showed that there are the crystallized hydrated newgrowths with smaller dispersive capacity in composition with the complex modifying agent than the ones without introduction of admixtures. The increasing of concentration of hydrated calcium sulfoaluminate in pores and capillaries, the increasing of the specific surface area of hydrated phases both in the general structure of cement stone and in structure with regions of imperfections, the voids content decreasing lead to the material hardening.

4. By differential thermal and X-ray phase analysis established the mechanism of structure formation of cement stone in the composition with a complex modifying agent manifested in blocking effect SP and HP, resulting in a reduced amount of portlandite and high content of the starting phase the cement clinker, wherein the MTK is reacted with calcium hydroxide, which helps to seal material. Reduction of ettringite in the composition with a complex modifying agent is associated with precipitation of superplasticizing admix molecules on C_3A particles, which limits interaction with water.

References

1. Ibragimov R.A. The influence of binder modification by means of the superplasticizer and mechanical activation on the mechanical properties of the high-density concrete. *ZKG International.* 2016. No. 6. Pp. 34–39.
2. Kirsanova A.A., Kramar L.Y. Additives based on metakaolin features in concrete. *Conference Series: Materials Science and Engineering.* 2015. No. 71.
3. Kapriyelov S.S., Sheynfeld A.V., Kardumyan G.S. *Novyye modifitsirovannyye betony* [New modified concrete]. Moscow: Tipografiya «Paradiz», 2010. 258 p. (rus)
4. Kapriyelov S.S., Travush V.I., Karpenko N.I., Sheynfeld A.V., Kardumyan G.S., Kiseleva Yu.A., Prigozhenko O.V. Modifitsirovannyye betony novogo pokoleniya v sooruzheniyakh MMDTs «Moskva-Siti» [Modified concrete of a new generation in the buildings of the Moscow-City MIBC]. *Stroitelnyye materialy.* 2006.

Литература

1. Ibragimov R.A. The influence of binder modification by means of the superplasticizer and mechanical activation on the mechanical properties of the high-density concrete // ZKG International. 2016. № 6. Pp. 34-39.
2. Kirsanova A.A., Kramar L.Y. Additives based on metakaolin features in concrete // Conference Series: Materials Science and Engineering. 2015. № 71.
3. Каприелов С.С., Шейнфельд А.В., Кардумян Г.С. Новые модифицированные бетоны. М.: Типография «Парадиз». 2010. 258 с.
4. Каприелов С.С., Травуш В.И., Карпенко Н.И., Шейнфельд А.В., Кардумян Г.С., Киселева Ю.А., Пригоженко О.В. Модифицированные бетоны нового поколения в сооружениях ММДЦ «Москва-Сити» // Строительные материалы. 2006. № 10. С. 13–18.
5. Okamura H., Ouchi M. Self-compacting concrete //

No. 10. Pp. 13–18. (rus)

5. Okamura H., Ouchi M. Self-compacting concrete. *Advanced Concrete Technology.* 2003. No. 1. Pp. 5–15.
6. Izotov V.S., Ibragimov R.A. The influence of complex additives on the endurance strength of concrete. *ZKG: Zement - Kalk - Gips International.* 2013. Vol. 66. No. 9. Pp. 54–59.
7. Liu Z., Wang D., Zhang L., Shi L. Influence of molecular structure optimization of polycarboxylate superplasticizer on slurry dispertionand early mortar strength. *Tenth International conference on superplasticizers and other chemical admixtures in concrete.* Prague. 2012. Suppl. Vol. 1. Pp. 368–376.
8. Vovk A.I. Dobavki na osnove otechestvennykh polikarboksilatov [Additives based on native polycarboxylates]. *Stroitelnyye materialy, oborudovaniye, tekhnologii XXI veka.* 2012. No. 9(164). Pp. 31–33. (rus)
9. Nikishkin V.A. Usloviya raboty tsementnogo kamnya, obrabotannogo kremniyorganicheskimi gidrofobizatorami [Working conditions of cement stone treated with silicone hydrophobizators]. *Stroitelnyye materialy, oborudovaniye, tekhnologii XXI veka.* 2011. No. 10(153). Pp. 22–24. (rus)
10. Voytovich V.A., Khryapchenkova I.N., Yavorskiy A.A. Gidrofobizatsiya kak sposob povysheniya sroka sluzhby zdaniy (informatsiya) [Hydrophobization as a way of increasing the life of buildings (information)]. *Stroitelnyye materialy.* 2013. No. 12. Pp. 15–17. (rus)
11. Voytovich V.A., Khryapchenkova I.N. Napravleniya primeneniya gidrofobizatorov v stroitelstve (informatsiya) [Directions for using water repellents in construction (information)]. *Stroitelnyye materialy.* 2015. No. 7. P. 76. (rus)
12. Batrakov V.G. *Modifitsirovannyye betony. Teoriya i praktika* [Modified concrete. Theory and practice.]. Moscow, 1998. 768 p. (rus)
13. Stark J. Recent advances in the field of cement hydration and microstructure analysis. *Cement and Concrete Research.* 2011. No. 41. Pp. 666–678.
14. Li Q., Shui Z., Geng H., Huang Y. Chloride resistance of concrete with metakaolin addition and seawater mixing: a comparative study. *Construction and Building Materials.* 2015. Vol. 101. Pp. 184–192.
15. Rashad A.M. Metakaolin as cementitious material: history, scours, production and composition-a comprehensive overview. *Construction and Building Materials.* 2013. Vol. 41. Pp. 303–318.
16. Courard L., Darimont A., Schouterden M., Ferauche F., Willem X., Degeimbre R. Durability of mortars modified with metakaolin. *Cement and Concrete Research.* 2003. Vol. 33. No. 9. Pp. 1473–1479.
17. Kirsanova A.A., Kramar L.Ya. Organomineralnyye modifikatory na osnove metakaolina dlya tsementnykh betonov [Organometallic modifiers based on metakaolin for cement concretes]. *Stroitelnyye materialy.* 2013. No. 11. Pp. 54–56. (rus)
18. Sheynfeld A.V. Organomineralnyye modifikatory kak faktor, povyshayushchiy dolgovechnost zhelezobetonnykh konstruktsiy [Organomineralic modifiers as a factor increasing the durability of reinforced concrete structures]. *Beton i zhelezobeton.* 2014. No. 3. Pp.16–21. (rus)
19. Izotov V.S., Ibragimov R.A., Bogdanov R.R. Issledovaniye vliyaniya super- i giperplastifikatorov na osnovnyye svoystva tsementnogo testa [Investigation of the influence of super- and hyperplasticizers on the main properties of cement testing]. *Izvestiya KazGASU.* 2013. No. 2(24). Pp. 221–225. (rus)
20. Izotov V.S., Ibragimov R.A., Bogdanov R.R. Issledovaniye vliyaniya otechestvennykh gidrofobizatorov na osnovnyye svoystva tsementnogo testa i rastvora [Investigation of the effect of domestic hydrophobisers on the main properties of cement paste and mortar]. *Izvestiya KazGASU.* 2013.

Advanced Concrete Technology. 2003. № 1. Pp. 5–15.

6. Izotov V.S., Ibragimov R.A. The influence of complex additives on the endurance strength of concrete // ZKG: Zement - Kalk - Gips International. 2013. Vol. 66. No. 9. Pp. 54–59.
7. Liu Z., Wang D., Zhang L., Shi L. Influence of molecular structure optimization of polycarboxylate superplasticizer on slurry dispertionand early mortar strength // Tenth International conference on superplasticizers and other chemical admixtures in concrete. Prague. 2012. Suppl. Vol. 1. Pp. 368–376.
8. Вовк А.И. Добавки на основе отечественных поликарбоксилатов // Строительные материалы, оборудование, технологии XXI века. 2012. № 9 (164). С. 31–33.
9. Никишкин В.А. Условия работы цементного камня, обработанного кремнийорганическими гидрофобизаторами // Строительные материалы, оборудование, технологии XXI века. 2011. № 10(153). С. 22–24.
10. Войтович В.А., Хряпченкова И.Н., Яворский А.А. Гидрофобизация как способ повышения срока службы зданий (информация) // Строительные материалы. 2013. № 12. С. 15–17.
11. Войтович В.А., Хряпченкова И.Н. Направления применения гидрофобизаторов в строительстве (информация) // Строительные материалы. 2015. № 7. С. 76.
12. Батраков В.Г. Модифицированные бетоны. Теория и практика. М., 1998. 768 с.
13. Stark J. Recent advances in the field of cement hydration and microstructure analysis // Cement and Concrete Research. 2011. No. 41. Pp. 666–678.
14. Li Q., Shui Z., Geng H., Huang Y. Chloride resistance of concrete with metakaolin addition and seawater mixing: a comparative study // Construction and Building Materials. 2015. Vol. 101. Pp. 184–192.
15. Rashad A.M. Metakaolin as cementitious material: history, scours, production and composition-a comprehensive overview // Construction and Building Materials. 2013. Vol. 41. Pp. 303–318.
16. Courard L., Darimont A., Schouterden M., Ferauche F., Willem X., Degeimbre R. Durability of mortars modified with metakaolin. Cement and Concrete Research. 2003. Vol. 33. No. 9. Pp. 1473–1479.
17. Кирсанова А.А., Крамар Л.Я. Органоминеральные модификаторы на основе метакаолина для цементных бетонов // Строительные материалы. 2013. № 11. С. 54–56.
18. Шейнфельд А.В. Органоминеральные модификаторы как фактор, повышающий долговечность железобетонных конструкций // Бетон и железобетон. 2014. № 3. С. 16–21.
19. Изотов В.С., Ибрагимов Р.А., Богданов Р.Р. Исследование влияния супер- и гиперпластификаторов на основные свойства цементного теста // Известия КазГАСУ. 2013. № 2(24). С. 221–225.
20. Изотов В.С., Ибрагимов Р.А., Богданов Р.Р. Исследование влияния отечественных гидрофобизаторов на основные свойства цементного теста и раствора // Известия КазГАСУ. 2013. № 4(26). С. 207–210.
21. Гамалий Е.А., Трофимов Б.Я., Крамар Л.Я. Структура и свойства цементного камня с добавками микрокремнезема и поликарбоксилатного пластификатора // Вестник Южно-Уральского государственного университета. Серия: Строительство и архитектура. 2009. № 16(149). С. 29–35.
22. Kim H.-S., Lee S.-H., Moon H.-Y. Strength properties and durability aspects of high strength concrete using Korean

Богданов Р.Р., Ибрагимов Р.А. Процессы гидратации и структурообразования модифицированного самоуплотняющегося бетона // Инженерно-строительный журнал. 2017. № 5(73). С. 14–24.

No. 4(26). Pp. 207–210. (rus)

21. Gamalij E.A., Trofimov B.Ja., Kramar L.Ja. Struktura i svojstva cementnogo kamnja s dobavkami mikrokremnezema i polikarboksilatnogo plastifikatora [Structure and properties of cement stone with additives of microsilica and polycarboxylate plasticizer]. *Vestnik Juzhno-Ural'skogo gosudarstvennogo universiteta.* Serija: Stroitel'stvo i arhitektura. 2009. No. 16(149). Pp. 29–35. (rus)
22. Kim H.-S., Lee S.-H., Moon H.-Y. Strength properties and durability aspects of high strength concrete using Korean metakaolin. *Construction and Building Materials Journal.* 2007. No. 1. P. 128.
23. Teylor Kh.F. Khimiya tsementa [Chemistry of cement]. Moscow: Mir., 1996. 560 p.

metakaolin. // Construction and Building Materials Journal. 2007. № 1. P. 128.

23. Тейлор Х.Ф. Химия цемента. Пер. с англ. М.: Мир, 1996. 560 с.

Ruslan Bogdanov,
+79172339001; bogdanov.r.r@yandex.ru

Ruslan Ibragimov,
89297223248; rusmag007@yandex.ru

Руслан Равильевич Богданов,
+79172339001;
эл. почта: bogdanov.r.r@yandex.ru

Руслан Абдирашитович Ибрагимов,
89297223248; эл. почта: rusmag007@yandex.ru

Bogdanov R.R., Ibragimov R.A. Process of hydration and structure formation of the modified self-compacting concrete. *Magazine of Civil Engineering*. 2017. No. 5. Pp. 14–24. doi: 10.18720/MCE.73.2.

doi: 10.18720/MCE.73.3

Semi-rigid steel beam-to-column connections

Податливые соединения стальных балок с колоннами

V.M. Tusnina,
National Research Moscow State Civil Engineering University, Moscow, Russia

Канд. техн. наук, доцент В.М. Туснина,
Национальный исследовательский Московский государственный строительный университет, г. Москва, Россия

Key words: semi-rigid joint; steel frame; beam; stiffness; rotational angle; support moment

Ключевые слова: податливый узел; стальной каркас; ригель; жесткость; угол поворота; опорный момент

Abstract. Steel frameworks are widely used construction of multistory buildings for different purposes. In the practical framework calculations, the girder-column joint connections are taken as either absolutely rigid or hinged ones. The analysis of the actual behaviour of the frame joint connections shows that they normally occupy an intermediate position in the joints classification into "rigid" and "hinged" ones, i.e. they have certain pliability. Such pliability is characterized by different grades of stiffness that depends on a specific design solution of a joint. Therefore, to avoid possible material errors, the statistical calculations of frames should consider layouts with the joints that are able to support the corresponding amount of bending moments. This article contains the results of experimental and theoretical research of the actual behaviour of the girder-column connection semi-rigid joints using ABAQUS 6.13 computing complex, which enables us to solve problems by the finite elements method with due regard to the geometrical and physical nonlinearity. We consider the design of a beam-to-column connection with connecting elements in the form of paired vertical angles bolted to the beam wall and to the column flange. Based on the comparative analysis of the results of the numerical analysis and on the experimental data, the actual behaviour of the structure has been found and the stiffness of the joint type to be considered has been determined.

Аннотация. В строительстве многоэтажных зданий различного назначения широко применяются стальные каркасы. Узловые сопряжения ригелей с колоннами при практических расчетах рам принимаются либо абсолютно жесткими, либо шарнирными. Анализ действительной работы узловых соединений рам показывает, что они, как правило, занимают промежуточное положение в классификации узлов на «жесткие» и «шарнирные», то есть обладают некоторой податливостью. Такая податливость характеризуется различной степенью жесткости, зависящей от конкретного конструктивного решения узла. Поэтому во избежание возможно существенных ошибок в статических расчетах рам должны рассматриваться схемы с узлами, способными воспринимать соответствующую долю изгибающих моментов. В настоящей статье приводятся результаты экспериментально-теоретических исследований действительной работы податливых узлов сопряжения ригелей с колоннами с использованием вычислительного комплекса ABAQUS 6.13, позволяющего решать задачи методом конечных элементов с учетом геометрической и физической нелинейности. Рассматривается конструкция узла «ригель-колонна» с соединительными элементами в виде парных вертикальных уголков, прикрепляемых к стенке балки и полке колонны с помощью болтов. На основе сравнительного анализа результатов численного расчета и экспериментальных данных выявлена действительная работа конструкции и определена жесткость рассматриваемого типа узла.

Introduction

Metal frameworks of multistory buildings and facilities are represented a complex of structural elements connected in joints. The reliability of a facility in general is equally determined by the reliability of its separate load-carrying structural elements and the faultless work of their joint connections.

Local forces that are characterized by significant bearing reactions in the form of concentrated forces and bending moments occur in the places of connection between girders and columns in a framework building system under operational loads. Flowing from one element to another within small contact areas, those forces lead to uneven distribution of stress within the joint area, which causes

Туснина В.М. Податливые соединения стальных балок с колоннами // Инженерно-строительный журнал. 2017. № 5(73). С. 25–39.

development of excessive deformations, as well as occurrence and development of cracks, etc. That is an evidence of the fact that the girder-column connections are the most critical joints in the framework buildings [4, 5–7, 9, 12–14].

As of today, for practical calculation of frames in the framework building systems, the beam-to-column joints are normally taken as divided into the following two types: absolutely rigid and hinged. The results of experimental and theoretical research on the behaviour of beam-to-column connection joints in steel frameworks show that they have certain pliability that is characterized by different grades of stiffness affecting both the actual behaviour of the frame as a whole and the distribution of the metal in its main elements, columns and girders.

The results of both experimental and theoretical research of the actual behaviour of semi-rigid beam-column joints by both foreign and domestic scientists clearly demonstrate the influence of the stiffness of such connections on the load-bearing capacity of the columns. Thus, the academic papers state that the load-bearing capacity of the columns in the frames with semi-rigid joints are underestimated at the average of 40 % in comparison to the frames that have hinged beam-to-column connections. On the other hand, the load-bearing capacity of the columns in the frames that have semi-rigid joints might be unreasonably increased, if they are considered as rigid [10, 11, 14–16, 23, 24, 27, 35].

Semi-rigid beam-to-column connection joints in braced frameworks are sufficiently diverse in terms of design solution; however, they are all characterized by the presence of steel plate flexible elements that contribute to relatively free rotation of the beam within a joint when working under load. In addition, the connection elements show the development of plastic deformations, and the connected elements show a change in the stress and strain-state in comparison to rigid joints. It is particularly important to take into account the grade of stiffness of the beam-to-column joint connections in the structures working beyond the elastic limit.

It is obviously possible to receive a reliable picture of the stress-strain state of joints of frames in an elastic-plastic stage of work on the basis of the numerical methods of calculation which are widely used at design of buildings today. So the analysis of numerical researches of semi-rigid joints taking into account geometrical and physical nonlinearity is provided in works [1, 6, 17–20, 22, 25–34].

Taking into consideration the fact that the joint pliability depends on a considerable variety of factors conditioned by the peculiarities of the design solution of a beam-to-column connection, it is quite difficult to assess. However, many scientists have attempted to resolve this problem to a greater or lesser degree of proximity; based on the results of their experimental and theoretical research, it can be concluded that the main factor that determines the joint pliability is the deformation of the connection elements, which can be up to 80% of the total joint deformation and directly depends on its design solution. The rest of the deformations occurring in a semi-rigid beam-to-column connection, such as a bend of a column flange, section shear and column bend deformations within the joint area, etc., have practically no influence on its flexibility [7, 10, 11, 15, 23, 27, 35].

The foreign and domestic experience of design and construction of multistory buildings shows that the design solutions of beam-to-column connection joints with double angles are the most appropriate for braced frameworks due to their constructability and low metal consumption.

The purpose of this work was studying stress-strain state and destruction of bolted joint with double angles in an elastic-plastic stage of work on the basis of the comparative analysis of numerical calculation with use of the ABAQUS 6.13 [2] computer system and experimental data [35].

The objectives of the research included the following:

- assessment of the limit state of the structure;
- study of the distribution of internal forces within the joint areas of a frame fragment;
- identification of the locations of the highest stress concentration within a joint;
- analysis of the strain state of connection angles, beam and column;
- angle stiffness assessment.

Methods

The study of the stress-strain state considered type of joint was carried out on the example of the constructive decision with connecting elements in the form of the double angles bolted to the beam wall and to the column flange (Fig. 1) as an example.

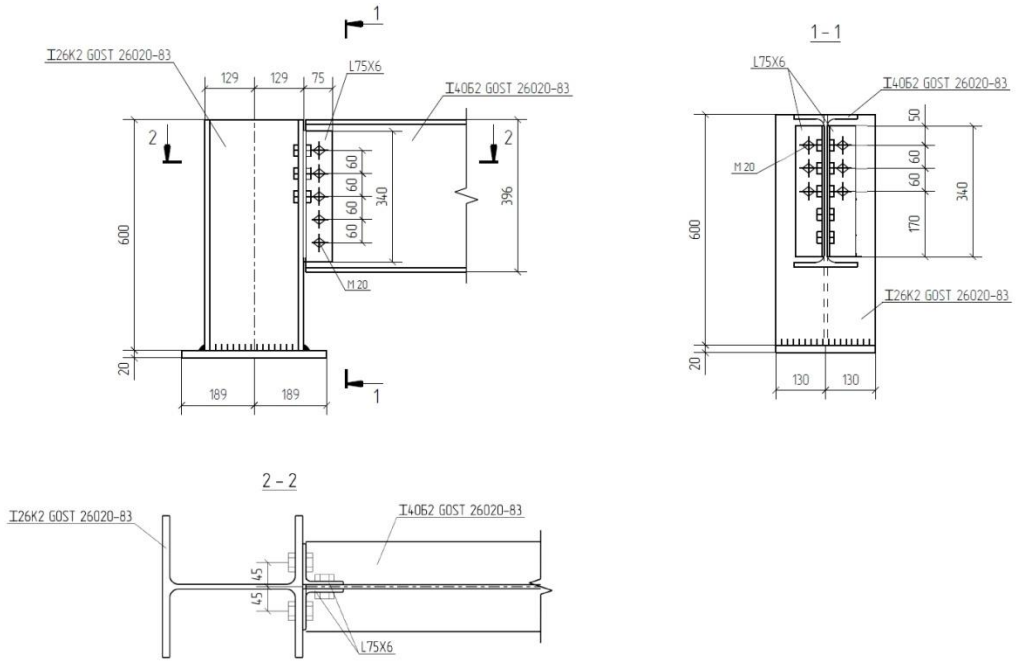

Figure 1. A design solution of a bolted joint with double vertical angles

To make the experimental model as close to the natural conditions as possible, it was made in the form of a U-shaped framework fragment with a beam made of a normal (Б type per Russian classification) wide-flanged I-beam and posts made of a column (К type per Russian classification) wide-flanged beams. Taking into consideration the fact that the influence of the column stiffness on the joint behaviour is insignificant, the fragment height was determined as possibly small. We took sufficient height of the beam section to allow significant angles of rotation and deflection. To increase the load and extend the stage of beam elastic work, the load was applied on span quarters (Fig. 2).

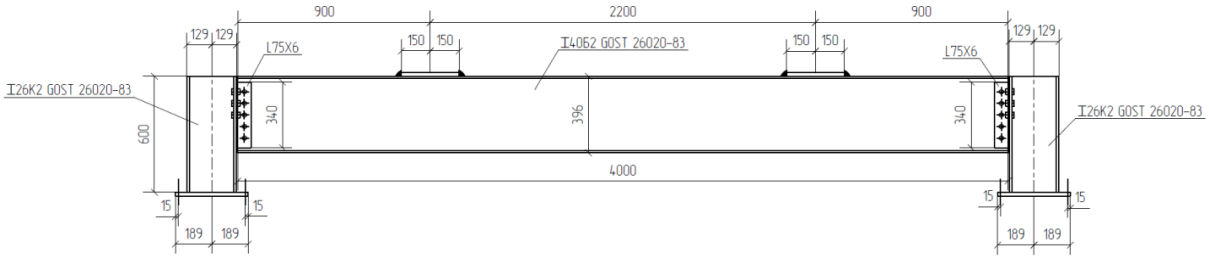

Figure 2. Scheme of the structure to be considered

Figure 3 shows a scheme of sample testing in a natural experiment, as well as a frame joint with measuring instruments.

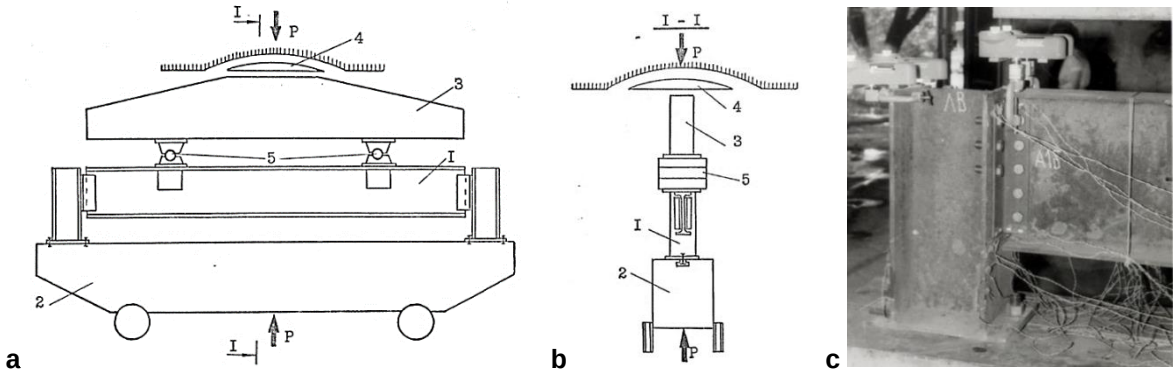

Figure 3. Static testing of a frame fragment
a – scheme of static testing of frame fragment; b – frame joint with measurement instruments; 1 – frame; 2 – large cart; 3 – cross-arm; 4 – press ball hinge; 5 – hinges

Туснина В.М. Податливые соединения стальных балок с колоннами // Инженерно-строительный журнал. 2017. № 5(73). С. 25–39.

The experiment was carried out using M20 normal precision bolts of strength grade 5.8 without pretension. Double vertical angels 75x6 (length 340 mm) were made of S345 low-alloy steel, and the beam (40Б2 profile) was made of S245 steel.

The numerical research was carried out using ABAQUS 6.13 computing complex, which allows to resolve the problems of the structural mechanics and the materials resistance applying the finite elements method. An explicit solver (Abaqus/Explicit) [2] was used to solve the problem considering the geometrical and physical nonlinearity and to compare the results to the experiment data [35].

According to the testing, the load was applied on two nodes located in the gravity centre of absolutely rigid bodies in a quasi-static manner during 10 seconds with a limit total value of 1000 kN.

The structural elements and the joint parts were made using a standard model (Plasticity), that allows to consider not only the physical nonlinearity and the descending unloading branch during the material's work beyond the elastic limit, but also the structure damage (Ductile Damage) when achieving the limit stress values typical for steel [3] in the joints elements.

The finite-element computing model was formed by volume octagonal finite elements (C3D8). The mesh was condensed using tetrahedrons (C3D10) in order to obtain a more precise picture of the stress state of the joints for the connection parts and the beam area adjacent to a joint. The mesh was performed under the condition of including no less than 2 elements based on the thickness of the parts.

Figure 4 shows the finite-element model.

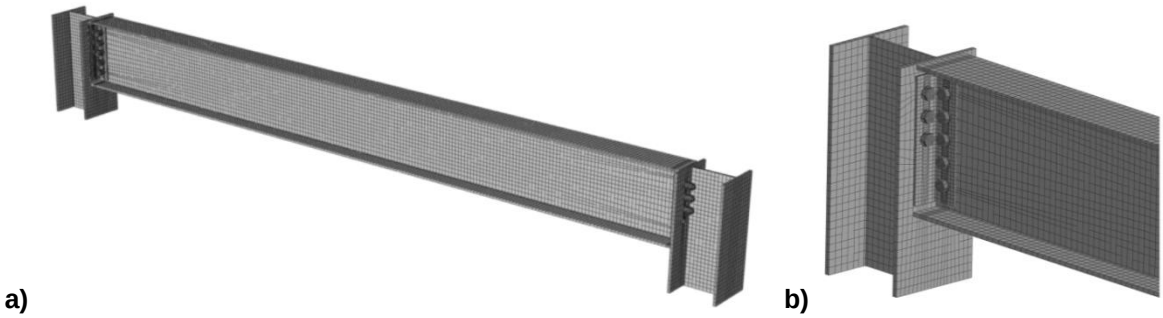

a) **b)**

Figure 4. Finite-element model:
a – general view of the frame; b – beam-to-column connection joint

Results and Discussion

It was established experimentally [35] that the exhaustion of the load-bearing capacity of the structure consisted in the loss of beam stability at the plastic stage of work of the flange in the simple bending area. In addition, local loss of flange stability was noted as well (Fig. 5b).

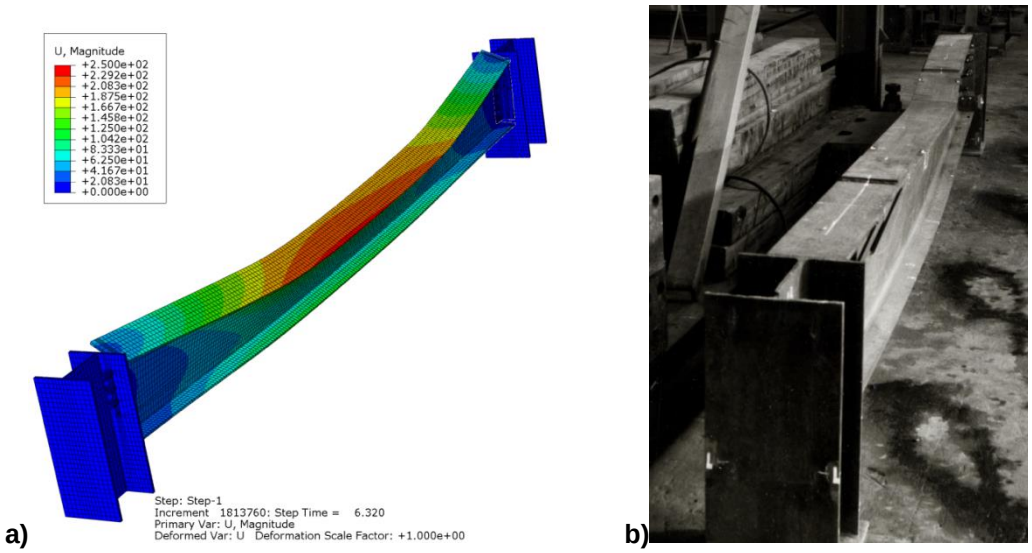

a) **b)**

Figure 5. Structure limit state:
a – numerical analysis; b – experiment

The numerical analysis confirmed the nature of damage of the tested structure established by the testing (Fig. 5a). The results of the numerical calculation showed that the beam transition into the elastic-plastic stage of work occurs at P = 500 kN; however, no structural damage occurs in this case, and the structure keeps working in case of further load increasing. This can be explained by the restraining effect of the neighbouring "rigid" areas on the development of deformations in the plastic areas. Joint damage in the form of angle rupture close to the back edge occurred at the load of P = 632 kN (Fig. 6).

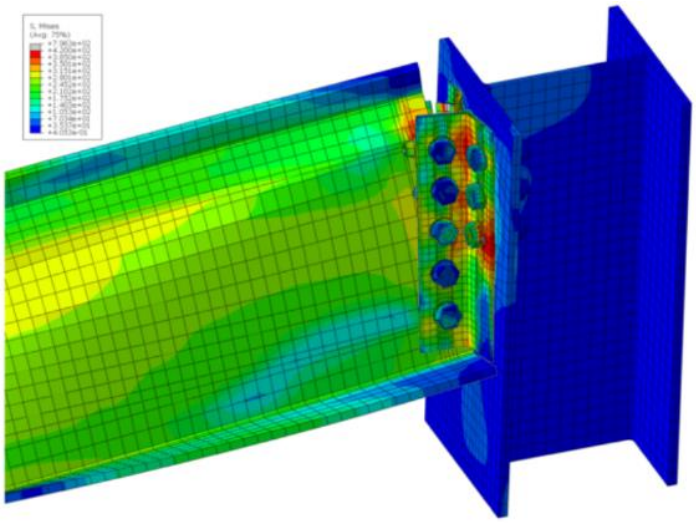

Figure 6. Joint damage at P=632 kN (Abaqus)

The general nature of the structure's work under load reflects the "load-deflection" dependence. The load deflection dependence graphs (fig. 7) obtained on the basis of the experiment [35] and numerical calculation data show that the elastic-plastic stage of work of the beam within the wide area of a simple bend occurs at the load of 500 kN, which is characterized by a sharp increase in the inclination angle at that moment.

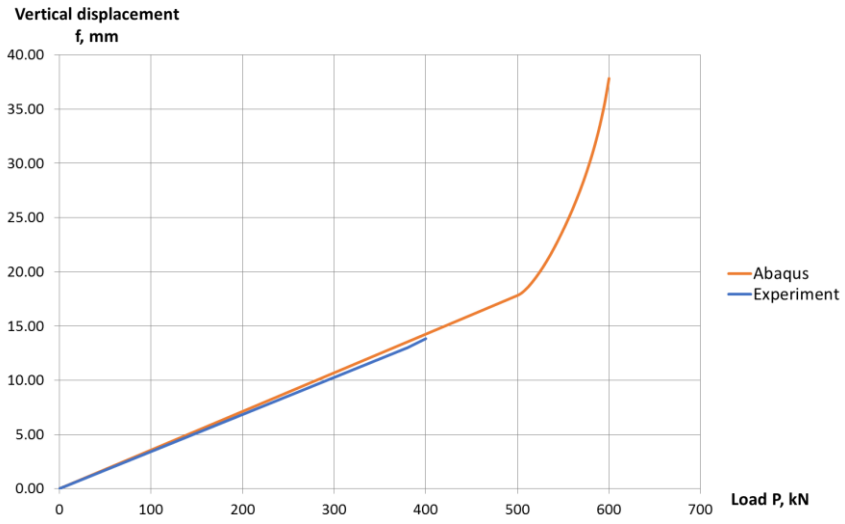

Figure 7. The "load-deflection" dependence graph

Туснина В.М. Податливые соединения стальных балок с колоннами // Инженерно-строительный журнал. 2017. № 5(73). С. 25–39.

There is no conflict between the numerical calculation and the experiment data [35], and the difference between the corresponding values does not exceed 4% (Table 1).

Table 1. The comparison of the vertical displacements of the beam middle point

Load *P*, kN	Vertical displacement of the beam middle point *f*, mm		Difference, %
	Abaqus	*Experiment*	
0	0	0	0
48	1.71	1.64	-3.99 %
100	3.56	3.42	-3.99 %
148	5.27	5.06	-3.99 %
200	7.13	6.84	-3.99 %
248	8.84	8.48	-3.99 %
300	10.69	10.26	-3.99 %
348	12.40	11.91	-3.99 %
400	14.25	13.83	-2.94 %
448	15.96	-	-
500	17.82	-	-

Figure 8 contains the graphs of dependence of the rotational angle of the beam support section on the load that were made based on the experimental data [35] and the numerical calculation results. Sufficient similarity is noted at the stage of elastic work of the joint. The figure shows that the numerical curve (Abaqus) has two typical break points corresponding to the load (P_{lim}) at which a plastic mechanism is formed within the connection angles, and to the load (P_T) at which the primary yield occurs in the area of a simple bending of the beam. At this moment, a plastic hinge is formed within the joint, and the nature of the "load-rotational angle" dependence changes, since the load-bearing joint loses the capacity of elastic restraint and the girder works in the frame system as a simply supported beam.

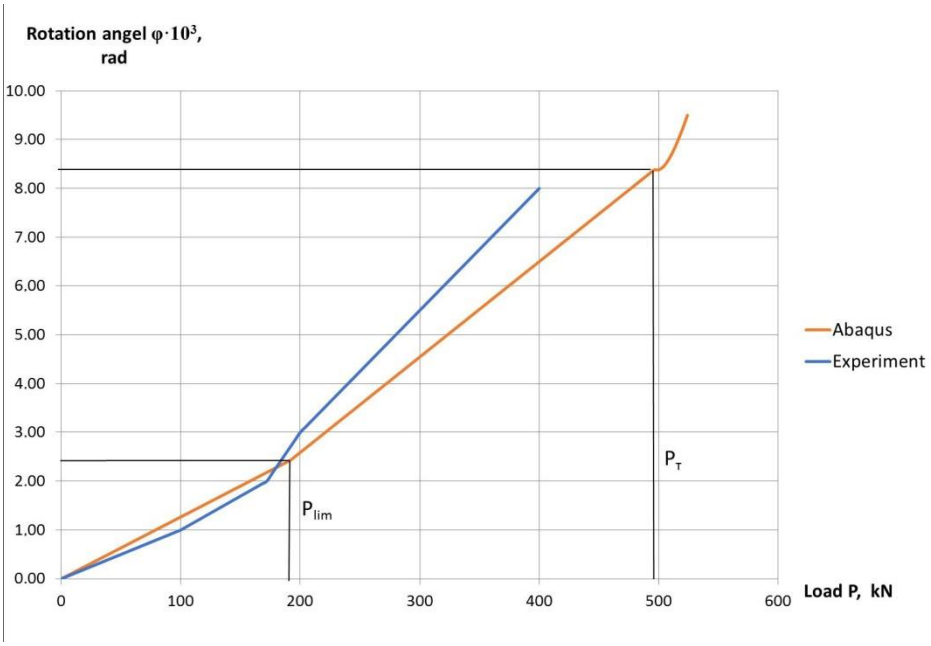

Figure 8. The graph of "load-rotation angle" dependence

Table 2. The comparison of the values of rotational angel of support cross-section

Load *P*, kN	Rotational angel of support cross-section $\varphi \cdot 10^3$, rad		Difference, %
	Abaqus	*Experiment*	
0	0	0	0
48	0.61	0.48	-21.09 %
100	1.27	1.00	-21.09 %
148	1.88	1.67	-11.14 %
200	2.59	3.00	13.68 %
248	3.53	4.20	15.99 %
300	4.55	5.50	17.36 %
348	5.48	6.70	18.15 %
400	6.50	8.00	18.74 %
448	7.44	-	-
500	8.38	-	-

Beside a significant bevelling (horizontal displacement of the angle back side in respect of the column flange), the deformations of the connection angles bolted to the beam and the column are characterized by a strong approximation of the back sides in the upper and their separation from each other in the lower part of the joint. In this case, the angles rotate within the plane of the column flange. This is explained by the fact that, beside the bending moment out of the plane of the "column" angle flange, there is a moment acting in the plane of the flange, rotating the connection angle. Therefore, a couple of forces acting in this area brings the angle back sides together in the upper part and separates them in the lower part. The deformations of the holes of the connected elements, which are inherent to bolted connections, contribute to that to a large extent. According to the testing results, the value of the limit bevelling of the angles amounted to 11 mm [35], and according to the results of the numerical calculation, it amounted to 7 mm.

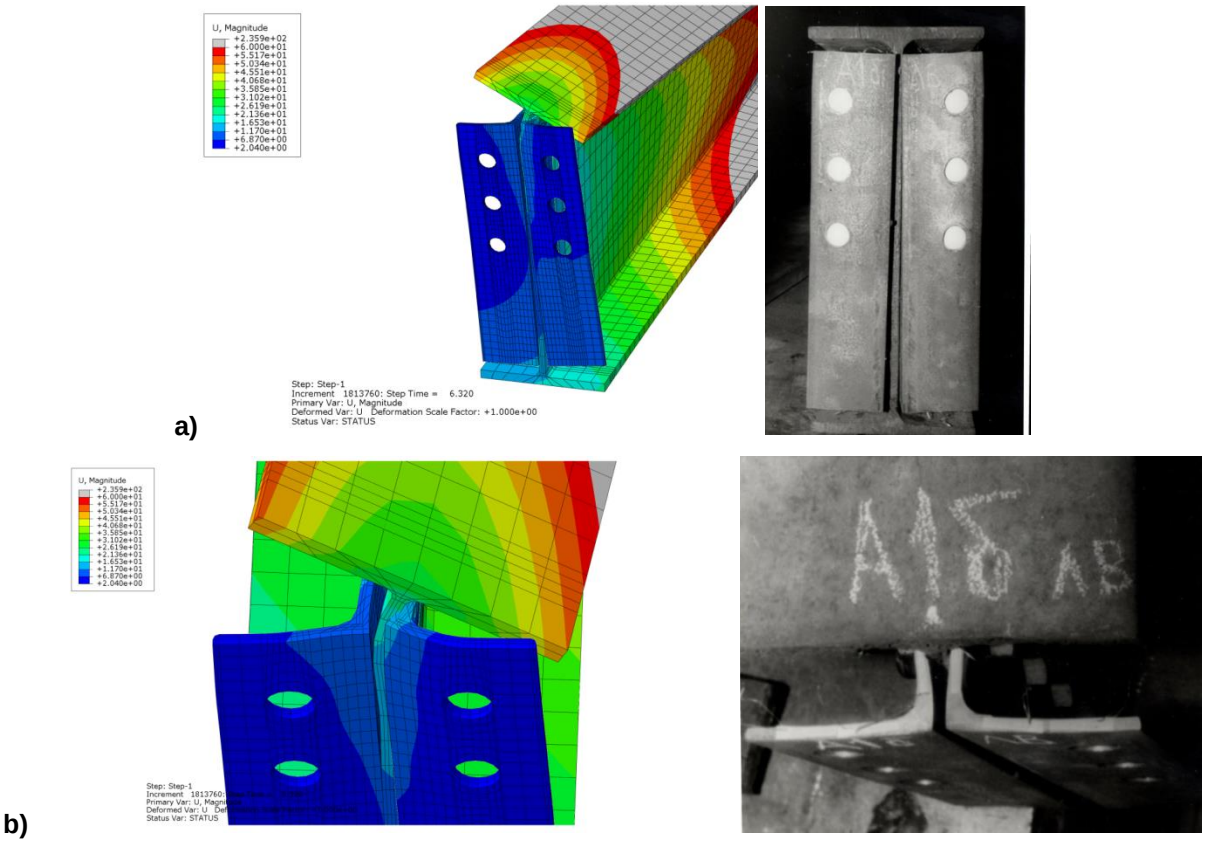

Figure 9. Strain state of joint elements:
a – strain state of angles (view of column flanges); b – strain state of angles (top view)

Туснина В.М. Податливые соединения стальных балок с колоннами // Инженерно-строительный журнал. 2017. № 5(73). С. 25–39.

The stress state of the tested structure is clearly demonstrated by the graphs of "load-span moment" dependence (Fig. 10). The linear dependence of the "load-span moment" curves can be seen up to the load of P = 500 kN. At this moment, the initial yield occurs in the simple bending area. In addition, the bending moment grows disproportionally to the load applied. Then, the beam's work reaches the next stage corresponding to the formation of an elastic hinge in the beam span section, when the span moment reaches its limit value and remains constant for some period until the exhaustion of the load-bearing capacity of the beam.

The pictures of the stress state of the beam at P = 500 kN in the form of isofields of normal and equivalent stresses obtained through a numerical calculation, as well as of the vertical displacement, are given on figures 11 and 12 respectively.

Table 3 contains the values of the span moment M_{sp} obtained both through a numerical analysis and experimentally [35], the difference between which does not exceed 6 %.

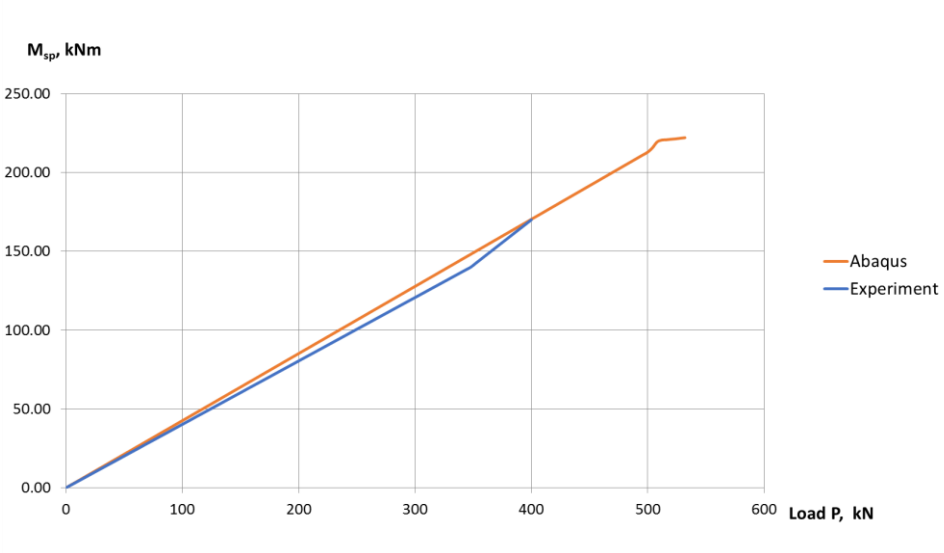

Figure 10. The graph of "span moment-load" dependence

Table 3. The comparison of the values of span moment

Load *P*, kN	Span moment M_{sp}, kNm		*Difference, %*
	Abaqus	*Experiment*	
0	0	0	0
48	20.44	19.31	-5.52%
100	42.58	40.23	-5.52%
148	63.02	59.54	-5.52%
200	85.16	80.46	-5.52%
248	105.60	99.77	-5.52%
300	127.74	120.69	-5.52%
348	148.18	140.00	-5.52%
400	170.32	170.00	-0.19%
448	190.76	-	-
500	212.91	-	-

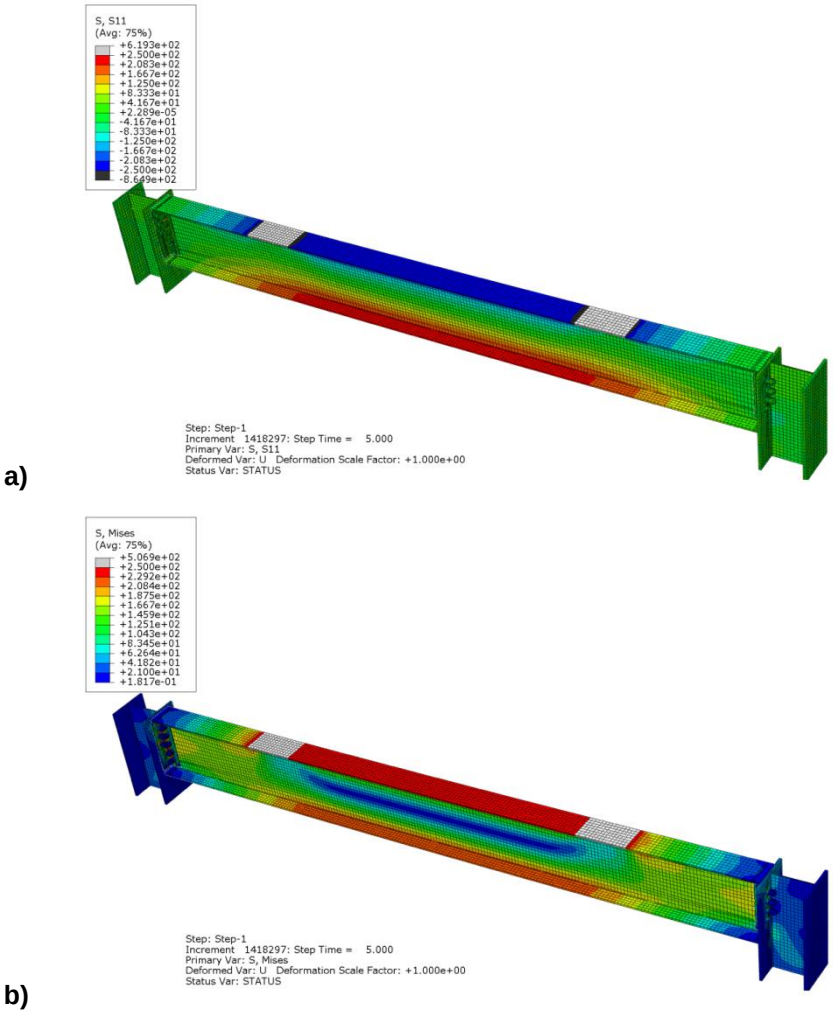

Figure 11. Stress state of the beam at P = 500 kN (numerical analysis): contour plots of normal (a) and equivalent (b) stresses within the beam (MPa)

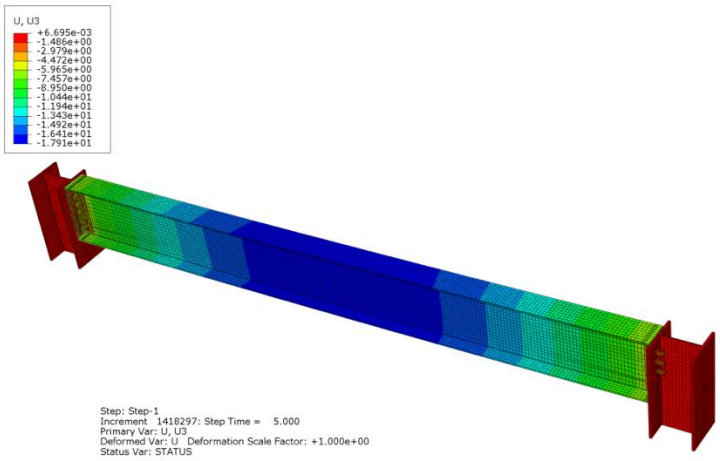

Figure 12. Vertical displacement (mm) of the beam at P = 500 kN (numerical analysis)

Numerical studies have revealed the general picture of the stress-state of connection angles and the adjacent column areas and beam (Figs.13, 14). The figures show that a strong bending nature of the stress-state is inherent to the "beam" flanges of angles. The horizontal stresses acting in the points along the diagonals of the "column" flanges of angles characterize the bending nature of deformation of these flanges from the plane with a restraint along the bolts axis and next to the angles curve.

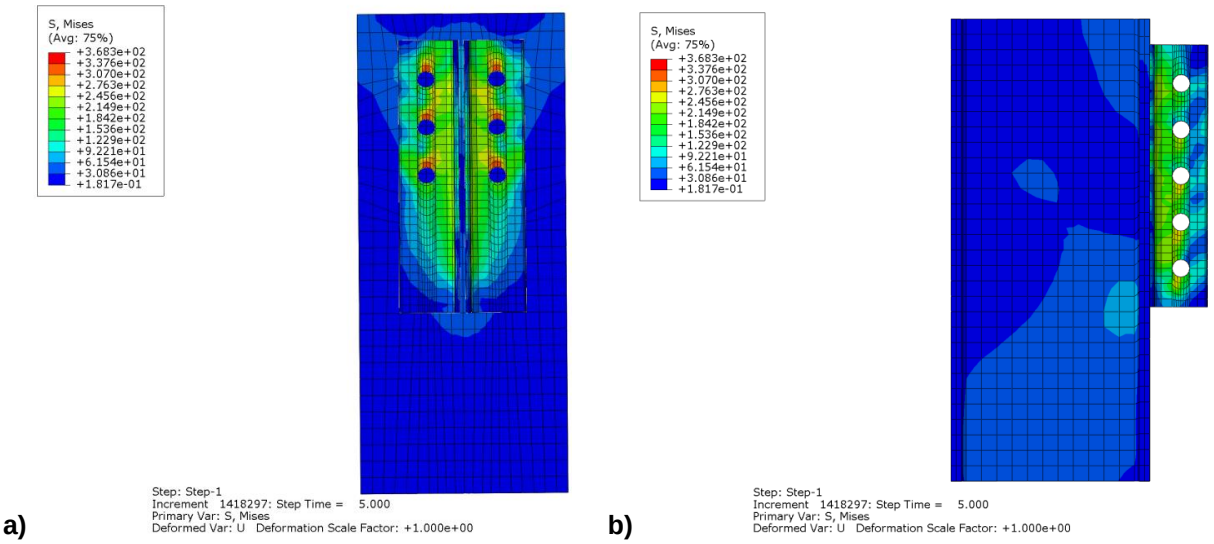

Figure 13. Stress state of the connection angles (numerical analysis): at P = 500 kN: a – "column" flanges; b – "beam" flanges

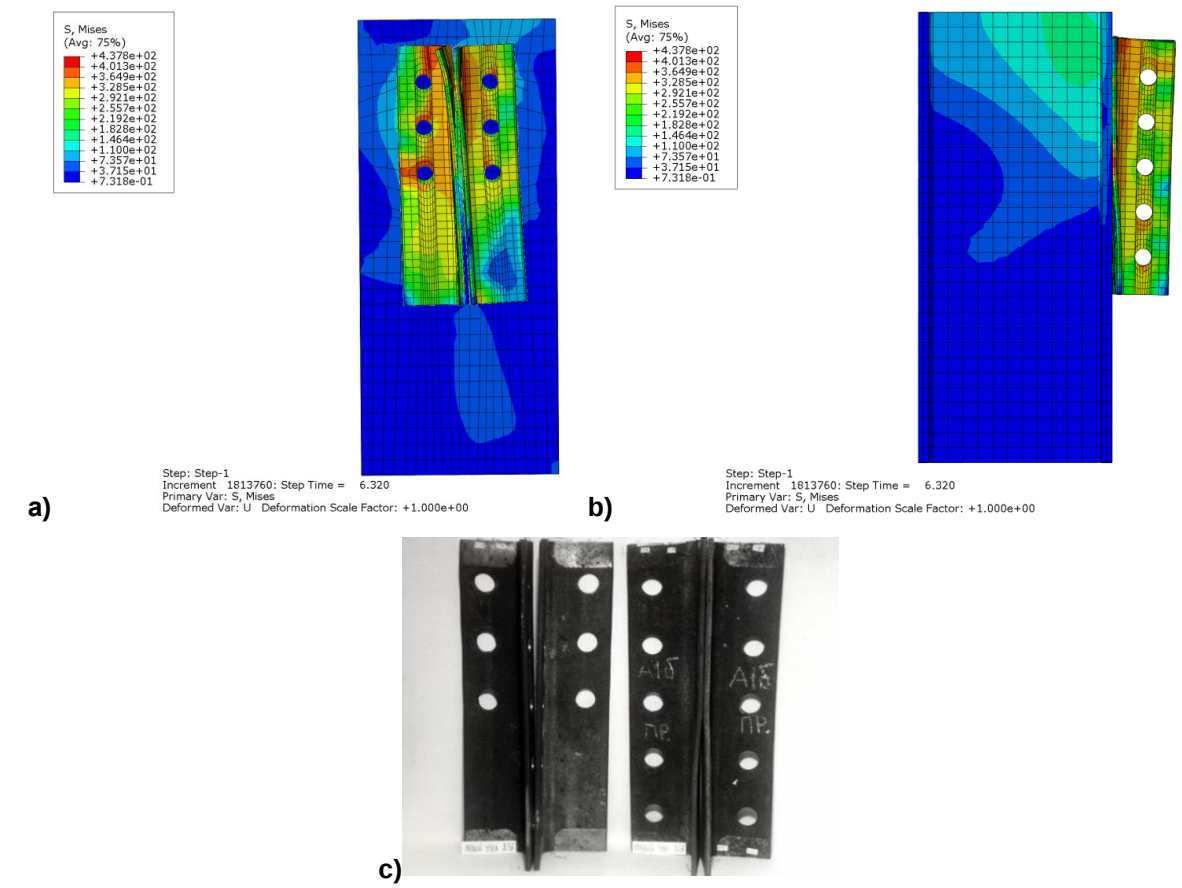

Figure 14. Stress state of the connection angles with damage of the following: a – "column" flanges (numerical analysis); b – "beam" flanges; c – "column" and "beam" flanges (experiment)

The structure of the beam-to-column bolted connection being considered has certain stiffness allowing the support moments to develop and be transferred to the column. The graphs of dependence of the support moment M_{sup} on the load made on the basis of the results of the numerical calculation and testing, are given on figure 15. The comparison of the results of the numerical analysis and the experiment [35] are given in Table 4.

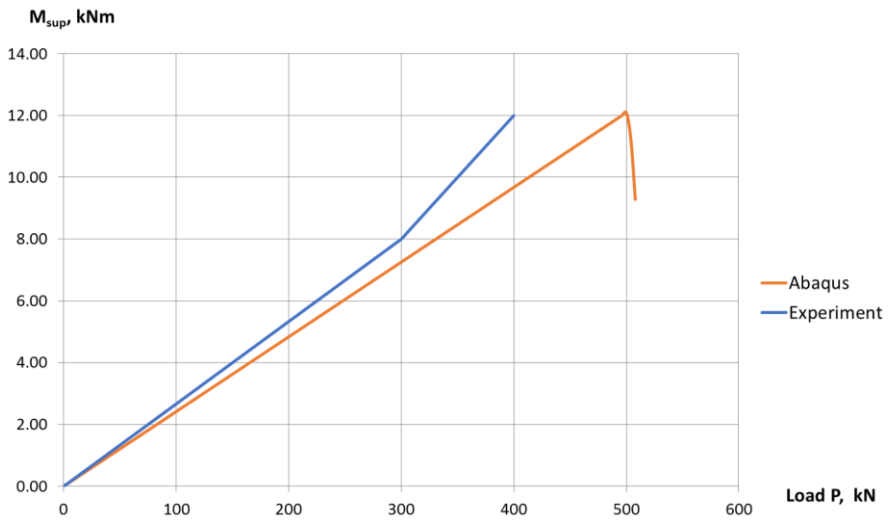

Figure 15. The graph of "support moment-load" dependence

Table 4. The comparison of the values of support moment

Load P, kN	Support moment M_{sup}, kNm		*Difference, %*	$k = \frac{M_{sup}}{M_{sup,theor}}$	
	Abaqus	*Experiment*		*Abaqus*	*Experiment*
0	0	0	0	-	-
48	1.16	1.28	9.29%	0.069	0.076
100	2.42	2.67	9.29%	0.069	0.076
148	3.58	3.95	9.29%	0.069	0.076
200	4.84	5.33	9.29%	0.069	0.076
248	6.00	6.61	9.29%	0.069	0.076
300	7.26	8.00	9.29%	0.069	0.076
348	8.42	9.92	15.14%	0.069	0.082
400	9.68	12.00	19.37%	0.069	0.086
448	10.84	14.40	24.74%	0.069	0.092
500	12.09	17.00	28.86%	0.069	0.097

The *C* factor of the beam restrain on support, which is equal to the relation of the support moment to the corresponding rotational angle of the beam end within the joint, is taken as the stiffness property of the semi-rigid frame joints:

$$C = \frac{M}{\varphi}, \quad (1)$$

where *M* is the bending moment acting on the support;

φ is the rotation angle of support cross-section of beam.

The qualitative analysis of the results of the numerical and experimental studies of the behaviour of a beam-to-column bolted joint connection with double vertical angles allowed us to determine the stiffness of the joint type being considered.

The graphs of "stiffness-load" dependence and the comparison of the numerical calculation and the testing results are given on figure 15 and in table 5 respectively.

It has been noted that the angle stiffness determined based on the experiment data exceeds the numerical one significantly at the initial stage of structure loading. However, the difference between their values is levelled and reaches the average of 15 % as the load increases.

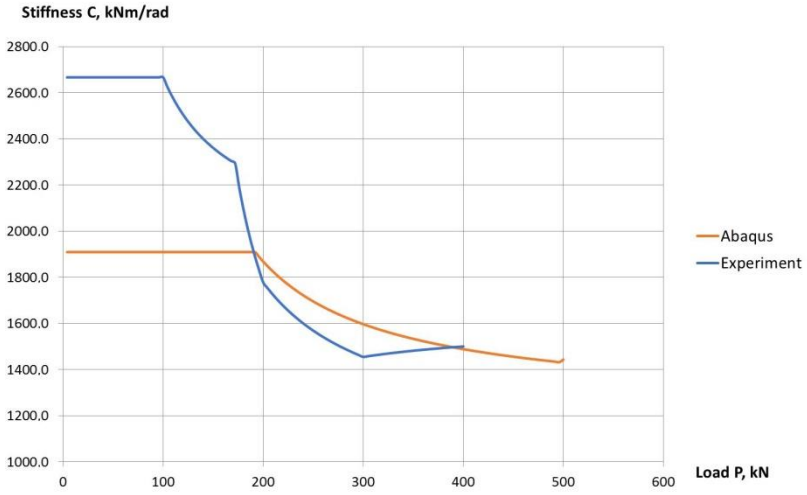

Figure 16. The graph of "stiffness-load" dependence

Table 5 The comparison of the joint stiffness

Load P, kN	Stiffness of the joint C, kNm/rad		*Difference, %*
	Abaqus	*Experiment*	
0	0	0	0
48	1,908.7	2,666.6	28.42%
100	1,908.7	2,666.6	28.42%
148	1,908.7	2,367.9	19.40%
200	1,868.1	1,777.7	-4.84%
248	1,700.2	1,574.6	-7.39%
300	1,596.6	1,454.5	-8.90%
348	1,535.0	1,480.6	-3.55%
400	1,488.4	1,500.0	0.77%
448	1,456.7	-	-
500	1,443.3	-	-

To verify the assessment of the pliability of the joint type being considered, the stiffness was determined using the methodology proposed by the authors of the paper [27], where the factor characterizing the beam restrain on support is calculated by the following formula:

$$k = \frac{M_{\text{sup}}}{M_{\text{sup},theor}}, \quad (2)$$

where M_{sup} is the bending moment acting on the support;

$M_{\text{sup, theor}}$ is the bending moment acting on the absolutely rigid support.

The values of the k factor obtained based on the testing and numerical calculation results are given in Table 4.

For approval of joint stiffness estimating, the coefficient of beam restraint on the support was calculated by the formula suggested in [35]:

$$C = \frac{3}{2E}\left(\frac{S}{th}\right)^3, \quad (3)$$

where E – elastic modulus of steel;

S – distance between butt of “column” flange of connecting angel and axes of bolts;

t – thickness of connecting angel;

g – height of connecting angel.

Stiffness of considered joint obtained by the kinematic theory of limit equilibrium method represented in [27] is 1789 kNm/rad. Stiffness was calculated in the moment of formation of “plastic” hinge in the “column” part of connecting angel when limit moment is acting in joint. This situation occurred in load about 200 kN, which is grafically demonstrated by rhe graphs of the “stiffness-load” dependences in Figure 16.

Conclusions

1. The picture of the stress-strain state and damage of semi-rigid joints of beam-to-column connection with double vertical angles is found.

2. It is established that the main factor determining the deformability of a joint is the deformation of the angles, which accounts for up to 87 % of the total deformation of the connection.

3. In the "column" flanges of connection angles, an early transition (at $P = 0.3\ P_{max}$) of the metal into the elastic-plastic stage with subsequent formation of linear plastic hinges in this area is noted.

4. The strain state of the connection angles is mainly characterized by a bend out of the plane of the flange attached to the column.

5. The design solution of the joints with vertical angles allows large angles of rotation of the beam support section, the value of which at the elastic stage of work achieves 75 % of the beam rotation angle under the condition of its simple support.

6. The assessment of the joint stiffness carried out allows to note that the structure with double vertical angles is able to support up to 8 % of the bending span moment within the beam.

In conclusion, it should be noted that the design solutions of the beam-to-column connection joints with double vertical angles, that are traditionally taken as hinged ones in the calculations of connection frameworks of multistory buildings, can be considered as semi-rigid joints supporting the corresponding support moment, the value of which depends on the peculiarities of their design solution, which is confirmed by the results of this research.

References

1. Vatin N., Bagautdinov R., Andreev K. Advanced method for semi-rigid joints design. *Applied Mechanics and Materials.* 2015. Vols. 725–726. Pp. 710–715.
2. *Abaqus Documentation*: Abaqus Analysis User's manual.
3. Silantyev A.S. Calculation of Strength of Oblique Sections of Flexural Reinforced Concrete Elements Using the Finite-Element Method in KE-Complexes Ansys and Abaqus. *Industrial and Civil Engineering.* 2012. No. 2. Pp. 71–74. (rus)
4. Li F.X., Xin B. Experimental research and finite element analysis on behavior of steel frame with semi-rigid connections. *Advanced Materials Research.* 2011. Vols. 168–170. Pp. 553–558.
5. Hu X.B., Yang Y.W., He G.J., Fan Y.L., Zhou P. A moment-shear story model for the design of steel frames with semi-rigid connections. *Applied Mechanics and Materials*. 2013. Vols. 256–259. Pp. 821–825.
6. Arul Jayachandran S., Marimuthu V., Prabha P., Sectharaman S., Pandian N. Investigation on the behaviour of semi-rigid endplate connections. *Advanced Steel Construction.* 2009. Vol. 5. No. 4. Pp. 432–451.
7. Frye M., Morris G., Glenn A. Analysis of flexibility connected steel frame. *Canadian Journal of Civil Engineering.* 1975. Vol. 2. Pp. 280–291.
8. Packer J., Morris G. A limit state design method for tension region of bolted beam column connections. *The Structural Engineer.* 1977. Vol. 55. No. 10. Pp. 446–458.
9. Morris G., Packer J. Beam-to-column connections in steel frames. *Canadian Journal of Civil Engineering.* 1987. Vol. 14. No. 1. Pp. 68–76.
10. Aggarwal A.K., Coates R.C. Strength criteria for bolted

Литература

1. Vatin N., Bagautdinov R., Andreev K. Advanced method for semi-rigid joints design // Applied Mechanics and Materials. 2015. Vols. 725–726. Pp. 710–715.
2. Abaqus Documentation: Abaqus Analysis User's manual.
3. Силантьев А.С. Расчет прочности наклонных сечений изгибаемых железобетонных элементов методом конечных элементов в КЭ-комплексах Ansys и Abaqus // Промышленное и гражданское строительство. 2012. № 2. С. 71–74.
4. Li F.X., Xin B. Experimental research and finite element analysis on behavior of steel frame with semi-rigid connections // Advanced Materials Research. 2011. Vols. 168–170. Pp. 553–558.
5. Hu X.B., Yang Y.W., He G.J., Fan Y.L., Zhou P. A moment-shear story model for the design of steel frames with semi-rigid connections // Applied Mechanics and Materials. 2013. Vols. 256–259. Pp. 821–825.
6. Arul Jayachandran S., Marimuthu V., Prabha P., Sectharaman S., Pandian N. Investigation on the behaviour of semi-rigid endplate connections // Advanced Steel Construction. 2009. Vol. 5. № 4. Pp. 432–451.
7. Frye M., Morris G., Glenn A. Analysis of flexibility connected steel frame // Canadian Journal of Civil Engineering. 1975. Vol. 2. Pp. 280–291.
8. Packer J., Morris G. A Limit State Design Method for Tension Region of Bolted Beam Column Connections // The Structural Engineer. 1977. Vol. 55. № 10. Pp. 446–458.
9. Morris G., Packer J. Beam-to-column connections in steel frames // Canadian Journal of Civil Engineering. 1987. Vol. 14. № 1. Pp. 68–76.

Туснина В.М. Податливые соединения стальных балок с колоннами // Инженерно-строительный журнал. 2017. № 5(73). С. 25–39.

beam-column Connections. *Journal of Construction Steel Research.* 1987. Vol. 7. No. 3. 213 p.

11. Lui E.M., Chen W.P. Analysis and behavior of flexibly-jointed frames. *Engineering Structures.* 1986. Vol. 8 Pp. 107–118.
12. Khart F., Khenn V., Zontag Kh. *Atlas stalnykh konstruktsiy. Mnogoetazhnyye zdaniya* [Atlas of steel structures. Multi-storey buildings]. M.: Stroyizdat, 1977. 351 p. (rus)
13. *Joints in Steel Construction: Simple Connection Publication* P212. 2002. 490 p.
14. Troitskiy P.N., Levitanskiy I.V. Opornyye soyedineniya razreznykh balok na vertikalnykh nakladkakh, privarivayemykh s stenke balki (uzly UNS) [The supporting joints of the split beams on vertical pads welded from the beam wall (UNS nodes)]. *Proyektirovaniye metallicheskikh konstruktsiy.* No. 4. Moscow: TsNIIproyektstalkonstruktsiya, 1970. 120 p. (rus)
15. Ananin M.Yu., Fomin N.I. Metod ucheta podatlivosti v uzlakh metallicheskikh konstruktsiy zdaniy [Method of accounting for compliance in the nodes of metal structures of buildings]. *Akademicheskiy vestnik URALNIIPROEKT RAASN.* 2010. No. 2. Pp. 72–74.
16. Nagao T., Tanaka T., Nanaba H. Performance of beam-column connections in steel structures. *13th World Conference on Earthquake Engineering.* Vancouver, B.C., Canada. 2004. Paper no. 1235.
17. Heinisuo M., Laine V., Lehtimaki E. Enlargement of the component method into 3D. *Proceedings of the Nordic Steel Construction Conference NSCC.* Malmo, Sweden. 2009. Pp. 430–437.
18. Heinisuo M., Laasonen M., Ronni H. Integration of joint design of steel structurres using product model. *Proceedings of the International Conference on Computing in Civil and Building Engineering ICCBE.* Nottingham. UK. 2010. Pp. 323–328.
19. Li G., Yu H., Fang C. Performance study on T-stub connected semi-rigid between rectangular tubular columns and H-shaped steel beams. *Frontiers of Structural and Civil Engineering.* 2013. Vol. 7. No. 3. Pp. 296–303.
20. Bzdawka K., Heinisuo M. Fin plate joint using component method of EN 1993-1-8. *Rakenteiden Mekaniikka (Journal of Structural mechanics).* 2010. Vol. 43. No. 1. Pp. 25–43.
21. Simoes da Silva L. Towards a consistent design approach for steel joints under generalized loading. *Journal of Constructional Steel Research.* 2008. Vol. 64. Pp. 1059–1075.
22. Simoes da Silva L., Girap Coelho A.M. An analytical evaluation of the response of steel joints under bending and axial force. *Computers and Structures.* 2001. Vol. 79. Pp. 873–881.
23. Ferdous W. Effect of beam-column joint stiffness on the design of beams. *23rd Australian Conference on the Mechanics of Structures and Materials.* 2014. Pp. 701–706.
24. Augustyn J., Kozlowski A. Teoretycsno-doswiadcsalna analisa sztywnosci I nosnosci wezla spawanego. *Insynieria I Budownictwo*. 1987. No. 5. Pp. 150–153.
25. Urbonas K., Daniunas A. Behaviour of semi-rigid steel beam-to-beam joints under bending and axial forces. *Journal of Constructional Steel Research.* 2006. Vol. 62. No. 12. Pp. 1244–1249.
26. Wang Q., Wang L., Jlang B., Li H., Liu Q.F. Finite element analysis of behavior in semi-rigid steel frames. *Advanced Materials Research.* 2011. Vols. 163–167. Pp. 102–105.
27. Tusnina O.A., Danilov A.I. The stiffness of rigid joints of beam with hollow section column. *Magazine of Civil Engineering*. 2016. No. 4. Pp. 40–51.
28. Bandyopadhyay M., Banik A. Numerical analysis of semi-rigid jointed steel frame using rotational springs. *International Conference on Structural Engineering and Mechanics* (ICSEM). 2013.

10. Aggarwal A.K., Coates R.C. Strength criteria for bolted beam-column connections // Journal of Construction Steel Research. 1987. Vol. 7. № 3. 213 p.
11. Lui E.M., Chen W.P. Analysis and behavior of flexibly-jointed frames // Engineering Structures.1986. Vol. 8 Pp. 107–118.
12. Харт Ф., Хенн В., Зонтаг Х. Атлас стальных конструкций. Многоэтажные здания. М.: Стройиздат, 1977. 351 с.
13. Joints in Steel Construction: Simple Connection Publication P212. 2002. 490 p.
14. Троицкий П.Н., Левитанский И.В. Опорные соединения разрезных балок на вертикальных накладках, привариваемых с стенке балки (узлы УНС) // Проектирование металлических конструкций. № 4. М.: ЦНИИпроектстальконструкция, 1970. 120 с.
15. Ананьин М.Ю., Фомин Н.И. Метод учета податливости в узлах металлических конструкций зданий // Академический вестник УРАЛНИИПРОЕКТ РААСН. 2010. № 2. С. 72–74.
16. Nagao T., Tanaka T., Nanaba H. Performance of beam-column connections in steel structures // 13th World Conference on Earthquake Engineering. Vancouver, B.C., Canada. 2004. Paper № 1235.
17. Heinisuo M., Laine V., Lehtimaki E. Enlargement of the component method into 3D // Proceedings of the Nordic Steel Construction Conference NSCC. Malmo, Sweden. 2009. Pp. 430–437.
18. Heinisuo M., Laasonen M., Ronni H. Integration of joint design of steel structurres using product model // Proceedings of the International Conference on Computing in Civil and Building Engineering ICCBE. Nottingham. UK. 2010. Pp. 323–328.
19. Li G., Yu H., Fang C. Performance study on T-stub connected semi-rigid between rectangular tubular columns and H-shaped steel beams // Frontiers of Structural and Civil Engineering. 2013. Vol. 7. № 3. Pp. 296–303.
20. Bzdawka K., Heinisuo M. Fin plate joint using component method of EN 1993-1-8 // Rakenteiden Mekaniikka (Journal of Structural mechanics). 2010. Vol. 43. № 1. Pp. 25–43.
21. Simoes da Silva L. Towards a consistent design approach for steel joints under generalized loading // Journal of Constructional Steel Research. 2008. Vol. 64. Pp. 1059–1075.
22. Simoes da Silva L., Girap Coelho A.M. An analytical evaluation of the response of steel joints under bending and axial force // Computers and Structures. 2001. Vol. 79. Pp. 873–881.
23. Ferdous W. Effect of beam-column joint stiffness on the design of beams // 23rd Australian Conference on the Mechanics of Structures and Materials. 2014. Pp. 701–706.
24. Augustyn J., Kozlowski A. Teoretycsno-doswiadcsalna analisa sztywnosci I nosnosci wezla spawanego // Insynieria I Budownictwo. 1987. № 5. Pp. 150–153.
25. Urbonas K., Daniunas A. Behaviour of semi-rigid steel beam-to-beam joints under bending and axial forces // Journal of Constructional Steel Research. 2006. Vol. 62. № 12. Pp. 1244–1249.
26. Wang Q., Wang L., Jlang B., Li H., Liu Q.F. Finite element analysis of behavior in semi-rigid steel frames // Advanced Materials Research. 2011. Vols. 163–167. Pp. 102–105.
27. Туснина О.А. Данилов А.И. Жесткость рамных узлов сопряжения ригеля с колонной коробчатого сечения // Инженерно-строительный журнал. 2016. № 4. С. 40–51. (англ.)
28. Bandyopadhyay M., Banik A. Numerical analysis of semi-rigid jointed steel frame using rotational springs // International conference on structural engineering and mechanics (ICSEM). 2013.
29. Nogueiro P., Simoes Da Silva L., Bento R., Simoes R.

Tusnina V.M. Semi-rigid steel beam-to-column connections. *Magazine of Civil Engineering*. 2017. No. 5. Pp. 25–39. doi: 10.18720/MCE.73.3.

29. Nogueiro P., Simoes Da Silva L., Bento R., Simoes R. Experimental behavior of standardized European end-plate under arbitrary cyclic loading. *Proceedings of SDSS 06-International Colloquium on Stability and Ductility of Steel Structures.* 2006.
30. Liu M., Burns S.A. Multiple fully stressed designs of steel frame structures with semi-rigid connections. *International Journal for Numerical Methods in Engineering.* 2003. Vol. 58. No. 6. Pp. 821–838.
31. Degertekin S.O., Hayalioglu M.S. Design of non-liner semi-rigid steel frames with semi-rigid column bases. *Electronic Journal of Structural Engineering.* 2004. Vol. 4. Pp. 1–16.
32. Lee S.S., Moon T.S. Moment-rotation model of semi-rigid connections with angles. *Engineering Structures.* 2002. Vol. 24. Pp. 227–237.
33. Liu J., Huang X.Y., Hao J.P., Zhou G.G., Pehg D.F. A second-order inelastic analytical method on semi-rigid connections steel frame. *Advanced Materials Research.* 2011. Vols. 163–167. Pp. 760–765.
34. Bandyopadhyay M., Banik A.K., Datta T.K. Numerical modeling of compound element for static inelastic analysis of steel frames with semi-rigid connections. *Advances in Structural Engineering.* 2015. Vol. 3. Pp. 543–558.
35. Tusnina V.M. *Nesushchaya sposobnost i deformativnost podatlivykh uzlov stalnykh karkasov mnogoetazhnykh zdaniy.* Diss. kand. tekhn. nauk 05.23.01 [Bearing capacity and deformability of compliant knots of steel frames of multi-storey buildings. PhD Thesis] / Tusnina Valentina Matveyevna. Moscow, 1989. 166 p.

Experimental behavior of standardized European end-plate under arbitrary cyclic loading // Proceedings of SDSS 06-International Colloquium on Stability and Ductility of Steel Structures. 2006.
30. Liu M., Burns S.A. Multiple fully stressed designs of steel frame structures with semi-rigid connections // International Journal for Numerical Methods in Engineering. 2003. Vol. 58. № 6. Pp. 821–838.
31. Degertekin S.O., Hayalioglu M.S. Design of non-liner semi-rigid steel frames with semi-rigid column bases // Electronic Journal of Structural Engineering. 2004. Vol. 4. Pp. 1–16.
32. Lee S.S., Moon T.S. Moment-rotation model of semi-rigid connections with angles // Engineering Structures. 2002. Vol. 24. Pp. 227–237.
33. Liu J., Huang X.Y., Hao J.P., Zhou G.G., Pehg D.F. A second-order inelastic analytical method on semi-rigid connections steel frame // Advanced Materials Research. 2011. Vols. 163–167. Pp. 760–765.
34. Bandyopadhyay M., Banik A.K., Datta T.K. Numerical modeling of compound element for static inelastic analysis of steel frames with semi-rigid connections // Advances in Structural Engineering. 2015. Vol. 3. Pp. 543–558.
35. Туснина В.М. Несущая способность и деформативность податливых узлов стальных каркасов многоэтажных зданий. Дисс. канд. техн. наук 05.23.01 / Туснина Валентина Матвеевна. М., 1989. 166 с.

Valentina Tusnina,
+7(916)5107224; valmalaz@mail.ru

Валентина Матвеевна Туснина,
+7(916)5107224; эл. почта: valmalaz@mail.ru

Туснина В.М. Податливые соединения стальных балок с колоннами // Инженерно-строительный журнал. 2017. № 5(73). С. 25–39.

doi: 10.18720/MCE.73.4

Effect of rustication joints on air mode in ventilated facade

Влияние рустов на воздушный режим в вентилируемом фасаде

M.R. Petritchenko,
S.A. Subbotina,
F.F. Khairutdinova,
E.V. Reich,
D.V. Nemova,
V.Ya. Olshevskiy,
V.V. Sergeev,
Peter the Great St. Petersburg Polytechnic University, St. Petersburg, Russia

Д-р техн. наук, заведующий кафедрой М.Р. Петриченко,
студент С.А. Субботина,
студент Ф.Ф. Хайрутдинова,
студент Е.В. Рейх,
канд. техн. наук, доцент, директор центра Д.В. Немова,
аспирант В.Я. Ольшевский,
д-р техн. наук, доцент, член-корреспондент РАН, проректор по научной работе В.В. Сергеев,
Санкт-Петербургский политехнический университет Петра Великого, г. Санкт-Петербург, Россия

Key words: ventilated facade; enclosing structure; heat-gravitational motion; average velocity; ventilated air gap; energy efficiency

Ключевые слова: вентилируемый фасад; ограждающие конструкции; термогравитационное движение воздуха; средняя скорость; воздушный зазор; энергоэффективность

Abstract. Ventilated facade is a contemporary facade system that is popular due to its energy efficiency. There are different configurations of the façade systems, among other things, various spacing between rustication joints. Cold air penetrates through them, thereby, influences air circulation. In this paper, theoretical estimate of air flow data is carried out by applying Boussinesq's hydrostatic model. Research of an impact of rustication joints interval on air flow data via physical simulation is performed for different façade configurations. Based on the results obtained, the most optimal solution is the design of a ventilated facade without rustication joints, or with the largest joints interval value.

Аннотация. Двойные вентилируемые фасады – это современные фасадные системы, ставшие популярными благодаря своей энергоэффективности. Существуют различные конфигурации данных систем, в том числе могут варьироваться расстояния между рустами. Проникая через них, холодный воздух оказывает влияние на циркуляцию воздуха. В статье представлен теоретический расчет парамаетров воздушного потока с помощью гидростатической модели Буссинеска. Также для различных конфигураций фасада проведено физическое моделирование для оценки влияния расстояния между рустами на параметры воздушного потока. Основываясь на полученных результатах, можно сказать, что оптимальным конструктивным решением вентилируемого фасада является отсутствие рустов, либо максимальное расстояние между ними.

Introduction

Nowadays ventilated facades (VF) are widely used due to their energy efficiency excellence in comparison with other enclosing structures. VF is a multilayer structure, consisted of wall itself, insulation layer, air gap and cladding, bonded with metal framing. This structure diminishes heat loss of the building, therefore increasing its energy efficiency. One of the basic work principle of the ventilated facades is excess moisture removal from the insulation. This effect occurs due to air gap, where heated air along the hot surface come to the output of the structure.

Petritchenko M.R., Subbotina S.A., Khairutdinova F.F., Reich E.V., Nemova D.V., Olshevskiy V.Ya., Sergeev V.V. Effect of rustication joints on air mode in ventilated facade. *Magazine of Civil Engineering*. 2017. No. 5. Pp. 40–48. doi: 10.18720/MCE.73.4.

There are openings between tiles of the cladding in real structures of the VF – rustication joints. Cold air penetrates through these openings. Nowadays impact of rustication joints on air mode is under investigated, in spite of the fact that presence of rustication joints may cause air circulation change.

Analysis of ventilated facades has started recently. Fundamental understanding of the work's principles is of importance for proper operation of the façade and energy efficiency maximizing. Thereby, a lot of scientists research these constructions [2–3, 6, 15–18]. Several researches are focused on the influence of various factors on the operation of ventilated facades [7–8; 19–20]. Also, since ventilated facades are an energy-efficient design, they had been used in smart buildings [10–14].

Feasibility study on a usage of numerical model for analyzing the performance of VF was carried out by F. Peci Lópeza, R.L. Jensenb, P. Heiselbergb, M. Ruiz de Adana Santiagoa [1]. They have performed numerical and physical simulation of natural ventilation inside the façade and approved usage of numerical model subject to certain parameters.

Nizovtsev M.I., Belyi V.T., Sterlygov A.N. [5] have carried out a numerical simulation of thermal resistances of heat-insulating panels. Basing on calculations, they suggested facades, thermally insulated with ventilated channels, for providing low moisture content and good heat-insulating properties of the walls.

In modern construction using of ventilated facades as an enclosure structure has increased. This type of systems is characterized by high heat-shielding properties in comparison with other popular types of walling. Consequently, the question of the optimal ventilated facades construction becomes relevant.

The aim of this study is an experimental evaluation of the impact of rustication joints interval on velocity in the air gap of ventilated façade. To accomplish this aim, such challenges should be figured out:

1. To perform theoretical estimate of airflow data in the vertical channel.
2. To perform physical simulation of heat-gravitational motion in the air gap in different cases of rustication joints interval value.
3. To suggest recommendations for choosing the appropriate spacing between rustication joints.

Theoretical estimate

There are different cladding types of the ventilated facades:

- porcelain stoneware;
- composite tiles;
- aluminum tiles;
- fiber cement tiles;
- terracotta tiles and others.

Most commonly, spacing (rustication joints) between tiles take place in every type of cladding. Firstly, rustication joints are necessary for reasons of design – for thermal distortion compensation. It helps to prevent crack initiation at the façade. However, rustication joints can markedly affect on airflow data in the vertical channel.

The most significant flow characteristic for determination of façade's energy efficiency is an average velocity. In case of heat-gravitational air mode average velocity can be estimated by applying Boussinesq's hydrostatic model [4]:

$$v = \varphi \sqrt{\frac{T_h - T_c}{T_h}} \sqrt{2gL}\,, \qquad (1)$$

where: φ – velocity coefficient,

T_h – temperature of the heated surface,

T_c – temperature of the cold surface,

L – length of the air gap.

$$\varphi = \frac{1}{\sqrt{1+\lambda\frac{L}{h}+\zeta}}, \quad (2)$$

where: λ – pipe friction number,

ζ – coefficient of local head loss.

For the narrow channels: h – width of the air gap.

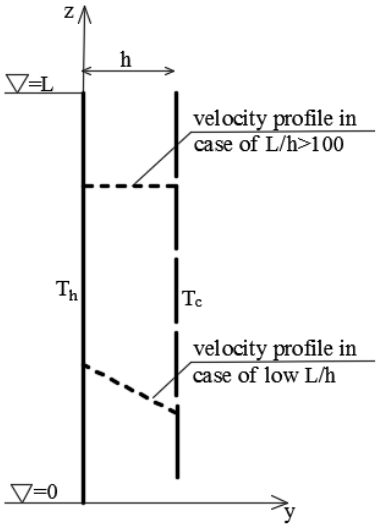

Figure 1. Spacing parameters and velocity

Wide channels perform as a vertical plane in unlimited space. That is why for calculation of the head loss it is relevant to substitute h with the boundary layer thickness of buoyant force δ. Channel is considered to be narrow if h/δ=O(1). In case of h>>δ, channel is wide, and boundary layer does not fulfill the width of the channel.

Basing on Eckert's theory:

$$\delta = \sqrt[4]{\frac{4\nu^2 z}{g}} \le \sqrt[4]{\frac{4\nu^2 L}{g}}, \quad (3)$$

where: ν – gas viscosity,

z –vertical coordinate, z≤L

Therefore, φ can be calculated by the following formula:

$$\varphi = \frac{1}{\sqrt{1+\lambda\frac{L}{\delta}+\zeta}}, \quad (4)$$

For the air gap with rustication joints, open input and output in case of low value of L/h velocity attains its maximum alongside the hot surface. Approximating to the cold surface, velocity value decreases (Fig.1.) In case of L/h>100 velocity profile straightens over the width of the channel.

Physical simulation

Heat-gravitational motion can be simulated on the physical model of the vertical air gap, that is represented an installation with height of 2050 mm and width of 600 mm, and air gap varying from 20 to 300 mm. One of the sides of the installation is fixed, faced with the aluminum sheets and has 3 heat sources (3 heating elements, with 1 kW of power per unit) for imitation of uniformly heated building's wall. Second side is simulating cladding, and it is unheated and movable. It allows varying the width of air gap.

Petritchenko M.R., Subbotina S.A., Khairutdinova F.F., Reich E.V., Nemova D.V., Olshevskiy V.Ya., Sergeev V.V. Effect of rustication joints on air mode in ventilated facade. *Magazine of Civil Engineering*. 2017. No. 5. Pp. 40–48. doi: 10.18720/MCE.73.4.

This side consists of wooden sheets with the height of 300 mm, divided by the spacing of 5 mm, simulating rustication joints.

To change spacing between rustication joints, some of them are sealed. Air access from beneath can be modified via special attachments, air outlet from the top is free. Visual appearance of the installation is presented below (Fig.2).

Figure 2. Installation for physical simulation

Series of experiments for studying impact of rustication joints interval on airflow data was carried out in different configurations:

1. Absence of rustication joints – all joints are sealed (imitation of the ideal channel);
2. Value of the interval is equal to 0.6 m – some rustication joints are sealed;
3. Value of the interval is equal to 0.3 m – all rustication joints are opened for air access.

Installation diagram is shown. (Fig.3.)

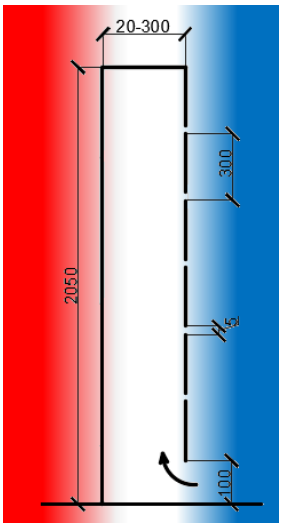

Figure 3. Installation diagram

In the first case width of the gap was constant and was equal to 100 mm for every configuration. Velocity was measured at different height marks.

In the second case air gap width was varying from 20 to 300 mm and all measures were taken at one height mark.

For all cases:

- Height of the air layer was constant and equal to 2050 mm;
- Fixed side was uniformly heated over the length;

- Air access from beneath is provided by the gap of 100 mm – open input.

All experiment were carried out with the use of thermal anemometer (Fig.4). Thermal anemometer is designed for measurement of temperature and velocity of an air flow. Operation principle is based upon the measurement of characteristics of platinum actuators.

Figure 4. Thermal anemometer

Device's minimum velocity in the range of measurement is equal to 0.1 m/s, instrumental uncertainty: for velocity ± 5 %, for temperature ± 0.2 °C.

Temperature in the lab was equal 21.9 °C, temperature of the heated surface was equal to 43.6 °C.

Average velocity of the air flow was measured in the vertical channel for every case and configuration of the installation, and was in the range of 0–0.5 m/s.

Variables for data processing were:

- Vertical coordinate Z and average velocity v;
- The ratio L/h and Froude number $v/(gL)^{0,5}$.

By means of calculated dependences, that were presented above, it is possible to calculate velocity φ and local head loss ξ coefficients. Pipe friction coefficient λ for the ideal channel was also calculated.

Results

Obtained results for the first case are presented in the Figure 5, for the second case – in the Figures 6–10.

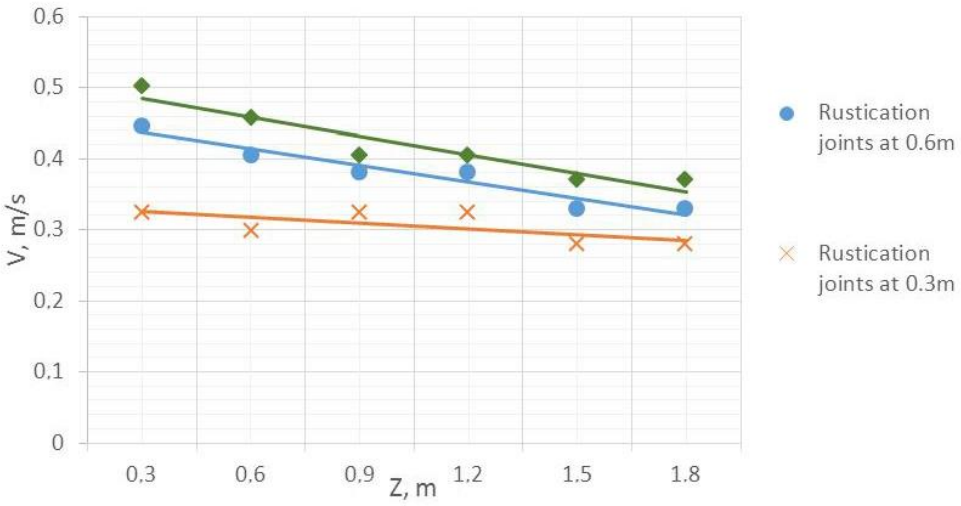

Figure 5. Velocity distribution on vertical coordinate Z

Petritchenko M.R., Subbotina S.A., Khairutdinova F.F., Reich E.V., Nemova D.V., Olshevskiy V.Ya., Sergeev V.V. Effect of rustication joints on air mode in ventilated facade. *Magazine of Civil Engineering*. 2017. No. 5. Pp. 40–48. doi: 10.18720/MCE.73.4.

In Figure 5 it can be seen that velocity of the air flow attains its maximum in the ideal channel, whose movable side is continuous (absence of rustication joints). In case of presented rustication joints with the interval value equal to 0.6 m air velocity decreases in average at 9 %. Rustication joints at 0.3 m diminish velocity at 19 % more. Velocity contrast is well demonstrated at low height marks.

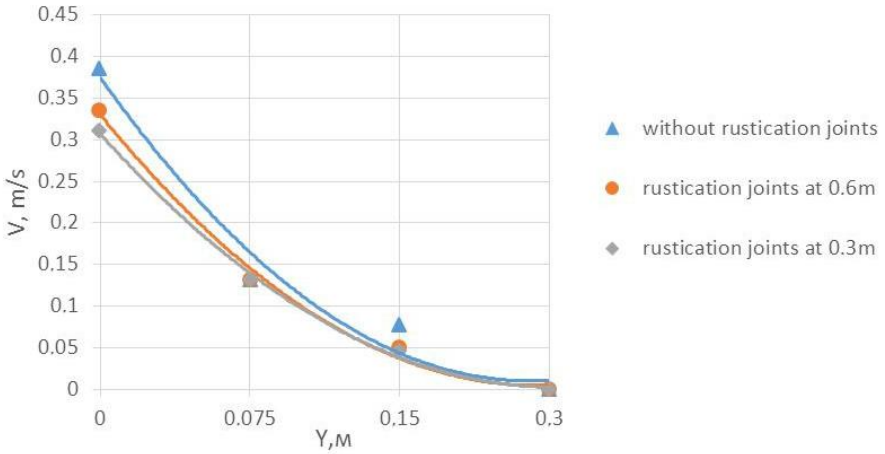

Figure 6. Velocity profile across the width of the air gap at 0.3 m

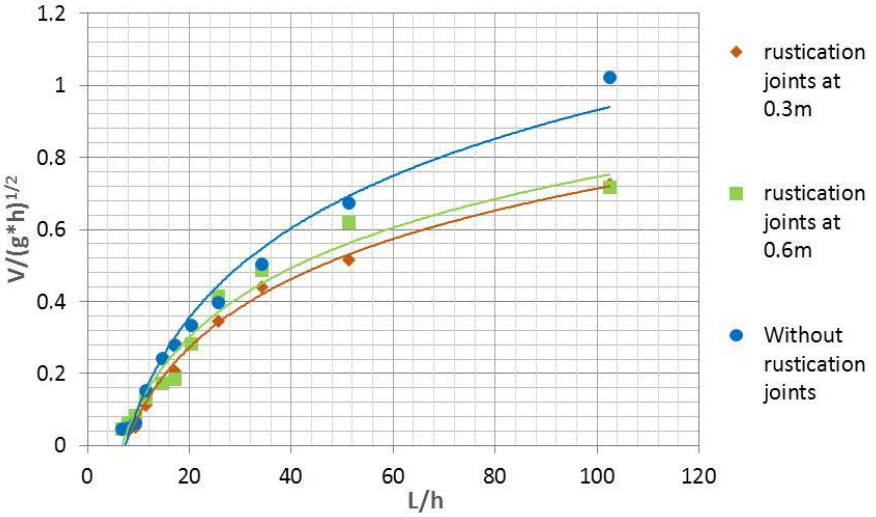

Figure 7. Dependence of Froude number on geometric parameters of the air gap

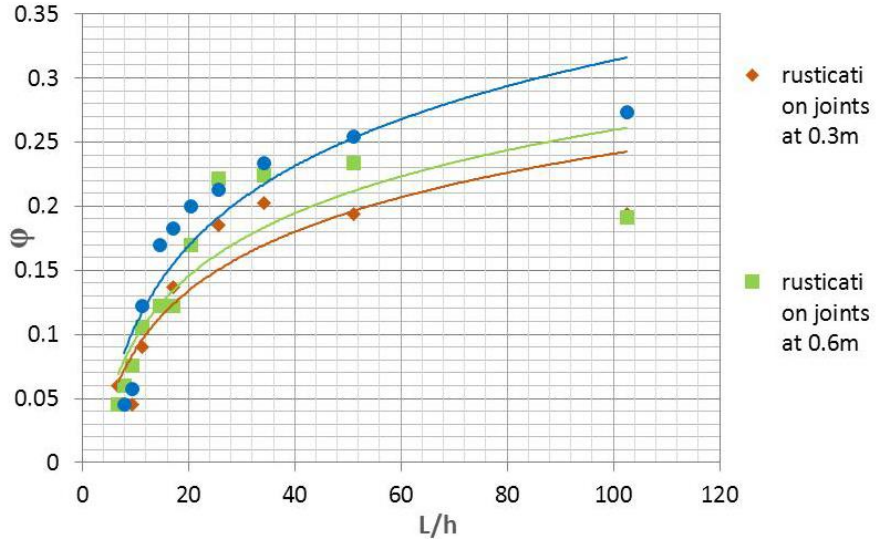

Figure 8. Dependence of velocity coefficient φ on geometric parameters of the air gap

Петриченко М.Р., Субботина С.А., Хайрутдинова Ф.Ф., Рейх Е.В.,. Немова Д.В., Ольшевский В.Я., Сергеев В.В. Влияние рустов на воздушный режим в вентилируемом фасаде // Инженерно-строительный журнал. 2017. № 5(73). С. 40–48.

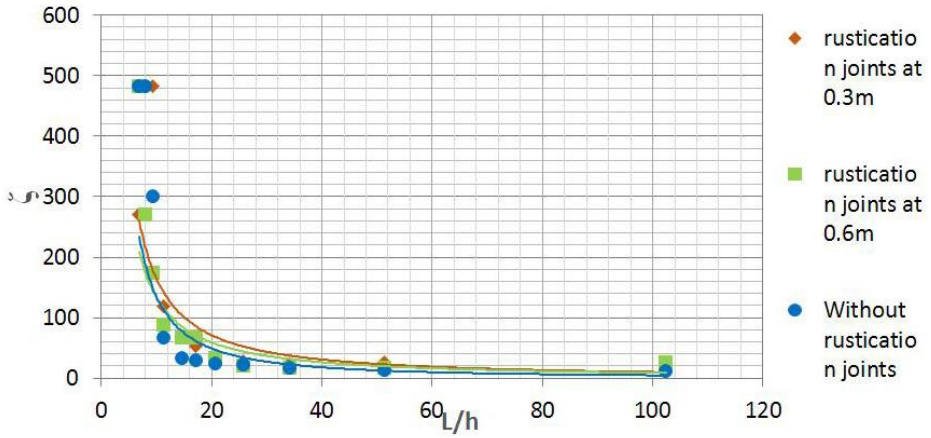

Figure 9. Dependence of local head loss coefficient ζ on geometric parameters of the air gap

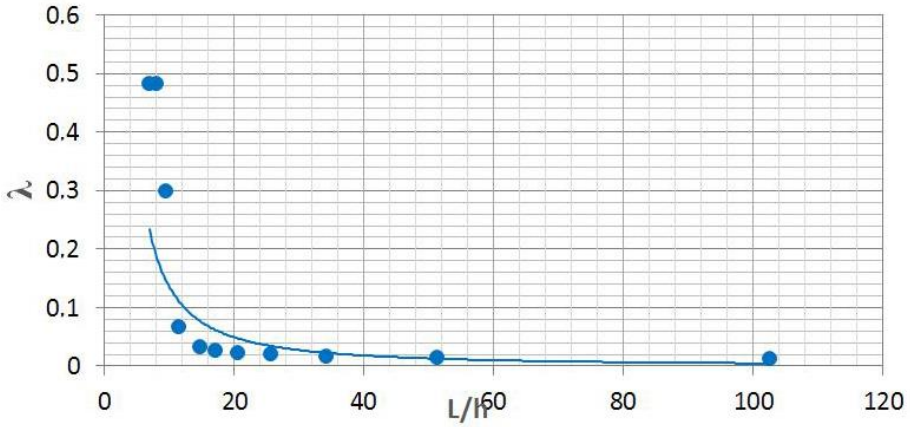

Figure 10. Dependence of pipe friction coefficient λ on geometric parameters of the air gap without rustication joints

In these dependences for the second case it can be seen that:

1. Velocity attaints its maximum alongside the hot surface, and there is no air circulation along the cold surface. Besides, for the width of the gap of 0.3 m impact of rustication joints interval on velocity value is precious little (Fig. 6). When the width of the air gap satisfies a condition $h \geq 0.22$ m, then velocity goes below 0.1 m/s, that is lower than instrumental uncertainty. In this case, experimental results are unreliable.
2. Aside from the width of air gap (h), average velocity, as in the first case, is lower at frequent rustication joints (Fig. 7).
3. Frequently pitched rustication joints diminish velocity coefficient (Fig. 8) and increase local hydraulic resistance (Fig. 9).

Discussion

In this study, we have performed physical simulation of heat-gravitational motion inside of the air gap at different spacing between rustication joints.

Research of the influence of outlet geometry on the airflow and temperatures in the ventilated façade was carried out by E. Šagát, L. Matějka, J. Pěnčík in their paper [16]. This experiment was performed for open joint ventilated façade. A. Fallahi, F. Haghighat, H. Elsadi suggested design approach [6], that involves the integration of passive thermal mass technique. These researches were carried out for the ventilated façade without considering interval value. In our study, we have ascertained, that different spacing between rustication joints also influences ventilated façade performance.

All-in-all results suggest, that interval influences on airflow data. Frequently pitched rustication joints diminish velocity coefficient and increase local hydraulic resistance regardless of width of the air

gap. Apparently, cold air penetrates through them, afterwards it descends, thereby decreasing average velocity.

It should be noted, that all measurements were taken without weather impact. Impact of rustication joints on airflow data will increase, in case of wind correction.

Conclusions

1. Average velocity of the air flow depends on spacing between rustication joints and on air gap width.
2. Obtained results show, that velocity attains its maximum in the ideal channel without rustication joints. As the interval is reduced, average velocity decreases because of cold air penetrating. It leads to heat-gravitational motion inversion.
3. The most appropriate design is the façade without rustication joints, or facade with the maximal spacing between them. In comparison with current configurations, the most appropriate interval is equal to 0.6 m.

References

1. Peci López F., Jensen R.L., Heiselberg P., Ruiz de Adana Santiago M. Experimental analysis and model validation of an opaque ventilated façade. *Building and Environment.* 2012. Vol. 56. Pp. 265–275.
2. Patania F., Gagliano A., Nocera F., Ferlito A., Galesi A. Thermofluid-dynamic analysis of ventilated facades. *Energy and Buildings.* 2010. Vol. 42. Pp. 1148–1155.
3. Suareza C., Joubertb P., Molinaa J.L., Sánchez F.J. Heat transfer and mass flow correlations for ventilated facades. *Energy and Buildings.* 2011. Vol. 43. Pp. 3696–3703.
4. Borovkov, V.M., Zysin, L.V., Sergeev, V.V. Itogi i nauchno-tekhnicheskiye problemy ispol'zovaniya rastitel'noy biomassy i organosoderzhashchikh otkhodov v energetike [The totals and technological problems of usage of vegetative biomass and organic waste in power engineering]. *Izvestiya Akademii Nauk. Energetika.* 2002. No. (6). Pp. 13–24 (rus)
5. Nizovtsev M.I., Belyi V.T., Sterlygov A.N. The facade system with ventilated channels for thermal insulation of newly constructed and renovated buildings. *Energy and Buildings.* 2014. Vol. 75. Pp. 60–69.
6. Fallahi A., Haghighat F., Elsadi H. Energy performance assessment of double-skin facade with thermal mass. *Energy and Buildings.* 2010. Vol. 42. Pp. 1499–1509.
7. Borodinecs A., Nazarova J., Zajacs A., Malyshev A., Pronin V. Specifics of building envelope air leakage problems and airtightness measurements. *MATEC Web of Conferences.* 2016. Vol. 73. 02020.
8. Gaujena B., Borodinecs A., Zemitis J., Prozuments A. Influence of building envelope thermal mass on heating design temperature. *Materials Science and Engineering*. 2015. Vol. 96. 012031.
9. Sergeev V.V., Aleshina A.S. Gas-generator combined-cycle plant equipped with a high-head heat-recovery boiler. *Thermal Engineering.* 2011. No. 58(3). Pp. 268–270.
10. Zajacs A., Zemitis J., Tihomirova K., Borodinecs A. Concept of smart city: first experience from city of Riga. *Journal of Sustainable architecture and Civil Engineering.* 2014. No. 2(7). Pp. 54–59.
11. Kaklauskas A. Passive House Model for Quantitative and Qualitative Analyses and Its Intelligent System. *Energy and Buildings.* 2012. Vol. 50. Pp. 7–18.
12. Gamayunova O., Vatin N. The role of the state and citizens to improve energy efficiency. *Applied Mechanics and Materials.* 2015. Vols. 725–726. Pp. 1493–1498.
13. Perlova E., Karpova S., Rakova X.M., Bondarenko E., Platonova M., Gorshkov A. The architectural concept of the building with low energy consumption. *Applied*

Литература

1. Peci López F., Jensen R.L., Heiselberg P., Ruiz de Adana Santiago M. Experimental analysis and model validation of an opaque ventilated facade // Building and Environment. 2012. Vol. 56. Pp. 265–275.
2. Patania F., Gagliano A., Nocera F., Ferlito A., Galesi A. Thermofluid-dynamic analysis of ventilated facades // Energy and Buildings. 2010. Vol. 42. Pp. 1148–1155.
3. Suareza C., Joubertb P., Molinaa J.L., Sánchez F.J. Heat transfer and mass flow correlations for ventilated facades // Energy and Buildings. 2011. Vol. 43. Pp. 3696–3703.
4. Боровков В.М., Зысин Л.В., Сергеев В.В. Итоги и научно-технические проблемы использования растительной биомассы и органосодержащих отходов в энергетике // Известия АН. Энергетика. 2002. № 6. С. 13–24.
5. Nizovtsev M.I., Belyi V.T., Sterlygov A.N. The facade system with ventilated channels for thermal insulation of newly constructed and renovated buildings // Energy and Buildings. 2014. Vol. 75. Pp. 60–69.
6. Fallahi A., Haghighat F., Elsadi H. Energy performance assessment of double-skin facade with thermal mass // Energy and Buildings. 2010. Vol. 42. Pp. 1499–1509.
7. Borodinecs A., Nazarova J., Zajacs A., Malyshev A., Pronin V. Specifics of building envelope air leakage problems and airtightness measurements // MATEC Web of Conferences. 2016. Vol. 73. 02020.
8. Gaujena B., Borodinecs A., Zemitis J., Prozuments A. Influence of building envelope thermal mass on heating design temperature // Materials Science and Engineering. 2015. Vol. 96. 012031.
9. Sergeev V.V., Aleshina A.S. Gas-generator combined-cycle plant equipped with a high-head heat-recovery boiler // Thermal Engineering. 2011. № 58(3). Pp. 268–270.
10. Zajacs A., Zemitis J., Tihomirova K., Borodinecs A. Concept of smart city: first experience from city of Riga // Journal of Sustainable Architecture and Civil Engineering. 2014. № 2(7). Pp. 54–59.
11. Kaklauskas A. Passive house model for quantitative and qualitative analyses and its intelligent system // Energy and Buildings. 2012. Vol. 50. Pp. 7–18.
12. Gamayunova O., Vatin N. The role of the state and citizens to improve energy efficiency // Applied Mechanics and Materials. 2015. Vols. 725–726. Pp. 1493–1498.
13. Perlova E., Karpova S., Rakova X.M., Bondarenko E., Platonova M., Gorshkov A. The architectural concept of the building with low energy consumption // Applied Mechanics and Materials. 2015. Vols. 725–726. Pp 1580–1588.
14. Harmati N., Jakšić Ž., Vatin N. Heat balance method

Петриченко М.Р., Субботина С.А., Хайрутдинова Ф.Ф., Рейх Е.В.,. Немова Д.В., Ольшевский В.Я., Сергеев В.В. Влияние рустов на воздушный режим в вентилируемом фасаде // Инженерно-строительный журнал. 2017. № 5(73). С. 40–48.

Mechanics and Materials. 2015 Vols. 725–726. Pp. 1580–1588.

14. Harmati N., Jakšić Ž., Vatin N., Heat balance method application in building energy performance simulation. *Applied Mechanics and Materials.* 2015. Vols. 725–726. Pp. 1572–1579.
15. Šagát E., Matějka L. Experimental assessment of the influence of wind speed on the airflow and temperatures in the open joint ventilated façade cavity. *Applied Mechanics and Materials.* 2016. Vol. 835. Pp. 444–449.
16. Šagát E., Matějka L., Pěnčík J. Experimental assessment of the influence of outlet geometry on the airflow and temperatures in the ventilated façade cavity. *Applied Mechanics and Materials.* 2016. Vol. 824. Pp. 641–648.
17. Saari J., Sermyagina E., Kaikko J., Vakkilainen E., Sergeev V. Integration of hydrothermal carbonization and a CHP plant: Part 2 – operational and economic analysis. *Energy.* 2016. No. 113. Pp. 574–585.
18. Ryabukhina S., Simankina T., Koshkarova M., Sokolovskii N., Ryzhkov O. Combined thermal insulating module of mounted vented facades. *MATEC Web of Conferences*. 2016. Vol. 73. 02005.
19. Kornienko S.V. Testing of calculation method of the enclosing structures temperature-humidity conditions on results of indoor climate in-situ measurements. *Magazine of Civil Engineering.* 2012. No. 2. Pp. 18–23. (rus)
20. Grinfeldi G.I., Gorshkov A.S., Vatin N.I. Tests results strength and thermophysical properties of aerated concrete block wall samples with the use of polyurethane adhesive. *Advanced Materials Research.* 2014. Vols. 941–944. Pp. 786–790.

application in building energy performance simulation // Applied Mechanics and Materials. 2015. Vols. 725–726. Pp. 1572–1579.

15. Šagát E., Matějka L. Experimental assessment of the influence of wind speed on the airflow and temperatures in the open joint ventilated façade cavity // Applied Mechanics and Materials. 2016. Vol. 835. Pp. 444–449.
16. Šagát E., Matějka L., Pěnčík J. Experimental assessment of the influence of outlet geometry on the airflow and temperatures in the ventilated façade cavity // Applied Mechanics and Materials. 2016. Vol. 824. Pp. 641–648.
17. Saari J., Sermyagina E., Kaikko J., Vakkilainen E., Sergeev, V. Integration of hydrothermal carbonization and a CHP plant: Part 2 – operational and economic analysis // Energy. 2016. № 113. Pp. 574–585
18. Ryabukhina S., Simankina T., Koshkarova M., Sokolovskii N., Ryzhkov O. Combined thermal insulating module of mounted vented facades // MATEC Web of Conferences. 2016. Vol. 73. 02005.
19. Корниенко С.В. Тестирование метода расчета температурно-влажностного режима ограждающих конструкций на результатах натурных измерений параметров микроклимата помещений // Инженерно-строительный журнал. 2012. № 2(28). С. 18–23.
20. Grinfeldi G.I., Gorshkov A.S., Vatin N.I. Tests results strength and thermophysical properties of aerated concrete block wall samples with the use of polyurethane adhesive. Advanced Materials Research. 2014. Vols. 941–944. Pp. 786–790.

Mikhail Petritchenko,
+7(921)3300429; fonpetrich@mail.ru

Svetlana Subbotina,
+7(921)5606981; svetlana.subbotina94@mail.ru

Faina Khairutdinova,
+7(952)2159789; faina.spbstu@gmail.com

Elizaveta Reich,
+7(960)2439533; lisa_reich@mail.ru

Darya Nemova,
+7(921)8900267; darya.nemova@ice.spbstu.ru

Vyacheslav Olshevskiy,
+7(911)9199526; 79119199526@yandex.ru

Vitaliy Sergeev,
+7(921)9805437; sergeev_vitaly@mail.ru

Михаил Романович Петриченко,
+7(921)3300429; эл. почта: fonpetrich@mail.ru

Светлана Александровна Субботина,
+7(921)5606981;
эл. почта: svetlana.subbotina94@mail.ru

Фаина Фанилевна Хайрутдинова,
+7(952)2159789;
эл. почта: faina.spbstu@gmail.com

Елизавета Викторовна Рейх,
+7(960)2439533; эл. почта: lisa_reich@mail.ru

Дарья Викторовна Немова,
+7(921)8900267;
эл. почта: darya.nemova@ice.spbstu.ru

Вячеслав Янушевич Ольшевский,
+79119199526;
эл. почта: 79119199526@yandex.ru

Виталий Владимирович Сергеев,
+7(921)9805437;
эл. почта: sergeev_vitaly@mail.ru

Petritchenko M.R., Subbotina S.A., Khairutdinova F.F., Reich E.V., Nemova D.V., Olshevskiy V.Ya., Sergeev V.V. Effect of rustication joints on air mode in ventilated facade. *Magazine of Civil Engineering*. 2017. No. 5. Pp. 40–48. doi: 10.18720/MCE.73.4.

doi: 10.18720/MCE.73.5

The algorithm and accuracy of definition of heattechnical indicators of buildings

Алгоритм и точность определения теплотехнических показателей зданий

L.N. Danilevski,
S.L. Danilevsky,
State enterprise "NIPTIS Housing Institute named after Ataev S.S.", Minsk, Republik of Belarus

Д-р техн. наук, первый заместитель директора Л.Н. Данилевский,
старший научный сотрудник С.Л. Данилевский,
Государственное предприятие "Институт жилища – НИПТИС им. Атаева С. С.", г. Минск, Республика Беларусь

Key words: specific consumption of thermal energy on heating; settlement service conditions; measurements; coefficient of specific heatlosses; statistical characteristics; classification of buildings

Ключевые слова: удельное потребление тепловой энергии на отопление; расчетные условия эксплуатации; измерения; коэффициент удельных теплопотерь; статистические характеристики; классификация зданий

Abstract. The object of the given research is the thermotechnical characteristics of buildings. The problem of thermotechnical indicators measurement arises at the acceptance of the buildings in use and also while performing work on energy classification of buildings in use. The two-level procedure of specific consumption definition of thermal energy for heating is offered: the coefficient of heat losses of the building is defined, and then the specific consumption of thermal energy for heating for settlement conditions is estimated. The given article suggests the optimal algorithm of the coefficient of heat losses determination according to the consumption of thermal energy for the buildings, not depending from the outdoor air temperature and the power of household thermal emissions of the building. There are also the results of the estimation of the coefficient of the coefficient of heat losses and specific consumption of thermal energy for heating for the conditions estimation according to the long-term observation for high-rise buildings. There are also the estimation of the RMS error of determining the coefficient of the coefficient of heat losses and specific thermal energy consumption for heating for the conditions estimation, as well as the 75 % confidence interval for this indicator. The results can be used for the buildings in use energy classification.

Аннотация. Объектом исследования являются теплотехнические характеристики зданий. Проблема измерения теплотехнических показателей возникает при приемке зданий в эксплуатацию, а также при выполнении работ по энергетической классификации зданий в процессе эксплуатации. Предлагается двухступенчатая процедура определения удельного потребления тепловой энергии на отопление: определяется коэффициент теплопотерь здания, затем рассчитывается удельное потребление тепловой энергии на отопление для расчетных условий. Представлен оптимальный алгоритм определения коэффициента теплопотерь по данным потребления тепловой энергии на отопление в здании, не зависящий, от температуры воздуха и мощности бытовых тепловыделений в здании. Определена потенциальная точность определения указанного коэффициента в зависимости от климатических условий и погрешности измерения температуры наружного воздуха. Приведены результаты определения коэффициента теплопотерь и удельного потребление тепловой энергии на отопление для расчетных условий по данным многолетних наблюдений для многоэтажных зданий. Вычислены значения среднеквадратичной погрешности определения коэффициента удельных теплопотерь и удельного потребление тепловой энергии на отопление для расчетных условий, а также 75 % доверительный интервал для этого показателя. Полученные результаты могут быть использованы для выполнения энергетической классификации эксплуатируемых зданий.

Данилевский Л.Н., Данилевский С.Л. Алгоритм и точность определения теплотехнических показателей зданий // Инженерно-строительный журнал. 2017. № 5(73). С. 49–61.

Introduction

The requirements for the heat engineering characteristics of buildings change together with the cost of energy resources. If in [1] the requirements for resistance to heat release of enclosing structures were chosen only for the sake of thermal comfort, in [2, 3] normalized values for the heat resistance for protecting structures was established, and in [3, 4] standardized values for the specific annual heat consumption for heating of buildings was estimated. Specific annual heat consumption for heating is also set in the normative documents of the EU, [5], RF [6] RK [7]. From the regulatory requirements to the mentioned indicator logically follows the need to develop measuring techniques providing the verification of compliance of performance indicator values calculated at the stage of acceptance of the buildings as well as at the other stages of its use.

Currently, to assess the thermal performance of the building in most cases methods of thermal control [8–10] are used. However, its use lets estimate the thermal defects in the exterior building enclosure and do not provide us with the ideas of specific energy characteristics of the building.

In [11] the methodology and results of determination of heat transfer resistance exterior walls of buildings in use are given. The considerable complexity of methods with a small sufficiently result should be noted. It is almost impossible to define thermal resistance of all external fences of the building with the method proposed in [11]. The results are selective with no statistical evaluation of the accuracy and reliability of the results.

Definition and comparative analysis of values of specific heat energy consumption for heating of buildings is, as a rule, made in specific conditions [12], Russia, [13]. However, the indicator "specific annual consumption of thermal energy for heating" refers not to the building as a structural system, and characterizes it with the account of climatic conditions, inhabitation of the building and its operation conditions. Therefore, the value of the indicator of specific consumption of thermal energy for heating measured under the specific climatic conditions and under operating conditions differing from design, may differ significantly from the calculated. It should also be added that the complete inhabitation of the building occurs a few years after putting it in use, therefore, the consumption of thermal energy for heating and ventilation during this period may differ significantly from the design value.

[19] suggests the concept of the specific thermal characteristic of the building which value is equal to the relation of specific power of thermal losses at a difference of temperatures in 1K to building volume. This quantity does not depend on the service conditions and characterizes the building as a thermal power object. For residential buildings it is more convenient to standardize this quantity not to volume, but to the heated area of the building which value can be received from the maintenance organization. In our opinion, the name "Coefficient of heat losses" of the building is more suitable for this quantity. Knowing this indicator, it is possible to calculate quantity of specific consumption of thermal energy on heating of the building for any settlement conditions [20].

The way of determination of the coefficient of heat losses for the general and separate accounting of thermal energy on heating and hot water supply is investigated in [21–25]. It is offered to determine the value of a specific consumption of thermal energy on heating for settlement conditions by the calculations for this indicator.

The necessity to define the thermal energy specific consumption for heating arises while performing the following tasks:

- At the acceptance in use of new buildings and buildings after thermal modernization;
- While performing energy certification of the buildings in use;
- To estimate the thermal protection design quality of the building and to provide the feedback between the project and the constructed object for the purpose of its iteration.

By now in the well-known literature there is no information which would allow determining the possible accuracy of definition of this indicator, as well as no data on an error of its definition for the buildings in use.

It should also be noted that in normative and scientific literature there is no specific requirements to the accuracy of measurement of a specific indicator expense of thermal energy on heating of the operated buildings.

Requirements to the accuracy of definition of specific consumption of thermal energy on heating for settlement conditions

In the Republic of Belarus the classification of buildings by specific consumption of thermal energy on heating and ventilation for settlement conditions is accepted [3]. While solving the problem of the building in use reference to a certain class, it is necessary to consider the possible accuracy of definition of specific consumption of thermal energy on heating and ventilation.

Buildings of the classes B, A and A^+ are allowed to design and construction in the Republic of Belarus. The class B for multistoried buildings is characterized with a range of values from 30 to 48 kWh/m^2 for a heating season. The accuracy of the measurement of this indicator should provide the possibility of a clear classification of the building to a particular class. E.g., the value of an error of measurements of ±4 W / (m2K) allows to range the specified range into 5 intervals of unambiguous reference of the building to the specified class. The increase in accuracy of measurements respectively increases the quantity of the intervals and decreases the uncertainty of its reference for a certain class.

Table 1 presents the number of ranges of intervals depending on the control precision for high-rise buildings of different classes.

Table 1. Quantity of Ranges of Split Intervals depending on the precision of measurements

Classes of buildings with more than 7 levels	Range of values of indicator, kWh/m^2	Reasonable range of indicator, kWh/m^2	Accuracy of definition of kWh/(m^{2}a)							
			±2		±4		±6		±8	
			Quantity of ranges For two ranges of indicators		Quantity of intervals For two ranges of indicators		Quantity of intervals For two ranges of indicators		Quantity of intervals For two ranges of indicators	
			range 1	range 2						
D	81 - 60	89 - 69	10	10	5	5	3	3	2	2
C	59 - 49	69 - 49	5	10	3	5	2	3	2	2
B	48 - 30	49 -29	10	10	5	5	3	3	2	2
A	29 - 25	29 -19	3	10	2	5	1	3	1	2
A^+	<25	<19	12	10	6	5	4	3	3	2

From the data shown in Table 1, we can conclude that the choice of division of the ranges into classes is irrational. The above-mentioned ranges of the indicator q_u for classes A and C will lead to an increase of the number of errors in determining the class of the building compared to the others, since the number of measurement intervals in a specified range-tries is twice less than in the others. The appropriate division into ranges proposed in the table does not break the logic of the division into classes, and makes it possible to reduce the uncertainty of attribution of the building to a particular class.

The optimal solution for the coefficient of heat losses

In [26] it is proposed to take into account the energy costs of hot water supply by data out of a heating season for determining the coefficient of heat losses of the building in the case of general energy account for heating and hot water supply. This approach can lead to considerable mistakes while estimating the coefficient. Besides, offered in [26] method of calculating annual energy consumption and value of consumption at zero degrees Celsius is not rational.

In [20–23] the coefficient of heat losses of the building, f_1, is estimated together with the following assumptions:

– Air temperature inside the building is known and equal to some extent to the constant value;

- the power of the household thermal emissions remains constant during the entire measurement period;
- Insolation is negligible in comparison with the other components of thermal balance.

The compliance of the above-stated requirements during one heating season and especially during several heating seasons is problematic. In practice, these requirements are not fulfilled which leads to decrease in accuracy of measurements.

The algorithm offered in [24] measures the temperature of external air and the energy spent for the hot water preparation on the measuring intervals. But there are still some requirements to the constant temperature values about in the building and the power of household thermal emissions during each heating season. The system of the equations in [24–25] for the definition of f_1 in the heating season k consists of the equations like follows:

$$p_i^k = f_1 \cdot \left(t_{0i}^k - t_i^k\right) - f_{2i}^k + \widetilde{u_i}, \text{ i=1,…,N; k=1, …,K;} \quad (1)$$

where f_1 – coefficient of heat losses of the building of W/(m^{2}K);

f_{2i}^k – the power of the building thermal emissions in a heating season k, and the measuring interval i which is supposed to be constant during one heating season, W/m^2;

t_{0i}^k – air temperature in the building in a heating season k and a measuring interval i which is also supposed to be constant during one heating season, K;.

t_i^k – the temperature of the outdoor air on the interval i of the heating season k, K;

p_i^k– a specific power of a source of heating of the building on the interval i of the heating season k, W/m^2;

N – quantity of intervals of measurement in one heating season;

K – quantity of heating seasons, information on which is used for the f_1 value definition.

$\widetilde{u_i}$ – an uncorrelated interfering component on the interval i which arises from the inaccuracy of temperature and energy measurement, and also owing to the deviation of air temperature and power of thermal emissions in the building from the constant values, W/m^2.

In order to increase the accuracy of measurements, the algorithm of f_1 value definition is proposed to be changed as follows:

- The electricity meter counters estimate the average power of the thermal energy consumed by the building on heating on several time intervals during one or more heating seasons;
- Duration of the time intervals gets out of a ratio:

$$\tau >> \tau_0,$$

where τ_0 is a constant of loss of heat time of the building, s;

- For the same intervals of time the average temperature of the outdoor air, e.g., according to the hydrometeocenter is estimated.

For the chosen measuring intervals of each heating season we make a system of the equations (1) in which the sequence of the equations in system corresponds to the sequence of the chosen measurement intervals. Then we subtract the next equations systems (1) made for a concrete heating season to get a new system of the equations for each heating season with a quantity of the equations in system, equal to N-1. While subtraction the corresponding coefficients and free members of the equations are subtracted. Then we unite the systems of the equations received for each heating season in the general system and solve it concerning f_1.

The total system of the equations is as follows (2):

$$\begin{gathered} q_1^k = f_1 \cdot T_1^k + \widetilde{u_1} \\ q_i^k = f_1 \cdot T_i^k + \widetilde{u_i} \\ q_{n-1}^k = f_1 \cdot T_{n-1}^k + \widetilde{u_{n-1}} \end{gathered} \quad (2)$$

where $q_i^k = p_i^k - p_{i+1}^k T_i^k = t_i^k - t_{i+1}^k$, i=1,…, N; k=1, …, K;

p_i and p_{i+1} - the specific power of a source of heating of the building on i and $i+1$ intervals of the heating season k, W/m^2.

t_i^k *и* t_{i+1}^k- the average temperature of the outdoor air on i and i+1 intervals of heating season k, K.

The total quantity of equations is equal to the system K*(N-1)

Such an approach to the equations system formation allows:

- To reduce labor input of measurements since it is enough to obtain information on average value of temperature of external air and there is no need to take temperature in the building:
- To increase the precision of measurements by the increase of the initial information volume;
- To reduce the measurement uncertainty associated with the violation of the requirement of constant values of temperature, power, domestic heat and intensity of the insolation during each heating season.

Change in parameters in the neighboring time intervals is not abrupt because of the inertia of these quantities in blocks of flats and to a less extent than during the heating season.

The changes in solar activity in the adjacent months of the heating season is also smaller than the dispersion for the season and, especially, for several heating seasons. For example, Table 2 shows the value of the energy of solar radiation coming to the multilevel, designed for Minsk.

Table 2. Energy of Insolation coming to the multilevel dwelling in Minsk

Single-section 19-floors 132-rooms dwelling in a series 111-90 MAPID, Minsk:					
Months of a heating season	November	December	January	February	March
Insolation, W/m^2	0.018	0.015	0.027	0.050	0.074

Using the least squares method [27] to solve the system of equations (2), we obtain a formula for determining the coefficient of the specific heat losses of a building:

$$f_1 = \frac{\sum_{k=1}^{K}\sum_{i=1}^{N} q_i^k T_i^k}{\sum_{k=1}^{K}\sum_{i=1}^{N}(T_i^k)^2} \tag{3}$$

Usage of the method of least squares to solve the system of equations gives the minimum value of f_1 estimate variance [27] and is optimum in sense of providing the minimum mean square error for an objective.

On the known value of coefficient determine specific consumption of thermal energy on heating for settlement service conditions by a formula:

$$q_h = 0.024 \cdot N(\Delta t_{sr} \cdot f_1 - \xi(f_2 + \varsigma \cdot q_s)), \tag{4}$$

where: $\Delta t_{sr} = (t_{in.} - t_{out.})$, K,

q_h – the Specific average annual power of a power source on heating and ventilation for settlement conditions, W / (м^{2}а);

f_1 – specific coefficient of thermal losses of the building, W / (m^{2}K);

f_2 – the specific power of internal thermal emissions in the building accepted for calculations for W/m^2;

t_{in} – settlement air temperature in the building, equal 18 °C;

t_{out} – the average temperature of external air in in a heating season according to climatic conditions of the area on [29];

q_{sr} – the average stream of the solar radiation coming to the building, according to requirements [29];

ζ and ξ – the coefficients considering type of system of regulation and coefficient of assimilation of solar energy in the building, respectively.

The potential accuracy of coefficient of heat losses determination

Assuming the values q_i^k and T_i^k - uncorrelated random variables, in accordance with the principles of the transfer of errors for independent variables in [27], we receive:

$$\sigma_f^2 = \left(\frac{\partial f_1}{\partial T}\right)^2 \cdot \sigma_T^2 + \left(\frac{\partial f_1}{\partial q}\right)^2 \cdot \sigma_q^2, \quad (5)$$

From (3) we receive the derivatives:

$$\frac{\partial f_1}{\partial T} = \frac{\overline{q} \cdot \overline{T^2} - 2 \cdot \overline{qT} \cdot \overline{T}}{\left(\overline{T^2}\right)^2}, \quad (6)$$

$$\frac{\partial f_1}{\partial q} = \frac{\overline{T}}{\overline{T^2}}, \quad (7)$$

With the following designations:

$$\bar{T} = \sum_{k=1}^{K} \sum_{i=1}^{N} T_i^k \quad ; \overline{T^2} = \sum_{k=1}^{K} \sum_{i=1}^{N} (T_i^k)^2;$$
$$\bar{q} = \sum_{k=1}^{K} \sum_{i=1}^{N} q_i^k; \ \overline{(qT)} = \sum_{k=1}^{K} \sum_{i=1}^{N} q_i^k T_i^k \quad (8)$$

Substituting (6) and (7) in (5), and taking into account (8) we get the dependence of the standard square deviation for f_1 value from the error of determination of temperature and power:

$$\sigma_f = \frac{\sqrt{\left(\overline{q}^2 + 4 \cdot (f_1)^2 \cdot \overline{T}^2 + 4 \cdot \overline{q} \cdot \overline{T} \cdot f_1\right) \cdot \sigma_T^2 + \overline{T}^2 \cdot \sigma_q^2}}{\overline{T^2}} \quad (9)$$

From (9) it is possible to obtain the minimum value of an error of dispersion estimation coefficient of heat losses of the building for the known values of uncertainty of determination of power and temperature of the outdoor air.

From (9) we can conclude that besides the values of σ_q and σ_T the accuracy of f_1 determination also depends on the condition of the changes. The decrease in the value of $\overline{T^2}$, i.e., reducing the difference between the outdoor air temperatures at various measurement intervals leads to an increase of the estimation of σ_f uncertainty.

The real uncertainty of measurement of f_1 may exceed the obtained value, since the initial formula does not take into account outcome all possible changes in solar activity, the capacity of the internal heat sources and the temperature of the air inside the building. The measurement accuracy could also depend on the number and duration of measurement intervals, the quality controller of a heat supply, etc.

Results and Discussion

We should determine the potential accuracy of measurements of coefficient of heat losses for average climatic conditions of the cities of Republic of Belarus [28] and the Russian Federation [29]. With this purpose we calculate on a formula (8) for given values of f_1 the range of possible variations of σ_f. In Figure 1 there is a graph of dependence of size σ_f for the range of f_1 values, from 0.4 to 1.8, and climatic conditions of various cities. Calculations are performed for N = 5 (November, December, January, February, March).

σ_T=1K; σ_q=1W/m^2;

From the data provided on Figure 1 it is possible to conclude that the value of the RMS-deviation increases together with the increase of f_1 value and for softer climatic conditions.

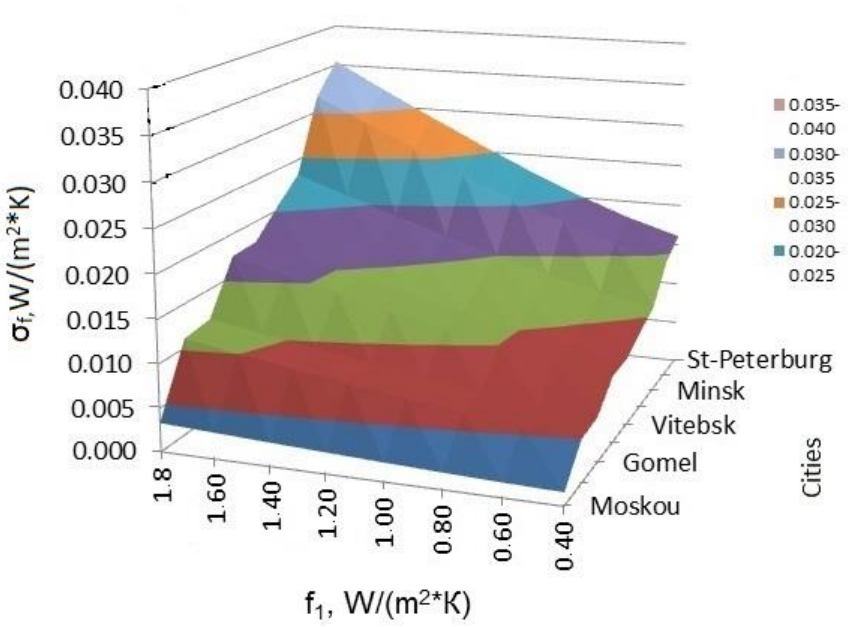

Figure 1. Dependence of the value of σ_f for the range of f_1 values and climatic conditions of various cities

Table 3 shows the average values of dispersion of coefficient estimation of the coefficient of heat losses calculated for the regional centers of the Republic of Belarus.

Table 3. An average error of determination of coefficient of heat losses for the RB regional centers. σ_T=1K; σ_q=1 W / (m^2)

f_1 ,w/(m^{2}K)	1.8	1.6	1.4	1.2	1	0.8	0.6	0.4
σ_f, w/(m^{2}K)	0.042	0.039	0.035	0.032	0.029	0.026	0.024	0.022

Figures 2 and 3 show the dependence of the value of *σf* for a range of changes to the RMS error σT and σq for Minsk and Krasnoyarsk. In both graphs the increases in the values of σ_T and σ_q lead to an increase in the error of determining the coefficient of the coefficient of heat losses, σ_f. However, on the graph for Minsk the range of values of σf are from 0.003 to 0.03 W/(m^{2}K), but for Krasnoyarsk values of σ_f are in the range from 0.0015 to 0.014. Therefore, the accuracy of determining the values of the coefficient of the coefficient of heat losses increases for the more severe climatic conditions.

Recalculation of the RMS deviation σ_f for coefficient of heat losses definition in an error of definition of specific consumption of thermal energy on heating is carried out on a formula:

$$\sigma_q = \sigma_f \cdot \mathrm{G} * 0.024, \quad (10)$$

where σ_q – a the RMS deviation of definition of specific consumption of thermal energy on heating, kWh / (m^2 year);

G – quantity of the degree – days of a heating season, K*d.

According to (10), to value σ_f =*0.01* W / (m^2*K) corresponds σ_q=*0.9* to kWh / (m^2 a) for Minsk, and σ_q=*1.6* kWh / (m^2 a) for Krasnoyarsk.

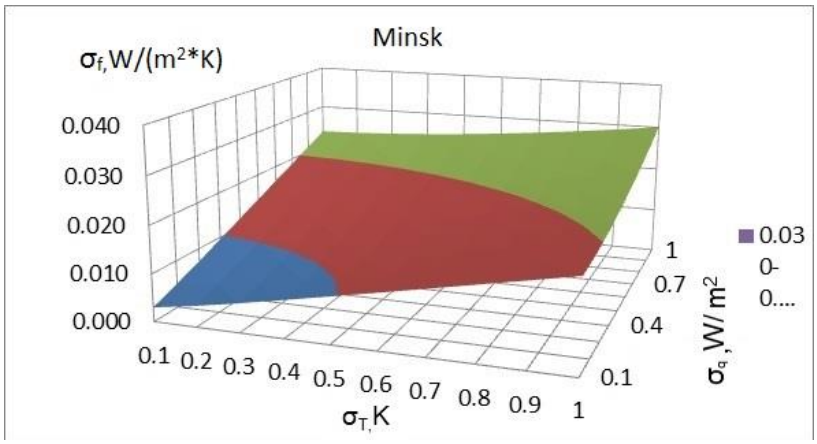

Figure 2. Schedule of Dependence of σf for the range of changes of the RMS deviation σT and σq for Minsk

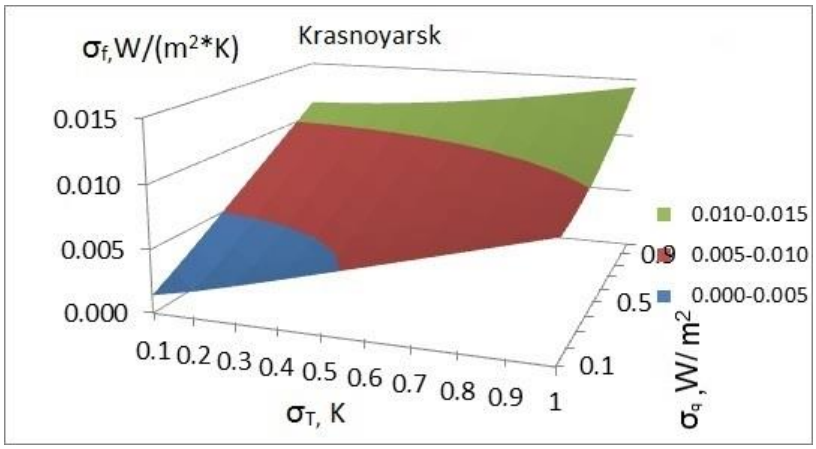

Figure 3. Schedule of Dependence of σf for the range of changes of the RMS deviation σT and σq for Krasnoyarsk

Statistical characteristics of f_1 value estimation on long-term observations

If for the preliminary estimations of the potential accuracy of determining the values of σ_f we used the principles of errors transfer for the independent variables from [27], for processing experimental data to determine the values of of the coefficient of heat losses by the results of many years of observations we use the methods of experimental data processing [30].

We should consider statistical characteristics of estimation of *f_1 value* on long-term observations. We should introduce some designations:

$$S^2 = \frac{1}{(N-1)} \sum_{k=1}^{K} \sum_{i=1}^{N} (q_i^k - f_1 \cdot T_i^k)^2 \quad (11)$$

Then the sample variance, σ_f, is equal [25]:

$$\sigma_f = \frac{S}{\sqrt{T^2}} \quad (12)$$

According to [30] 100(1-γ) % confidential range of estimation of f_1 is determined by a formula (3) and is in range:

$$f_1 - \frac{t_{N-1;1-\gamma/2} \cdot S}{\sqrt{T^2}} \le f_{10} \le f_1 + \frac{t_{N-1;1-\gamma/2} \cdot S}{\sqrt{T^2}} \quad (13)$$

where $t_{N-1;1-\gamma/2}$ – the corresponding value of the Student's t-test [30].

Figure 4 shows f_1 values for the multilevel Minsk buildings determined by the values of heat consumption in three heating seasons, 2011–2012, 2012–2013 and 2013–2014. On axis of abscissa

there is the conditional number of buildings. To calculate the coefficients the monthly data on consumption of thermal energy from November to March inclusive were chosen. I.e., the processing was performed at 15 months in the three heating seasons, in accordance with the algorithm described in this article. The range of variation of the obtained values of the conversion factor of the coefficient of heat losses in the range from 0.6 to 1.4, which corresponds to the measurable implementation of specific consumption of thermal energy on heating for the calculation of the conditions of Minsk from 55 to 125 kWh/(m^2*year), as shown in Figure 5.

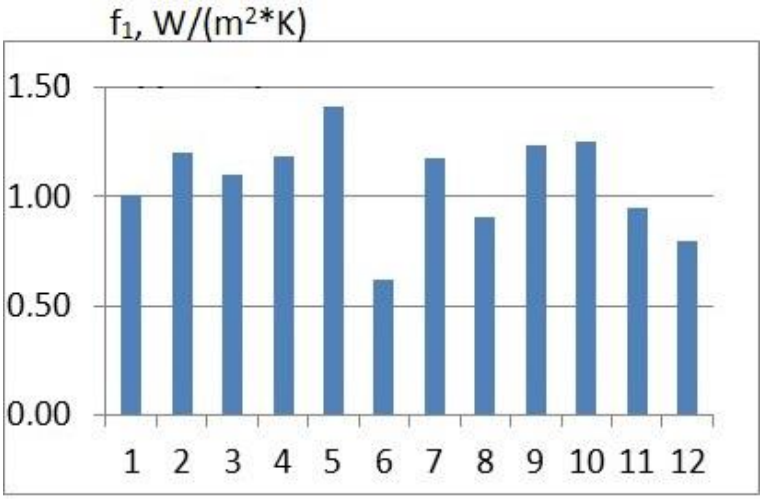

Figure 4. Values of coefficient of the coefficient of heat losses, f_1, for multilevel buildings in Minsk

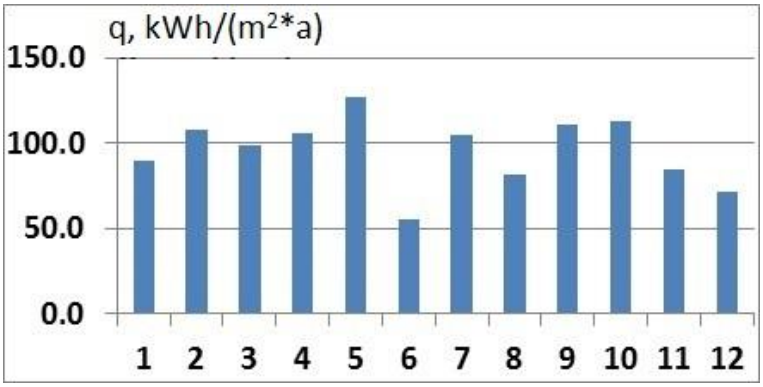

Figure 5. Values of specific consumption of thermal energy for calculated conditions of Minsk (f_1 values of fig. 4)

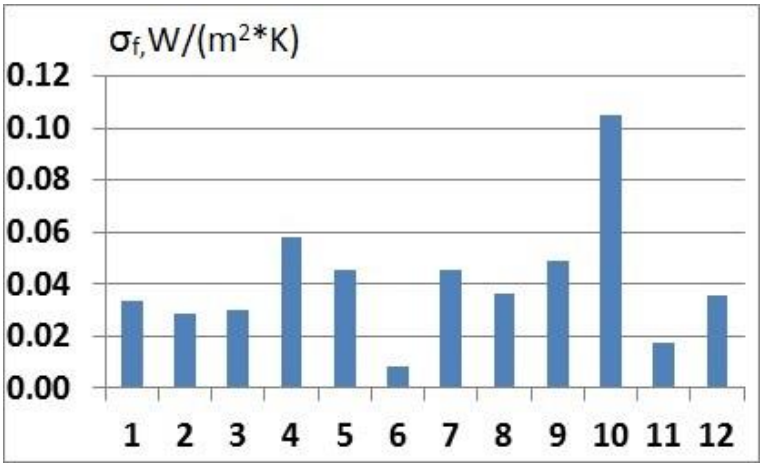

Figure 6. The values of the RMS deviation of determination of the coefficient of heat losses, σ_f (f_1 values of fig. 4)

Figure 6 shows the value of the RMS deviation of determination of coefficient of specific-value, σ_f, calculated according to expression (14). The values are in range from 0.01 to 0.04 W/(m²K) with an average of 0.03 W/(m²K). For buildings # 4 and #10 significantly exceed this value that demands an additional research of the reasons of excess.

Figure 7 shows the values of the RMS deviation of determination of specific consumption of thermal energy for heating σ_q and a confidence range of determination of this value for 75 % of probability. The values of the RMS deviation of determination of specific consumption of thermal energy for heating are mostly in the range from 1 to 4 kWh/(m²), and confidence interval of 3 to 6 kWh/(m²).

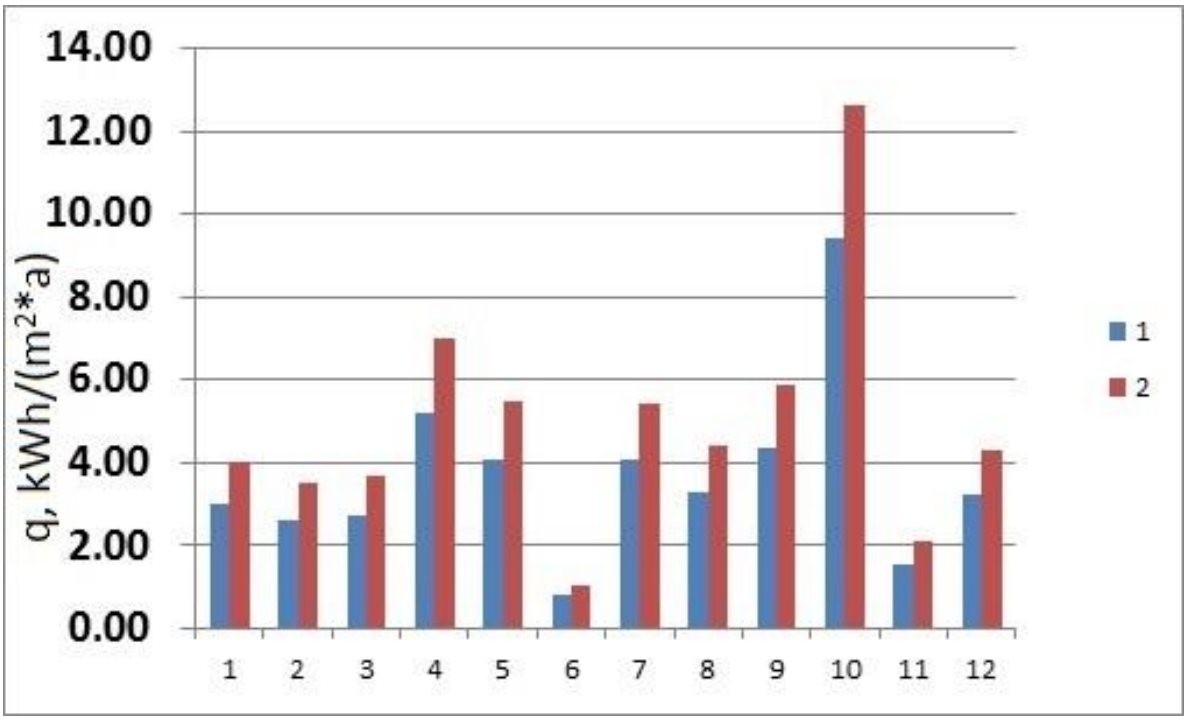

Figure 7. The values of the RMS deviation of determination of specific consumption of thermal energy on heating σ_q – row 1 and a confidential interval of determination of this size for 75 % of probability, row 2 (f_1 values of fig. 3)

Comparison of the received accuracy of measurements with data from Table 1 shows that the values of an deviation received at measurements give the chance of splitting ranges for each of classes of buildings on consumption of thermal energy on heating (at the offered adjustment of ranges) on 5–10 intervals. Such quantity of intervals will give 80–90 % of cases of errorless classification of buildings to a particular class.

The comparative analysis of sample variance of definition of values of coefficient of coefficient of heat losses of the building and specific consumption of thermal energy for settlement conditions and potential accuracy of measurements confirmed their practical coincidence for the potential accuracy of measurements corresponding to values σ_q = 1 W/m² and σ_T = 1K. This circumstance gives an opportunity to switch from Student's distribution to normal distribution with use of integral of mistakes [25] during the processing of experimental data and assessment of confidential intervals.

Conclusions

The article investigates a new method of determination of specific consumption of thermal energy for heating and ventilation of the buildings in use with in order to provide their classification. Besides, it contains a research of dependence of a statistical error of determining the rate of accuracy of measurement baseline information for different climatic conditions.

In contrast to the known methods, the method proposed provides the possibility of joint processing of information for the consumption of thermal energy on heating for several heating seasons, which significantly increases the reliability and the accuracy of the measurements. At the same time there is a decrease in the deviation connected with the change of the air temperature, in the power of the household heat emissions and in the intensity of the solar energy into the building during each heating season and from season to season.

Danilevsky L.N., Danilevsky S.L. The algorithm and accuracy of definition of heattechnical indicators of buildings. *Magazine of Civil Engineering*. 2017. No. 5. Pp. 49–61. doi: 10.18720/MCE.73.5.

The following tasks were solved:

- We developed the optimal by the criterion of minimizing the RMS deviation algorithm, determining the coefficient of the specific heat according to long-term monitoring of heat consumption for heating of the building, independent, in contrast to the already known, from changes in air temperature, the power of the household releases and intensity of the solar energy into the building during the period of measurement (collecting measurement data);
- We developed a mathematical model of dependence of potential accuracy of determination of the specified coefficient depending on the accuracy of determination of air temperature and power of system of heating in the building for various climatic conditions;
- We offered a new principle of the buildings in use classification by consumption of thermal energy on heating in which ranges of classes of buildings are coordinated to the accuracy of measurement of an indicator of classification that provides a possibility of unambiguous reference of the building to a certain class at a use stage;
- We defined the coefficient of the coefficient of heat losses according to long-term observations for a number of buildings in use via the algorithm proposed in the article, besides, the specific thermal energy consumption for heating for the calculated conditions was determined with the known value of the coefficient;
- For the considered buildings we estimated the values of a mean square error of determination of coefficient of the coefficient of heat losses, the specific thermal energy consumption on heating for settlement conditions and 75% confidential interval for this indicator.

According to the comparative analysis of sample variance value and the confidence interval of specific consumption estimation of thermal energy on heating of buildings in use for the calculated conditions, together with the theoretical values of potential accuracy of the measurements we can draw the following conclusions:

- The general tendencies in the change of the RMS deviation of determining the coefficient of the coefficient of heat losses of buildings in use are consistent with the results of the calculation of the potential accuracy of measurements by the offered mathematical model;
- The range of values of σ_f in the experimental studies corresponds with the calculation of the potential measurement accuracy for deviation values to determine the power and temperature, and is: $\sigma_q = 1$ W/m^2 and $\sigma_t = 1$K which corresponds to the possible accuracy of obtaining the initial information.

The statistical analysis of the results of determining the coefficient of the coefficient of heat losses and the specific thermal energy consumption on heating for the buildings in use for the calculated conditions via the method proposed demonstrated the feasibility of its use and allowed us to estimate the metrological characteristics depending on the accuracy of the measurements of the initial variables: temperatures of the outdoor air and energy consumed for heating.

The article suggests the decomposition of the ranges of classes of buildings by their consumption of thermal energy on heating, which provides 80–90% cases of errorless classification to a certain class when performing measurements for the buildings in use.

On the basis of the obtained results we can conclude that during the processing of experimental data and the estimation of confidence intervals on the potential accuracy of measurements and confirmed with experimental results allow us to switch from Student's t-test distribution to the standard distribution with use of the error integral.

Reference

1. *TKP 45-2.04-43-2006.* Stroitel'naya teplotekhnika. Stroitel'nye normy proektirovaniya [Construction heating engineer. Construction norms of design] Minsk: Interstate Council for standardization, metrology and certification: Belarusian. State Institute of standardization and certification, 2006. 35 p. (rus)
2. *SNB 3.02.04-03*-2003.* Zhilyye doma [Residential buildings]. Minsk: Ministry of Architecture and Construction of the Republic of Belarus, 2016. (rus)
3. *TKP 45-2.04-196-2010.* Teplovaya zashchita zdaniy. Teploenergeticheskiye kharakteristiki. Pravila opredeleniya

Литература

1. ТКП 45-2.04-43-2006. Строительная теплотехника. Строительные нормы проектирования. Минск: Межгос. Совет по стандартизации, метрологии и сертификации: Белорус. Гос. Ин-т стандартизации и сертификации, 2006. 35 с.
2. СНБ 3.02.04-03*-2003. Жилые здания. Мінск: Міністэрства архітэктуры і будаўніцтва Рэспублікі Беларусь, 2016.
3. ТКП 45-2.04-196-2010. Тепловая защита зданий. Теплоэнергетические характеристики. Правила определения. Минск: Межгос. Совет по

Данилевский Л.Н., Данилевский С.Л. Алгоритм и точность определения теплотехнических показателей зданий // Инженерно-строительный журнал. 2017. № 5(73). С. 49–61.

[Thermal protection of buildings. Heat power characteristics. Rules of definition]. Minsk: Interstate Council for standardization, metrology and certification: Belarusian. State Institute of standardization and certification, 2010. (rus)

4. Vasil'yev G.P., Lichman V.A., Yurchenko I.A., Kolesova M.V. Method of assessment of coefficient of heattechnical uniformity from the analysis of thermograms. *Magazine of Civil Engineering.* 2016. No. 6(66). Pp. 60–67.
5. Korniyenko S.V., Vatin N.I., Gorshkov A.S. Natural heatphysical tests of residential buildings from gas-concrete blocks. *Magazine of Civil Engineering*. 2016. No. 4(64). Pp. 10–25.
6. Levin Ye.V., Okunev A.Yu. Teplovizionnyye obsledovaniya stroitel'nykh ob"yektov. Metodicheskiye pogreshnosti, voznikayushchiye za schet neopredelennosti koeffitsiyenta emissii v usloviyakh razlichnogo fonovogo izlucheniya [Thermovision inspections of construction objects. The methodical errors arising due to uncertainty of coefficient of issue in the conditions of various background radiation]. *BST. 2016.* No. 6. Pp. 30–33. (rus)
7. Kryshov S.I., Kurilyuk I.S. Opyt GBU «TSEIIS» po eksperimental'noy otsenke effektivnosti energosberegayushchikh meropriyatiy v zhilykh i obshchestvennykh zdaniyakh. [Experiment of SBU “CEIIS” by experimental assessment of efficiency of energy saving actions in residential and public buildings]. Trudy seminara “Analiz i prognoz razvitiya otrasley toplivno-energeticheskogo kompleksa” [Works of a seminar "Analysis and the forecast of development of branches of fuel and energy complex"]. Moscow: INP RAS publishing house, 2015. Pp. 20–40. (rus)
8. *BS EN 13829: Thermal performance of buildings*. Determination of air permeability of buildings. Fan pressurization method, 2001.
9. Siddall M. Thermal Bypass: The Impact apon performance of natural and forced convection. *Proceedings of the 13th International Passive House Conference.* Darmstadt, 2009. Pp. 355–360.
10. Siddall M. Long Term experience of the passivhousstandard in North East England: does airtightness decay. *20 Internationale Passivhaustagung.* Darmstadt, 2016. Pp. 389–394.
11. Knissel J., Grossklos M. Luftqualitetsgeführte volumenstromregelung und kontinuerliche erfassung des fensteröffnungszutands. *12. Internationale Passivhaustagung.* Darmstadt, 2008. Pp. 179–184.
12. Kalender V., Heidt F.D. Entwicklung einre Handwerker – Blower – Door. *4. Passivhaus Tagung.* Kassel, 2000. Pp. 409–416.
13. Peper S. Luftdichtheit bei passivhäusern erfahrungen aus über 200 realisierten objekten drucktest ohne blower door. *4. Passivhaus Tagung.* Kassel, 2000. Pp. 367–381.
14. Kirtschig T. Messergebnisse aus dem ENERGON in ULM. *20. Internationale Passivhaustagung.* Darmstadt, 2016. Pp. 253–260.
15. Feist W., Ebel W., Peper S., Hasper W. Langzeiterfahrungen und messergebnisse aus dem ersten passivhaus in Darmstadt-Kranichstein. *20. Internationale Passivhaustagung.* Darmstadt, 2016. Pp. 279–287.
16. Plesser S., Gőrtnes A., Ahrens-Hein O-N., Wissler M. Evalution von 8 Passivhaus-Kitas in Hannover. *19. Internationale Passivhaustagung.* Leipzig, 2015. Pp. 469–474.
17. Hofman A., Hessler F. Technisches Monitoring. *19. Internationale Passivhaustagung.* Leipzig, 2015. Pp. 179–184.
18. Pfluger R., Peper S. Ergebnisse der Messungen in der Passivhaussiedlung Hannover Kronsberg. *4. Passivhaus Tagung.* Kassel, 2000. Pp. 443–456.
19. Bogoslovskiy, V.N. Aspekty sozdaniya zdaniya s

стандартизации, метрологии и сертификации: Белорус. Гос. Ин-т стандартизации и сертификации, 2010.

4. Васильев Г.П., Личман В.А., Юрченко И.А., Колесова М.В. Метод оценки коэффициента теплотехнической однородности из анализа термограмм // Инженерно-строительный журнал. 2016. № 6(66). С. 60–67.
5. Корниенко С.В., Ватин Н.И., Горшков А.С. Натурные теплофизические испытания жилых зданий из газобетонных блоков // Инженерно-строительный журнал. 2016. № 4(64). С. 10–25.
6. Левин Е.В., Окунев А.Ю. Тепловизионные обследования строительных объектов. Методические погрешности, возникающие за счет неопределенности коэффициента эмиссии в условиях различного фонового излучения // БСТ. 2016. № 6. С. 30–33.
7. Крышов С.И., Курилюк И.С. Опыт ГБУ «ЦЭИИС» по экспериментальной оценке эффективности энергосберегающих мероприятий в жилых и общественных зданиях // Труды семинара «Анализ и прогноз развития отраслей топливно-энергетического комплекса». Москва: Издательство ИНП РАН, 2015. С. 20–40.
8. BS EN 13829: Thermal performance of buildings. Determination of air permeability of buildings. Fan pressurization method, 2001.
9. Siddall M. Thermal Bypass: The Impact apon performance of natural and forced convection // Proceedings of the 13th International Passive House Conference. Darmstadt, 2009. Pp. 355–360.
10. Siddall M. Long Term experience of the passivhousstandard in North East England: does airtightness decay // 20 Internationale Passivhaustagung. Darmstadt, 2016. Pp. 389–394.
11. Knissel J., Grossklos M. Luftqualitetsgeführte volumenstromregelung und kontinuerliche erfassung des fensteröffnungszutands // 12. Internationale Passivhaustagung. Darmstadt, 2008. Pp. 179–184.
12. Kalender V., Heidt F.D. Entwicklung einre Handwerker – Blower – Door // 4. Passivhaus Tagung. Kassel, 2000.4 Pp. 409–416.
13. Peper S. Luftdichtheit bei passivhäusern erfahrungen aus über 200 realisierten objekten drucktest ohne blower door // 4. Passivhaus Tagung. Kassel, 2000. Pp. 367–381.
14. Kirtschig T. Messergebnisse aus dem ENERGON in ULM // 20. Internationale Passivhaustagung. Darmstadt, 2016. Pp. 253–260.
15. Feist W., Ebel W., Peper S., Hasper W. Langzeiterfahrungen und messergebnisse aus dem ersten passivhaus in Darmstadt-Kranichstein // 20. Internationale Passivhaustagung. Darmstadt, 2016. Pp. 279–287.
16. Plesser S., Gőrtnes A., Ahrens-Hein O-N., Wissler M. Evalution von 8 Passivhaus-Kitas in Hannover // 19. Internationale Passivhaustagung. Leipzig, 2015. Pp. 469–474.
17. Hofman A., Hessler F. Technisches Monitoring // 19. Internationale Passivhaustagung. Leipzig, 2015. Pp. 179–184.
18. Pfluger R., Peper S. Ergebnisse der Messungen in der Passivhaussiedlung Hannover Kronsberg // 4. Passivhaus Tagung. Kassel, 2000. Pp. 443–456.
19. Богословский В.Н. Аспекты создания здания с эффективным использованием энергии //АВОК. 2000. № 5. С. 34–39.
20. Данилевский Л.Н. Способ определения общего коэффициента теплопередаче здания. Патэнт на вынаходства №18898 РБ по заявке от 20.12.2010 г. № a20101504 МПК(2009) G 01 N 25/00.
21. Данилевский Л.Н. Методика определения теплоэнергетических характеристик эксплуатируемых

Danilevsky L.N., Danilevsky S.L. The algorithm and accuracy of definition of heattechnical indicators of buildings. *Magazine of Civil Engineering*. 2017. No. 5. Pp. 49–61. doi: 10.18720/MCE.73.5.

effektivnym ispol'zovaniyem energii [Aspects of creation of the building with effective use of energy]. *ABOK*. 2000. No. 5. Pp. 34–39. (rus)

20. Danilevskiy L.N. *Sposob opredeleniya obshchego koeffitsiyenta teploperedache zdaniya* [Way of determination of the general coefficient to a building heat transfer]. L.N. Danilevskiy. Patent for the withdrawal No. 18898 RB on the application dated 20.12.2010 No. a20101504 IPC (2009) G 01 N 25/00. (rus)
21. Danilevskiy L.N. Metodika opredeleniya teploenergeticheskikh kharakteristik ekspluatiruyemykh zdaniy [Technique of definition of heat power characteristics of the operated buildings]. *Construction science and technology*. 2010. No. 6. Pp. 31–35. (rus)
22. *State Standard of the Republic of Belarus STB 2409-2015.* Metod opredeleniya udel'nogo raskhoda teplovoy energii na otopleniye i ventilyatsiyu ekspluatiruyemykh zhilykh zdaniy [Method for determining the specific consumption of heat energy for heating and ventilation of operated residential buildings]. Minsk, 2015. 42 p. (rus)
23. Danilevskiy L.N., Terekhov S.V., Terekhova I.A., Korizna I.A. Metod opredeleniya udel'nogo raskhoda teplovoy energii na otopleniye i ventilyatsiyu mnogokvartirnykh zhilykh zdaniy i usloviya yego primeneniya [Method of determination of specific heat consumption for heating and ventilation of multi-apartment residential buildings and conditions of its application]. *Architecture and Construction*. 2014. No. 1. Pp. 52–58. (rus)
24. Danilevskiy L.N., Danilevskiy S.L. *Sposob opredeleniya udel'nogo koeffitsiyenta teplovykh poter' zdaniya* [A method for determining the specific coefficient of thermal losses of a building]. L.N. Danilevskiy, S. L. Danilevskiy. Application for the grant of a patent of the Republic of Belarus for invention, No. a20150303. 03.06.2015. (rus)
25. Danilevskiy L.N., Danilevskiy S.L. Opredeleniye teploenergeticheskikh kharakteristik i energeticheskaya klassifikatsiya ekspluatiruyemykh zhilykh zdaniy [Determination of the thermal power characteristics and energy classification of the exploited residential buildings]. *BST*. 2016. No. 6. Pp. 45–47. (rus)
26. *EN 15603:2008 Enery performance of buildings – overall use and definition of energy ratings.* CEN. European Commitee vor Standardisation, 2008.
27. Khudson D. *Statistika dlya fizikov* [Statistics for physicists]. Moscow: Mir, 1970. 296 p. (rus)
28. *Changing No 1 2.04.02-2000 BNB.* Budaŭníchaya klímatalogíya [Construction climatology]. 33 p. (bel)
29. *Actualized version of SNIP 23-01-99.* Stroitel'naya klimatologiya [Construction climatology]. Ministry of Regional Development of the Russian Federation. Moscow, 2012. 108 p. (rus)
30. Dzhonson N., Lion F. Statistika i planirovaniye eksperimenta v tekhnike i nauke. Metody obrabotki dannyh [Statistics and experiment planning in engineering and science. Methods of data processing]. Moscow: Mir, 1980. 610 p. (rus)

зданий // Строительная наука и техника. 2010. № 6. С. 31–35.

22. Метод определения удельного расхода тепловой энергии на отопление и вентиляцию эксплуатируемых жилых зданий. Государственный стандарт Республики Беларусь СТБ 2409-2015. Минск, 2015. 42 с.
23. Данилевский Л.Н., Терехов С.В., Терехова И.А., Коризна И.А. Метод определения удельного расхода тепловой энергии на отопление и вентиляцию многоквартирных жилых зданий и условия его применения // Архитектура и строительство. 2014. № 1. С. 52–58.
24. Данилевский Л.Н., Данилевский, С.Л. Способ определения удельного коэффициента тепловых потерь здания // Заявление о выдаче патента РБ на изобретение, № a20150303 от 03.06.2015.
25. Данилевский Л.Н., Данилевский С.Л. Определение теплоэнергетических характеристик и энергетическая классификация эксплуатируемых жилых зданий // БСТ. 2016. № 6. С. 45–47.
26. EN 15603:2008 Enery performance of buildings – overall use and definition of energy ratings. CEN. European Commitee vor Standardisation, 2008.
27. Худсон Д. Статистика для физиков. Москва: «Мир», 1970г. 296 с.
28. Змяненне № 1 БНБ 2.04.02-2000. Будаўнічая кліматалогія. 33 с.
29. Актуализированная версия СНиП 23-01-99. Строительная климатология. Министерство регионального развития Российской Федерации. Москва, 2012. 108 с.
30. Джонсон Н., Лион Ф. Статистика и планирование эксперимента в технике и науке. Методы обработки данных. Москва: «Мир», 1980г. 610 с.

Leonid Danilevski,
+3(7533)3003911; leonik@tut.by

Sergey Danilevsky,
+3(7617)3663272; niptis-7@tut.by

Леонид Николаевич Данилевский,
+3(7533)3003911; эл. почта: leonik@tut.by

Сергей Леонидович Данилевский,
+3(7617)3663272; эл. почта: niptis-7@tut.by

Данилевский Л.Н., Данилевский С.Л. Алгоритм и точность определения теплотехнических показателей зданий // Инженерно-строительный журнал. 2017. № 5(73). С. 49–61.

doi: 10.18720/MCE.73.6

The probabilistic-statistical modeling of the external climate in the cooling period

Вероятностно-статистическое моделирование наружного климата в охладительный период

O.D. Samarin,
National Research Moscow State University of Civil Engineering, Moscow, Russia

Канд. техн. наук, доцент О.Д. Самарин,
Национальный исследовательский Московский государственный строительный университет, Москва, Россия

Key words: probabilistic-statistical model; climate; typical year; safety index; Monte-Carlo procedure; temperature; the cooling period

Ключевые слова: вероятностно-статистическая модель; климат; типовой год; коэффициент обеспеченности; метод Монте-Карло; температура; охладительный период

Abstract. Currently, the successful development of construction industry depends on the improved energy performance of buildings, structures and facilities, as well on the quality estimation of the outdoor climate. The problem of feasibly more accurate determination of energy consumption by climatic systems in buildings is a very high-priority task now because of decrease of energy and fuel sources and because of actualization of building standards in many countries. That is why it is very important to find simple but enough accurate dependences between climatic parameters in the heating as well as in the cooling seasons of a year. In the paper the modern principles accepted in different countries for the selection of the design climate information for the design of building envelopes and systems to ensure building microclimate are considered. Main shortcomings of the methods, including the concept of "typical year", are shown and the advantages of generating climate data arrays programmatically with the use of a pseudorandom number generator are described. Some results of the calculation of current temperature of the external air during the warm period of the year with different safety are presented using numerical modeling with Monte-Carlo procedure. The possibility of practical implementation of probabilistic-statistical principle of climatic data for some calculations relating to climatic systems and thermal regime of the building are shown. The comparison of the obtained values with the analytical expression for the normal distribution of random variables is presented and relationships for the selection of its main parameters according to the existing climatic manuals are proposed.

Аннотация. В настоящее время успешное развитие строительной отрасли зависит от повышения энергетической эффективности зданий, строений и сооружений и в то же время от качественной оценки параметров наружного климата. Задача возможно более точного определения энергопотребления климатическими системами зданий имеет очень большое значение в связи с исчерпанием запасов органического топлива и других ресурсов, а также в связи с актуализацией нормативной базы многих стран в области строительства. Поэтому очень важно располагать простыми, но одновременно достаточно точными зависимостями между климатическими параметрами как в отопительный, так и в охладительный периоды года. В работе рассмотрены принятые в настоящее время в различных странах принципы выбора расчетной климатической информации для проектирования ограждающих конструкций и систем обеспечения микроклимата зданий. Отмечены основные недостатки методик, включающих понятие «типового года», и описаны преимущества генерации массивов климатических данных программным способом с применением датчиков псевдослучайных чисел. Приведены некоторые результаты расчета срочной температуры наружного воздуха в теплый период года с различной обеспеченностью при помощи численного моделирования методом Монте-Карло. Показана возможность практической реализации вероятностно-статистического принципа формирования климатических данных для некоторых расчетов, касающихся систем климатизации и теплового режима здания. Представлено сопоставление полученных значений с аналитическим выражением для нормального закона распределения случайной величины и предложены соотношения для подбора ее основных параметров по имеющимся нормативным данным в области строительной климатологии.

Samarin O.D. The probabilistic-statistical modeling of the external climate in the cooling period. *Magazine of Civil Engineering*. 2017. No. 5. Pp. 62–69. doi: 10.18720/MCE.73.6.

Introduction

One of the main approaches to determination of design parameters of external climate for designing external enclosures and climatic system of buildings is based on using factor k_h (so called safety index), which represents the likelihood that actual value of considered parameter upon operation of the building will not exceed set thresholds i.e. it will not exceed this threshold in hot period of the year and will not be lower in cold period. The expression for k_h should have the following view [1]:

$$k_h = 1 - \frac{\Delta N}{N} \text{ or } k_h = 1 - \frac{\Delta z}{z}, \quad (1)$$

where N is a total number of supervision events when the parameter exceeds established threshold; z is general time of supervisions; Δz is a duration of time interval when the parameters exceeds threshold value. The first variant is used for evaluation of discrete events k_h, for example, the coldest five days or days, and the second variant is used for determination of the level of general climatic parameters for hot and cold period. However, definite conditions may require parameters under other value k_h that differs from those, for which the values are represented in the source. Especially, this relates to significant and responsible facilities when customer requires high reliability and, respectively, value k_h.

Therefore, in this paper, the object of study is the design outdoor temperature for design of the microclimate systems during the cooling period of the year with a specified safety index. Probabilistic-statistical model of external climate allows determination of scientifically grounded level for this temperature. It can be shown that this model efficiently describes basic ratio between different parameters [2–3] regardless the availability of two main factors that affect formation of these parameters, i.e. regular seasonal trend and fluctuations against this trend that are actually close to random ones.

This method has definite benefits over so-called “typical year” [4–10] that is accepted in many cases and described in details in the last versions of recommendations ASHRAE [11–12]. Eventually, they provide for the selection of so-called “typical meteorological months” chosen from long-time data base (the last variant for the period from 1982 to 2006). Moreover, the data for each day and hour of each month of the year can be selected from different years of considered period, i.e. they are real, so that resultant deviation from the average temperature for this period doesn’t exceed 0.1 °C. Then the massive is analyzed for the respective parameters (in particular, temperature) with necessary reliability. In [13–14] some elements of probabilistic-statistical models were presented, but, again, it is not aimed at obtaining in-depth evaluation of dependencies. So, the benefits of probability/statistical method relate to the absence of the need in the search for accumulation of the large volume of climatic data and their special selection so that these data correspond to the requirements applied to their representatively. Moreover, there is no need in loading of such large amount of data to software. Finally, the method based on ‘typical year’ is less oriented at obtaining any point estimates, including determination of certain external air temperatures t_{ex} with set reliability. The latter is necessary for the correct selection of processes of the supply air treatment in the cooling period and for calculation of installed power of air-conditioning equipment. In the practice of building regulation in several countries, including the Russian Federation and some others, that the safety index of climate parameters forms the basis of their definition, therefore, the application of probabilistic-statistical modeling will allow the most simple way to solve the problem of selection of HVAC equipment within design conditions of the cooling period with any k_h required by the customer.

Generally speaking, the recommendations of the ASHRAE, especially [12], also provide for the regulation of temperatures t_{ex} using a certain analogue of k_h, namely the indication of temperature values the ambient air dry bulb temperature corresponding to 0.4, 1.0, or 2.0 % annual cumulative frequency of occurrence (warm conditions). Unlike the k_h's is that at use of formula (1) in the denominator will be the duration of the cooling period only and not the whole year. However, here the frequency is fixed, and for intermediate values, the corresponding data do not exist.

A slightly different approach is proposed in [15], where t_{ex} is associated with the characteristics of the thermal resistance of the premises and solutions for automatic control of climate systems, but in spite of the physical validity, it is difficult to apply at the stage of making preliminary decisions due to the lack of reliable data on the characteristics of the object of regulation.

Thus, the purpose of this study is to determine key design parameters of external climate in warm season with arbitrary safety index with the help of probabilistic-statistical model. Objectives of the study are to build an algorithm that implements this model, and obtaining analytical dependences for the calculated outside temperature according to the results of approximation results software generation.

Самарин О.Д. Вероятностно-статистическое моделирование наружного климата в охладительный период // Инженерно-строительный журнал. 2017. № 5(73). С. 62–69.

Methods

Probabilistic-statistical model is based on determination of urgent ambient air temperature and associated correlation enthalpy as a random value distributed under normal law and characterized by certain expected mean *M(t)* and mean-square deviation σ_t. It should be noted that regular and stochastic factors that determine the behavior of urgent temperature can be tracked separately without significant complication of the algorithm upon computer-based calculations. In studies case, seasonal trend was simulated by the input of float mean that varied within the year under sinusoidal law within the amplitude A_t that corresponds to the half of the difference of average temperatures of the hottest and the coldest month with the maximum near July 31, i.e. on 210th day from the beginning of the year. Then stochastic component with corresponding value σ_t was applied to resultant value. This was performed by means of quasi-random number counter that generates values that are subject to normal distribution law. Considered approach is one of the variants of Monte-Carlo procedure. In variant of ECM program, realized by the author, the generated was performed for the period of 100 years. Then obtained temperatures were ranked in ascending order. This allows building unknown dependency of t_{ex} from k_h.

Results and Discussion

On figure 1, red line indicates results for climatic conditions of Moscow. In this case, mean annual temperature t_{mean} that is equal to +5.4 °C was taken as expected mean. Value A_t of 13.25 °C was considered and the value of amplitude of daily rate of urgent temperatures in hot period, i.e. 9.6 °C was taken as σ_t. It should be noted that in climatic terms the amplitude is considered as the difference between maximum and minimum value within a day since half size value of mathematic amplitude should be used as σ_t for modeling the behavior of not urgent but mean daily temperatures. Moreover, not directly k_h but the probability of contrary event (urgent temperature exceeds its current value, i.e. $1 - k_h$) is taken as independent variable. This is not fundamental importance but it will simplify obtained approximate relationships.

Black line on figure 1 shows approximation of disclosed dependency in the following form (2):

$$t_{ex} = a \ln\left(1-k_h\right) + b \tag{2}$$

Acceding to the results of regression analysis a = –4.51, b = 9.1 and correlation ratio r = 0.996. Obviously, this expression ensures rather high degree of approximation, considering its simplicity and statistical nature of used initial data that inevitably have variation.

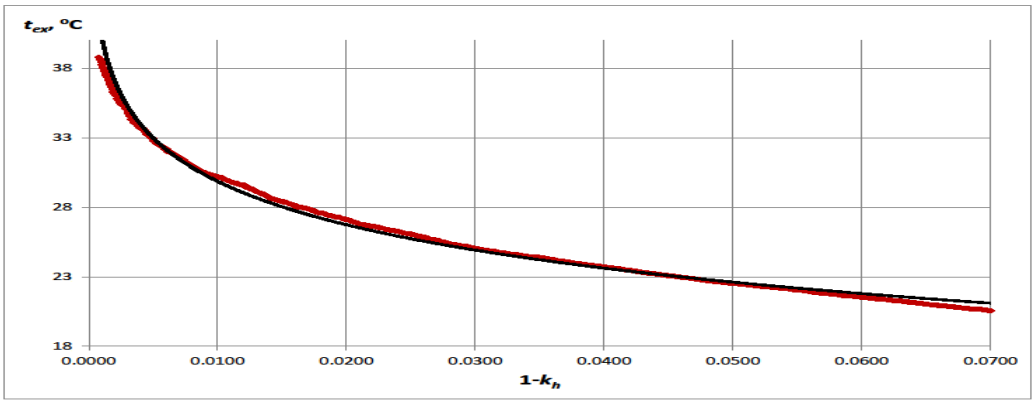

Figure 1. Results of software generation t_{ex} depending on $1 - k_h$ and their approximation (2)

It should be noted that the use of theoretical dependency that directly derives from main probabilistic-statistical model gives higher deviation as we can see on the Figure 2 where red continuous line indicates calculation results by program and black dotted line indicates calculation by formula (3):

$$t_{ex} = t_{mean} + \sigma_t \sqrt{-1.592 \ln\left[1-\left(1-2k_h\right)^2\right]} \tag{3}$$

Samarin O.D. The probabilistic-statistical modeling of the external climate in the cooling period. *Magazine of Civil Engineering*. 2017. No. 5. Pp. 62–69. doi: 10.18720/MCE.73.6.

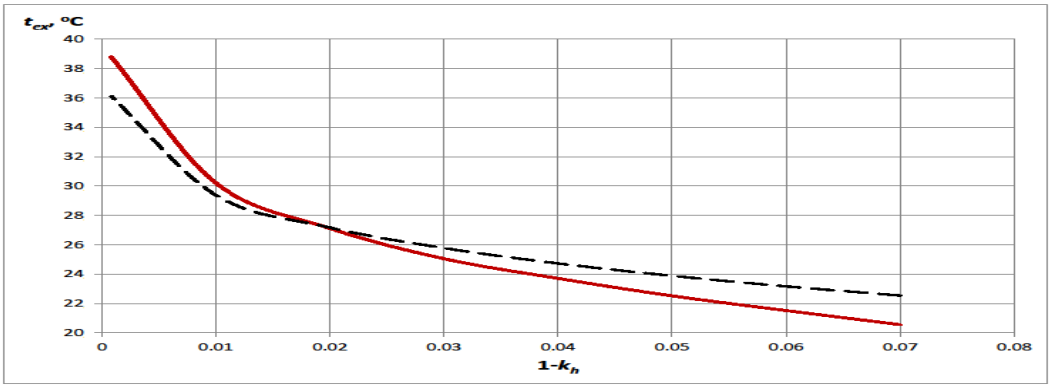

Figure 2. The results of software generation t_{ex} depending on 1 – k_h and their comparison with data (3)

This formula is built, considering known approximate expression for error function *erf* at large values of the argument since the model based on normal distribution law provides the dependency in the following from [2–3]:

$$k_h = \frac{1}{2}\left(1+erf\left[\frac{t_{ex}-t_{mean}}{\sigma_t\sqrt{2}}\right]\right) \tag{4}$$

It can be assumed that revealed difference is associated with model refinement that is realized in the software and relates to tracking of seasonal nature of the change of external temperature.

Since probabilistic-statistical model provides for the unity of the mechanism for formation of urgent temperature regardless definite construction area and, respectively, the generality of corresponding dependencies, there are solid grounds for stating that the expression in the form (2) is true for all cases and differs only in *a* and *b* values. Therefore, the main task of probabilistic-statistical modeling was to find common type of control $t_{ex} = f(k_h)$, and definite level of numerical radios may be selected by identification of the model, considering available fixed points.

Considering arbitrary probability of fixed temperature values from (2), we find:

$$a=\frac{t_{ex1}-t_{ex2}}{\ln\left(\frac{1-k_{h1}}{1-k_{h2}}\right)};$$
$$b=t_{ex1}-a\ln\left(1-k_{h1}\right)=t_{ex2}-a\ln\left(1-k_{h2}\right), \tag{5}$$

where t_{ex1} и t_{ex2} are design external air temperatures basing on the data of this or that source with respective reliability k_{h1} and k_{h2}. For instance, for Moscow t_{ex1} = +23 °C and t_{ex2} = +26 °C at k_{h1} = 0.95 and k_{h2} = 0.98, respectively, where we find a = –3.3, b = 13.1. These values differ from values obtained from the results of approximation of software generation data but, as it was mentioned above, the purpose of this generation was to disclose dependency form (2). However, the nature of the curves on Figure 1, especially approximating dependency, suggests that their difference from normative values is not very high and does not exceed one degree.

The accuracy and reliability of the results obtained by using dependence (2) with the coefficients calculated by the expressions (5), can be seen from the graphs in figures 3 and 3a. Here, the solid line shows the results of calculations by the proposed method, and dotted line – data from existing observations [13]. In the figure 3, lines 1 refer to the conditions of Moscow; the lines 2 represent the city with substantially more hot and dry climate – Samara. The graph in the Figure 3a refers to the intermediate parameters of Khabarovsk. It is easy to see that the agreement is pretty good, noticeable discrepancies arise only at very high $k_h \to 1$, which can be explained by the presence of a minimum time interval of averaging measurement results ambient temperature (typically one hour), so that its extreme values in hourly aggregates do not fall. The red lines show the data of ASHRAE [12] with the appropriate conversion. As it can be seen, here the similarity is also quite satisfactory.

Самарин О.Д. Вероятностно-статистическое моделирование наружного климата в охладительный период // Инженерно-строительный журнал. 2017. № 5(73). С. 62–69.

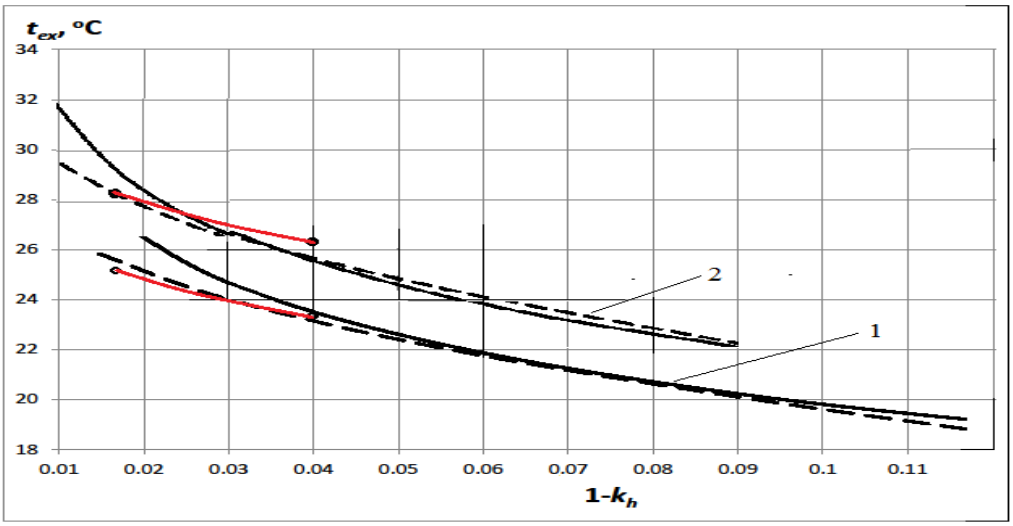

Figure 3. Comparison of calculations by formulas (2), (5) with climate data for Moscow and Samara

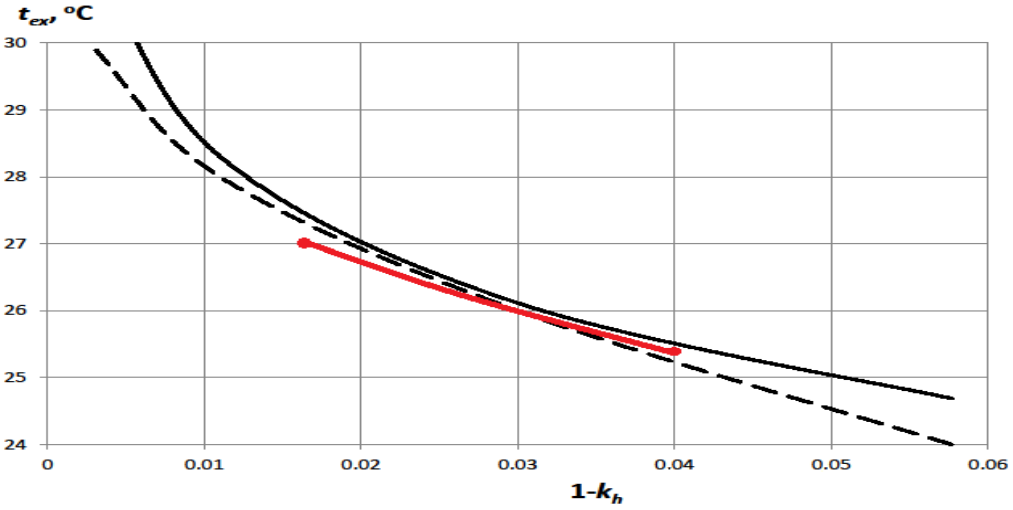

Figure 3a. Comparison of calculations by formulas (2), (5) with climate data for Khabarovsk

If you conduct additional calculations on above-mentioned ECM program at different A_t within the limits from 10 to 15 °C, which is peculiar for most countries of Central and Eastern Europe, it is possible to obtain ratios for parameters *a* and *b* in the following forms through further regressive analysis:

$$a=-0.325A_t\ ;\ b=0.275A_t+t_{mean}\ , \tag{6}$$

where $A_t=\frac{t_{hm}-t_{cm}}{2}$.

Correlation ratio is not less than 0.99. t_{hm} and t_{cm} are temperatures of the hottest and the coldest month in considered region, i.e. A_t value is nothing else but the amplitude of annual cycle of mean monthly temperatures [2–3]. Moreover, it was understood that there is correlation ratio between σ_t and A_t in considered target area:

$$\sigma_t=(0.67\pm0.13)A_t\ . \tag{7}$$

Thus, the most probable change of σ_t after A_t is considered in (6) automatically. Since values t_{hm}, t_{cm} and t_{mean} for any rather large settlement can be taken from normative and reference documents that are valid in this or that country, it is possible to conclude that the ratio (2), considering (6), is easy-to-use since it requires maximum quantity of accessible initial data.

Samarin O.D. The probabilistic-statistical modeling of the external climate in the cooling period. *Magazine of Civil Engineering*. 2017. No. 5. Pp. 62–69. doi: 10.18720/MCE.73.6.

In this respect, the data offered by ASHRAE [11, 12], is less convenient because, first, does not contain the necessary analytical dependences, but only discrete values of temperatures and other parameters, and secondly, forcing users to resort to self-selecting the required values from the available array. The same applies to more recent studies [4–10], as they support the same methodological approach. Analytical relations are given for example in [7], but they refer to average temperatures, without considering the stochastic component, and [14, 16], despite the elements of probability and statistical consideration, are not aimed at providing analytical assessments.

It should also be noted that models using probabilistic-statistical approach are especially suitable for calculation of annual power consumption of the building upon estimation of energy saving class that is very critical today in the context of depletion of the reserves of organic fuel and increased attention to energy conservation that is observed in most European and other countries [17–22]. Although discussed in the present work a variant of probabilistic-statistical modeling aimed, as mentioned, primarily on the calculation of climatic parameters for estimating installed capacity of HVAC equipment with the required security, in principle it can be used to calculate annual energy consumption. It is enough to integrate the product of the expression containing the difference between t_{ex} (2) and the corresponding temperature of supply or internal air t_{in} for the value $1 - k_h$, because from (1) the difference $1 - k_h$ shows the relative number of hours standing t_{ex}, which is greater than the current value. Then, for example, by expressing additionally the required value $1 - k_h$ from (2) using the set value t_{in}, the degree-days of cooling period can be calculated to determine the total cold consumption by the expression:

$$D_d = 24 \exp\left(\frac{t_{in} - b}{a}\right)\left(t_{in} - a\right). \quad (8)$$

Taking by the requirements of ASHRAE [13] the boundary value t_{in} = +15.11 °C (65 °F) and the values of *a* and *b*, obtained when plotting figure 3, we can calculate for Moscow D_d = 116 K•day, for Samara 215 K•day. The actual values in [12] are, respectively, 107 and 199 K•day, i.e. the divergence is of only about 8 percent, which is sufficient for engineering calculations considering the simplicity of the obtained relationships.

Conclusion

1. It is confirmed that the probability/statistical modeling can be used for creation of climatic data array upon definite calculations associated with thermal mode of rooms and environmental control systems and selection of design parameters of external climate with required reliability;

2. It has been shown that probability/statistical modeling is suitable for development of simplified models, aimed at determining integral characteristics of the building, enclosures and engineering systems for definite time;

3. It is proved that the results of the probabilistic-statistical modeling reliably and with acceptable accuracy for practice reflect the real data of climate observations from different sources for a significant number of construction areas;

4. Using the probabilistic-statistical model, the formulas are obtained for calculating the design temperature of external air in cooling period for the design of cooling systems and the degree-days of cooling period to determine the total energy consumption with any required safety index;

5. Accessible results are represented in engineering form with use of only basic values that are available from existing sources and can be used in design practice.

References

1. Kuvshinov Yu.Ya. *Energosberezheniye v sisteme obespecheniya mikroklimata zdaniy* [Energy saving in the building microclimate system]. Moscow: MSUCE – ASV Publ. 2010. 320 p. (rus)
2. Samarin O.D. O podtverzhdenii veroyatnostno-statisticheskikh sootnosheniy mezhdu raschetnymi parametrami naruzhnogo klimata [On verifying of probable and statistical correlation between design parameters of external climate]. *Izvestiya vuzov. Stroitel'stvo.* 2014. No. 3. Pp. 66–69. (rus)
3. Samarin O.D. Veroyatnostno-statisticheskiy vybor massivov predstavitel'nykh klimaticheskikh dannykh [On the probable and statistical choice of arrays of representative cliate data] // *Vestnik MGSU*. 2016. No. 2. Pp. 98–105. (rus)
4. Malyavina E.G., Ivanov D.S. Razrabotka raschetnogo

Литература

1. Кувшинов Ю.Я. Энергосбережение в системе обеспечения микроклимата зданий. М.: МГСУ – Изд-во Ассоциации строительных вузов, 2010. 320 с.
2. Самарин О.Д. О подтверждении вероятностно-статистических соотношений между расчетными параметрами наружного климата // Известия вузов. Строительство. 2014. № 3. С. 66–69.
3. Самарин О.Д. Вероятностно-статистический выбор массивов представительных климатических данных // Вестник МГСУ. 2016. № 2. С. 98–105.
4. Малявина Е.Г., Иванов Д.С. Разработка расчетного «типового» года для определения теплопотерь заглубленных в грунт частей здания // Труды Главной геофизической обсерватории им. А.И. Воейкова. 2014.

Самарин О.Д. Вероятностно-статистическое моделирование наружного климата в охладительный период // Инженерно-строительный журнал. 2017. № 5(73). С. 62–69.

"tipovogo" goda dlya opredeleniya teplopoter' zaglublennykh v grunt chastey zdaniya [The development of the design "typical" year for definition of heat losses of soiled parts of buildings]. *Trudy Glavnoy geofizicheskoy observatorii im. A.I.Voeykova* [Papers of the Main geophysical observatory named A.I.Voeykov]. 2014. No. 571. Pp. 182–191. (rus)

5. Gagarin V.G., Ivanov D.S., Malyavina E. G. Razrabotka klimatologicheskoy informacii v forme specializirovannogo "tipovogo goda" [The development of climatic information in the form of specialized "typical year"]. *Vestnik VolgGASU.* Ser.: Str-vo i archit. 2013. No. 31(50). P. 1. Pp. 343–349. (rus)
6. Kryuchkova O. Yu. Inzhenernaya metodika rascheta godovykh zatrat energii i vody central'nymi ustanovkami kondicionirovaniya vozdukha [The engineering procedure of calculation of annual water and energy consumption by the central air conditioning units]. *Internet-vestnik VolgGASU.* Ser.: Politematicheskaya. 2013. Vol. 4(29). [Electronic resource]. System requirements: Windows 7. URL: http://vestnik.vgasu.ru/attachments/ Kryuchkova-2013_4(29).pdf. (rus)
7. Zukowski M., Sadowska B., Sarosiek W. *Assessment of the cooling potential of an earth-tube heat exchanger in residential buildings.* Vilnius : VGTU Publishers, 2011. Vol. 2. Pp. 830–834.
8. Ecevit A., Akinoglu B. G., Aksoy B. Generation of a typical meteorological year using sunshine duration data. *Energy*. 2002. Vol. 27. No. 10. Pp. 947–954.
9. Masson V. A physically-based scheme for the urban energy budget in atmospheric models. *Boundary-Layer Meteorology.* 2000. Vol. 94. No. 3. Pp. 357–397.
10. Wang J., Zhai Z., Jing Y., Zhang C. Influence analysis of building types and climate zones on energetic, economic and environmental performances of BCHP systems. *Applied Energy.* 2011. No. 88(9). Pp. 3097–3112.
11. *Weather Year for Energy Calculations.* Atlanta : American Society of Heating, Refrigerating, and AirConditioning Engineers, Inc. (ASHRAE), 1985.
12. *Handbook 2009 – Fundamentals*. Chapter 14. Climatic Design Information. Atlanta : American Society of Heating, Refrigerating, and AirConditioning Engineers, Inc. (ASHRAE), 2009.
13. *Stroitel'naya klimatologiya.* Spravochnoye posobie k SNiP 23-01-99* [Building climatology. User manual to SNiP 23-01-99*]. Under ed. of V.K.Savin. Moscow: NIISF Publ., 2006. 260 p. (rus)
14. Naji S., Alengaram U.J., Jumaat M.Z., Shamshirband S., Basser H., Keivani A., Petković D. Application of adaptive neuro-fuzzy methodology for estimating building energy consumption. *Renewable and Sustainable Energy Reviews.* 2016. Vol. 53. Pp. 1520–1528.
15. Sotnikov A.G. Analytic method of determination of the external design parameters in the microclimate systems of buildings. Magazine of Civil Engineering. 2013. No. 2. Pp. 3–12. (rus)
16. Wang X., Mei Y., Li W., Kong Y., Cong X. Influence of sub-daily variation on multi-fractal detrended analysis of wind speed time series. *PLoS ONE.* 2016. Vol. 11. No. 1. Pp. 6014–6284.
17. Kobysheva N.V., Klyuyeva M.V., Kulagin D.A. Klimaticheskiye riski teplosnabzheniya gorodov [Climatic risks of city heat supply]. *Trudy Glavnoy geofizicheskoy observatorii im. A.I.Voeykova* [Papers of the Main Voeykov's Geophysical Observatory]. 2015. No. 578. Pp. 75–85. (rus)
18. Kornienko S.V. Metod resheniya trekhmernoy zadachi sovmestnogo nestacionarnogo teplo- i vlagoperenosa dlya ograzhdayushchikh konstrukciy zdaniy [The procedure of solving the three-dimensional problem of joint heat and moisture transfer for the building enclosures]. *News of higher educational institutions. Construction.* 2006. No. 2. Pp. 108–110. (rus)

№ 571. С. 182–191.

5. Гагарин В.Г., Иванов Д.С., Малявина Е.Г. Разработка климатологической информации в форме специализированного «типового года» // Вестник ВолгГАСУ. Сер.: Стр-во и архит. 2013. № 31(50). Ч. 1. Города России. Проблемы проектирования и реализации. С. 343–349.
6. Крючкова О.Ю. Инженерная методика расчета годовых затрат энергии и воды центральными уста-новками кондиционирования воздуха // Интернет-вестник ВолгГАСУ. Сер.: Политематическая. 2013. № 4(29). [Электронный ресурс]. Систем. требования: Windows 7. URL: http://vestnik.vgasu.ru/attachments/ Kryuchkova-2013_4(29).pdf
7. Zukowski M., Sadowska B., Sarosiek W. Assessment of the cooling potential of an earth-tube heat exchanger in residential buildings. Vilnius: VGTU Publishers, 2011. Vol. 2. Pp. 830–834.
8. Ecevit A., Akinoglu B. G., Aksoy B. Generation of a typical meteorological 2017 using sunshine duration data // Energy. 2002. Vol. 27. No. 10. Pp. 947–954.
9. Masson V. A physically-based scheme for the urban energy budget in atmospheric models // Boundary-Layer Meteorology. 2000. Vol. 94. No. 3. Pp. 357–397.
10. Wang J., Zhai Z., Jing Y., Zhang C. Influence analysis of building types and climate zones on energetic, economic and environmental performances of BCHP systems // Applied Energy. 2011. No. 88(9). Pp. 3097–3112.
11. Weather Year for Energy Calculations. Atlanta: American Society of Heating, Refrigerating, and AirConditioning Engineers, Inc. (ASHRAE), 1985.
12. Handbook 2009 – Fundamentals. Chapter 14. Climatic Design Information. Atlanta : American Society of Heating, Refrigerating, and AirConditioning Engineers, Inc. (ASHRAE), 2009.
13. Строительная климатология. Справочное пособие к СНиП 23-01-99*. Под ред. В.К.Савина. М.: НИ-ИСФ. 2006. 260 с.
14. Naji S., Alengaram U.J., Jumaat M.Z., Shamshirband S., Basser H., Keivani A., Petković D. Application of adaptive neuro-fuzzy methodology for estimating building energy consumption // Renewable and Sustainable Energy Reviews. 2016. Vol. 53. Pp. 1520–1528.
15. Сотников А. Г. Аналитическая методика определения наружных расчетных параметров в системах микроклимата зданий // Инженерно-строительный журнал. 2013. № 2. С. 3–12.
16. Wang X., Mei Y., Li W., Kong Y., Cong X. Influence of sub-daily variation on multi-fractal detrended analysis of wind speed time series. PLoS ONE. 2016. Vol. 11. No. 1. Pp. 6014–6284.
17. Кобышева Н.В., Клюева М.В., Кулагин Д.А. Климатические риски теплоснабжения городов // Труды Главной геофизической обсерватории им. А.И.Воейкова. 2015. № 578. С. 75–85.
18. Корниенко С.В. Метод решения трехмерной задачи совместного нестационарного тепло- и влагопереноса для ограждающих конструкций зданий // Известия высших учебных заведений. Строительство. 2006. № 2. С. 108–110.
19. Гагарин В.Г., Козлов В.В. О нормировании теплозащиты и требованиях расхода энергии на ото-пление и вентиляцию в проекте актуализированной редакции СНиП «Тепловая защита зданий» // Вестник Волгоградского государственного архитектурно-строительного университета. Серия: Строительство и архитектура. 2013. № 31-2 (50). С. 468–474.
20. Рымаров А.Г., Савичев В.В. Особенности работы регенеративной системы вентиляции административного здания // Вестник МГСУ. 2013. № 3.

Samarin O.D. The probabilistic-statistical modeling of the external climate in the cooling period. *Magazine of Civil Engineering*. 2017. No. 5. Pp. 62–69. doi: 10.18720/MCE.73.6.

19. Gagarin V.G., Kozlov V.V. O normirovanii teplozashchityi I trebovaniyakh raskhoda energii na otoplenie I ventilytsiyu v proekte aktualizirovannogoy redaktsii SNiP «Teplovaya zashchita zdanij» [About rationing thermal protection requirements and energy consumption for heating and ventilation in the project version of the updated SNIP "Thermal Protection of Buildings"]. *Vestnik VolgGASU Seriya: Stroitel'stvo i arkhitektura.* 2013. No. 31-2(50). Pp. 468–474. (rus)
20. Rymarov A.G., Savichev V.V. Osobennosti raboty regenerativnoy sistemy ventilyacii administrativnogo zdaniya [Features of operation of the regenerative ventilating system of the administrative building]. *Vestnik MGSU*. 2013. No. 3. Pp. 174–177. (rus)
21. Jedinák R. Energy Efficiency of Building Envelopes. *Advanced Materials Research.* 2013. Vol. 855. Pp. 39–42.
22. Hani A., Koiv T.-A. Energy Consumption Monitoring Analysis for Residential, Educational and Public Buildings. *Smart Grid and Renewable Energy.* 2012. Vol. 3. No. 3. Pp. 231–238.

C. 174–177.

21. Jedinák R. Energy Efficiency of Building Envelopes // Advanced Materials Research. 2013. Vol. 855. Pp. 39–42.
22. Hani A., Koiv T.-A. Energy Consumption Monitoring Analysis for Residential, Educational and Public Buildings // Smart Grid and Renewable Energy. 2012. Vol. 3. No. 3. Pp. 231–238.

Oleg Samarin,
+7(916)107-77-01; samarin-oleg@mail.ru

Олег Дмитриевич Самарин,
+7(916)107-77-01;
эл. почта: samarin-oleg@mail.ru

Самарин О.Д. Вероятностно-статистическое моделирование наружного климата в охладительный период // Инженерно-строительный журнал. 2017. № 5(73). С. 62–69.

doi: 10.18720/MCE.73.7

The impact of superplasticizers on the radiation changes in Portland cement stone and concretes

Влияние суперпластификаторов на радиационные изменения портландцементного камня и бетонов

A.V. Denisov,
National Research Moscow State Civil Engineering University, Moscow, Russia

Канд. техн. наук, доцент А.В. Денисов,
Национальный исследовательский Московский государственный строительный университет, г. Москва, Россия

Key words: superplasticizers; Portland cement stone; concretes; civil engineering; radiation changes in volume, strength and deformation modulus; effect of neutron radiation from nuclear reactors

Ключевые слова: суперпластификаторы; портландцементный камень; бетоны; радиационные изменения объема; прочности и модуля деформации; действие нейтронного излучения ядерных реакторов

Abstract. The authors have estimated the effect of advanced superplasticizers of types Muraplast, Reamin, Weiss SM, Polyplast SP-1 and Melflux on radiation changes in Portland cement stone and concretes of radiation protection, based on experimental data from available literature, about the effect of such superplasticizers on thermal changes of Portland cement stone and the known analogy between thermal and radiation changes in Portland cement stone exposed to neutrons. The estimate of radiation changes in volume and compression strength of Portland cement stone used proposed ratios between the effect of superplasticizers on thermal and radiation changes in Portland cement stone, obtained through processing the published experimental results about the effect of superplasticizers S-3 and S-4 on radiation and thermal changes in Portland cement stone. Radiation changes in volume, crack formation, compression strength and deformation modulus of concretes, were measured with developed and tested methods for analysis of radiation changes in concretes based on information on changes of their components (aggregates and Portland cement stone). It has been established that advanced superplasticizers generally diminish radiation changes in Portland cement stone and concretes. The authors have demonstrated the extent by which such changes are reduced depending on various factors. It has been found that the effect of superplasticizers is in inverse proportion to the water-to-cement ratio of the mix as cement stone is made, by increasing the content of superplasticizer in the mix (for water reducing), and it depends on the fluency of fast neutrons.

Аннотация. Выполнено расчетное определение влияния современных суперпластификаторов Muraplast, Reamin, Weiss SM, Полипласт СП-1 и Melflux на радиационные изменения портландцементного камня и бетонов радиационной защиты на основании имеющихся в литературе экспериментальных данные по влиянию этих суперпластификаторов на термические изменения портландцементного камня и известной аналогии между термическими и радиационными изменениями портландцементного камня под действием нейтронов. Расчетное определение радиационных изменений объема и прочности на сжатие портландцементного камня выполнено с использованием предложенных коэффициентов связи между влиянием суперпластификаторов на термические и на радиационные изменения портландцементного камня, полученных на основании обработки имеющихся в литературе экспериментальных данных по влиянию суперпластификаторов С-3 и С-4 на радиационные и термические изменения портландцементного камня. Радиационные изменения объема, трещинообразования, прочности при сжатии и модуля деформации бетонов проведено на основании имеющихся разработанных и апробированных методов аналитического определения радиационных изменений бетонов по данным об изменениях их составляющих (заполнителей и портландцементного камня). Установлено, что современные суперпластификаторы в основном уменьшают радиационные изменения портландцементного камня и бетонов. Показано, в какой степени уменьшаются эти изменения в зависимости от различных факторов. Установлено, что эффект влияния суперпластификаторов возрастает с уменьшением водоцементного отношения смеси при изготовлении цементных камней за счет увеличения содержания суперпластификатора в смеси (при водоредуцировании) и зависит от флюенса быстрых нейтронов.

Денисов А.В. Влияние суперпластификаторов на радиационные изменения портландцементного камня и бетонов // Инженерно-строительный журнал. 2017. № 5(73). С. 70–87.

Introduction

Among the main objectives within the Russian Federation 2035 energy strategy in nuclear power is the objective to reduce specific costs of building new nuclear power plants (NPP) as a financial competitive edge, with safety as top priority. One way to address the issue is that NPP construction, including the structures of nuclear reactor radiation protection, should use concrete mixes and concretes with properties modified as required for the purpose.

In order to modify and improve the construction technology and operation properties of concretes, manufacturers use a whole range of chemical additives, particularly superplasticizers, primarily polycarboxylates [1–11]. Published works executed in the Russian Federation [12–19] contain evidence that superplasticizers are also able to raise thermal and radiation resistance of concretes to neutrons, because they mainly reduce thermal and radiation changes in Portland cement stone as a key component of concrete. With this as basis, the paper [18] validates the possibility of concretes with high radiation resistance for nuclear power plants by using superplasticizers based on polycarboxylate ethers.

Among the publications of foreign authors of works devoted to the study of the influence of superplasticizers on the radiation changes in Portland cement stone and concrete, weren`t found. Not considered these issues and in most major foreign reviews [20–25].

At the same time, both in early studies [13, 14], as summarized in [15], and in later studies [16–18], the effect of superplasticizers and other chemical additives on radiation resistance of concretes, was assessed based on how the additives change the properties of Portland cement stone as a component of concrete. In fact, only papers [14–15] gave some results from research of superplasticizer effects on radiation changes in Portland cement stone exposed to the most harmful ionizing radiation neutron radiation that emanates from nuclear reactors. However, those studies only covered superplasticizers S-3 and S-4 (Dophen) – polycondensates, based on sulfonated naphthaleneformaldehyde, developed during 1970s. In [16–18], the effect of superplasticizers on radiation resistance of Portland cement stone was researched based on the resulting thermal changes in Portland cement stone heated to high temperatures. This was done using the fast method – proposed and validated in [14], then improved in [16–18] – of finding (or rather, verifying) the radiation resistance of cement stone [19]. The method is based on comparing the relative changes of the properties of the investigated cement stone with addition, with change of properties of the radiation-resistant cement stone without additives (reference sample) after short-term heating. Modify the properties of each of the compositions is determined in relation to the properties until it is warm. The results of comparing the changes in the properties of the composition with the additive and without the additive composition are judged on the influence of additives on the radiation changes and radiation resistance of cement stone.

Essentially, the studies covered in [13, 14] and summarized in [15] helped to do the following:

- to learn, how specific studied superplasticizers S-3 and S-4 influence on thermal and radiation changes in Portland cement stone (exposed to neutrons);
- to set an analogy in the mechanisms of radiation and thermal changes in Portland cement stone, which temperatures cause which results of radiation, up to researched level of fast neutron fluency;
- based on the above analogy, developing a method to quickly measure radiation resistance of Portland cement stone by results of heating test, after 5 hours at temperatures 150, 350, 600 and 900 °C.

Nevertheless, at the papers [13, 14] researchers never examined the quantitative relation between the effect of chemical additives on radiation and thermal changes in Portland cement stone, as necessary to identify radiation changes after the thermal test. They merely found approximate temperatures that correspond to certain neutron fluency levels in terms of concurrent processes. In addition, they failed to demonstrate how radiation changes of concretes change/decrease when the researched additives are used.

Research represented in studies [16–18] demonstrates that modern superplasticizers either increase thermal change immaterially or decrease it, and thus they must either slightly increase or decrease radiation changes in Portland cement stone; therefore they can be used to raise radiation resistance of concretes. However, the studies never established the extent of radiation changes in Portland cement stone and concretes caused by the use of said superplasticizers.

Among the publications of foreign authors of works devoted to the study of the influence of superplasticizers on the radiation changes in Portland cement stone and concrete, weren`t found. Not considered these issues and in most major foreign reviews [20–25].

Denisov A.V. The impact of superplasticizers on the radiation changes in Portland cement stone and concretes. *Magazine of Civil Engineering*. 2017. No. 5. Pp. 70–87. doi: 10.18720/MCE.73.7.

The purpose of present article is estimation of effects of modern superplasticizers on radiation changes in Portland cement stone and concretes based on experimental data [16–18] about effect of such superplasticizers on thermal changes in Portland cement stone. Perfomed calculations are based on processed and analyzed available experimental data [12–15] about the effects of superplasticizers S-3 and S-4 on radiation and thermal changes in Portland cement stone, and also based on available designed and tested analytical methods of measuring radiation changes in concretes based on data on changes in their components (aggregate and Portland cement stone) [15, 26–28]. From the given publications [12–15] used the data about change of the sizes and volume of Portland cement stones without additives with water cement relation W/C = 0.255-0.26 and with superplasticizers S-3 (0.5–0.8 %) and S-4 (0.8–1.1 %) with W/C = 0.225 after an irradiation in nuclear reactor IBR-2 to fluency of fast neutrons in IBR-2 reactor, from 0.1×10^{24} neutron/m^2 to 1.4×10^{24} neutron/m^2 and after heating within 5 hours at temperatures 150 °C, 350 °C, 600 °C and 900 °C.The paper also examines purely radiation-related changes in Portland cement stone and concretes exposed to neutrons, because radiation from nuclear reactors causes not only radiation changes, but also thermal changes by heating, along with neutron radiation, as can be demonstrated by the results of heating.

Research Methodology

According to the summary contained in [15, 29], vital effects of radiation on Portland cement stone include shrinking size and volume as concrete shrinks when it loses water, and also change of strength, mainly towards weakening. Changes of density and thermal conductivity coefficient, as reviewed in [15], are immaterial. According to [15, 29], change of mass by dehydration and change of strength correlate with changing size and volume, while intensity of gas release can be calculated based on figures that represent change of material weight with dehydration and condition of radiation, as discussed in [30, 31]. Therefore, the focus was on volume change.

To estimate radiation changes in Portland cement stone with superplasticizers, we considered the analogy of the processes of radiation and thermal changes in Portland cement stone, as demonstrated in [14].

We used coefficient K_{RT} to describe the ratio between the effect of superplasticizer additives on change of volume Portland cement stone caused by radiation and heat (according to [19] after 5 hours of heating), expressed as:

$$K_{RT} = \frac{1 - (\Delta V_{CSR} / V_{CS0})_A / (\Delta V_{CSR} / V_{CS0})_{WA}}{1 - (\Delta V_{CST} / V_{CS0})_A / (\Delta V_{CST} / V_{CS0})_{WA}}, \quad (1)$$

where $(\Delta V_{CSR} / V_{CS0})_A$ and $(\Delta V_{CSR} / V_{CS0})_{WA}$ – relative change of volume of Portland cement stone with and without additive after exposure to radiation, %;

$(\Delta V_{CST} / V_{CS0})_A$ and $(\Delta V_{CST} / V_{WC0})_{WA}$ – relative change of volume of Portland cement stone with and without additive after 5 hours of heating, %.

Values of coefficients K_{RT} were found by processing the experimental data available in [12, 14, 15] on effect of superplasticizers S-3 and S-4 on thermal [12] and radiation [14, 15] changes in Portland cement stone.

For all data used herein, relative change of volume of Portland cement stone after heating $\Delta V_{CST} / V_{CS0}$ and radiation $\Delta V_{CSR} / V_{CS0}$, was found by relative change of size $\Delta h / h_0$ and was assumed to be $3\Delta h / h_0$.

Based on the resulting coefficients K_{RT} calculates radiation change in Portland cement stone with various modern superplasticizers, whose effects were studied in [16–18], after heating with the method recommended resistance in [14, 19] to measure radiation.

Radiation change of volume of Portland cement stone without additives were found using the formula found in [15, 29], proving that dependency of radiation change of volume $\Delta V_{ЦКР} / \Delta V_{ЦК0}$ of Portland cement stone (pure radiation, no thermal changes by heating that goes along with radiation) on the fluency of neutrons with energy greater than 0.8 MeV regardless the type of Portland cement, W/C ratio and age of stone, can be approximated with the expression:

$$\Delta V_{CSR} / V_{CS0} = a_R (F_{FN} k_F)^{b_R}, \quad (2)$$

where $a_R = -3.31\%$; $b_R = 1.22$;

F_{FN} – fluency of fast neutrons with energy above 0.8 MeV, neutron/m^2;

k_F = 10^{-24} m^2/neutron – normalizing factor.

For Portland cement stone without additives, we assumed $a_R = -3.31\%$, $b_R = 1.22$.

For Portland cement stone with additives, following the analogy of mechanisms of radiation and thermal changes in Portland cement stone established in [14], value a_R was adjusted by coefficient K_{PT} and then found with the formula:

$$a_R = -3.31\{1 - K_{RT}[1 - (\Delta V_{CST} / V_{CS0})_A / (\Delta V_{CST} / V_{CS0})_{WA}]\}, \quad (3)$$

Radiation changes in strength of Portland cement stone, within and without additives, were found using the formula recommended in [15, 29], which connects the relative residual strength of Portland cement stone after both radiation and heating, with change of volume:

$$R_{CSR} / R_{CS0} = 1/(A + B\Delta V_{CSR} / V_{CS0}), \quad (4)$$

where R_{CSR} / R_{SC0} – relative weakening of Portland cement stone caused by radiation impact, as ratio of strength after radiation R_{CSR} and strength before radiation R_{CS0}, fractional unit;

A and B – parameters, assumed for aged Portland cement stone (8 months and more, considering time it takes to erect nuclear reactors and NPP buildings) under [15, 23]: $A = 1$; $B = -0.23\%^{-1}$.

Use of ultrasound passing time to measure changes in strength proved impractical, because according to data analysis of [14, 15], no reliable correlation exists between change of ultrasound penetration time and change of compression strength after irradiation in the reactor. Besides, according to data analysis offered in [13–18], correlation observed between changes in size and velocity of ultrasound is even less dependable, while their averaged ratios differ greatly for exposure to radiation and heat.

Based on data on radiation changes in Portland cement stone with various modern superplasticizers, we calculated relative radiation-induced change of volume, relative cracking ratio, relative loss of strength and deformation modulus of concretes. We used analytical methods to measure radiation changes in concretes by data on radiation changes of their components, as described in [15, 26–28].

To estimate material influences on radiation changes of concrete aggregate, this research calculated and compared net contributions of radiation changes in Portland cement stone. Such calculations assumed that the aggregate is made of specific material whose volume and properties are not changed by exposure to radiation.

Our calculations treated a typical concrete with averaged production mix with relative aggregate content by volume (sand + crushed rock) $V_{s+cr} = 0.70$.

The approximation was that the true W/C ratio (considering the water need of the aggregate) of Portland cement in the concrete is the same as in the researched mixes of Portland cement stones.

Using the methodology described in [15, 26–28], change of volume, relative crack ratio, changes in compression strength and elasticity modulus of the concrete, due to radiation shrinkage and weakening of Portland cement stone (with and without additives), for aggregates not changed by radiation, is found using these formulas:

$$\frac{\Delta V_{CR}}{V_{C0}} = 100\left\{\left[1-(C_{comp}^{s+cr})^{1/3}\right]\left(1+\frac{\Delta V_{CSR}}{V_{CS0}}\frac{1}{100}\right)^{1/3}\right\}^{3} - 100 \approx \left[1-(C_{comp}^{s+cr})^{1/3}\right]\frac{\Delta V_{CSR}}{V_{CS0}} \quad (5)$$

$$V_{CRRC} = \Delta V_{CR} / V_{C0} - (1 - V_{s+cr})\Delta V_{CSRP} / V_{CS0}, \quad (6)$$

$$R_{CR} / R_{C0} = (R_{CSR} / R_{CS0}) / [1 + (A_C V_{CRRC})^2] \quad (7)$$

$$E_{CR} / E_{C0} = 0{,}85(R_{CR} / R_{C0})^{1.8} + 0.15, \quad (8)$$

where $\Delta V_{CR} / V_{C0}$ – radiation-induced relative change of volume of concrete, as ratio of absolute change of volume of concrete ΔV_{CR} to volume prior to radiation exposure V_{C0}, % ;

V_{CRRC} – radiation-induced relative crack ratio in concrete due to radiation impact, as the ratio of cracks caused by radiation impact, to the material's volume before radiation impact, %;

R_{CR} / R_{C0} – radiation-induced relative weakening of concrete due to radiation impact, as the ratio of strength after radiation R_{CR} to strength before radiation R_{C0}, fractional unit;

E_{CR} / E_{C0} – radiation-induced relative change in deformation modulus of concrete due to radiation impact, as the ratio of deformation modulus after radiation E_{CR}, to initial deformation modulus E_{C0}, fractional unit;

C_{comp}^{s+cr} – degree of aggregate consolidation (sand and crushed rock) in concrete, by the formula:

$$C_{comp}^{s+cr} = V_{s+cr} / V_{comp}^{s+cr} \quad (9)$$

where V_{s+cr} – relative content of aggregate (sand and crushed rock) by volume in concrete, assumed herein to be 0.70, as mentioned above;

V_{comp}^{s+cr} – relative volume that the aggregate such as sand and crushed rock can have in packed state (without layers of Portland cement), measured by bulk density of vibration-packed aggregate.

From [15], our calculations assumed $V_{comp}^{s+cr} = 0.86$ as the approximated mean value.

As discussed in [16–18], the mixes of Portland cement stone, additives of superplasticizers used, respective batch ratios and water-to-cement ratios (W/C) are listed in Tables 1 and 2 below.

Thermal changes in samples of such mixes, after they were heated to different temperatures for 5 hours, are quoted from [16–18] and listed in Tables 3 and 4.

Table 1.Information on composition of Portland cement stone, as discussed in [16–18]

No.	Additive marking	Superplasticizer group by [1]*	Manufacturer	Batch ratio recommended, %	Batch ratio used, %	W/C ratio, rel. units
0	No additive	–	–	–	–	0.26
1	Muraplast FK 48	II (NF)	MC-Bauchemie	0.2–2.0	0.6	0.24
2	Muraplast FK 63	IV (P)	MC-Bauchemie	0.2–2.5	0.6	0.25
3	Reamin MF-100	I (MF)	Kuban Polymer	0.3–1.0	0.4	0.24
4	Weiss SM	IV (P)	Weiss Reagens	No data	0.4	0.24
5	Poliplast SP-1 (S-3)	II (NF)	OOO Poliplast-Uralsib	0.4–0.8	0.4	0.24

*MF – based on sulfonated melamin-formaldehyde polycondensates; NF – based on sulfonated naphthalene-formaldehyde polycondensates; P – polycarboxylate-based.

Table 2. Information on composition of Portland cement stone, as discussed in [18]

No.	Additive marking	Superplasticizer group by [1]	Lateral chain length, and steric effect, by [18]	Batch ratio recommended, %	Batch ratio used, %	W/C ratio, rel. units
0	No additive	–	–	–	–	0.26
1.1	Melflux 1641f	IV (P)	Short lateral chains, minor steric effect	0.05–0.50	0.05	0.25
1.2					0.50	0.20
2.1	Melflux 4930f	IV (P)	Very long lateral chains, very high steric effect	0.05–1.00	0.05	0.25
2.2					1.00	0.20
3.1	Melflux 5581f	IV (P)	Long lateral chains, high steric effect	0.03–0.50	0.03	0.26
3.2					0.50	0.20
4.1	Melflux 6681f	IV (P)	Medium lateral chains, medium steric effect	0.05–1.00	0.05	0.25
4.2					1.00	0.19

Table 3. Thermal changes in Portland cement stone, according to [16–18], after brief heating for 5 hours to temperatures 150 °C to 900 °C

Mix No. by Table 1	Average relative change in size $\Delta h / h_0$, weight $\Delta m / m_0$ and ultrasound velocity $\Delta v / v_0$ in samples after 5 hours of heating to different temperatures											
	150 °C			350 °C			600 °C			900 °C		
	$\frac{\Delta h}{h_0}$, %	$\frac{\Delta m}{m_0}$, %	$\frac{\Delta v}{v_0}$, %	$\frac{\Delta h}{h_0}$, %	$\frac{\Delta m}{m_0}$, %	$\frac{\Delta v}{v_0}$, %	$\frac{\Delta h}{h_0}$, %	$\frac{\Delta m}{m_0}$, %	$\frac{\Delta v}{v_0}$, %	$\frac{\Delta h}{h_0}$, %	$\frac{\Delta m}{m_0}$, %	$\frac{\Delta v}{v_0}$, %
Portland cement stone, without additives												
0	0.02	–3.28	0.13	–1.06	–6.32	–3.23	–1.97	–6.59	–5.61	–2.43	–11.95	–15.00
Portland cement stone, with different groups of superplasticizers												
1	–0.29	–4.31	–0.98	–1.13	–7.39	–5.26	–2.19	–8.17	–5.41	–2.57	–13.39	–13.00
2	–0.27	–4.85	–1.98	–1.00	–8.12	–5.79	–2.02	–9.06	–4.62	–2.53	–14.09	–15.50
3	–0.32	–4.47	–2.60	–1.06	–7.65	–6.40	–2.10	–8.70	–6.65	–2.66	–13.90	–9.71
4	–0.30	–4.91	–2.10	–0.96	–7.75	–2.32	–1.95	–8.82	–4.80	–2.41	–14.09	–13.20
5	–0.30	–4.38	–0.16	–1.06	–7.13	–1.53	–2.09	–8.25	–6.04	–2.59	–13.47	–13.30

Table 4. Information on thermal changes in Portland cement stone, according to [18], after brief heating for 5 hours to temperatures 150 °C to 900 °C

Mix No. by Table 2	Average relative change in size $\Delta h / h_0$, weight $\Delta m / m_0$ and ultrasound velocity $\Delta v / v_0$ in samples after 5 hours of heating to different temperatures											
	150 °C			350 °C			600 °C			900 °C		
	$\frac{\Delta h}{h_0}$, %	$\frac{\Delta m}{m_0}$, %	$\frac{\Delta v}{v_0}$, %	$\frac{\Delta h}{h_0}$, %	$\frac{\Delta m}{m_0}$, %	$\frac{\Delta v}{v_0}$, %	$\frac{\Delta h}{h_0}$, %	$\frac{\Delta m}{m_0}$, %	$\frac{\Delta v}{v_0}$, %	$\frac{\Delta h}{h_0}$, %	$\frac{\Delta m}{m_0}$, %	$\frac{\Delta v}{v_0}$, %
Portland cement stone without additives												
0	–0.17	–1.65	–1.35	–0.76	–4.89	–8.38	–1.58	–9.28	–20.33	–2.18	–11.11	–22.37
Portland cement stone, with various superplasticizers based on polycarboxylate ethers												
1.1	–0.14	–1.81	–2.16	–0.75	–5.48	–3.63	–1.36	–9.85	–9.78	–1.83	–11.40	–15.25
1.2	–0.11	–1.43	–2.31	–0.54	–4.22	–4.94	–1.10	–6.89	–6.78	–1.31	–9.01	–15.62
2.1	–0.18	–1.87	–1.94	–0.76	–5.54	–7.18	–1.63	–10.04	–14.66	–2.38	–11.69	–18.81
2.2	–0.14	–1.00	–2.31	–0.54	–3.60	–7.49	–1.15	–6.22	–9.76	–1.45	–8.66	–15.58
3.1	–0.15	–1.73	–2.63	–0.81	–5.58	–6.76	–1.76	–10.12	–16.97	–2.67	–11.84	–21.34
3.2	–0.14	–1.95	–1.34	–0.63	–5.68	–4.73	–1.33	–9.24	–8.30	–1.70	–11.41	–15.80
4.1	–0.14	–1.59	–1.79	–0.80	–5.39	–4.11	–1.68	–9.97	–13.20	–2.47	–11.72	–17.77
4.2	–0.11	–1.30	–1.28	–0.50	–4.22	–3.33	–1.20	–7.15	–5.27	–1.55	–9.55	–17.16

Results of Research and Discussion

Examination of data offered in [12, and 14, 15] reveals that coefficient K_{RT} of the connection between effects of additives on thermal and radiation-induced changes in Portland cement stone with and without superplasticizers, were 2.5 to 0.5, and depended on the temperature in relation to which the connection is established, and on neutron fluency (Fig. 1). Effects of the superplasticizer type (S-3 or S-4) were not observed.

Analysis demonstrates that the dependency can be described with this expression:

$$K_{RT} = a_r (k_F F_{IBR})^2 + b_r (k_F F_{IBR}) + c_r , \quad (10)$$

where F_{IBR} – fluency of fast neutrons in IBR-2 reactor, neutron/m^2;

k_F =1×10^{-24} m^2/neutron – normalizing factor;

a_r, b_r and c_r – coefficients dependent on the heating temperature compared to effect of the additives on radiation-induced changes, whereof the received values are:

- a_r = -0.383, b_r = -0.003, c_r = 1.25 – taking as basis the results after 5 hours of heating at 150 °C;
- a_r = -0.522, b_r = -0131, c_r = 1.922 – taking as basis the results after 5 hours of heating at 350 °C;
- a_r = -0.750, b_r = -0.094, c_r = 2.534 – taking as basis the results after 5 hours of heating at 600 °C;
- a_r = -0.282, b_r = 0.370, c_r = 1.674 – taking as basis the results after 5 hours of heating at 900 °C.

Calculations with formula (10) considered the following circumstances:

1. According to [15, 29], radiation-induced changes in Portland cement stone are mainly caused by neutrons with energy charges above 0.8 MeV, so radiation changes in Portland cement stone should be bound to the fluency value of such neutrons.
2. According to [15], there is apparent difference between Portland cement stone exposed to radiation in an impulse reactor such as IBR-2 and the results of other reactors. The results

presented in [16] prove that by efficient influence on Portland cement stone, fluency of fast neutrons in IBR-2 impulse reactors is equivalent to that of neutrons with charges greater than 0.8 MeV in other reactors, the ratio being 0.3 approximately. This may be explained by the impulse operation principle of reactor IBR-2 as different for the constant mode in other reactor; another possible explanation is the specific nature of the neutron spectrum in the channel of reactor IBR-2 where exposure is done, as compared to the spectra in the channels of other reactors.

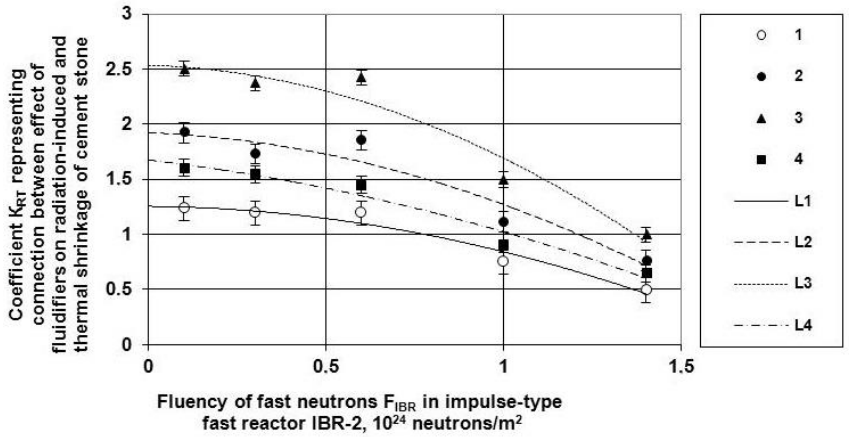

Fig. 1. Dependence of coefficient K_{RT} representing the effect of superplasticizers on radiation-induced and thermal change of volume of Portland cement stone, on fluency of fast neutrons in impulse-type fast reactor IBR-2, based on comparison of Portland cement stone exposed to radiation in reactor with same briefly (5 hours) heated at 150, 350, 600 and 900 °C

We used test results with Portland cement stone of various mixes with superplasticizers S-3 and S-4 and also ones without additives treated in impulse reactor IBR-2 at 30–40 °C, as described in [14, 15], plus test results of the same mixes briefly (5 hours) heated at 150, 350, 600 and 900 °C, as presented in [12].

1 – on the data at 150 °C; 2 – on the data at 350 °C; 3 – on the data at 600 °C; 4 – on the data at 900 °C;

L1 – approximation line by data after 150 °C; L2 – approximation line by data after 350 °C;

L3 – approximation line by data after 600 °C; L4 – approximation line by data after 900 °C.

Therefore, respective to fluency of neutrons with charge above 0.8 MeV in typical reactors coefficient K_{RT} was found with the adjusted formula:

$$K_{RT} = a_r (k_F F_{FN} / 0.3)^2 + b_r (k_F F_{FN} / 0.3) + c_r , \quad (11)$$

where F_{FN} – fluency of fast neutrons with charge above 0.8 MeV, neutron/m^2.

Because we assumed the results presented in [14,15] for impulse reactor IBR-2 as basis to find coefficients K_{PT}, the radiation-induced changes in Portland cement stone with different modern superplasticizers had to be found for the following fluency of neutrons, the effects of which were covered in [14, 15], but converted to fluency of neutrons with charge above 0.8 MeV in other reactors: $0.1 \times 10^{24} \times 0.3 = 0.03 \times 10^{24}$ neutron/m^2; $0.3 \times 10^{24} \times 0.3 = 0.09 \times 10^{24}$ neutron/m^2; $0.6 \times 10^{24} \times 0.3 = 0.18 \times 10^{24}$ neutron/m^2; $1 \times 10^{24} \times 0.3 = 0.3 \times 10^{24}$ neutron/m^2; $1.4 \times 10^{24} \times 0.3 = 0.42 \times 10^{24}$ neutron/m^2.

Calculated radiation changes in Portland cement stones with different superplasticizers taking as basis the results of heating for 5 hours at 350 °C are presented in Tables 5 and 6, and in Figures 2–5.

Tables 5 and 6, and Figures 2–5 make it obvious that in the fluency range of fast neutrons with charges above 0.8 MeV between 0.03×10^{24} and 0.42×10^{24} neutron/m^2, radiation-induced changes in Portland cement stones tend to increase along with growing fluency of fast neutrons, specifically:

– -relative decrease of volume from 0.016 %–0.052 % to 0.867 %–1.203 %;

- relative residual strength from 0.99–0.996 to 0.783–0.834, which corresponds to relative decrease of strength by the value range of 0.4–1 % to 21.7–16.6 %.

Table 5. Calculated radiation-induced changes in Portland cement stones with and without different superplasticizer additives, examined in [16–18]

Mix No. in Table 1.	Relative changes in volume $\Delta V_{CSR}/V_{CS0}$ and relative residual strength R_{CSR}/R_{CS0} of Portland cement stone radiation-treated with various fluency of fast neutrons with charge above 0.8 MEV									
	F_{FN} = 0.03×10^{24} neutron/m^2		F_{FN} = 0.09×10^{24} neutron/m^2		F_{FN} = 0.18×10^{24} neutron/m^2		F_{FN} = 0.3×10^{24} neutron/m^2		F_{FN} = 0.42×10^{24} neutron/m^2	
	$\frac{\Delta V_{CSR}}{V_{CS0}}$, %	$\frac{R_{CSR}}{R_{CS0}}$, rel. units	$\frac{\Delta V_{CSR}}{V_{CS0}}$, %	$\frac{R_{CSR}}{R_{CS0}}$, rel. units	$\frac{\Delta V_{CSR}}{V_{CS0}}$, %	$\frac{R_{CSR}}{R_{CS0}}$, rel. units	$\frac{\Delta V_{CSR}}{V_{CS0}}$, %	$\frac{R_{CSR}}{R_{CS0}}$, rel. units	$\frac{\Delta V_{CSR}}{V_{CS0}}$, %	$\frac{R_{CSR}}{R_{CS0}}$, rel. units
0	-0.046	0.990	-0.175	0.961	-0.409	0.914	-0.762	0.851	-1.149	0.791
1	-0.052	0.988	-0.197	0.957	-0.453	0.906	-0.826	0.840	-1.203	0.783
2	-0.041	0.991	-0.157	0.965	-0.370	0.922	-0.707	0.860	-1.102	0.798
3	-0.046	0.990	-0.175	0.961	-0.409	0.914	-0.762	0.851	-1.149	0.791
4	-0.038	0.991	-0.145	0.968	-0.345	0.927	-0.671	0.866	-1.071	0.802
5	-0.046	0.990	-0.175	0.961	-0.409	0.914	-0.762	0.851	-1.149	0.791

Table 6. Calculated radiation-induced changes in Portland cement stones with and without various superplasticizers based on polycarboxylated ethers. examined in [18]

Mix No. in Table 2.	Relative changes in volume $\Delta V_{CSR}/V_{CS0}$ and relative residual strength R_{CSR}/R_{CS0} of Portland cement stone radiation-treated with various fluency of fast neutrons with charge above 0.8 MeV									
	F_{FN} = 0.03×10^{24} neutron/m^2		F_{FN} = 0.09×10^{24} neutron/m^2		F_{FN} = 0.18×10^{24} neutron/m^2		F_{FN} = 0.3×10^{24} neutron/m^2		F_{FN} = 0.42×10^{24} neutron/m^2	
	$\frac{\Delta V_{CSR}}{V_{CS0}}$, %	$\frac{R_{CSR}}{R_{CS0}}$, rel. units	$\frac{\Delta V_{CSR}}{V_{CS0}}$, %	$\frac{R_{CSR}}{R_{CS0}}$, rel. units	$\frac{\Delta V_{CSR}}{V_{CS0}}$, %	$\frac{R_{CSR}}{R_{CS0}}$, rel. units	$\frac{\Delta V_{CSR}}{V_{CS0}}$, %	$\frac{R_{CSR}}{R_{CS0}}$, rel. units	$\frac{\Delta V_{CSR}}{V_{CS0}}$, %	$\frac{R_{CSR}}{R_{CS0}}$, rel. units
0	-0.046	0.990	-0.175	0.961	-0.409	0.914	-0.762	0.851	-1.149	0.791
1.1	-0.045	0.990	-0.171	0.962	-0.400	0.916	-0.749	0.853	-1.138	0.793
1.2	-0.021	0.995	-0.082	0.981	-0.212	0.953	-0.482	0.900	-0.911	0.827
2.1	-0.046	0.990	-0.175	0.961	-0.409	0.914	-0.762	0.851	-1.149	0.791
2.2	-0.021	0.995	-0.082	0.981	-0.212	0.953	-0.482	0.900	-0.911	0.827
3.1	-0.052	0.988	-0.197	0.957	-0.453	0.906	-0.826	0.840	-1.203	0.783
3.2	-0.031	0.993	-0.120	0.973	-0.293	0.937	-0.597	0.879	-1.008	0.812
4.1	-0.051	0.989	-0.192	0.958	-0.444	0.907	-0.813	0.842	-1.192	0.785
4.2	-0.016	0.996	-0.065	0.985	-0.177	0.961	-0.431	0.910	-0.867	0.834

Where superplasticizers are used, relative radiation change of volume of Portland cement stone with superplasticizer, compared to changes in that without additives typically fall 1.0–2.8 times, though strength is lost to a lesser degree: mainly by up to 6 %.

At water-cement ratio W/C = 0.25 – 0.26 radiation-induced changes in Portland cement stones with superplasticizers of group I (MF) and group II (NF) tend to be somewhat above the radiation changes in Portland cement stone without additives, but in the case of superplasticizers of group IV (P) are either commensurable or weaker than the changes in Portland cement stone without additives.

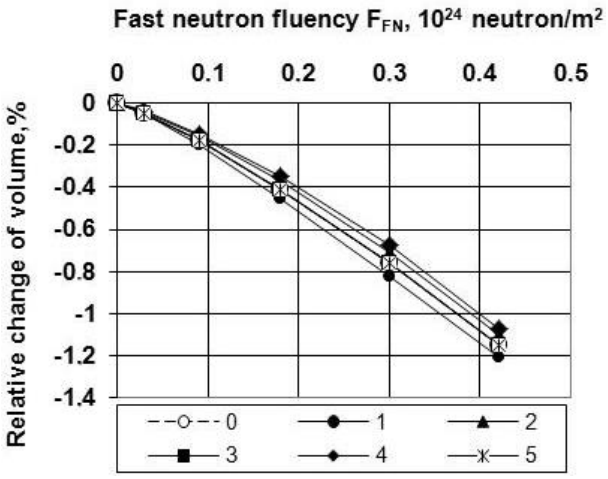

Figure 2. Dependence of calculated radiation change in volume of Portland cement stones with and without various superplasticizers, on fluency of fast neutrons with charge above 0.8 MeV

0, 1, 2, 3, 4, 5 – numbers of Portland cement stone mix in Table 1.

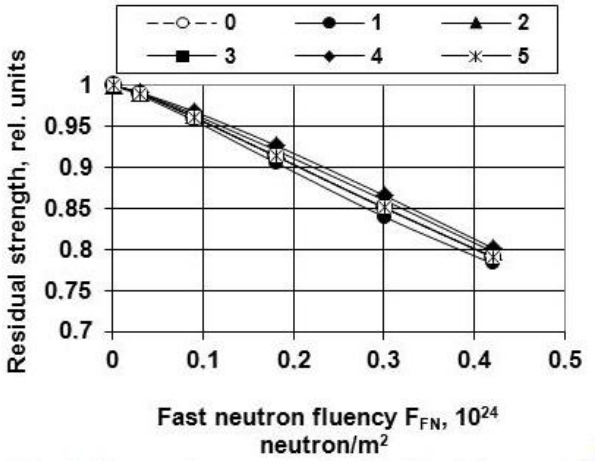

Figure 3. Dependence of calculated relative residual strength to compression in Portland cement stones with and without various superplasticizers, on fluency of fast neutrons with charge above 0.8 MeV

0, 1, 2, 3, 4, 5 – numbers of Portland cement stone mix in Table 1.

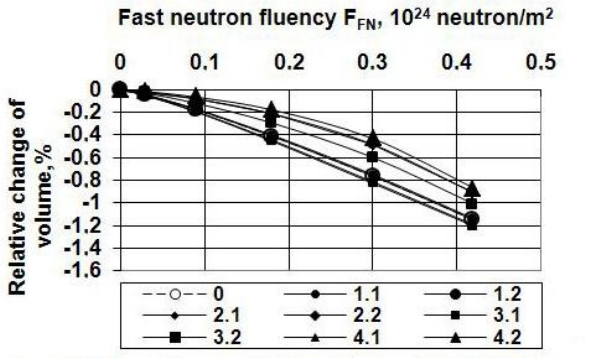

Figure 4. Dependence of calculated radiation change in volume of Portland cement stones with and without various superplasticizers based on polycarboxylated ethers, on fluency of fast neutrons with charge above 0.8 MeV

0, 1.1, 1.2, 2.1, 2.2, 3.1, 3.2, 4.1, 4.2 – numbers of Portland cement stone mix in Table 2.

Denisov A.V. The impact of superplasticizers on the radiation changes in Portland cement stone and concretes. *Magazine of Civil Engineering*. 2017. No. 5. Pp. 70–87. doi: 10.18720/MCE.73.7.

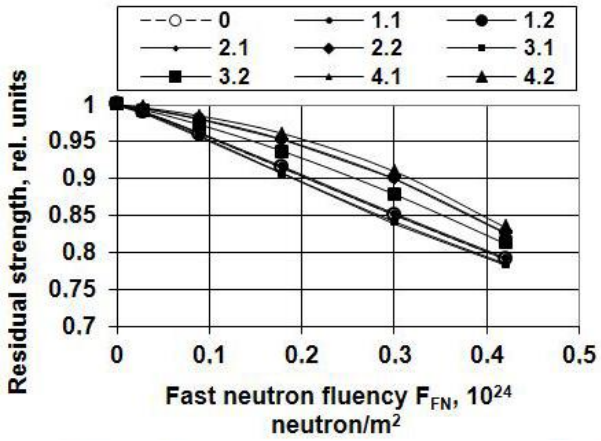

Figure 5. Dependence of calculated relative residual strength to compression in Portland cement stones with and without various superplasticizers based on polycarboxylated ethers, on fluency of fast neutrons with charge above 0.8 MeV

0, 1.1, 1.2, 2.1, 2.2, 3.1, 3.2, 4.1, 4.2 – numbers of Portland cement stone mix in Table 2.

The reducing effect on radiation change of volume of Portland cement stone is increased by superplasticizers, if higher content of superplasticizer in the mix lowers the water-to-cement ratio of manufactured Portland cement stone in the range between 0.25–0.26 and 0.19–0.20 (Fig. 6). Such W/C ratio dependency was also observed with the heating test results (Fig. 7).

From composition of Portland cement stone investigated at low W/C = 0.19-0.20 the greatest drop in radiation change was observed with superplasticizers Melflux 1641f, Melflux 4930f, and Melflux 6681f.

Thus we observed immaterial influence of superplasticizers on radiation-induced but especially on thermal changes in volume and strength of Portland cement stone with a constant W/C ratio, but we saw a decrease of radiation and thermal changes in cement stone with lower W/C ratios, and the decrease was in inverse proportion to the W/C ratio. This means that the effect of superplasticizers on radiation and thermal changes in Portland cement stone is mainly explained by their influence on the material's general porosity. We know from [1–3, 6, 10] that although superplasticizers added at a constant W/C ratio does decrease capillary porosity, the gel porosity will increase, and so general porosity remains practically unchanged, therefore the effect of superplasticizers is immaterial. With the W/C ratio lower, both the capillary and the gel porosity will go down [32], so the effect of the superplasticizer will grow.

The factor of porosity can be explained by the fact that after Portland cement stone is heated to less than 550 °C and treated with neutron radiation, change of volume (shrinkage) is caused by water oozing from the material's pores.The lower the material's porosity, the less will be the meaning stretching forces and material deformations around pores, which were water-saturated prior to heating or radiation. Since such forces and deformations are weakened by dehydration, this causes reduction of volumes (shrinkages) of Portland cement stone. The lower porosity, the less will the material shrink with dehydration and the loss of strength will become lower. Certainly, loss of chemically bound water (decomposition of portlandite and other crystalline hydrates around 550–600 °C) and decomposition of tiff (at 800–900 °C) represents a different shrinkage mechanism of Portland cement, but seen the results of heating described in [17–19] (Table 3, 4) at 600 °C and 900 °C, the effect patterns of the W/C ratio – and therefore of porosity – will be the same as when water is lost from the pores after 150 °C and 350 °C

The same effects of the W/C ratio and porosity with a similar mechanism for heating up to 550 °C were observed with shrinkage of cement stone and concretes as they hardened [33].

Meanwhile, quoting from the thermal tests described in [16–18] (Table 3 and 4), loss of cement stone weight after heating is not unambiguously caused by shrinkage and loss of volume. As the superplasticizer is added with a constant W/C ratio, the degree of weight loss due to dehydration increases, but loss of volume hardly progresses. As superplasticizers are added and the W/C ratio gets lower, shrinkage will be the less, the less is the extent of weight loss. Therefore, adding the superplasticizers changes the ratio of weight loss to shrinkage compared to that in cement stone without additives in the mix.

Notably, research failed to observe any significant unambiguous effect on thermal and radiation changes in the cement stone, from lateral chain length or by the extent of steric effect of polycarboxylate

superplasticizer discussed in [18], or the amount of portlandite and tiff formed in cement stone, as shown in [18].

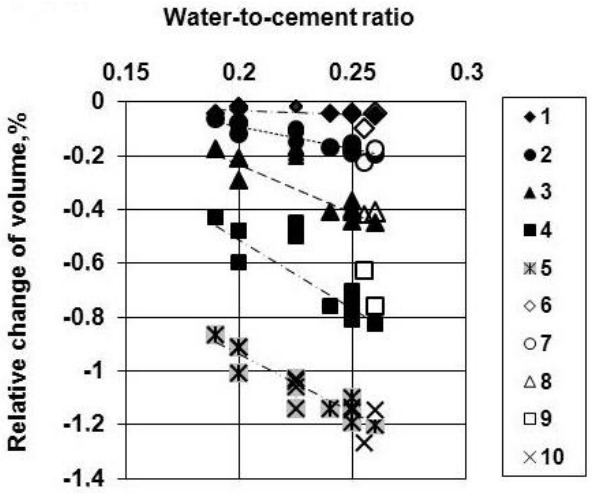

Figure 6. Water-to-cement ratio dependence of radiation-change of volume of Portland cement stones with and without various superplasticizers additives – after radiation treatment with different fluency of fast neutrons charged above 0.8 MeV

1–5 – with additives; 6–10 – without additives; 1 and 6 – fluency 0.03×10^{24} neutron/m^2; 2 and 7 – fluency 0.09×10^{24} neutron/m^2; 3 and 8 – fluency 0.18×10^{24} neutron/m^2; 4 and 9 – fluency 0.3×10^{24} neutron/m^2; 5 and 10 – fluency 0.42×10^{24} neutron/m^2.

For W/C ratio = 0.19, 0.20, 0.24, 0.25 and 0.26, we quote calculated radiation-induced changes in volume of Portland cement stones with and without various modern superplasticizers, examined in [16–18] after 5 hours of heating.

For W/C ratio 0.225 and 0.255, we quote radiation-induced (less thermal-induce) changes in volume of Portland cement stones with and without superplasticizers S-3 and S-4, examined in [14, 15] after treatment in reactor IBR-2.

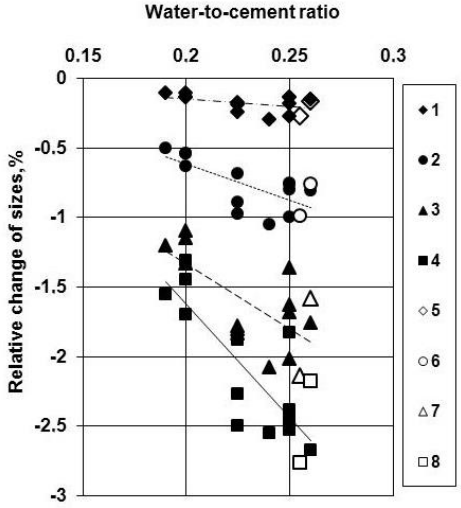

Figure 7. Water-to-cement ratio dependence of radiation-change of volume of Portland cement stones with and without various superplasticizers additives – after brief (5 hours) heat treatment at various temperatures

1–4 – with additives; 5–8 – without additives;

1 and 5 – after 150° C; 2 and 6 – after 350 °C;

3 and 7 – after 600° C; 4 and 8 – after 900 °C.

For W/C ratio = 0.19, 0.20, 0.24, 0.25 and 0.26 we quote data with various modern superplasticizers as presented in [16–18].

Denisov A.V. The impact of superplasticizers on the radiation changes in Portland cement stone and concretes. *Magazine of Civil Engineering*. 2017. No. 5. Pp. 70–87. doi: 10.18720/MCE.73.7.

For W/C ratio= 0.225 and 0.255, we quote data with and without superplasticizers S-3 and S-4, as presented in [12].

Results of calculations with use of formulas (5) – (8) of radiation changes in concretes with various superplasticizers due to radiation changes in volume and strength of Portland cement stone are represented in Table 7–10. Considered, that the true W/C ratio Portland cement stone in concrete, taking into account the water demand of aggregates is approximately the same as the samples of Portland cement stones. Although in the manufacture of concrete W/C ratio by number is typically greater than in the manufacture of cement stones. In this connection in calculations of radiation changes in concretes used the data of tables 5 and 6.

Table 7. Calculated radiation-induced changes in volume of concrete and relative micro-cracking ratio due to radiation changes in Portland cement stone, listed in Table 5

Mix No. in Table 1 in concrete	Relative volume changes $\Delta V_{CR}/V_{C0}$ and relative cracking ratio V_{CRRC} for concretes with various Portland cement stone radiation-treated with various fluency of fast neutrons with charge above 0.8 MeV									
	F_{FN} = 0.03×10²⁴ neutron/m²		F_{FN} = 0.09×10²⁴ neutron/m²		F_{FN} = 0.18×10²⁴ neutron/m²		F_{FN} = 0.3×10²⁴ neutron/m²		F_{FN} = 0.42×10²⁴ neutron/m²	
	$\frac{\Delta V_{CR}}{V_{C0}}$, %	V_{CRRC}, %	$\frac{\Delta V_{CR}}{V_{C0}}$, %	V_{CRRC}, %	$\frac{\Delta V_{CR}}{V_{C0}}$, %	V_{CRRC}, %	$\frac{\Delta V_{CR}}{V_{C0}}$, %	V_{CRRC}, %	$\frac{\Delta V_{CR}}{V_{C0}}$, %	V_{CRRC}, %
0	-0.003	0.011	-0.012	0.041	-0.027	0.095	-0.051	0.177	-0.076	0.268
1	-0.003	0.012	-0.013	0.046	-0.030	0.106	-0.055	0.192	-0.080	0.280
2	-0.003	0.010	-0.010	0.037	-0.025	0.086	-0.047	0.165	-0.073	0.257
3	-0.003	0.011	-0.012	0.041	-0.027	0.095	-0.051	0.177	-0.076	0.268
4	-0.002	0.009	-0.010	0.034	-0.023	0.080	-0.044	0.156	-0.071	0.249
5	-0.003	0.011	-0.012	0.041	-0.027	0.095	-0.051	0.177	-0.076	0.268

Table 8. Calculated radiation-induced changes in strength and deformation modulus due to radiation changes in Portland cement stone, listed in Table 5

Mix No. in Table 1 in concrete	Relative residual strength R_{CR}/R_{C0} and relative residual deformation modulus E_{CR}/E_{C0} of concretes with various Portland cement stone radiation-treated with various fluency of fast neutrons with charge above 0.8 MeV									
	F_{FN} = 0.03×10²⁴ neutron/m²		F_{FN} = 0.09×10²⁴ neutron/m²		F_{FN} = 0.18×10²⁴ neutron/m²		F_{FN} = 0.3×10²⁴ neutron/m²		F_{FN} = 0.42×10²⁴ neutron/m²	
	$\frac{R_{CR}}{R_{C0}}$, rel. units	$\frac{E_{CR}}{E_{C0}}$, rel. units	$\frac{R_{CR}}{R_{C0}}$, rel. units	$\frac{E_{CR}}{E_{C0}}$, rel. units	$\frac{R_{CR}}{R_{C0}}$, rel. units	$\frac{E_{CR}}{E_{C0}}$, rel. units	$\frac{R_{CR}}{R_{C0}}$, rel. units	$\frac{E_{CR}}{E_{C0}}$, rel. units	$\frac{R_{CR}}{R_{C0}}$, rel. units	$\frac{E_{CR}}{E_{C0}}$, rel. units
0	0.990	0.984	0.961	0.941	0.913	0.872	0.848	0.782	0.785	0.700
1	0.988	0.982	0.957	0.935	0.905	0.860	0.837	0.767	0.777	0.690
2	0.991	0.986	0.965	0.947	0.921	0.883	0.858	0.795	0.792	0.709
3	0.990	0.984	0.961	0.941	0.913	0.872	0.848	0.782	0.785	0.700
4	0.991	0.987	0.968	0.951	0.926	0.890	0.864	0.804	0.797	0.715
5	0.990	0.984	0.961	0.941	0.913	0.872	0.848	0.782	0.785	0.700

Денисов А.В. Влияние суперпластификаторов на радиационные изменения портландцементного камня и бетонов // Инженерно-строительный журнал. 2017. № 5(73). С. 70–87.

Table 9. Calculated radiation-induced changes in volume of concrete and relative micro-cracking ratio due to radiation changes in Portland cement stone, listed in Table 6

Mix No. in Table 1 in concrete	Relative changes in volume $\Delta V_{CR}/V_{C0}$ and relative cracking ratio V_{CRRC} for concretes with various Portland cement stone, radiation-treated with various fluency of fast neutrons with charge above 0.8 MeV									
	F_{FN} = 0.03×10²⁴ neutron/m²		F_{FN} = 0.09×10²⁴ neutron/m²		F_{FN} = 0.18×10²⁴ neutron/m²		F_{FN} = 0.3×10²⁴ neutron/m²		F_{FN} = 0.42×10²⁴ neutron/m²	
	$\frac{\Delta V_{CR}}{V_{C0}}$, %	V_{CRRC}, %	$\frac{\Delta V_{CR}}{V_{C0}}$, %	V_{CRRC}, %	$\frac{\Delta V_{CR}}{V_{C0}}$, %	V_{CRRC}, %	$\frac{\Delta V_{CR}}{V_{C0}}$, %	V_{CRRC}, %	$\frac{\Delta V_{CR}}{V_{C0}}$, %	V_{CRRC}, %
0	-0.003	0.011	-0.012	0.041	-0.027	0.095	-0.051	0.177	-0.076	0.268
1.1	-0.003	0.010	-0.011	0.040	-0.026	0.093	-0.050	0.175	-0.075	0.265
1.2	-0.001	0.005	-0.005	0.019	-0.014	0.049	-0.032	0.112	-0.060	0.212
2.1	-0.003	0.011	-0.012	0.041	-0.027	0.095	-0.051	0.177	-0.076	0.268
2.2	-0.001	0.005	-0.005	0.019	-0.014	0.049	-0.032	0.112	-0.060	0.212
3.1	-0.003	0.012	-0.013	0.046	-0.030	0.106	-0.055	0.192	-0.080	0.280
3.2	-0.002	0.007	-0.008	0.028	-0.019	0.068	-0.040	0.139	-0.067	0.235
4.1	-0.003	0.012	-0.013	0.045	-0.029	0.103	-0.054	0.189	-0.079	0.278
4.2	-0.001	0.004	-0.004	0.015	-0.012	0.041	-0.029	0.100	-0.058	0.202

Table 10.Calculated radiation-induced changes in strength and deformation modulus due to radiation changes in Portland cement stone, listed in Table 6

Mix No. in Table 2 in concrete	Relative residual strength R_{CR}/R_{C0} and relative residual deformation modulus E_{CR}/E_{C0} of concretes with various Portland cement stone, radiation-treated with various fluency of fast neutrons with charge above 0.8 MeV									
	F_{FN} = 0.03×10²⁴ neutron/m²		F_{FN} = 0.09×10²⁴ neutron/m²		F_{FN} = 0.18×10²⁴ neutron/m²		F_{FN} = 0.3×10²⁴ neutron/m²		F_{FN} = 0.42×10²⁴ neutron/m²	
	$\frac{R_{CR}}{R_{C0}}$, rel. units	$\frac{E_{CR}}{E_{C0}}$, rel. units	$\frac{R_{CR}}{R_{C0}}$, rel. units	$\frac{E_{CR}}{E_{C0}}$, rel. units	$\frac{R_{CR}}{R_{C0}}$, rel. units	$\frac{E_{CR}}{E_{C0}}$, rel. units	$\frac{R_{CR}}{R_{C0}}$, rel. units	$\frac{E_{CR}}{E_{C0}}$, rel. units	$\frac{R_{CR}}{R_{C0}}$, rel. units	$\frac{E_{CR}}{E_{C0}}$, rel. units
0	0.990	0.984	0.961	0.941	0.913	0.872	0.848	0.782	0.785	0.700
1.1	0.990	0.984	0.962	0.943	0.915	0.874	0.850	0.785	0.787	0.702
1.2	0.995	0.993	0.981	0.972	0.953	0.930	0.899	0.852	0.823	0.749
2.1	0.990	0.984	0.961	0.941	0.913	0.872	0.848	0.782	0.785	0.700
2.2	0.995	0.993	0.981	0.972	0.953	0.930	0.899	0.852	0.823	0.749
3.1	0.988	0.982	0.957	0.935	0.905	0.860	0.837	0.767	0.777	0.690
3.2	0.993	0.989	0.973	0.959	0.937	0.905	0.878	0.822	0.807	0.728
4.1	0.989	0.982	0.957	0.936	0.906	0.862	0.839	0.770	0.779	0.692
4.2	0.996	0.994	0.985	0.977	0.961	0.941	0.909	0.866	0.830	0.758

Tables 7–10 show that in the fast neutron fluency range between 0.03×10²⁴ and 0.42×10²⁴ neutron/m², radiation-induced changes in concretes due to radiation-caused changes in volume and strength of Portland cement stone will grow along with the fluency of fast neutrons and will be:

- relative decrease in volume between 0.001 %–0.003 % and 0.058–0.076 %;
- relative micro-crack ratio between 0.004 %–0.012 % and 0.202–0.280 %;
- relative residual strength between 0.984–0.996 and 0.777–0.830.
- relative residual modulus of deformation between 0.984–0.994 and 0.690–0.758.

Denisov A.V. The impact of superplasticizers on the radiation changes in Portland cement stone and concretes. *Magazine of Civil Engineering*. 2017. No. 5. Pp. 70–87. doi: 10.18720/MCE.73.7.

Change of volume of concretes is about 15 times less than that for Portland cement stones; micro-crack ratio is about 0.25 of change in volume of Portland cement stone by modulus; its residual strength is not much lower than that of Portland cement stones, and residual deformation modulus is a bit lower than the residual strength, by up to 7 %. Effect of superplasticizer type, quantity and W/C ratio are the same as for Portland cement stone.

Depending on radiation-induced change of aggregate, not considered for our calculations due to the vast range of their type-specific values, real-life radiation-induced changes of concretes will differ from the data that only considers changes of cement stone. However, absolute differences in radiation changes due to the effect of superplasticizers will be the same as if aggregate changes are considered; therefore, the conclusion about the superplasticizer effect on radiation-induced changes in concretes is true for any aggregate.

Conclusion

1. To estimate the effect of modern superplasticizers on radiation-induced changes in Portland cement stone, based on experimental data on the effect of modern superplasticizers on thermal changes in Portland cement stone available in published literature, we propose the use of coefficient K_{RT} that describes the ratio of superplasticizer additive effect on radiation and thermal change of volumes of Portland cement stone.

2. It has been established that the value of coefficient K_{RT} describing the relation between the effect of additives on thermal change of volume (after 5 hours of heating) and radiation change of volume (after exposure to neutrons) of Portland cement stone with and without superplasticizers, varies between 2.5 and 06, and depends on the temperature that underlies the relation, and on fluency of fast neutrons. Now we have analytical expressions to describe the dependence of coefficients K_{RT} on fast neutron fluency under various heating temperatures during thermal tests. Relation between the superplasticizer type and K_{RT} has not been found.

3. Based on received values of coefficient K_{RT} it has been established that superplasticizers used tend to decrease relative radiation shrinkage of Portland cement stone compared to stone without additives by some 1.0–2.8 times, while weakening is much lower, mainly up to 6 %. At water-cement ratio W/C = 0.25 – 0.26 radiation-induced changes in Portland cement stones with superplasticizers of group I (MF) and group II (NF) tend to be somewhat above the radiation changes in Portland cement stone without additives, but in the case of superplasticizers of group IV (P) are either commensurable or weaker than the changes in Portland cement stone without additives.

4. The reducing effect on radiation change of volume of Portland cement stone is increased by superplasticizers, if higher content of superplasticizer in the mix lowers the water-to-cement ratio of manufactured Portland cement stone in the range between 0.25–0.26 and 0.19–0.20. Such W/C ratio dependency was also observed with the heating test results.

5. From compositions of Portland cement stones investigated at low W/C = 0.19–0.20 the greatest drop in radiation change was observed with superplasticizers Melflux 1641f, Melflux 4930f, and Melflux 6681f. Researchers have not observed any significant and unambiguous influence on thermal and radiation changes of cement stone by such factors as lateral link length, steric effect of polycarboxylate superplasticizers, and the amount of portlandite and tiff formed in cement stone.

6. Based on available tried and trusted analytical methods of measuring radiation changes in concrete using data about changes in their components (aggregate and Portland cement stone), we have calculated radiation-induced changes in concretes with different added superplasticizers due to radiation and thermal changes in the volume and strength of Portland cement stone.

7. It has been established that radiation change of volume of concretes is approximately 15 times less than change of volume of Portland cement stones, the micro-cracking ratio is about 0.23 of change of volume of Portland cement stone by modulus, and the residual strength is just a bit lower that that of Portland cement stones, while the residual deformation modulus is by up to 8 % less than the residual strength. Relative effect of the superplasticizer type, quantity and W/C ratio is the same as with Portland cement stone.

8. The results of calculations suggest that the use of modern superplasticizers, particularly ones that are polycarboxylate-based, tend to reduce radiation-induced changes (especially change of volume)

Денисов А.В. Влияние суперпластификаторов на радиационные изменения портландцементного камня и бетонов // Инженерно-строительный журнал. 2017. № 5(73). С. 70–87.

of Portland cement stone and concrete. The effect of radiation change reduction is in inverse proportion with the water-to-cement ratio.

References

1. Batrakov V.G., Kapriyelov S.S., Sheynfeld A.V., Silina E.S. Modificirovannyye betony v praktike sovremennogo stroitelstva [The modified concrete In practice of modern construction]. *Promyshlennoye i grazhdanskoye stroitel'stvo.* 2002. No 9. Pp. 23-25. (rus)
2. Puertas F., Santos H., Palacios M. and Martınez-Ramırez S. Polycarboxylate superplasticiser admixtures: effect on hydration, microstructure and rheological behaviour in cement pastes. *Advances in Cement Research.* 2005. Vol. 17. No. 2. Pp. 77–89.
3. Izotov V.S., Sokolova Yu.A. *Himicheskiye dobavki dlya modifikacii betona: monografiya* [Chemical additives for modification of concrete] Moscow: Kazanskiy Gosudarstvennyy arhitekturno-stroitelnyy universitet: Izdatelstvo «Paleotip», 2006. 244 p. (rus)
4. El-Gamal S.M.A., Al-Nowaiser F.M., Al-Baity A.O. Effect of superplasticizers on the hydration kinetic and mechanical properties of Portland cement pastes. *Journal of Advanced Research.* 2012. Vol. 3. No. 2. Pp. 119–124.
5. Mardani-Aghabaglou A., Tuyan M., Yılmaz G., Arıöz Ö., Ramyar K. Effect of different types of superplasticizer on fresh, rheological and strength properties of self-consolidating concrete. *Construction and Building Materials.* 2013. Vol. 47. Pp. 1020–1025.
6. Nowak-Michta A. Influence of superplasticizer on porosity structures in hardened concretes. *Procedia Engineering.* 2015. Vol. 108. Pp. 262–269.
7. Janowska-Renkas E. The influence of the chemical structure of polycarboxylic superplasticizers on their effectiveness in cement pastes. *Procedia Engineering.* 2015. Vol. 108. Pp. 575–583.
8. Korovkin M.O., Yeroshkina N.A., Pokshin V.R., Koshkin A.G. Sravnitelnyye issledovaniya effektivnosti superplastifikatorov [Comparative research on the effectiveness of superplasticizer]. *Obrazovaniye i nauka v sovremennom mire. Innovacii.* 2016. No. 6-1. Pp. 149–157. (rus)
9. Smirnova O.M. Compatibility of portland cement and polycarboxylate-based superplasticizers in high-strength concrete for precast constructions. *Magazine of Civil Engineering.* 2016. No. 6. Pp. 12–22.
10. Huang H., Qian C., Zhao F., Qu J., Guo J., Danzinger M. Improvement on microstructure of concrete by polycarboxylate superplasticizer (PCE) and its influence on durability of concrete. *Construction and Building Materials.* 2016. Vol. 110. Pp. 293–299.
11. Nkinamubanzi P.-C., Mantellato S., Flatt R.J. 16–Superplasticizers in practice. *Science and Technology of Concrete Admixtures.* 2016. Pp. 353–377.
12. Falikman V.R., Veselova V.I., Yershov V.Yu., Muzalevskiy L.P. Povedeniye cementnogo kamnya s himicheskimi dobavkami v usloviyah kratkovremennogo vozdeystviya vysokih temperature [Behavior of a cement stone with chemical additives in the conditions of short-term influence of high temperatures]. *Voprosy atomnoy nauki i tekhniki. Ser. Proyektirovaniye i stroitelstvo.* 1987. No. 1. Pp. 3–15. (rus)
13. Yershov V.Yu., Dubrovskiy V.B., Muzalevskiy L.P., Kolesnikov N.A. Povedeniye cementnogo kamnya s himicheskimi dobavkami v usloviyah dlitelnogo vozdeystviya vysokikh temperature [Behaviour of a cement stone with chemical additives in the conditions of long influence of high temperatures]. *Voprosy atomnoy nauki i tekhniki. Ser. Proyektirovaniye i stroitelstvo.* 1988. No. 2. Pp. 120–129. (rus)
14. Yershov V.Yu. *Radiatsionnaya stoykost portlandcementnogo kamnya s himicheskimi i mineralnymi*

Литература

1. Батраков В.Г., Каприелов С.С., Шейнфельд А.В., Силина Е. С. Модифицированные бетоны в практике современного строительства // Промышленное и гражданское строительство. 2002. № 9. С. 23–25.
2. Puertas F., Santos H., Palacios M. and Martınez-Ramırez S. Polycarboxylate superplasticiser admixtures: effect on hydration, microstructure and rheological behaviour in cement pastes // Advances in Cement Research. 2005. Vol. 17. № 2. Pp. 77–89.
3. Изотов В.С., Соколова Ю.А. Химические добавки для модификации бетона: монография. М.: Казанский Государственный архитектурно-строительный университет: Издательство «Палеотип», 2006. 244 с.
4. El-Gamal S.M.A., Al-Nowaiser F.M., Al-Baity A.O. Effect of superplasticizers on the hydration kinetic and mechanical properties of Portland cement pastes // Journal of Advanced Research. 2012. Vol. 3. № 2. Pp. 119–124.
5. Mardani-Aghabaglou A., Tuyan M., Yılmaz G., Arıöz Ö., Ramyar K. Effect of different types of superplasticizer on fresh, rheological and strength properties of self-consolidating concrete // Construction and Building Materials. 2013. Vol. 47. Pp. 1020–1025.
6. Nowak-Michta A. Influence of superplasticizer on porosity structures in hardened concretes // Procedia Engineering. 2015. Vol 108. Pp. 262–269.
7. Janowska-Renkas E. The influence of the chemical structure of polycarboxylic superplasticizers on their effectiveness in cement pastes // Procedia Engineering. 2015. Vol. 108. Pp. 575–583.
8. Коровкин М.О., Ерошкина Н.А., Покшин В.Р., Кошкин А.Г. Сравнительные исследования эффективности суперпластификаторов // Образование и наука в современном мире. Инновации. 2016. № 6-1. С. 149–157.
9. Смирнова О.М. Совместимость портландцемента и суперпластификаторов на поликарбоксилатной основе для получения высокопрочного бетона сборных конструкций // Инженерно-строительный журнал. 2016. № 6. С. 12–22.
10. Huang H., Qian C., Zhao F., Qu J., Guo J., Danzinger M. Improvement on microstructure of concrete by polycarboxylate superplasticizer (PCE) and its influence on durability of concrete // Construction and Building Materials. 2016. Vol. 110. Pp. 293–299.
11. Nkinamubanzi P.-C., Mantellato S., Flatt R.J. 16–Superplasticizers in practice // Science and Technology of Concrete Admixtures. 2016. Pp. 353–377.
12. Фаликман В.Р., Веселова В.И., Ершов В.Ю., Музалевский Л.П. Поведение цементного камня с химическими добавками в условиях кратковременного воздействия высоких температур // Вопросы атомной науки и техники. Сер. Проектирование и строительство. 1987. № 1. С. 3–15.
13. Ершов В.Ю., Дубровский В.Б., Музалевский Л.П., Колесников Н.А. Поведение цементного камня с химическими добавками в условиях длительного воздействия высоких температур // Вопросы атомной науки и техники. Сер. Проектирование и строительство. 1988. № 2. С. 120–129.
14. Ершов В.Ю. Радиационная стойкость портландцементного камня с химическими и минеральными добавками. Дисс. на соискю учен. степ. к.т.н. М., 1992. 185 с.
15. Денисов А.В., Дубровский В.Б., Соловьев В.Н. Радиационная стойкость минеральных и полимерных строительных материалов. М.: Издательский дом МЭИ,

Denisov A.V. The impact of superplasticizers on the radiation changes in Portland cement stone and concretes. *Magazine of Civil Engineering*. 2017. No. 5. Pp. 70–87. doi: 10.18720/MCE.73.7.

dobavkami [Radiating stability portland cement stone with chemical and mineral additives]. PhD dissertation. Moscow, 1992. 185 p. (rus)

15. Denisov A.V., Dubrovskiy V.B., Solovev V.N. Radiatsionnaya stoykost mineralnyh i polimernyh stroitelnyh materialov [Radiating stability of mineral and polymeric building materials]. Moscow: Izdatelskiy dom MEI, 2012. 284 p. (rus)
16. Medvedev V., Pustovgar A. Evaluation method of radiation stability of hardened cement paste with chemical additives. *Annual meeting on nuclear technology 2013 Documentation.* Berlin, 2013. 1142 p.
17. Medvedev V., Pustovgar A. Influence of chemical additives on radiation stability of concrete.theoretical basis and evaluation method. *Applied Mechanics and Materials*. 2015. Vol. 725–726. Pp. 377–382.
18. Medvedev V.V. *Povysheniye radiatsionnoy stoykosti betonov za schet primeneniya effektivnyh superplastifikatorov* [Increase of radiating stability of concrete at the expense of application effective supersofteners]. PhD dissertation. Moscow, 2015. 181 p. (rus)
19. Yershov V.Yu., Muzalevskij L.P., Dubrovskij V.B. *Copyright certificate No. 1641089 on invention: Sposob opredelenija radiacionnoj stojkosti cementnogo kamnja* [Hardened cement paste radiation stability determination method]. (rus)
20. Hilsdorf H.K., Kropp J., Koch H.J. The effects of nuclear radiation on the mechanical properties of concrete. *Proceedings of the Douglas McHenry International Symposium on Concrete and Concrete Structures, ACI SP 55-10, American Concrete Institute, Mexico City, Mexico*. 1978. Pp. 223–251.
21. Kaplan M.F. *Concrete Radiation Shielding: Nuclear Physics, Concrete Properties, Design, and Construction.* John Wiley & Sons, New York, NY, USA, 1989.
22. William K., Xi Y., Naus D. A review of the effects of radiation on microstructure and properties of concretes used innuclear power plants. *Tech. Rep. NUREG/CR-7171 ORNL/TM-2013/263, US Nuclear Regulatory Commission, Oak RidgeNational Laboratory.* 2013.
23. Field K.G., Remec I., Pape Y.Le. Radiation effects in concrete for nuclear power plants – Part I: Quantification of radiation exposure and radiation effects. *Nuclear Engineering and Design.* 2015. Vol. 282. Pp. 126–143.
24. Pape Y.Le, Field K.G., Remec I. Radiation effects in concrete for nuclear power plants, Part II: Perspective from micromechanical modeling. *Nuclear Engineering and Design.* 2015. Vol. 282. Pp. 144–157.
25. Pomaro B. A review on radiation damage in concrete for nuclear facilities. *Experiments to Modeling. Modelling and Simulation in Engineering.* 2016. Vol. 2016. Article ID 4165746, 10 p.
26. Muzalevskiy L.P. Prognozirovaniye stepeni izmeneniya prochnosti i radiatsionnyh deformaciy betona [Forecasting of degree of change of durability and radiating deformations of concrete]. *Trudy Tretey Vsesoyuznoy nauchnoy konferencii po zashchite ot ioniziruyushchih izlucheniy yaderno-tekhnicheskih ustanovok* [Works of the Third All-Union scientific conference on protection from Ionising radiation of Nuclear-technical installations]. Vol. 5. Tbilisi: Iz-vo TGU, 1985. Pp. 116–125. (rus)
27. Muzalevskiy L.P. *Radiatsionnye izmeneniya tyazhelyh betonov i metod ih analiticheskogo opredeleniya* [Radiating changes of heavy concrete and method of their analytical definition]. PhD dissertation. Moscow, 1989. 240 p. (rus)
28. Denisov A.V., Dubrovskiy V.B., Muzalevskiy L.P. Prognozirovaniye radiatsionnyh izmeneniy neorganicheskih stroitelnyh materialov [Forecasting of radiating changes of inorganic building materials]. *Voprosy atomnoy nauki i tekhniki. Ser. Proyektirovaniye i stroitelstvo.* 1990. No. 3. 2012. 284 c.
16. Medvedev V., Pustovgar A. Evaluation method of radiation stability of hardened cement paste with chemical additives // Annual meeting on nuclear technology 2013 Documentation. Berlin, 2013. 1142 p.
17. Medvedev V., Pustovgar A. Influence of Chemical Additives on Radiation Stability of Concrete. Theoretical Basis and Evaluation Method // Applied Mechanics and Materials. 2015. Vol. 725–726. Pp. 377–382.
18. Медведев В.В. Повышение радиационной стойкости бетонов за счет применения эффективных суперпластификаторов. Дисс. на соиск. учен. степ. к.т.н. М., 2015. 181 с.
19. Ершов В.Ю, Музалевский Л.П., Дубровский В.Б. Авторское свидетельство № 1641089 на изобретение: «Способ определения радиационной стойкости цементного камня».
20. Hilsdorf H.K., Kropp J., Koch H.J. The effects of nuclear radiation on the mechanical properties of concrete // Proceedings of the Douglas McHenry International Symposium on Concrete and Concrete Structures, ACI SP 55-10, American Concrete Institute, Mexico City, Mexico, 1978. Pp. 223–251.
21. Kaplan M.F. Concrete Radiation Shielding: Nuclear Physics, Concrete Properties, Design, and Construction. John Wiley & Sons, New York, NY, USA, 1989.
22. William K., Xi Y., Naus D. A review of the effects of radiation on microstructure and properties of concretes used innuclear power plants. Tech. Rep. NUREG/CR-7171 ORNL/TM-2013/263, US Nuclear Regulatory Commission, Oak RidgeNational Laboratory, 2013.
23. Field K.G., Remec I., Pape Y. Le. Radiation effects in concrete for nuclear power plants – Part I: Quantification of radiation exposure and radiation effects // Nuclear Engineering and Design. 2015. Vol. 282. Pp. 126–143.
24. Pape Y.Le, Field K.G., Remec I. Radiation effects in concrete for nuclear power plants, Part II: Perspective from micromechanical modeling // Nuclear Engineering and Design. 2015. Vol. 282. Pp. 144–157.
25. Pomaro B. A review on radiation damage in concrete for nuclear facilities // Experiments to Modeling. Modelling and Simulation in Engineering. 2016. Vol. 2016, Article ID 4165746, 10 p.
26. Музалевский Л.П. Прогнозирование степени изменения прочности и радиационных деформаций бетона // Труды Третьей Всесоюзной научной конференции по защите от ионизирующих излучений ядерно-технических установок. том V. Тбилиси: Из-во ТГУ, 1985. С. 116–125.
27. Музалевский Л.П. Радиационные изменения тяжелых бетонов и метод их аналитического определения: Дисс. на соиск. учен. степ. к.т.н. М., 1989. 240 с.
28. Денисов А.В., Дубровский В.Б., Музалевский Л.П. Прогнозирование радиационных изменений неорганических строительных материалов // Вопросы атомной науки и техники. Сер. Проектирование и строительство. 1990. № 3. С. 98–102.
29. Денисов А.В., Дубровский В.Б., Ершов В.Ю., Кореневский В.В., Музалевский Л.П., Сугак Е.Б. Радиационно-температурные изменения свойств портландцементного камня бетона и зависимости для их прогнозирования // Вопросы атомной науки и техники. Сер. Проектирование и строительство. 1989. № 2. С. 20–35.
30. Денисов А.В., Кирьянов Б.С., Мосеев Л.И., Музалевский Л.П., Сугак Е.Б. Газовыделение из компонентов бетона при реакторном облучении // Вопросы атомной науки и техники. Сер. Проектирование и строительство. 1988. № 2. С. 109–119.
31. Денисов А.В. Прогнозирование радиационного

Денисов А.В. Влияние суперпластификаторов на радиационные изменения портландцементного камня и бетонов // Инженерно-строительный журнал. 2017. № 5(73). С. 70–87.

Pp. 98–102. (rus)

29. Denisov A.V., Dubrovskiy V.B., Yershov V.Yu., Korenevskiy V.V., Muzalevskiy L.P., Sugak E.B. Radiatsionno-temperaturnyye izmeneniya svoystv portlandcementnogo kamnya betona i zavisimosti dlya ih prognozirovaniya [Radiation-thermal changes of properties of hardened cement paste and functions for their predictions]. *Voprosy atomnoy nauki i tekhniki. Ser. Proyektirovaniyye i stroitelstvo.* 1989. No. 2. Pp. 20–35. (rus)
30. Denisov A.V., Kiryanov B.S., Moseyev L. I., Muzalevskiy L. P., Sugak E.B. Gazovydeleniye iz komponentov betona pri reaktornom obluchenii [Gas evolution from concrete components at an irradiation in a nuclear reactor]. *Voprosy atomnoy nauki i tekhniki. Ser.: Proyektirovaniye i stroitelstvo.* 1988. No. 2. Pp. 109–119. (rus)
31. Denisov A.V. Prognozirovaniye radiatsionnogo gazovydeleniya iz betonov zashchity yadernyh reaktorov [Forecasting of radiating gas evolution from concrete of protection of nuclear reactors]. *Vestnik MGSU.* 2011. No. 8. Pp. 274–280. (rus)
32. Sheykin A.E. *Struktura, prochnost i treshchinostoykost tsementnogo kamnya* [Structure, durability and crack resistance of cement stone]. Moscow: Stroyizdat, 1974. 192 p. (rus)
33. Nesvetayev G.V., Shcherbinina T.A. K voprosu normirovaniya usadki tsementnykh betonov [About regulation of drying shrinkage of cement concrete]. *Naukovedenie.* 2015. Vol. 7. No. 5.

газовыделения из бетонов защиты ядерных реакторов // Вестник МГСУ. 2011. № 8. С. 274–280.

32. Шейкин А.Е. Структура, прочность и трещиностойкость цементного камня. М.: Стройиздат, 1974. 192 с.
33. Несветаев Г.В., Щербинина Т.А. К вопросу нормирования усадки цементных бетонов // Интернет-журнал «НАУКОВЕДЕНИЕ». 2015. Т. 7. № 5.

Aleksandr Denisov,
+7(499)1832583; den-al-v@inbox.ru

Александр Викторович Денисов,
+7(499)1832583; эл. почта: den-al-v@inbox.ru

Denisov A.V. The impact of superplasticizers on the radiation changes in Portland cement stone and concretes. *Magazine of Civil Engineering*. 2017. No. 5. Pp. 70–87. doi: 10.18720/MCE.73.7.

doi: 10.18720/MCE.73.8

Design methods of timber-concrete composite ceiling structure

Методы проектирования деревожелезобетонной композитной потолочной конструкции

M. Al Ali,
V. Bajzecerova,
V. Kvocak,
Technical University in Košice, Košice, Slovak Republic

Канд. техн. наук М. Ал Али,
канд. техн. наук В. Байзечерова
д-р техн. наук В. Квочак
Технический университет г. Кошице, Кошице, Словакия

Key words: timber-concrete; composite structures, Design methods, γ-method

Ключевые слова: деревожелезобетонные элементы; композитные конструкции; методы проектирования; γ-метод

Abstract. Timber-concrete composite structural members are increasingly used in the case of restoration of wooden ceilings. In the other hand, their use also increases in the case of new buildings. Design methods of the composite structures have been evolving since their first use. This expressive evolution of design methods is related to extensive research in this area in last three decades. This paper presents basic information about realisation, experimental and numerical analysis of timber-concrete composite ceiling with nail connections. The design of the mentioned ceiling was realised according to the relevant standards and recommendations in that time. The paper also presents a comparison between the design results of this composite ceiling and deflections measured during experimental short term loading process with the currently widely used analytical calculation model, so called γ-method. This method takes into account the joint compliance of the used nails. In addition, creep behaviour of used materials and concrete shrinkage were implemented in this calculation model. Comparison of the numerical and experimental results shows, that the current method better reflects the real stiffness of the ceiling structure. On the base of mentioned calculation model, the final deformation of the ceiling was also predicted.

Аннотация. При восстановлении деревянных потолочный конструкций все чаще используются древожелезобетонные композитные элементы. С другой стороны, их использование также увеличивается при строительстве новых зданий. Методы проектирования композитных конструкций эволюционировали с момента их первого использования. Эта значительная эволюция методов проектирования связана с обширными исследованиями в этой области за последние три десятилетия. В данной статье представлена основная информация о проведении, экспериментальном и численном анализе деревянного композитного потолка с гвоздевым соединением. Конструкция данного потолка была выполнена в соответствии со стандартами и рекомендациями, действующими на момент проектирования. Также представлено сравнение проектных результатов данного потолка и прогибов, измеренных во время экспериментального краткосрочного процесса загрузки, с широко используемой в настоящее время аналитической моделью расчета, так называемым γ-методом. Этот метод учитывает соответствие используемых гвоздей. Кроме того, в этой расчетной модели были учтены ползучесть используемых материалов и усадка бетона. Сравнение численных и экспериментальных результатов показывает, что текущий метод лучше отражает реальную жесткость потолочной конструкции. На основе указанной расчетной модели также была предсказана окончательная деформация потолка.

Introduction

Composite timber-concrete structures are created by joining several materials with different mechanical and physical properties. First attempts to join timber and concrete were made in the 20ies and 30ies of the last century. The first patent in this field was registered in Germany by Otto Schaub in 1939 [1]. In 1960, bearing structure of timber ceiling was strengthened as a part of the reconstruction of a historic building in Bratislava – Slovakia by joining timber beams with concrete slab using nails [2]. As a result, in 1966, Jozef Poštulka was granted a patent. Later in the 80ies, increased interest in the composite timber-concrete structures has been recorded. The development progressed especially in the

Ал Али М., Байзечерова В., Квочак В. Методы проектирования деревожелезобетонной композитной потолочной конструкции // Инженерно-строительный журнал. 2017. № 5(73). С. 88–95.

field of shear connectors, which resulted in a wide range of joining systems. In the next period, this structural system began to be used not only for renovation of old buildings, but increasingly also in new buildings because of the favourable structural and physical properties.

In the case of the timber part of the ceiling, beams with rectangular cross-sections, eventually solid wood planks are the most commonly used. The use of logs is not excluded [3], especially when used for temporary bridges and bridges on forest roads. It is, of course, possible to couple flat wood-based materials, such as vertical laminated nailed boards [4], glued laminated timber [5], cross laminated timber (CLT) [6, 7], eventually using of more resistant materials, such as laminated veneer lumber (LVL) [8].

The choice of concrete type depends on the size of the load. In usual ceilings and bridge constructions of smaller spans, it is possible to design concrete slabs not only from conventional concrete mixtures (from C12/25 to C50/60), but also from lightweight concrete (LC8/9 up to LC45/50), [6, 9]. For higher load sizes and larger spans, different types of high-grade concrete can be used, [10]. Usually, if the entire concrete layer is in the compressed area, strengthening of the concrete by means of main bearing reinforcement is not necessary. In order to reduce the shrinkage cracks, it is possible to use a structural reinforcement in two directions, eventually, fibre reinforced concrete can be also used [4 and 11]. Shrinkage of the concrete significantly affects the strain of composite timber-concrete elements [12], therefore, the ingredients that reduce the concrete shrinkage can be considered. Another possibility of reducing the undesirable influence of concrete shrinkage can be prefabrication of the concrete slab and subsequent coupling with the timber part using suitable connection means [13] or by gluing [10, 14].

The insuring of composite action between the concrete slab and timber elements can be provided by mechanical or glued connection. In the case of less exposed structures of smaller spans, it is economically advantageous to use dowel-type mechanical shear connectors, such as nails [2, 15]. However, the higher stiffness of coupling can be achieved using a pair of screws in the arrangement at an angle of 45° [16, 17]. The choice of shear connectors, their dimensions, their number and spacing depend on the shear force size in the chink between the wood and the concrete. In the case of joining flat wood-based materials, such as vertically laminated boards, the use of groove joints is appropriate [4, 18, 19]. In this case, the transmission of the shear force in the chink is mainly given by the shear strength of the concrete. The highest stiffness of the coupling can be achieved by gluing [5, 14, 20]. Epoxy adhesives allow bonding not only hardened concrete slab with the timber elements, but also to bond fresh concrete with an epoxy bonding agent. Besides the above mentioned, there are a large number of different shear connectors, such as perforated belts, steel strips with pressed mandrels, grooves in combination with pin joints, various heavy coupling systems for heavy loads for joining the prefabricated concrete slabs [13, 21, 22].

Number of methods were developed for calculation of composite structures. Historically, first used method was the method of idealized cross-section, based on modification factor *n* [2]. In this method, the composite action is considered as ideal rigid. Over the time, many researches and realized constructions proved, that the composite action using conventional dowel-type mechanical shear connectors can not be considered as ideal rigid, particularly in terms of element deflection. In the 60ies, Möhler [23] derived a calculation model of mechanically jointed timber beams with flexible connection. This method has proven to be appropriate and sufficient for the calculation of composite timber-concrete elements [17]. In the next period, the behaviour of these composites under long-term loading has been investigated and several rheological models have been proposed [16, 24, 25]. In addition to analytical and finite element methods, probabilistic methods based on probabilistic deterioration models are also being developed in this area [26].

From the above presented literature review is evident, that the possibilities and methods for design and calculation of these types of composite structures are very extensive. Therefore, within the presented research, the most common and most affordable type of timber-concrete composite ceiling was selected. The main idea of the realised research was to verify and confront the experimentally measured values with the results, obtained using various design methods.

In this paper, numerical and experimental analysis and results of realised timber-concrete composite ceiling with nail connections are presented. The design of the mentioned ceiling was realised according to the relevant standards and recommendations in that time. The paper also presents the comparison between the design results of this composite ceiling and deflections measured during experimental short-term loading process with the currently widely used analytical calculation model, so called γ-method.

Realisation, Methods and Calculation Models

Realisation of the composite ceiling structure

Timber-concrete composite slab was realised within a construction having rectangular shape of dimensions 30x12 m. Two external and one inner walls with spans 2x6 m created the vertical bearing system of the structure. Two-span continuous steel beams, spaced by 3.0 m, were set on the bearing walls. These beams created the main bearing system of the ceiling. At the same time, the steel beams provided a system for transfer of horizontal forces from the roof truss structure. The cross-section of timber beams had a dimensions 120x140 mm. These beams, axially spaced by 805 mm (Figs. 1, 2a), were lying onto the lower flange of the steel beams. The timber beams were covered by 25 mm thick boards, placed perpendicularly to the beams and fixed to them by nails. In the calculation, timber of strength 10 MPa and Young's modulus 10 000 MPa was considered.

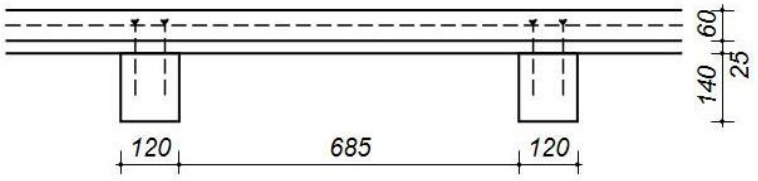

Figure 1. Layout scheme of the ceiling elements

Before hammering nails of dimensions 180/6.3 mm, holes were bored into the timber beams by means of prepared steel pattern plate to prevent the wood cleavage. Borer of diameter 5.5 mm was used to bore holes 80 mm deep, so that 1/3 of the nail length was hammered into the non-bored wood and the nail would protrude from the board by 40 mm.

After hammering the nails, welded net reinforcement was placed and the concrete slab of 60 mm thickness was poured (Fig. 2b). After concrete hardening the reinforced concrete slab started to act as a composite timber-concrete ceiling structure. In the calculation, concrete of strength 11.5 MPa and Young's modulus 27 000 MPa was considered.

a)  **b)** 

Figure 2. a) Layout of steel and timber elements, b) View during realization

Short-term loading test

Deflections of the timber beams were measured in the centre of their span and on the steel beams, in the placing spot of the timber beams. The measurement was carried out using mechanical indicators, as shown in Figure 3a.

Concrete roof tiles were used to create the load for the short-term loading test. The weight of one roof tile is 4.5 kg. The roof tiles were laid in nine rows in the direction of timber beams and in five rows in direction perpendicular to timber beams. By this way, an uniform load was created on an area of 3x2.4 m. The position of the load is illustrated in Figure 3b.

Before starting of the loading test, initial values on the deflection indicators were recorded and considered in the evaluation of final results. In the first stage, the loading test started with five layers of roof tiles uniformly spread onto defined area (3x2.4 m), which represents the load of 1.406 kN/m^2 and 1.132 kN/m uniform load on the monitored beam. The load was gradually increased by adding roof tiles layers as shown in Fig. 3b. In the final loading stage, the load reached a value of 6.48 kN/m^2, which represents 5.216 kN/m uniform load on the monitored beam. The measured deflections are presented in Figure 5.

Ал Али М., Байзечерова В., Квочак В. Методы проектирования деревожелезобетонной композитной потолочной конструкции // Инженерно-строительный журнал. 2017. № 5(73). С. 88–95.

a)  b) 

Figure 3. a) Set-up of the mechanical indicators, b) Process of loading

Calculation models and methods

Mentioned composite ceiling structure was designed according to relevant, in that time valid recommendation [2], i.e. method of idealized cross-section, based on modification factor *n*. For the verification of obtained results, 3D finite element model was created with consideration of the core and bases of this method. After the implementation of γ-method into new valid standards [27], calculation of the ceiling was carried out using this method to compare the old and new results.

Idealized cross-section method

In this method, the composite cross-section is replaced by timber cross-section with moment of inertia I_i, equated to moment of inertia of the original cross-section, taking into account the rigid connection between timber and concrete. Moment of inertia of the idealized cross-section is calculated according to following equation:

$$I_i = I_t + A_t a_t^2 + n\left(I_c + A_c a_c^2\right), \tag{1}$$

where I_i – moment of inertia of idealized cross-section, I_c – moment of inertia of concrete part, I_t – moment of inertia of timber part, A_c – cross-sectional area of concrete part, A_t – cross-sectional area of timber part, a_t – the distance between the centre of gravity of timber part and idealized cross section, a_c – the distance between the centre of gravity of concrete part and idealized cross section, n – modification factor defined as:

$$n = E_c / E_t, \tag{2}$$

where E_c – Young's modulus of elasticity of concrete in bending, E_t – Young's modulus of elasticity of timber.

Equations for calculation of normal and shear stress distribution can be found in [2, 4]. For the design of composite timber-concrete elements, serviceability limit state is often the determining. Deflection, caused by the considered short term loading δ can be calculated as:

$$\delta = \frac{5}{384}\frac{gL^4}{E_t I_i}. \tag{3}$$

Results of mentioned realized structure, calculated according to this method are presented in Table 1. The relationship between the load and the deflection is determined as $0.284q$, where q is the loading of the ceiling in kN/m^2, see Fig. 5. The stiffness of the timber formwork was disregarded in the calculations.

Finite element modelling (FEM)

The model consisted of simply supported timber beams, timber formwork, and concrete slab in accordance with the parameters in Chapter 2.1. Suitable software (FEAT), allowing the creation of surface connection between timber formwork and beams was used. This software also allows the creation of rigid far-connections between the concrete slab and the timber beams. No connections were generated between the timber formwork and the concrete slab. Fig. 4 illustrates a part of the calculation model. Deflections in the mid-span of the beams and stresses in the cross-section, obtained from the FE calculation model, are presented in Figure 5 and Table 1. Results of presented model proved the favourable effect of the timber formwork onto the general stiffness of the composite ceiling.

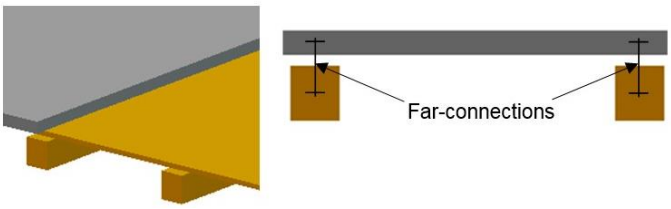

Figure 4. Part of the 3D FE model of the composite ceiling

γ-method

Currently, widely used analytical calculation model, so called *γ*-method, is based on the linear elastic solution of the simply supported timber-concrete composite beam. This method considers interlayer slip of joined layers, caused by the flexibility of shear connectors. The effective bending stiffness (EI_{ef}) of the simply supported composite beam according to this method, included in [27], can be calculated as:

$$(EI)_{ef} = E_c I_c + E_t I_t + \gamma E_c A_c a_c^2 + E_t A_t a_t^2, \quad (4)$$

where γ-factor is defined as:

$$\gamma = \left[1 + \pi^2 E_c A_c s / (K\ L^2)\right]^{-1}, \quad (5)$$

where *s* is the spacing between the connectors, *L* is the span of the beam, *K* is the slip modulus of the connectors.

The slip modulus *K* can be obtained experimentally, but some analytical equations for determination of modulus *K* are included in [27]. In our case, calculated value of the slip modulus for the ultimate limit state K_u was 6287 N/mm and for the serviceability limit state K_{ser} was 9431 N/mm.

Equations for determination of normal stress distribution are given by [16]. Deflection, caused by the considered short-term loading *δ* can be calculated as:

$$\delta = \frac{5}{384} \frac{gL^4}{(EI)_{ef}} \cdot \quad (3)$$

Results, obtained using this method are presented in Table 1. The relationship between the load and the deflection is determined as 0.654*q*, where *q* is the loading of the ceiling in kN/m^2, see Figure 5. The stiffness of the timber formwork was disregarded in the calculation. The effective width of the concrete slab was considered in the calculation according to [28]. The part of concrete cross-section, where a tensile stress arose, was not included when determining the stiffness of the composite cross-section.

Results

The results of measured and calculated deflections in the mid-span of above mentioned realized ceiling structure are illustrated in Figure 5.

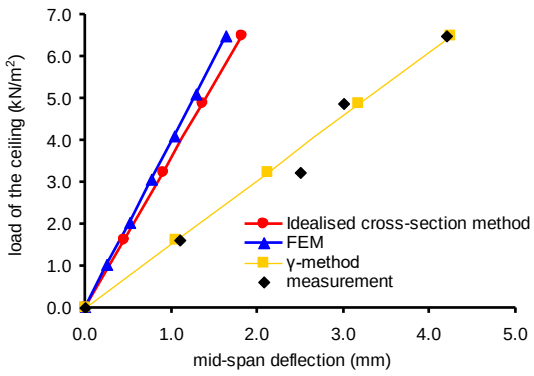

Figure 5. Comparison of measured and calculated values of the deflections

Ал Али М., Байзечерова В., Квочак В. Методы проектирования деревожелезобетонной композитной потолочной конструкции // Инженерно-строительный журнал. 2017. № 5(73). С. 88–95.

Calculated values of the stresses and deflections in the mid-span according to above mentioned methods and models are listed in Table 1. These results were determined with considering the design loading value of 5.2 kN/m^2.

Table 1. Comparison of the results according to various calculation methods

	$\sigma_{c,top}$ (MPa)	$\sigma_{t,\ bottom}$ (MPa)	F_s (kN)	δ (mm)
Idealised cross-section method	1.88	2.85	2.6	1.83
Finite element method	1.42	2.34	2.73	1.033
γ-method	3.32	4.48	3.17	3.40

$\sigma_{c,top}$ is the normal stress in the top fibres of the concrete part in the mid-span, $\sigma_{t,bottom}$ is the normal stress in the bottom fibres of the timber part in the mid-span, F_s is the maximal shear force in the connectors.

Discussion

As mentioned, this paper deals with numerical analysis using various calculation methods, 3D simulation and experimental measurement of already realized timber-concrete composite structure. Obtained results from these methods [2, 15–17] are compared, confronted with the experimental measurements and discussed in this chapter.

As shown in Figure 5, the deflections were calculated according to three methods, described in Chapter 2.2. From the comparison of the illustrated results is evident, that the measured values are almost identical to the values obtained from the calculation, when using γ-method. Results of this investigation prove, that γ-method is enough accurate and sufficiently appropriate to be used for the calculation of composite timber-concrete structures during short term loading.

Despite the fact that during the short term loading test higher load values were applied, mentioned realised structure was designed in accordance with the regulations in force at that time. Design loading value of 5.2 kN/m^2 was considered for the calculation of the stresses and deflection of the composite structure. This design value of loading is determined by the normative properties of used material to be on the safe side.

As shown in Table 1, values of normal stresses, shear forces and deflections, calculated according to *γ*-method are higher than the values calculated according to other methods, which do not consider the flexibility of shear connectors. However, presented values of normal stresses in the all cases are far from the limit values. The reached shear forces are close to the limit values. The deflections of the structure from the considered short-term loading meet the acceptable values.

Conclusions

The paper presents results of realized composite timber-concrete structures, obtained by application of experimental test and different calculation methods, described in detail in Chapter 3. The obtained results showed the appropriate sufficiency of γ-method for calculation of these types of composite structures, especially for short term loading. Presented results in the paper proved that the composite action using the dowel-type of shear connectors can not be considered as ideal rigid. In spite of relatively high flexibility, smooth nails are very used due to their availability.

Although the design of realized structure was carried out using methods that do not completely describe the real behaviour of the solved composite structure, the design was conducted with a sufficient reserve, so it is on the safe side. The design author of the mentioned structure is in a permanent contact with the owner of the building. More than 15 years after the realization, any problems with construction were not recorded.

Acknowledgement

This paper is prepared within the research projects VEGA No. 1/0188/16 and No. 1/0538/16, supported by the Scientific Grant Agency of the Ministry of Education of Slovak Republic and by the Slovak Academy of Sciences.

Al Ali M., Bajzecerova V., Kvocak V. Design methods of timber-concrete composite ceiling structure. *Magazine of Civil Engineering*. 2017. No. 5. Pp. 88–95. doi: 10.18720/MCE.73.8.

References

1. Schaub O. *Verbunddecke aus Holzrippen und Betonplatte*. Patent No. DE 673556 C. 1939.
2. Postulka J., Sandanus J. Berechnungsverfahren für eine Holz-Beton-Verbunddecke mit Nägeln als Verbindungsmittel. *Bautechnik.* 1999. No. 76. Pp. 1026–1030.
3. Rautenstrauch K., Grosse M., Lehmann S. *Forschungsvorhaben Brettstapel-Beton-Verbund: Auswertung der experimentlallen Untersuchungen Teil 2.* Bauhaus-Universität Weimar, 2002.
4. Kanócz J., Bajzecerová V., Šteller Š. Timber-concrete composite elements with various composite connections. Part 2: Grooved connection. *Wood research.* 2014. No. 59(4). Pp. 627–638.
5. Kanócz J., Bajzecerová V., Šteller Š. Timber-concrete composite elements with various composite connections. Part 3: Adhesive connection. *Wood research.* 2015. No. 60(6). Pp. 939–952.
6. Kanócz J., Bajzecerová V. CLT-lightweight concrete composite beam with adhesive connection. *Proceedings of 13th World Conference of Timber Engineering WCTE 2016.* Vienna University of Technology, 2016. Pp. 1–8.
7. Jorge L., Habenbacher J., Dujic B. Timber-concrete composite systems with cross-laminated timber. *Proceedings of 10th. World Conference of Timber Engineering WCTE 2010.* Trentino, Italy, 2010. Pp. 1–8.
8. Yeoh D., Fragiacomo M., Deam B. Experimental behaviour of LVL–concrete composite floor beams at strength limit state. *Engineering Structures.* 2011. No. 33(9). Pp. 2697-2707.
9. Jorge L.F., Schänzlin J., Lopes S.M.R., Cruz H., Kuhlmann U. Time-dependent behaviour of timber lightweight concrete composite floors. *Engineering Structures.* 2010. No. 32(12). Pp. 3966–3973.
10. Schäfers M. *Entwickelung von hybriden Bauteilen aus Holz und hochfesten bzw. Ultrahochfesten Betonen. Experimentelle und theoretische Untersuchungen.* Kassel university presss GmbH, Kassel, 2010.
11. Kanócz J., Kuliková D. High performance timber-concrete composite slab system with fiber reinforced concrete. *Proceedings of 9th World conference on Timber Engineering WCTE 2006.* Portland, USA, 2006. Pp. 1–8.
12. Kanócz J., Bajzecerová V. Influence of rheological behaviors to load-carrying capacity of timber-concrete composite beams under long term loading. *Procedia Engineering*. 2012. No. 40. Pp. 20–25.
13. Lukaszewska E., Johnsson H., Fragiacomo M. Performance of connections for prefabricated timber–concrete composite floors. *Materials and Structures.* 2008. No. 41(9). Pp. 1533–1550.
14. Eisenhut L., Seim W., Kühlborn S. Adhesive-bonded timber-concrete composites – Experimental and numerical investigation of hygrothermal effects. *Engineering Structures.* 2016. No. 125. Pp. 167–178.
15. Kvočák V., Al Ali M. Design and realization of composite timber-concrete beams. *Proceedings of Advances and Trends in Engineering Sciences and Technologies II.* Leiden: CRC Press/Balkema, 2016.Pp. 21–26.
16. Kanócz J., Bajzecerová V., Šteller Š. Timber-concrete composite elements with various composite connections. Part 1: Screwed connection. *Wood research.* 2013. No. 58(4). Pp. 555–570.
17. Kenel A. Zur Berechnung von Holz/Beton-Verbundkonstruktionen, Entwickelung und Vergleich verschiedener Berechnungsmethoden. *Forschungs- und Arbeitsbericht 115/42, EMPA Abteilung Holz.* Dübendorf, Germany. 2000.
18. Kuhlmann U., Schänzlin J. Grooves as shear connectors

Литература

1. Schaub O. Verbunddecke aus Holzrippen und Betonplatte. Patent No. DE 673556 C. 1939.
2. Postulka J., Sandanus J. Berechnungsverfahren für eine Holz-Beton-Verbunddecke mit Nägeln als Verbindungsmittel // Bautechnik. 1999. № 76. Pp. 1026–1030.
3. Rautenstrauch K., Grosse M., Lehmann S. Forschungsvorhaben Brettstapel-Beton-Verbund: Auswertung der experimentlallen Untersuchungen Teil 2. Bauhaus-Universität Weimar, 2002.
4. Kanócz J., Bajzecerová V., Šteller Š. Timber-concrete composite elements with various composite connections. Part 2: Grooved connection // Wood research. 2014. № 59(4). Pp. 627–638.
5. Kanócz J., Bajzecerová V., Šteller Š. Timber-concrete composite elements with various composite connections. Part 3: Adhesive connection // Wood research. 2015. № 60(6). Pp. 939–952.
6. Kanócz J., Bajzecerová V. CLT-lightweight concrete composite beam with adhesive connection // Proceedings of 13th World Conference of Timber Engineering WCTE 2016. Vienna University of Technology, 2016. Pp. 1–8.
7. Jorge L., Habenbacher J., Dujic B. Timber-concrete composite systems with cross-laminated timber // Proceedings of 10th. World Conference of Timber Engineering WCTE 2010. Trentino, Italy, 2010. Pp. 1–8.
8. Yeoh D., Fragiacomo M., Deam B. Experimental behaviour of LVL–concrete composite floor beams at strength limit state // Engineering Structures. 2011. № 33(9). Pp. 2697–2707.
9. Jorge L.F., Schänzlin J., Lopes S.M.R., Cruz H., Kuhlmann U. Time-dependent behaviour of timber lightweight concrete composite floors // Engineering Structures. 2010. № 32(12). Pp. 3966–3973.
10. Schäfers M. Entwickelung von hybriden Bauteilen aus Holz und hochfesten bzw. Ultrahochfesten Betonen. Experimentelle und theoretische Untersuchungen. Kassel university presss GmbH, Kassel, 2010.
11. Kanócz J., Kuliková D. High performance timber-concrete composite slab system with fiber reinforced concrete // Proceedings of 9th World conference on Timber Engineering WCTE 2006. Portland, USA, 2006. Pp. 1–8.
12. Kanócz J., Bajzecerová V. Influence of rheological behaviors to load-carrying capacity of timber-concrete composite beams under long term loading // Procedia Engineering. 2012. № 40. Pp. 20–25.
13. Lukaszewska E., Johnsson H., Fragiacomo M. Performance of connections for prefabricated timber–concrete composite floors // Materials and Structures. 2008. № 41(9). Pp. 1533–1550.
14. Eisenhut L., Seim W., Kühlborn S. Adhesive-bonded timber-concrete composites – Experimental and numerical investigation of hygrothermal effects // Engineering Structures. 2016. № 125. Pp. 167–178.
15. Kvočák V., Al Ali M. Design and realization of composite timber-concrete beams // Proceedings of Advances and Trends in Engineering Sciences and Technologies II. Leiden: CRC Press/Balkema, 2016. Pp. 21–26.
16. Kanócz J., Bajzecerová V., Šteller Š. Timber-concrete composite elements with various composite connections. Part 1: Screwed connection // Wood research. 2013. № 58(4). Pp. 555–570.
17. Kenel A. Zur Berechnung von Holz/Beton-Verbundkonstruktionen, Entwickelung und Vergleich verschiedener Berechnungsmethoden // Forschungs- und Arbeitsbericht 115/42, EMPA Abteilung Holz. Dübendorf, Germany. 2000.
18. Kuhlmann U., Schänzlin J. Grooves as shear connectors

Ал Али М., Байзечерова В., Квочак В. Методы проектирования деревожелезобетонной композитной потолочной конструкции // Инженерно-строительный журнал. 2017. № 5(73). С. 88–95.

for timber-concrete composite decks. *Proceedings of the International RILEM Symposium, PRO 22, Joints in Timber Structures.* Stuttgart. 2001.

19. Michelfelder B. *Trag- und Verformungsverhalten von Kerven bei Brettstapel-beton-Verbunddecken. Institut für Konstruktion und Entwurf.* Universität Stuttgart. Dissertation. 2006.
20. Negrão J., Leitão de Oliveira C., Maia de Oliveira F., Cachim P. Glued composite timber-concrete beams. I: Interlayer connection specimen tests. *Journal of Structural Engineering.* 2010. No. 136(10). Pp. 1236–1245.
21. Kuklík P., Nechanický P., Kuklíková A. Development of prefabricated timber-concrete composite floors. *Proceedings of 11th World Conference of Timber Engineering WCTE 2012.* Auckland, New Zealand. Pp. 1–8.
22. Balogh J. at al. Fatigue Behavior of Notched Connections in Wood-Concrete Composties. *Proceedings of 11th World Conference of Timber Engineering WCTE 2012*. Auckland, New Zealand. 2012. Pp. 1–8.
23. Möhler K. *Über das Tragverhalten von Biegeträgern und Druckstäben mit zusammengesetzem Querschnitt und nachgiebigen Verbindungsmitteln.* Habilitationsschrift. Karlsruhe. 1956.
24. Fragiacomo M. Long-term behavior of timber-concrete composite beams. II: Numerical analysis and simplified evaluation. *Journal of Structural Engineering. ASCE.* 2006. No. 132(1). Pp. 23–33.
25. Schänzlin J. *Zum Langzeitverhalten von Brettstapel-Beton-Verbunddecken.* Institut für Konstruktion und Entwurf - Universität Stuttgart. Dissertation. 2003.
26. Velimirović N., et al. Time-dependent Reliability Analysis of Timber-Concrete Composite Beams. *Periodica Polytechnica Civil Engineering.* 2017. Pp. 1–9.
27. *EN 1995-1-1: 2004.* Eurocode 5: Design of Timber Structures–Part 1–1: General Rules and Rules for Buildings. European Committee for Standardization Brussels. Belgium. 2004.
28. *EN 1992-1-1: 2004.* Eurocode 2: Design of Concrete Structures–Part 1–1: General Rules and Rules for Buildings. European Committee for Standardization Brussels. Belgium. 2004.

for timber-concrete composite decks // Proceedings of the International RILEM Symposium, PRO 22, Joints in Timber Structures. Stuttgart. 2001.

19. Michelfelder B. Trag- und Verformungsverhalten von Kerven bei Brettstapel-beton-Verbunddecken. Institut für Konstruktion und Entwurf. Universität Stuttgart. Dissertation. 2006.
20. Negrão J., Leitão de Oliveira C., Maia de Oliveira F., Cachim P. Glued composite timber-concrete beams. I: Interlayer connection specimen tests // Journal of Structural Engineering. 2010. № 136(10). Pp. 1236–1245.
21. Kuklík P., Nechanický P., Kuklíková A. Development of prefabricated timber-concrete composite floors // Proceedings of 11th World Conference of Timber Engineering WCTE 2012. Auckland, New Zealand. Pp. 1–8.
22. Balogh J. at al. Fatigue Behavior of Notched Connections in Wood-Concrete Composties // Proceedings of 11th World Conference of Timber Engineering WCTE 2012. Auckland, New Zealand. Pp. 1–8.
23. Möhler K. Über das Tragverhalten von Biegeträgern und Druckstäben mit zusammengesetzem Querschnitt und nachgiebigen Verbindungsmitteln. Habilitationsschrift. Karlsruhe. 1956.
24. Fragiacomo M. Long-term behavior of timber-concrete composite beams. II: Numerical analysis and simplified evaluation // Journal of Structural Engineering. ASCE. 2006. № 132(1). Pp. 23–33.
25. Schänzlin J. Zum Langzeitverhalten von Brettstapel-Beton-Verbunddecken. Institut für Konstruktion und Entwurf - Universität Stuttgart. Dissertation. 2003.
26. Velimirović N., et al. Time-dependent Reliability Analysis of Timber-Concrete Composite Beams // Periodica Polytechnica Civil Engineering. 2017. Pp. 1–9.
27. EN 1995-1-1: 2004. Eurocode 5: Design of Timber Structures–Part 1–1: General Rules and Rules for Buildings. European Committee for Standardization Brussels. Belgium. 2004.
28. EN 1992-1-1: 2004. Eurocode 2: Design of Concrete Structures–Part 1–1: General Rules and Rules for Buildings. European Committee for Standardization Brussels. Belgium. 2004.

Mohamad Al Ali,
+421905359228; mohamad.alali@tuke.sk

Viktoria Bajzecerova,
+421556024289; viktoria.bajzecerova@tuke.sk

Vincent Kvocak,
+421556024112; vincent.kvocak@tuke.sk

Мохамад Ал Али,
+421905359228;
эл. почта: mohamad.alali@tuke.sk

Виктория Вайзечерова
+421556024289;
эл. почта: viktoria.bajzecerova@tuke.sk

Винсент Квочак
+421556024112;
эл. почта: vincent.kvocak@tuke.sk

Al Ali M., Bajzecerova V., Kvocak V. Design methods of timber-concrete composite ceiling structure. *Magazine of Civil Engineering*. 2017. No. 5. Pp. 88–95. doi: 10.18720/MCE.73.8.

doi: 10.18720/MCE.73.9

Stress-strain state of seepage-control walls in foundations of embankment dams

Напряжённо-деформированное состояние противофильтрационных стен в основании грунтовых плотин

M.P. Sainov,
V.V. Lubyanov,
National Research Moscow State Civil Engineering University, Moscow, Russia

Канд. техн. наук, доцент М.П. Саинов,
студент В.В. Лубьянов,
Национальный исследовательский Московский государственный строительный университет, г. Москва, Россия

Key words: cut-of wall; stress-strain state; clay-cement concrete; numerical modeling; strength

Ключевые слова: стена в грунте; напряжённо-деформированное состояние; глиноцементобетон; численное моделирование; прочность

Abstract. Results are considered of systematic study of stress-strain state (SSS) of a seepage-control wall arranged in the embankment dam foundation. The following factors affecting the wall SSS were studied: the wall depth, deformation modulus of the wall material, the pattern of the wall resting. Studies were conducted with the aid of numerical modeling. They revealed significant role of friction processes and slippage at the contact with soil on the wall SSS formation. It is friction through which soil transfers to the wall the compressive longitudinal forces which increase while the wall stiffness increases. It was also revealed that conditions of operation of suspended walls are more favorable that those of walls resting on rock. Empirical formulae were proposed which permit predicting the value of maximum compressive forces in the wall. Compressive strength of the wall was assessed. At that, it was taken into account that strength of plastic clay-cement concrete considerably increases if it is compressed from all sides as compared to uniaxial compression. A considerable role of accounting this effect was shown at selecting material for arrangement of the wall. It was obtained that to provide the wall strength it is necessary to have its material deformability exceeding the deformability of the surrounding soil not more than 5 fold. It was revealed that at perceiving by the wall the horizontal forces of seepage or hydrostatic pressure the longitudinal forces in it sharply decrease. It was obtained that then there is a danger of the wall tensile stress failure, because bend deformations in the wall cause irregular distribution of stresses in it. Especially it is hazardous for the walls made of rigid materials.

Аннотация. Рассматриваются результаты методического исследования напряжённо-деформированного состояния (НДС) противофильтрационной стены, устроенной в основании грунтовой плотины. Было исследовано влияние на НДС стены следующих факторов: глубина стены, модуль деформации материала стены, схема опирания стены. Исследования проводились путём численного моделирования. Они выявили значительную роль на формирование НДС стены процессов трения и проскальзывания на контакте с грунтом. Именно через трение грунт передаёт на стену значительные сжимающие продольные усилия, которые тем больше, чем больше жёсткость материала стены. Также выявлено, что условия работы висячих стен более благоприятные, чем у стен, опёртых на скалу. Предложены эмпирические формулы, которые позволяют спрогнозировать величину максимальных сжимающих напряжений в стене. Выполнена оценка прочности стены на сжатие. При этом учитывалось, что прочность пластичного глиноцементобетона существенно возрастает по сравнению с одноосным сжатием, если он сжат со всех сторон. Показана существенная роль учёта этого эффекта при выборе материала для устройства стены. Получено, что для обеспечения прочности стены необходимо, чтобы деформируемость её материала не более чем в 5 раз превышала деформируемость окружающего грунта. Обнаружено, что при восприятии стеной горизонтальных сил фильтрационного или гидростатического давления, продольные усилия в ней резко уменьшаются. Получено, что при этом возникает опасность нарушения прочности стены на растяжение, т.к. изгибные деформации стене вызывают в ней неравномерное распределение напряжений. Особенно это опасно для стен, которые выполнены из жёстких материалов.

Саинов М.П., Лубьянов В.В. Напряжённо-деформированное состояние противофильтрационных стен в основании грунтовых плотин // Инженерно-строительный журнал. 2017. № 5(73). С. 96–112.

Introduction

As it is known, very often deep curtains are arranged by a cutoff wall method for seepage control in foundations of embankment dams. The advantage of this type of curtains as compared to injections is the fact that they reliably intersect water permeable layer. At that, arrangement of the walls is cost-saving, because they have small thickness (0.6÷1.2 m). If the wall is made of materials based on cement (concrete, clay-cement concrete), in compliance with the existing standards[1] it may withstand considerable head gradient (more than 100). Due to this seepage-control walls may perceive great heads. At use of modern technologies their depth may reach 135 m as at Peribonka dam in Canada [1]. Therefore, the cutoff wall methodology at present is widely used in hydraulic construction against seepage. The examples may be dams Karkhe [2], Xialongdi [3], Kureika [4], Yumaguza [5], Sangtuda [6], Peribonka [1], Merowe [7], Sylvenstein [8] and others.

In order to provide safe operation of seepage-control walls (SCW) it is necessary to provide their crack growth resistance and strength. Therefore, to assess strength at SCW designing it is required to assess their stress-strain state (SSS).

By present time the issue of SCW SSS has not been sufficiently studied. SSS analyses of wall made of non-soil materials were conducted in Moscow Civil Engineering University by a number of authors
[9–12]. However, in most cases they referred to walls arranged in dam bodies.

Recently there appeared papers about SSS of SCW arranged in dam foundations [13–16]. A number of papers devoted to SSS of SCW have been also prepared by us [17–21]. It was established that walls in embankment dam foundations may subject to considerable compressive and tensile longitudinal stresses. We revealed that these stresses are more the more is the ratio between deformation moduli of the wall material and foundation soil. The results of our studies showed that to provide the wall strength it is necessary to have its material deformability exceeding the deformability of the surrounding soil not more than 5 fold which complies with ICOLD recommendations [22].

However, these studies were not of systematic character; their results refer only to particular considered conditions. This paper describes the results of more full systematic study of SSS of seepage-control walls arranged in foundations of embankment dams. The purpose of this work is to reveal operation conditions and peculiar features of CSW SSS in foundation of an embankment dam as well as to verify recommendations for selection of material for SCW. These studies also permit assessing the effect on SSS of such factors as material rigidity of the wall, its depth, and conditions of rest.

In the studies there considered a seepage-control wall made in the uniform non-soil foundation of 100 m high embankment dam. It is a rock-earthfill dam with a core. The dam shells are filled with gravel-pebble soil; the core is made of loam. The wall is arranged along the core axis (Fig.1). The scheme of the wall and core conjugation (with the aid of a cantilever or a concrete gallery) was not considered not to complicate the analysis of SCW operation conditions. The wall does not propagate into the dam core.

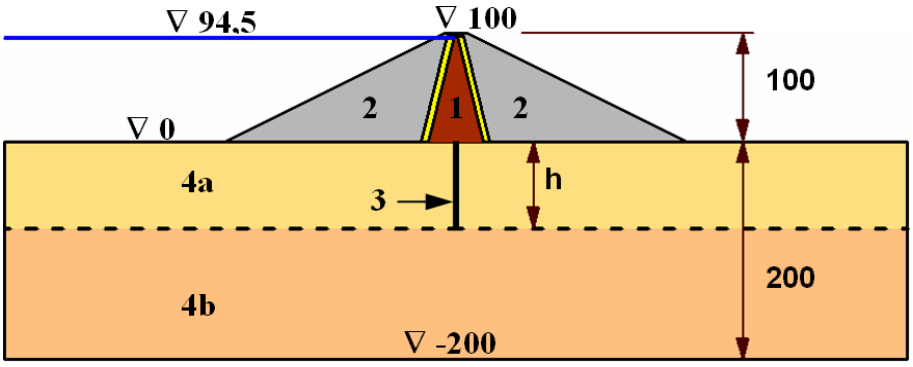

Figure 1. Design diagram of the wall in foundation of an embankment dam:
1 – loam core, 2 – shells of gravel-pebble, 3 – seepage-control wall, 4a, 4b – foundation layers

Two alternatives of foundation structure were considered. The first alternative is a homogenous structure of the earth foundation. In the second alternative the upper layer which is cut out by a wall, consists of earth and the lower layer refers to rock.

[1] Building Code SP 23.13330.2011. Foundations of hydraulic structures. Updated version of SNiP 2.02.02-85.

Sainov M.P., Lubyanov L.V. Stress-strain state of seepage-control walls in foundations of embankment dams. *Magazine of Civil Engineering*. 2017. No. 5. Pp. 96–112. doi: 10.18720/MCE.73.9.

Foundation soils were taken to be linearly deformable at active loading and unloading. Deformation modulus of the earth where the wall was arranged at active loading was taken equal 100 MPa and at unloading 500 MPa. This earth refers to gravel-pebble-sand soil. The earth Poisson's number was taken equal 0.35. Earth friction coefficient ($f = tg\ \varphi$) along the wall was taken equal 0.78 ($\varphi = 38°$); specific cohesion was absent.

Methods

Studies were conducted with the aid of numerical modeling by finite element method (FEM). Computations were conducted with use of software worked out by Dr. Ph. (Tech) M.P. Sainov [23].

Finite-element model of the structure covered the dam body and the foundation block. It was sufficiently detailed and comprised 1157 finite elements (Fig. 2). Width-wise the wall 3 rows of finite elements were distinguished. Among the finite elements 38 were contact elements; they simulated non-linear behavior at interaction of foundation soils with the wall. Besides, contact elements simulated possibility of occurrence of shear cracks in the soil mass above the wall top and the foot of the wall. At creation of a finite-element model the high-order finite elements were used with cubic approximation of displacements inside the element. The number of the model degrees of freedom comprised 11208.

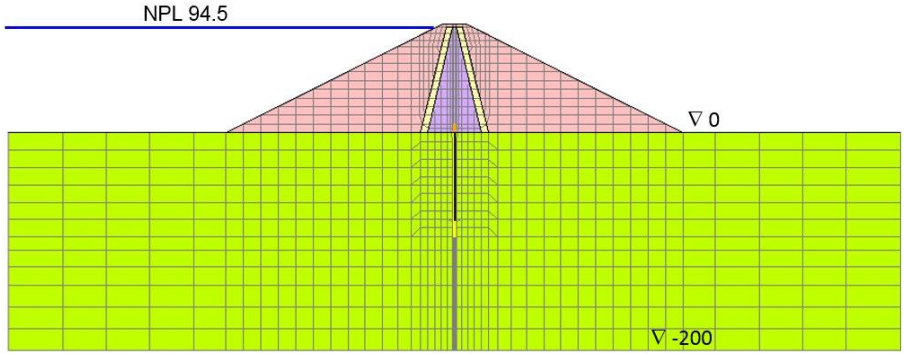

Figure 2. Diagram of FEM computational mesh

Studies were conducted for 6 design diagrams. The wall depth (20, 40 or 80 m) and conditions of its rest (suspended or resting). The resting wall was deepened into a rock layer with deformation modulus 5000 MPa; i.e. conditions of embedding were modeled. Parameters of design diagrams are given in Table 1.

Table 1. Parameters of design diagrams

No. of alternative	IA	IB	IC	IIA	IIB	IIC
Wall depth, m	80	40	20	80	40	20
Thickness of earth foundation under the wall, m	120	160	180	0	0	0
Conditions of rest	suspended			resting		

Rock on which the wall rested in the design was taken as waterproof. Therefore, in the alternatives of series II the resting wall took hydrostatic pressure of the upstream and downstream sides. In the alternatives of series I the suspended wall worked on taking loads from streamlining the wall by seepage flow. Therefore, to determine seepage loads in alternatives IA, IB, IC the seepage task was solved (Fig. 3). Analysis shows that suspended walls perceive horizontal forces 2–3 times as less as compared to resting walls.

For each of the design diagrams several alternatives of the wall materials were considered: from liquid plastic clay-cement concrete to reinforced concrete (Table 2).

Table 2. Parameters of wall material alternatives

Alternative	density, t/m³	deformation modulus [MPa]	Poisson's ratio	Uniaxial compression strength [MPa]	Angle of internal friction
1	1.93	100	0.30	1.27	30°
2	1.98	500	0.30	2.13	32°
3	2.10	1000	0.30	2.66	35°
4	2.12	5000	0.25	4.45	40°
5	2.40	29000	0.18	11.5	

These parameters were determined by us based on the results of experimental studies of clay-cement concrete properties conducted by other authors [5, 24–26]. For concrete, uniaxial compression strength (11.5 MPa) was adopted in compliance with Building Code SP 23.13330.2011.

32 design steps were considered. The first and the second step modeled the foundation SSS before the dam construction. The next step simulated the process of the wall arrangement by the trench method: trench excavation for the wall was modeled and its filling by the wall material. It was assumed that the wall material was not in the hardened state at perceiving its own weight. Its deformation modulus was taken equal 20% of the final one and Poisson's ratio was 0.45. At this step it was taken into account that non-hardened wall material could freely slip with respect to the trench walls.

At the next 16 steps there was model the process of the embankment layered construction. The next 13 steps modeled the process of the reservoir filling and the process of forming seepage (or hydrostatic) forces in the foundation. The task on stabilized seepage regime was solved for determining seepage forces (Fig. 3).

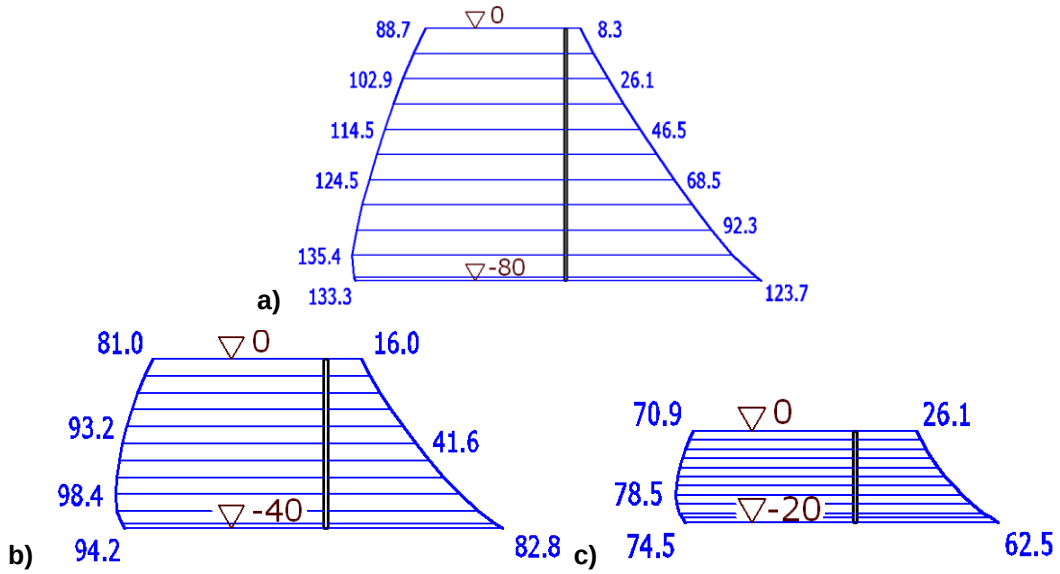

Figure 3. Seepage loads on the wall (in meters of water column): a – at wall depth 80m, b – at wall depth 40m, c – at wall depth 20 m

Results and Discussion

Analysis of the results of SCW SSS computations was conducted for two most dangerous moments of time:

1) moment of the dam construction completion,

2) moment of the reservoir filling completion.

As it was shown earlier [21], the first moment is dangerous from the point of view of hazardous failure of compression strength. At this moment the wall perceives maximum vertical load and has maximum compressive stresses. The wall vertical load appears due to settlements of the surrounding

earth mass under the action of the dam weight. This load is transferred to the wall by the foundation soil through friction on the contact “soil-wall”.

The second moment of time is dangerous from the point of view of possible appearance of tensile stresses in the wall. Tension in the wall may appear due to bend deformations, which the wall acquires at perceiving water pressure horizontal forces.

The results of analyses are given in Figures 4–15, 18–29 for some design alternatives in the form of curves of stresses and displacements. The curves of stresses given in the figures do not take into account stresses in the wall from its own weight.

Analysis of the results of SCW SSS computations for the moment of the dam construction completion shows the following:

- If the wall is made of rigid material, at the foundation settlements the considerable compressive longitudinal stresses are transferred to the wall. Due to this compressive stresses are concentrated in it.
- The more the wall material differs by deformability from the foundation soil, the higher are vertical compressive stresses y in it.
- For the alternatives where SCW is made of rigid materials (No. 3, No. 4, No. 5), there develops the typical process of the soil slip with respect to the wall due to the contact shear strength failure. The slip processes occur mainly in the upper part of the contact “wall-soil”.
- Due to this maximum compression is observed in the wall lower part.

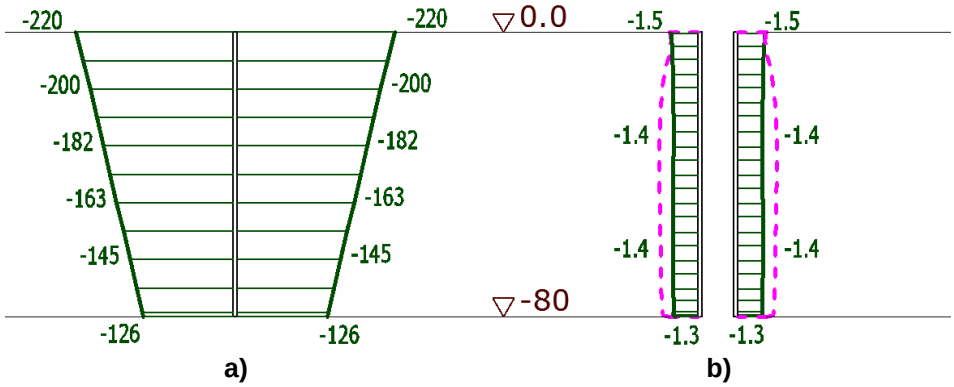

Figure 4. Wall SSS of alternative IA-1 for the moment of the dam construction completion: a – settlements (cm), b – vertical stresses (MPa) on the upstream and downstream faces

Green lines correspond to the curves for the wall. Pink-violet lines correspond to soil settlements. The dotted line indicates the wall material compressive strength.

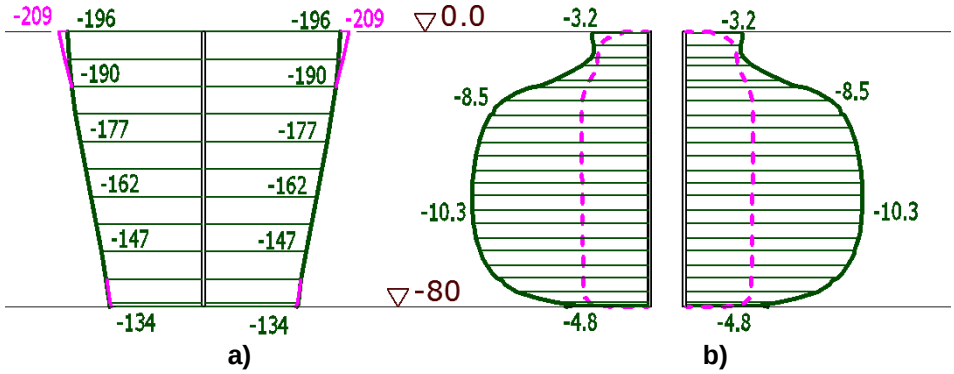

Figure 5. Wall SSS in alternative IA-3 for the moment of the dam construction completion. Legend see at Figure 4

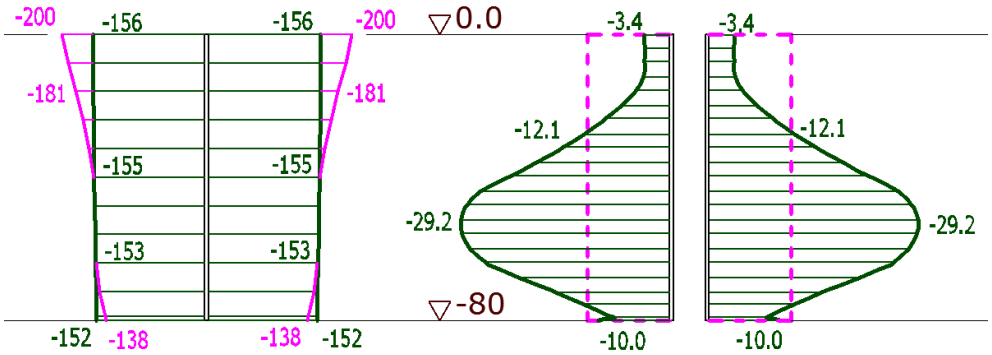

Figure 6. Wall SSS in alternative IA-5 for the moment of the dam construction completion. Legend see at Figure 4

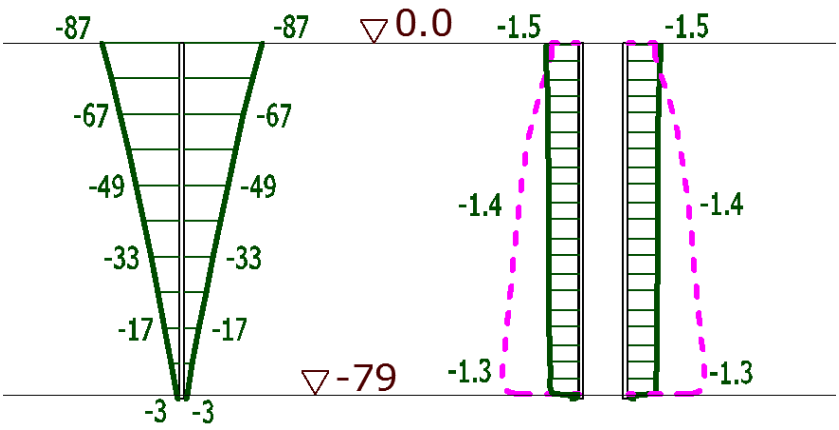

Fig.7. Wall SSS in alternative IIA-1 for the moment of the dam construction completion: a – settlements (cm), b – vertical stresses (MPa) on the upstream and downstream faces

Green lines correspond to the curves for the wall. Pink-violet lines correspond to soil settlements. The dotted line indicates the wall material compressive strength.

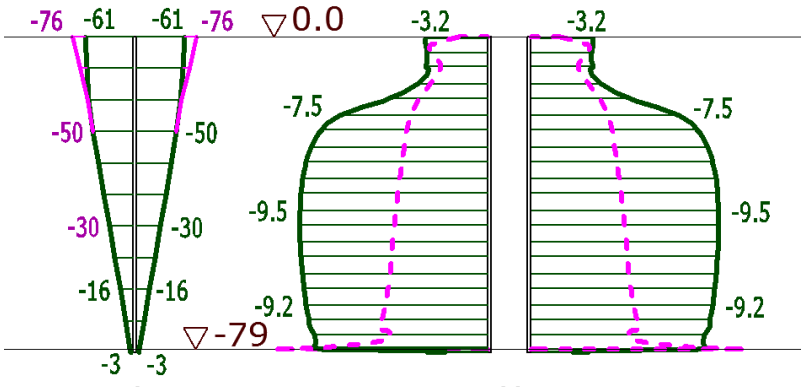

Figure 8. Wall SSS in alternative IIA-3 for the moment of the dam construction completion. Legend see at Figure 7

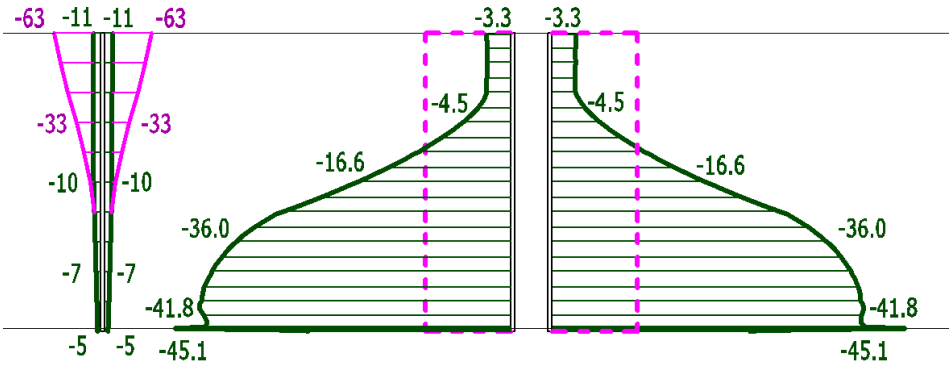

a) b)

Figure 9. Wall SSS in alternative IIA-5 for the moment of the dam construction completion. Legend see at Figure 7

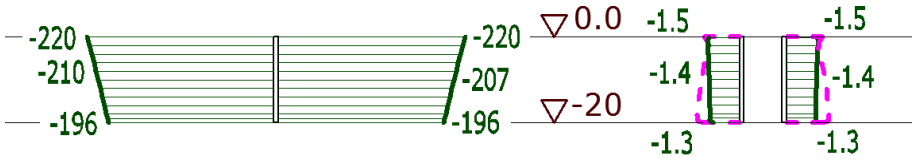

a) b)

Figure 10. Wall SSS in alternative IC-1 for the moment of the dam construction completion: a – settlements (cm), b – vertical stresses (MPa) on the upstream and downstream faces

Green lines correspond to the curves for the wall. Pink-violet lines correspond to soil settlements. The dotted line indicates the wall material compressive strength.

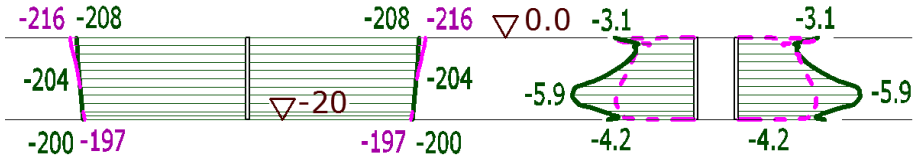

a) b)

Figure 11. Wall SSS in alternative IC-3 for the moment of the dam construction completion. Legend see at Figure 10

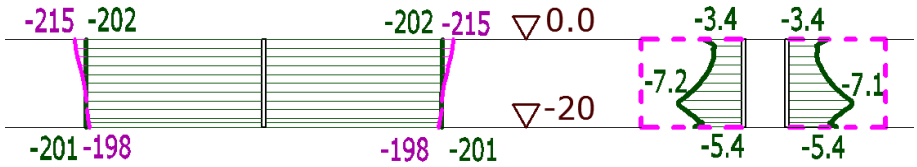

a) b)

Figure 12. Wall SSS in alternative IC-5 for the moment of the dam construction completion. Legend see at Figure 10

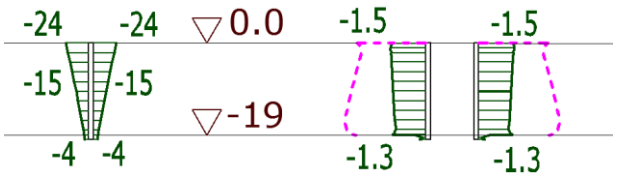

a) b)

Figure 13. Wall SSS in alternative IIC-1 for the moment of the dam construction completion. Legend see at Figure 10

Саинов М.П., Лубьянов В.В. Напряжённо-деформированное состояние противофильтрационных стен в основании грунтовых плотин // Инженерно-строительный журнал. 2017. № 5(73). С. 96–112.

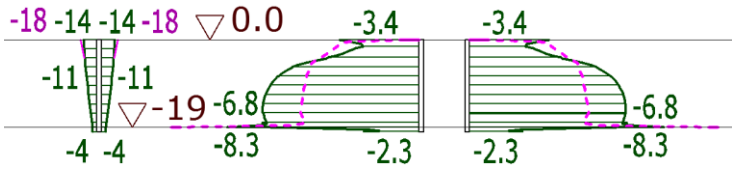

a) b)

Figure 14. Wall SSS in alternative IIC-3 for the moment of the dam construction completion. Legend see at Figure 10

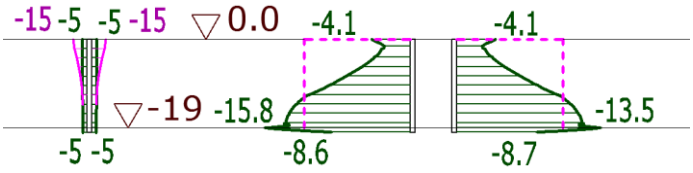

a) b)

Figure 15. Wall SSS in alternative IIC-5 for the moment of the dam construction completion. Legend see at Figure 10

For each design diagram there were drawn variation curves of maximum stresses σ_y^{max} depending on the ratio between deformation modulus E_{wall} and foundation deformation modulus E_{found} (Fig. 16).

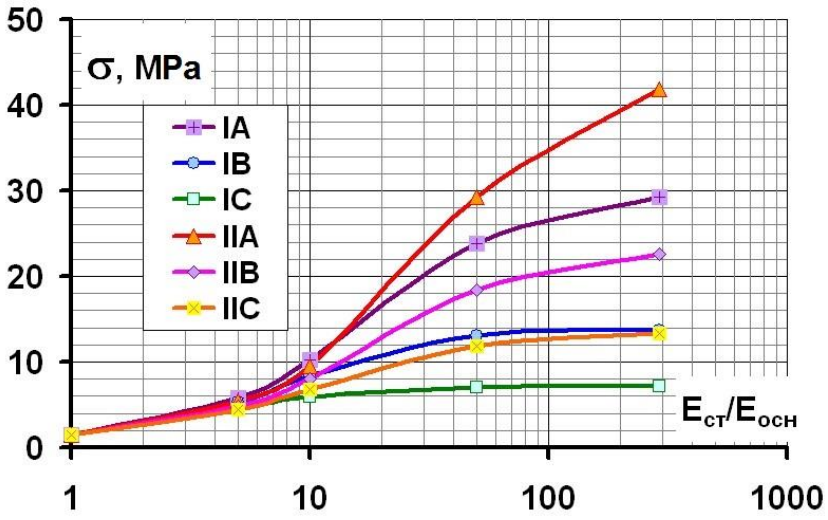

Figure 16. Variation of maximum values of longitudinal stresses in the wall depending on ratio E_{wall}/E_{found}

It is possible to distinguish two typical sections in this relationship. The first section is characterized by smooth increase of compressive stresses in the wall as the ratio E_{wall}/E_{found} increase. It is realized at E_{wall}/E_{found}. not exceeding 20. These conditions are characterized by weak development of slip processes at contact «wall-soil». Slip occurs only in the upper part of the contact; its shear strength is minimum.

At the first section the relationship between E_{wall}/E_{found} may be rather strictly described by the following relationship:

$$\sigma_y^{max} = A \cdot p \cdot \left(\frac{E_{ст}}{E_{осн}} \right)^n , \qquad (1)$$

where p – pressure transferred from the dam to the foundation,

A, n – empirical values.

By the results of analysis the pressure p amounted to approximately 1.5 MPa.

One of the empirical relationship parameters is always A≈1. The obtained values of index n are shown in Table 3.

Table 3. Values of index n

Design diagram	IA	IB	IC	IIA	IIB	IIC
n	0.84	0.78	0.70	0.76	0.73	0.66

Analysis of the obtained graphs (Fig. 16) shows that at the first section of relationship E_{wall}/E_{found} is characteristic the following:

- In the resting walls the maximum stress values y grow slightly less intensively than in suspended walls. This is explained by increase of contact "wall-soil" length where slip processes develop;
- Stress maximum values y have small dependence on the wall depth, though less deep walls have slightly less values of stress.

The study permitted revealing that the value of index n depends on the wall depth and conditions of the wall performance (suspended or resting). Dependence of n from the wall depth H may be described by relationship:

$$n = B\,H^{m} \qquad (2)$$

Empirical index B is within limits $0.46 \div 0.48$, and $m \approx 0.12 \div 0.13$ depending on boundary conditions of the wall operation conditions.

At the second section (at $E_{wall}/E_{found} > 10 \div 20$) the possibility of further increase of stresses in the wall is limited by intensive development of slip processes at contact "wall-foundation". The more is the length of the contact where shear strength fails, the higher are the values of stresses σ_y^{max} in the wall. Failure of the contact shear strength develops mainly from the wall upper end downward. Suspended walls have the contact strength failure near the lower end also.

Due to presence of slip there is limit value of maximum compressive stresses which may be transferred to the wall.

Analysis of the results shows that:

- The deeper is the wall, the higher is limiting compressive stress in it. For example, in diagram IA-5 (H=80 m) they comprised 29.2 MPa (Fig. 6b), and in diagram IC-5 (H = 20 m) – 7.2 MPa (Fig. 12b);
- In the walls resting on rock foundation the limit value of compressive stress is higher that in suspended walls. For example, in diagram IA-5 limit stresses amounted to 29.2 MPa (Fig. 6b), and in diagram IIA-5 – 41.8 MPa (Fig. 9b).

Thus, resting walls of large depth have more favorable SSS.

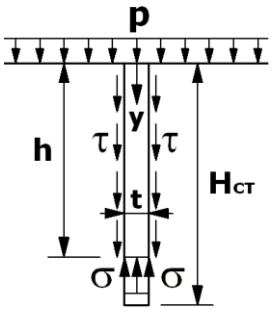

Figure 17. Diagram for the wall analysis

In [27] for the simplified design diagram (Fig. 17) we obtained an analytical dependence for determining the limit value:

$$\sigma_y^{пред} = p + \frac{h}{t}\left[\,2\,p\,\lambda\,\mathrm{tg}\,\varphi + 2c + \gamma\,\lambda\,\mathrm{tg}\,\varphi\,h\right], \qquad (3)$$

where h – length of the contact section, where shear strength failed,

t – wall thickness,

φ, c – angle of internal friction and specific cohesion at contact "wall-soil" respectively,

γ, λ – specific weight and coefficient of soil lateral pressure respectively.

Formula (3) shows that strength parameters of contact "soil-wall" considerably affect the limiting state of compressive stresses. The stronger is the contact the more are compressive stresses in the wall.

Dependence (3) also permits assessing the effect of depth on values of compressive stresses. Theoretically it is quadratic, however, the results of SSS analysis for the considered case show that the role of the quadratic term is small and stresses are actually increased linearly with growth of the wall depth.

This dependence also indicates on the method of decreasing compressive stresses in the wall, i.e. increase of the wall thickness.

However, analytical dependence (3) is approximate; it does not allow considering the effect of the foundation SSS peculiar features. The true values of compressive stresses in the wall may be obtained only by numerical modeling.

The obtained SCW SSS permitted us to assess the wall strength and reveal what material is the best for arranging SCW.

At assessing strength of the wall made of plastic material (for example, clay-cement concretes) we proposed to take into consideration the fact that SCW is in a complicated stress state. Experimental studies with clay-cement concrete show that its compressive strength increases when we have lateral compression [24–25]. This effect may be considered based on the theory of strength of Coulomb–Mohr. In compliance with this theory the material compressive strength proportionally increases with lateral compression growth:

$$R = R_1 + \sigma_1 \frac{1+\sin\varphi}{1-\sin\varphi}, \quad (4)$$

where R_1 – uniaxial compression strength,

σ_1 – compressive stress (maximum principal stress),

φ – angle of soil internal friction.

The wall compression is achieved by lateral pressure of the surrounding soil.

Analysis of meeting compressive strength conditions conducted for various alternatives showed the following:

- Consideration of lateral compression considerably improves the wall condition from the point of view of assessing compressive strength. Compression effect is especially noticed in the alternatives with liquid clay-cement concrete (alternative No. 1);
- In most alternatives compressive strength is not provided, even with consideration of strength growth at lateral compression;
- In most alternatives with liquid clay-cement concrete (Alternative No. 1) the most dangerous section is the wall top. In this section compressive stresses have maximum values and compressive strength values are minimum. It should be noted that SSS of foundation itself significantly affects SCW performance. By the results of analyses the foundation under the action of dam weight «sprawls». This results in the fact that the wall upper part turns to be weakly compressed by soil lateral pressure and the wall operation conditions are close to uniaxial compression state;
- In the alternatives of making SCW of rigid materials (alternatives Nos. 3–5) the most hazardous section is located in the wall lower part where compressive stresses are maximum;
- Operation conditions of suspended walls are more favorable, because compressive stresses in them are less and therefore, it is easier to provide the material strength;
- The only wall material whose strength was provided in any patterns and operation conditions is liquid clay-cement concrete (alternative No. 1). At that, safety factor in the wall upper part as a rule is close to 0;
- In operation mode of wall IC (suspended wall 20 m deep) (alternatives C) compressive strength was provided not only in alternative No.1 but also at arrangement of a concrete wall (alternative No. 5). This was achieved due to actually full slip of the foundation soil against a not deep wall.

This analysis shows that SCW operation conditions are very complicated; they depend on many factors, that is why it is not possible to formulate general recommendations for selection of material and providing SCW strength, which could be applicable to all possible SCW operation conditions. Depending

on loads transferred by the dam to the foundation, conditions of resting, the wall thickness and depth, foundation structures the SCW operation conditions may differ greatly. In each particular case it is necessary to conduct numerical studies of SCW SSS.

Tentative recommendations may be as follows:

- For arrangement of the wall it is desirable to use the material whose deformability differs from that of the surrounding soil by not more than 2 times. This recommendation differs from ICOLD recommendations [22] and makes the requirements tougher;
- For improvement of SSS and strength condition of the SCW upper part it is desirable to exclude direct transfer of the dam weight loads to it. For this purpose a concrete gallery may be provided above the wall separated from it by a gap (cavity);
- One more way of improving the strength state of SCW made of rigid materials is increase of its thickness. Increasing thickness of the wall will permit decreasing concentration of compressive stresses in it;
- In some cases the use of more rigid and strong material, reinforced concrete may be allowed for SCW arrangement and the required strength will be provided. This is possible in conditions if compressive forces transferred to the wall are not great. For example, this is possible due to slip at contact “soil-wall”. Therefore, of great importance are strength indices at contact “soil-wall”. With this respect it is necessary to note that at the wall construction by a trench method a so-called bentonite “casing” is formed with low strength indices. “Oiling” may greatly affect the rigid wall SSS.

The wall SSS analysis on the moment of perception by the wall of the seepage flow pressure shows cardinal change of SSS. At reservoir filling the wall shifted toward the downstream side and acquired bending deformations (Figs. 18–29b). Maximum shift is observed in the wall head.

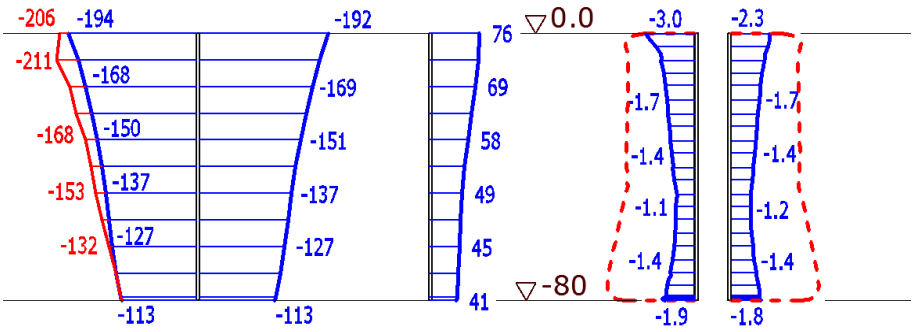

Figure 18. Wall SSS of alternative IA-1 as of the moment of reservoir filling completion: a – settlements (cm), b – displacements (cm), c– vertical stresses (MPa) on the upstream and downstream faces

Blue lines correspond to the curves for the wall. Red lines correspond to soil settlements. The dotted line indicates the wall material compressive strength.

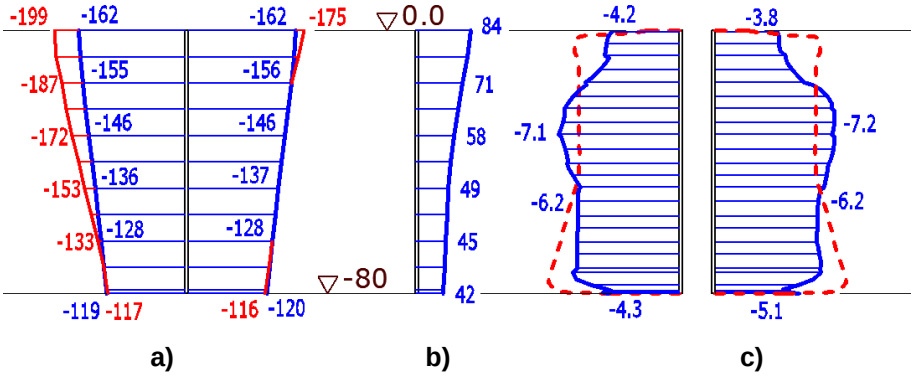

Figure 19. Wall SSS of alternative IA-3 as of the moment of reservoir filling completion. Legend see in Figure 18

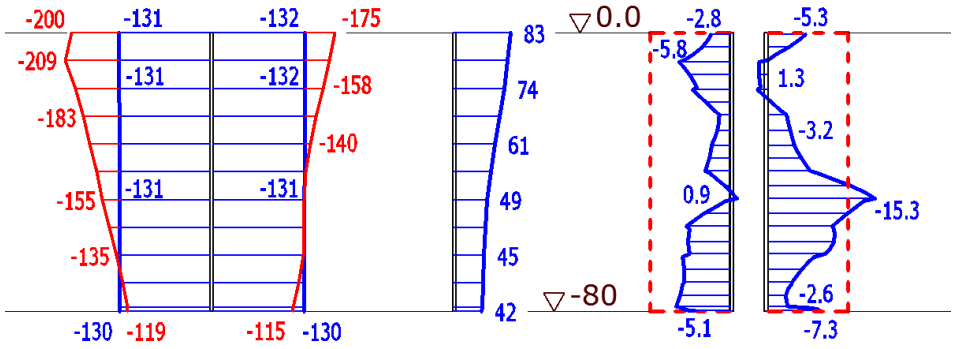

Figure 20. Wall SSS of alternative IA-5 as of the moment of reservoir filling completion. Legend see in Figure 18

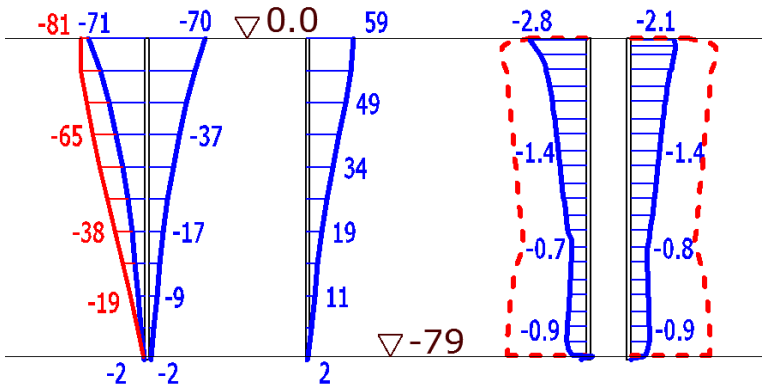

Figure 21. Wall SSS of alternative IIA-1 as of the moment of reservoir filling completion: a – settlements (cm), b – displacements (cm), c– vertical stresses (MPa) on the upstream and downstream faces

Blue lines correspond to the curves for the wall. Red lines correspond to soil settlements. The dotted line indicates the wall material compressive strength.

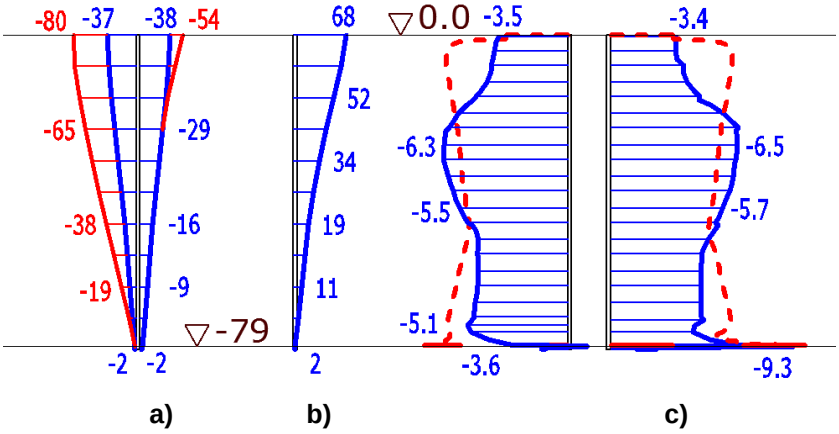

Figure 22. Wall SSS of alternative IIA-3 as of the moment of reservoir filling completion. Legend see in Figure 21

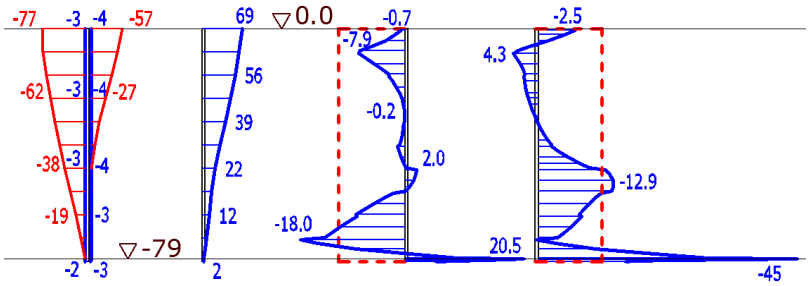

a) b) c)

Figure 23. Wall SSS of alternative IIA-5 as of the moment of reservoir filling completion. Legend see in Figure 21

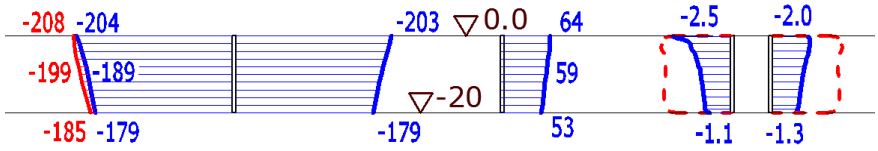

a) b) c)

Figure 24. Wall SSS of alternative IC-1 as of the moment of reservoir filling completion: a – settlements (cm), b – displacements (cm), c– vertical stresses (MPa) on the upstream and downstream faces

Blue lines correspond to the curves for the wall. Red lines correspond to soil settlements. The dotted line indicates the wall material compressive strength.

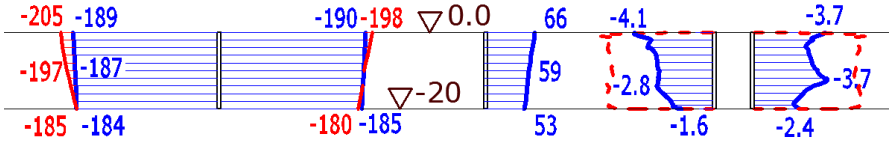

a) b) c)

Figure 25. Wall SSS of alternative IC-3 as of the moment of reservoir filling completion. Legend see in Figure 24

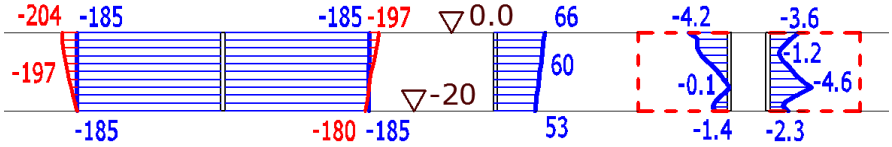

a) b) c)

Figure 26. Wall SSS of alternative IC-5 as of the moment of reservoir filling completion. Legend see in Figure 24

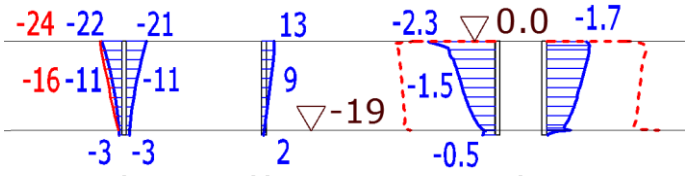

a) b) c)

Figure 27. Wall SSS of alternative IIC-1 as of the moment of reservoir filling completion. Legend see in Figure 24

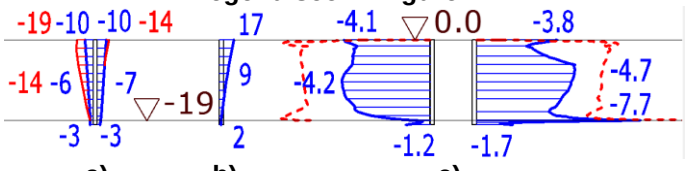

a) b) c)

Figure 28. Wall SSS of alternative IIC-3 as of the moment of reservoir filling completion. Legend see in Figure 24

Саинов М.П., Лубьянов В.В. Напряжённо-деформированное состояние противофильтрационных стен в основании грунтовых плотин // Инженерно-строительный журнал. 2017. № 5(73). С. 96–112.

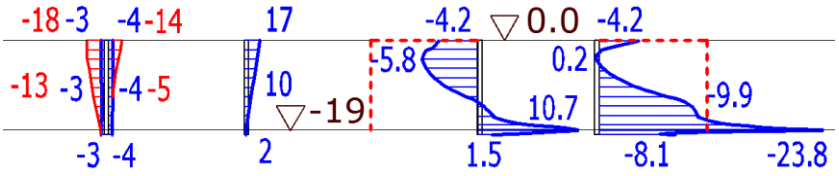

Figure 29. Wall SSS of alternative IC-5 as of the moment of reservoir filling completion. Legend see in Figure 24

Analysis of SCW SSS modeling shows the following:

- At perception of horizontal forces not only displacements occur but also the wall bend. At that, suspended SCW and resting walls displace and bend in different ways. Foot displacement of the walls resting on rock foundation is close to 0, but the wall top displacement is more than that of suspended walls. For example, the top displacement of the resting wall in alternative IIA-1 comprises 59 cm (Fig. 20b), and of the suspended wall in alternative IA-1 it is 76 cm (Fig. 20b). At that, bend of the suspended wall in alternative IIA-1 (57 cm) is much less than that of the resting wall in alternative IA-1 (35 cm). This difference in bends is explained by the fact that the resting walls take greater horizontal loads than the suspended ones;
- At perception of horizontal loads by the wall the vertical compressive forces perceived by it also considerably decreased. This is explained not only by the fact that weighing action contributes to decrease of pressure transferred to the foundation from the dam weight. Of great importance is development of slip processes along the upstream face of SCW (Figs. 17–28a). At the wall displacements toward the upstream side the normal stresses in the upstream contact “wall-soil” decrease, and consequently, its shear strength decreases also. Due to development of slip processes in the upstream contact “wall-soil” the vertical compressive forces transferred to the wall sharply decrease.
- Bend of the suspended wall is complicated. The upper part bends toward the downstream side and the lower part bends toward the upstream side. Due to the bend on one of the faces compressive stresses y decrease and on the other face they increase.
- For the walls made of clay-cement concrete there is hardly noticed non-uniformity in stress distribution. When the wall is made of reinforced concrete (alternative No. 5) compressive stresses pass to tensile stresses. For example, in alternative IA-5 tensile stresses reach 1.3 MPa (Fig. 19c) and exceed the concrete tensile strength.
- In the walls on rock foundations due to more displacements the bend deformations are expressed stronger. Due to the fact that in alternative IIA-5 the tensile stresses in the wall upper part reach 4.3 MPa (Fig. 22c). Besides, the resting wall character of bend deformations is complicated in the zone of embedment into the rock foundation. In the embedment zone the wall considerably bends toward the upstream side. In alternative IA-5 tensile stresses on the upstream face exceed 20 MPa (Fig. 22c).
- SSS of less deep walls is somewhat better. In alternative IIC-5 tensile stresses in the wall upper part do not exceed 0.2 MPa, and in the zone of embedment they amount to 10.7 MPa (Fig. 28c). Thus, for the walls embedded into a rigid rock foundation the most hazardous are tensile stresses in the embedment zone. We may arrive to the conclusion that the interface of SCW with rock should be provided not by its embedment into rock, but by arranging a more flexible connection. For example, it may be an earlier prepared zone of grouted impervious soil.

From the point of view of providing the dam compressive strength the wall strength state in the second design moment is more favorable than in the first one. This is explained by two reasons. The first reason refers to general decrease of compressive longitudinal forces in the wall. The second reason is attributed to the fact that at reservoir filling the wall is compressed under water pressure and due to this its material compressive strength increases.

Wall compressive strength is not provided only in use of rigid materials (alternatives Nos. 4–5, sometimes alternative No. 3).

Conclusion

1. SCW SSS analysis should be performed at least for two moments of time: The first is the moment of dam construction completion; the second refers to the moment of reservoir filling completion and formation of the seepage regime in the foundation. The first moment is dangerous from the point of

view of possible compressive strength failure, the second from the point of view of possible tensile strength failure.

SCW SSS in the foundation of a high embankment dam as of the moment of dam construction completion is characterized by concentration of considerable compressive longitudinal stresses. These stresses are greater the greater is the ratio between deformation moduli of the wall material and the foundation soil. After the reservoir filling the compressive stresses decrease, but this leads to possible appearance of tensile stresses in the wall. In the moment of reservoir filling completion the most hazardous for the wall are bend deformations.

2. Rigidity of the wall itself and conditions of interaction with surrounding soil mass have the greatest impact on formation of SCW SSS. The degree of developed slip processes at contact “soil-wall” plays a great role.

Besides, SCW SSS is affected by conditions of its rest (suspended or resting), foundation setting, the wall depth and thickness.

3. SSS of walls embedded into a rock foundation (resting walls) is less favorable than that of the suspended walls. At perception of vertical forces the resting wall maximum values of stresses turn to be slightly higher than those in suspended walls. Walls reaching water-tight stratum are subject to greater horizontal water pressure and therefore, greater displacements. They are characterized by greater bend deformations, especially in the zone of embedment into rock foundation. The zone of walls embedment into rock foundation is the most dangerous and unsafe section. At horizontal displacements of walls in the embedment, cracks may appear as a result of tensile strength failure as well as shear.

4. The empirical dependences proposed by us may be applied at the preliminary design stage for determining maximum values of compressive longitudinal stresses in SCW. However, these dependences are approximate. More reliable results may be obtained only by numerical modeling, because this is the only way of modeling slip processes at the contact of the wall with soil.

5. Deep walls operate in more complicated conditions than the wall of small deepness. The greater is the wall depth the higher are compressive stresses in it and the higher is the probability of compressive strength failure.

6. At assessing compressive strength of the walls made of plastic material, for example clay-cement concrete, it is necessary to take into account the effect of strength growth when we have lateral compression. As SCW are usually in the state of triaxial compression, account of this effect is of great importance.

7. For SCW constructed in a homogenous foundation it may be recommended to use the material whose deformation modulus is not more than 2 fold as compared to the deformation modulus of the surrounding soil. This meets ICOLD recommendations, but the difference is that it is tougher.

8. It is not recommended to use concrete and reinforced concrete for SCW arrangement. At foundation settlements considerable compressive stresses are concentrated in rigid walls, and at perception of horizontal forces the tensile stresses appear. It is especially dangerous to use concrete (reinforced concrete) for the walls arranged in soil and embedded into rock foundation.

However, there are cases when use of reinforced concrete may be allowed and justified. For example, reinforced concrete may be used for arranging suspended walls of small deepness.

9. At designing seepage-control walls there are several ways of their SSS regulation to provide strength. The first is using the material by deformability close to the enclosing soil. The second way is increasing the wall thickness. The third way is decrease of friction at contact “soil-wall” to decrease forces transferred to the wall by foundation soil, however, this way is not possible in practice. Besides, tangible effect may be reached by arranging a concrete gallery above the wall top, from which the wall will be separated by a gap. This will permit slight decrease of vertical compressive forces transferred to the wall.

References

1. Balian S. Cut-off wall construction at Peribonka dam. *International Water Power & Dam Construction.* 2007. Vol. 59(2). Pp. 42–44.
2. Mirghasemi A.A., Pakzad M., Shadravan B. The world’s largest cutoff wall at Karkheh dam. *Hydropower & Dams*. 2005. No. 2. Pp. 2–6.
3. Baranov A.Ye. Iz opyta proyektirovaniya i stroitelstva Yumaguzinskogo gidrouzla na r. Beloy [The Experience of

Литература

1. Balian S. Cut-off wall construction at Peribonka dam // International Water Power & Dam Construction. 2007. Vol. 59(2). Pp. 42–44.
2. Mirghasemi A.A., Pakzad M., Shadravan B. The world’s largest cutoff wall at Karkheh dam // Hydropower & Dams. 2005. № 2. Pp. 2–6.
3. Баранов А.Е. Из опыта проектирования и строительства Юмагузинского гидроузла на р.Белой //

Саинов М.П., Лубьянов В.В. Напряжённо-деформированное состояние противофильтрационных стен в основании грунтовых плотин // Инженерно-строительный журнал. 2017. № 5(73). С. 96–112.

Designing and Building Yumagusinskiy Hydoelectric Complex on the River Belaya]. *Vestnik MGSU*. 2006. No. 2. Pp. 112–122. (rus)

4. Radchenko V.G., Lopatina M.G., Nikolaychuk E.V., Radchenko S.V. Opyt vozvedeniya protivofil'tratsionnykh ustroystv i gruntotsementnykh smesey [Experience in the Construction of Antifiltering Devices and Soil-cement Compositions]. *Gidrotekhnicheskoe stroitel'stvo.* 2012. No. 6. Pp. 46–54. (rus)
5. Malyshev L.I., Shishov I.N., Kudrin K.P., Bardyugov V.G. Tekhnicheskie resheniya i rezul'taty rabot po sooruzheniyu protivofil'tratsionnoy steny v grunte v yadre i osnovanii Kureyskoy GES [Technical Solutions and Working Results in the Process of Building Filtration-proof Wall in the Soil of the Core and Foundation of Kureyskaya Water Power Plant]. *Gidrotekhnicheskoe stroitel'stvo.* 2001. No. 3. Pp. 31–36. (rus)
6. Coj M.S.D., Aldanov A.G., Radchenko V.G., Semenov Ju.D., Danilov A.S., Smolenkov V.Ju. Vozvedenie protivofil'tracionnoj zavesy metodom strujnoj cementacii v osnovanii plotiny Sangtudinskoj GJeS-1 [The erection of the anti-seepage curtain by the method of jet grouting in the base of the dam of Sangtudinskaya HPP-1]. *Gidrotekhnicheskoe stroitel'stvo.* 2008. No. 5. Pp. 32–37. (rus)
7. Ehrhardt T., Scheid Y., El Tayeb A. Design and construction of the rockfill dams and the cut-off wall at the Merowe Project [Entwurf und ausfuhrung der steinschuttdamme und der schlitzwand des Merowe-Projektes. *WasserWirtschaft.* 2011. No. 101(1-2). Pp. 36–42.
8. Noll H., Langhagen, K., Popp, M., Lang, T. Rehabilitation of the sylvenstein earth-fill dam - Design and construction of the cut off wall [Ertuchtigung des Sylvenstein-Staudamms - Planung und Ausfuhrung der Dichtwand]. *WasserWirtschaft*. 2013. Vol. 103. No. 5. Pp. 76–79.
9. Rasskazov L.N., Bestuzheva A.S., Sainov M.P. Betonnaya diafragma kak element rekonstruktsii gruntovoy plotiny [Concrete Membrane as an Element of Ground Water Dam Reconstruction]. *Gidrotekhnicheskoe stroitel'stvo*. 1999. No. 4. Pp. 10–16. (rus)
10. Sainov M.P. *Naprjazhjonno-deformirovannoe sostojanie protivofil'tracionnyh "sten v grunte" gruntovyh plotin* [The stress-strain state of the anti-seepage cutoff wall of the earth dams] (Dissertation for the degree of candidate of technical sciences). 2001. 255p. (rus
11. Dao Tuan An'. *Prostranstvennoe naprjazhjonno-deformirovannoe sostojanie gruntovyh plotin s tonkim protivofil'tracionnym jelementom* [Spatial stress-strain state of soil dams with a thin anti-seepage element] (Dissertation for the degree of candidate of technical sciences). 2002. 259 p. (rus)
12. Radzinskiy A.V., Rasskazov L.N., Sainov M.P. Plotina stometrovoy vysoty s glinotsementobetonnoy diafragmoy po tipu "stena v grunte" [Clay-cement Concrete Diaphragm of the Type "Slurry Wall" in the 100 Meter High Dam]. *Vestnik MGSU.* 2014. No. 9. Pp. 106–115. (rus)
13. Ding Y., Zhang Q., Zhang B. FEM analysis of stress-deformation characteristics of cut-off walls in high core rockfill dam. *Journal of Hydroelectric Engineering*. 2013. No. 32(3). Pp. 162–167.
14. Pan Y., He Y.-L., Zhou X.-X., Cao X.-X. Analysis of effect of canyon terrain on stress and displacement of cutoff wall in dam foundation with deep overburden. *Yantu Lixue/Rock and Soil Mechanics.* 2013. No. 34(7). Pp. 2023–2030.
15. Liu S.-H., Wang L.-J., Wang Z.-J., Bauer E. Numerical stress-deformation analysis of cut-off wall in clay-core rockfill dam on thick overburden. *Water Science and Engineering.* 2016. No. 9(3). Pp. 219–226.
16. Prokopovich V.S., Velichko A.S., Orishhuk R.N. Naprjazhenno-deformirovannoe sostojanie zemljanoj plotiny s glinocementobetonnoj diafragmoj (Na primere

Вестник МГСУ. 2006. № 2. С. 112–122.

4. Радченко В.Г., Лопатина М.Г., Николайчук Е.В., Радченко С.В. Опыт возведения противофильтрационных устройств из грунтоцементных смесей. // Гидротехническое строительство. 2012. № 12. С. 46–54.
5. Малышев Л.И., Шишов И.Н., Кудрин К.П., Бардюгов В.Г. Технические решения и результаты работ по сооружению противофильтрационной стены в грунте в ядре и основании Курейской ГЭС // Гидротехническое строительство. 2001. № 3. С. 31–36.
6. Цой М.С.Д., Алданов А.Г., Радченко В.Г., Семенов Ю.Д., Данилов А.С., Смоленков В.Ю. Возведение противофильтрационной завесы методом струйной цементации в основании плотины Сангтудинской ГЭС-1. // Гидротехническое строительство. 2008. № 5. С. 32–37
7. Ehrhardt T., Scheid Y., El Tayeb A. Design and construction of the rockfill dams and the cut-off wall at the Merowe Project [Entwurf und ausfuhrung der steinschuttdamme und der schlitzwand des Merowe-Projektes] // WasserWirtschaft. 2011. Vol. 101(1-2). Pp. 36–42.
8. Noll H., Langhagen K., Popp M., Lang T. Rehabilitation of the sylvenstein earth-fill dam - Design and construction of the cut off wall [Ertuchtigung des Sylvenstein-Staudamms - Planung und Ausfuhrung der Dichtwand] // WasserWirtschaft. 2013. Vol. 103. № 5. Pp. 76–79.
9. Рассказов Л.Н., Бестужева А.С., Саинов М.П. Бетонная диафрагма как элемент реконструкции грунтовой плотины // Гидротехническое строительство. 1999. № 4. С. 10–16.
10. Саинов М.П. Напряжённо-деформированное состояние противофильтрационных "стен в грунте" грунтовых плотин: дис. ... канд.техн.наук 05.23.07 / Саинов Михаил Петрович. – М., 2001. 255 с.
11. Дао Туан Ань. Пространственное напряжённо-деформированное состояние грунтовых плотин с тонким противофильтрационным элементом: дис. ... канд.техн.наук 05.23.07 / Дао Туан Ань. – М., 2002. 259 с.
12. Рассказов Л.Н., Радзинский А.В., Саинов М.П. Плотина высотой 100 м с глиноцементобетонной диафрагмой по типу "стена в грунте" // Вестник МГСУ. 2014. № 9. С. 106–115.
13. Ding Y., Zhang Q., Zhang B. FEM analysis of stress-deformation characteristics of cut-off walls in high core rockfill dam // Journal of Hydroelectric Engineering. 2013. № 32(3). Pp. 162–167.
14. Pan Y., He Y.-L., Zhou X.-X., Cao X.-X. Analysis of effect of canyon terrain on stress and displacement of cutoff wall in dam foundation with deep overburden // Yantu Lixue/Rock and Soil Mechanics. 2013. № 34(7). Pp. 2023–2030.
15. Liu S.-H., Wang L.-J., Wang Z.-J., Bauer E. Numerical stress-deformation analysis of cut-off wall in clay-core rockfill dam on thick overburden // Water Science and Engineering. 2016. № 9(3). Pp. 219–226.
16. Прокопович В.С., Величко А.С., Орищук Р.Н. Напряженно-деформированное состояние земляной плотины с глиноцементобетонной диафрагмой (На примере земляной плотины Гоцатлинской ГЭС) // Известия ВНИИГ им. Б.Е.Веденеева. 2016. Т. 282. С. 87–98.
17. Саинов М.П., Котов Ф.В. Оценка надежности диафрагмы из буронабивных свай в плотине средней высоты // Вестник МГСУ. 2014. № 1. С. 153–163.
18. ICOLD. Filling materials for watertight cut-off walls. 1985. Bulletin 51.
19. Саинов М.П. Вычислительная программа по расчёту напряжённо-деформированного состояния грунтовых

zemljanoj plotiny Gocatlinskoj GJeS) [The stress-strain state of an earth dam with slurry wall diaphragm (On the example of the earth dam of Gotsatlinskaya HPP)] // *Izvestija VNIIG im.B.E.Vedeneeva.* 2016. Vol. 282. Pp. 87–98. (rus)

17. Sainov M.P., Kotov F.V. Otsenka nadezhnosti diafragmy iz buronabivnykh svay v plotine sredney vysoty [Safety Assessment of a Bored Pile Diaphragm in a Mediumheight Dam]. *Vestnik MGSU.* 2014. No. 1. Pp. 153–163
18. ICOLD. Filling materials for watertight cut-off walls. 1985. Bulletin 51.
19. Sainov M.P. Vychislitelnaya programma po raschyotu napryazhyonno-deformirovannogo sostoyaniya gruntovykh plotin: opyt sozdaniya, metodiki i algoritmy [Computer program for the calculation of the stress-strain state of soil dams: the experience of creation, techniques and algorithms]. *International Journal for Computational Civil and Structural Engineering.* 2013. Vol. 9. No. 4. Pp. 208–225. (rus)
20. Rasskazov L.N., Radzinskiy A.V., Sainov M.P. Prochnost i deformiruyemost glinotsementobetona v slozhnom napryazhennom sostoyanii [Strength and Deformability of Clay-cement Concrete in Complex Stress State]. *Gidrotekhnicheskoye stroitelstvo*. 2014. No. 8. Pp. 29–33. (rus)
21. Pisheh Y.P., Mir Mohammad Hosseini, S.M. Stress-strain behavior of plastic concrete using monotonic triaxial compression tests. *Journal of Central South University of Technology (English Edition).* 2012. Vol. 19. No. 4. Pp. 1125–1131.
22. Hinchberger S., Weck J, Newsona T. Mechanical and hydraulic characterization of plastic concrete for seepage cut-off walls. *Canadian Geotechnical Journal*. 2010. No. 47(4). Pp. 461–471.
23. Sainov M.P. Priblizhjonnyj prognoz prochnosti protivofil'tracionnoj steny v osnovanii plotiny [Approximate prognosis of the strength of the anti-seepage wall at the base of the dam]. *Nauchnoe obozrenie*. 2017. No. 4. Pp. 34–38. (rus)

плотин: опыт создания, методики и алгоритмы // International Journal for Computational Civil and Structural Engineering. 2013. № 9(4). С. 208–225.

20. Рассказов Л.Н., Радзинский А.В., Саинов М.П. Прочность и деформируемость глиноцементобетона в сложном напряженном состоянии // Гидротехническое строительство. 2014. № 8. С. 29–33.
21. Pisheh Y.P., Mir Mohammad Hosseini S.M. Stress-strain behavior of plastic concrete using monotonic triaxial compression tests // Journal of Central South University of Technology (English Edition). 2012. Vol. 19. № 4. Pp. 1125–1131.
22. Hinchberger S., Weck J., Newsona T. Mechanical and hydraulic characterization of plastic concrete for seepage cut-off walls // Canadian Geotechnical Journal. 2010. № 47(4). Pp. 461–471.
23. Саинов М.П. Приближённый прогноз прочности противофильтрационной стены в основании плотины // Научное обозрение. 2017. № 4. С.34–38.

Mikhail Sainov,
+7(926)6078931; mp_sainov@mail.ru

Vladislav Lubyanov,
+7(909)9505567; lubyanovvv@yandex.ru

Михаил Петрович Саинов,
+7(926)6078931; эл. почта: mp_sainov@mail.ru

Владислав Валерьевич Лубьянов,
+7(909)9505567;
эл. почта: lubyanovvv@yandex.ru

Саинов М.П., Лубьянов В.В. Напряжённо-деформированное состояние противофильтрационных стен в основании грунтовых плотин // Инженерно-строительный журнал. 2017. № 5(73). С. 96–112.

Федеральное государственное автономное образовательное учреждение высшего образования
Санкт-Петербургский политехнический университет Петра Великого

ПОЛИТЕХ
Санкт-Петербургский политехнический университет Петра Великого

Инженерно-строительный институт
Центр дополнительных профессиональных программ

195251, г. Санкт-Петербург, Политехническая ул., 29,
тел/факс: 552-94-60, www.stroikursi.spbstu.ru,
stroikursi@mail.ru

Приглашает специалистов проектных и строительных организаций,
не имеющих базового профильного высшего образования
на курсы профессиональной переподготовки (от 500 часов)
по направлению «Строительство» по программам:

П-01 «Промышленное и гражданское строительство»

Программа включает учебные разделы:

- ***Основы строительного дела***
- ***Инженерное оборудование зданий и сооружений***
- ***Технология и контроль качества строительства***
- ***Основы проектирования зданий и сооружений***
- ***Автоматизация проектных работ с использованием AutoCAD***
- ***Автоматизация сметного дела в строительстве***
- ***Управление строительной организацией***
- ***Управление инвестиционно-строительными проектами. Выполнение функций технического заказчика***

П-02 «Экономика и управление в строительстве»

Программа включает учебные разделы:

- ***Основы строительного дела***
- ***Инженерное оборудование зданий и сооружений***
- ***Технология и контроль качества строительства***
- ***Управление инвестиционно-строительными проектами. Выполнение функций технического заказчика и генерального подрядчика***
- ***Управление строительной организацией***
- ***Экономика и ценообразование в строительстве***
- ***Управление строительной организацией***
- ***Организация, управление и планирование в строительстве***
- ***Автоматизация сметного дела в строительстве***

П-03 «Инженерные системы зданий и сооружений»

Программа включает учебные разделы:

- ***Основы механики жидкости и газа***
- ***Инженерное оборудование зданий и сооружений***
- ***Проектирование, монтаж и эксплуатация систем вентиляции и кондиционирования***
- ***Проектирование, монтаж и эксплуатация систем отопления и теплоснабжения***
- ***Проектирование, монтаж и эксплуатация систем водоснабжения и водоотведения***
- ***Автоматизация проектных работ с использованием AutoCAD***
- ***Электроснабжение и электрооборудование объектов***

П-04 «Проектирование и конструирование зданий и сооружений»

Программа включает учебные разделы:

- ***Основы сопротивления материалов и механики стержневых систем***
- ***Проектирование и расчет оснований и фундаментов зданий и сооружений***
- ***Проектирование и расчет железобетонных конструкций***
- ***Проектирование и расчет металлических конструкций***
- ***Проектирование зданий и сооружений с использованием AutoCAD***
- ***Расчет строительных конструкций с использованием SCAD Office***

П-05 «Контроль качества строительства»

Программа включает учебные разделы:

- ***Основы строительного дела***
- ***Инженерное оборудование зданий и сооружений***
- ***Технология и контроль качества строительства***
- ***Проектирование и расчет железобетонных конструкций***
- ***Проектирование и расчет металлических конструкций***
- ***Обследование строительных конструкций зданий и сооружений***
- ***Выполнение функций технического заказчика и генерального подрядчика***

По окончании курса слушателю выдается диплом о профессиональной переподготовке установленного образца, дающий право на ведение профессиональной деятельности